(12) INTERNATIONAL APPLICATION PUBLISHED UNDER THE PATENT COOPERATION TREATY (PCT)

(19) World Intellectual Property Organization
International Bureau

(43) International Publication Date
5 April 2007 (05.04.2007)

PCT

(10) International Publication Number
WO 2007/038378 A2

(51) International Patent Classification:
C21D 10/00 (2006.01)

(21) International Application Number:
PCT/US2006/037154

(22) International Filing Date:
22 September 2006 (22.09.2006)

(25) Filing Language: English

(26) Publication Language: English

(30) Priority Data:
60/719,551 23 September 2005 (23.09.2005) US
11/342,846 31 January 2006 (31.01.2006) US

(71) Applicant *(for all designated States except US)*: **UIT, L.L.C.** [US/US]; 5871 Old Ledds Rd., Birmingham, AL 35210 (US).

(72) Inventor; and

(75) Inventor/Applicant *(for US only)*: **STATNIKOV, Efim, S.** [RU/US]; 2942 Summit Place, Birmingham, AL 35243 (US).

(74) Agents: **RADOMSKY, Leon** et al.; FOLEY & LARDNER LLP, Washington Harbour, 3000 K Street, NW, Suite 500, Washington, DC 20007 (US).

(81) Designated States *(unless otherwise indicated, for every kind of national protection available)*: AE, AG, AL, AM, AT, AU, AZ, BA, BB, BG, BR, BW, BY, BZ, CA, CH, CN, CO, CR, CU, CZ, DE, DK, DM, DZ, EC, EE, EG, ES, FI, GB, GD, GE, GH, GM, HN, HR, HU, ID, IL, IN, IS, JP, KE, KG, KM, KN, KP, KR, KZ, LA, LC, LK, LR, LS, LT, LU, LV, LY, MA, MD, MG, MK, MN, MW, MX, MY, MZ, NA, NG, NI, NO, NZ, OM, PG, PH, PL, PT, RO, RS, RU, SC, SD, SE, SG, SK, SL, SM, SV, SY, TJ, TM, TN, TR, TT, TZ, UA, UG, US, UZ, VC, VN, ZA, ZM, ZW.

(84) Designated States *(unless otherwise indicated, for every kind of regional protection available)*: ARIPO (BW, GH, GM, KE, LS, MW, MZ, NA, SD, SL, SZ, TZ, UG, ZM, ZW), Eurasian (AM, AZ, BY, KG, KZ, MD, RU, TJ, TM), European (AT, BE, BG, CH, CY, CZ, DE, DK, EE, ES, FI, FR, GB, GR, HU, IE, IS, IT, LT, LU, LV, MC, NL, PL, PT, RO, SE, SI, SK, TR), OAPI (BF, BJ, CF, CG, CI, CM, GA, GN, GQ, GW, ML, MR, NE, SN, TD, TG).

Published:
— *without international search report and to be republished upon receipt of that report*

For two-letter codes and other abbreviations, refer to the "Guidance Notes on Codes and Abbreviations" appearing at the beginning of each regular issue of the PCT Gazette.

(54) **Title:** METHOD OF METAL PERFORMANCE IMPROVEMENT AND PROTECTION AGAINST DEGRADATION AND SUPPRESSION THEREOF BY ULTRASONIC IMPACT

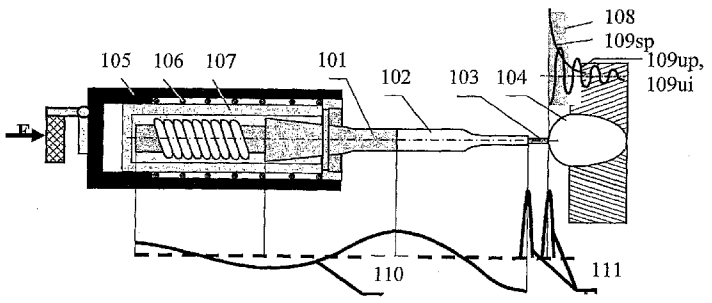

101 – MAGNETOSTRICTIVE TRANSDUCER
102 – WAVEGUIDE
103 – INDENTER
104 – TREATED SURFACE
105 – CASE (FIXED) WITH A HANDLE
106 – SPRING
107 – WATER-COOLED CASING OF TRANSDUCER
108 – PLASTIC DEFORMATION OF MATERIAL
109sp – SINGLE STRESS PULSES
109up– ULTRASONIC PERIODIC STRESS WAVE
109ui – ULTRASONIC (APERIODIC) IMPULSE STRESSES
110 – ULTRASONIC OSCILLATIONS
111 – IMPACT IMPULSES
F – PRESSING FORCE OF OS AGAINST TS

101, 102, 103 105, 106, 107 – FORM THE OSCILLATING SYSTEM (OS) WITH A RIGIDLY FIXED PROCESSING SETUP

(57) **Abstract:** A method of improving and strengthening the performance of metal and protecting the metal against degradation and suppression thereof by controlling ultrasonic impact is disclosed. The method addresses the problems of degradation of metal properties during prolonged service under external forces, thermodynamic fluctuations and negative environmental factors. The method also relates to the technologies oriented to protect against (prevent) and to suppress the danger of materials failure due to unfavorable change in performance over time. The well-known methods of "combating" metal degradation cover a wide range of technologies from metallurgical alloying during melting, casting, welding and application of coatings to various thermal treatments and effects on the surface. The invention provides a new versatile method of addressing degradation problems in all these cases.

WO 2007/038378 A2

METHOD OF METAL PERFORMANCE IMPROVEMENT AND PROTECTION AGAINST DEGRADATION AND SUPPRESSION THEREOF BY ULTRASONIC IMPACT

FIELD OF INVENTION

[0001] The invention relates to a method and algorithm of improving the performance of metal and protecting the metal against degradation and suppression thereof by ultrasonic impact. The invention addresses the problems of degradation of metal properties during prolonged service under external forces, thermodynamic fluctuations and negative environmental factors. The invention protects against, i.e., prevents, and suppresses the danger of material failure due to unfavorable change in performance over time. These problems commonly occur because of the damage of the original structure of the material/metal under known conditions that accompany the processes of environmental degradation of metals.

BACKGROUND OF THE INVENTION

[0002] Known in the art are U.S. Patent Nos. 6,171,415; 6,289,736; 6,458,225; 6,338,765; 6,722,175 and 6,843,957 and U.S. Serial No. 10/834,180 which disclose methods and means of the direct effect of ultrasonic impact treatment upon a material condition and properties, implying that the surface of a material and its subsurface layer are one integral substance of the effect and results.

[0003] Various types (classifications), causes, physics and mechanisms of degradation are known. For example, known in the art is Degradation of Mechanical Systems, by Berman A.F. (Novosibirsk: Nauka, 1998, - p. 320), which discloses the results of an investigation and formalization of structural organization of material degradation processes in structures, failure of structural components and breakdown of unique

mechanical systems affected by combined action of factors. The processes of materials damage and structural components failure due to corrosion cracking, hydrogen embrittlement, corrosion and mechanical fatigue and erosion are also described.

[0004] The results of experimental investigations, tests and service experience of mechanical systems (MS) are the informational basis to address the problems associated with support, maintenance and recovery of the reliability and safety of MS and technical systems (TS) consisting of mechanical systems. This work addresses the changes in reliability of MS due to degradation. The degradation of MS implies the process of irreversible changes in technical condition, malfunction and unsafe operation. Degradation of MS is the portion of the breakdown and accident accumulating process that entails a change in structural load-bearing capacity.

[0005] To provide reliability at fabrication stage, efforts are made, based on knowledge of possible degradation processes, to develop and improve design diagrams and models, establish diagnostic features and criteria of failures and limiting states, as well as to validate test methods, determine techniques to diagnose and predict the technical condition and protection methods to prevent extension of emergencies and accidents.

[0006] To ensure reliable and safe operation, knowledge of degradation processes enables effective controlling and assessing of the technical condition of MS and the causes of its change, updating the lifetime of components and frequency of diagnostics, improving diagnostic and prediction techniques and updating MS.

[0007] Mechanical systems make up the structural basis of almost any technical system. Hence, the strength and life of

load-bearing structures and mechanisms are paramount in the general methodology of reliability study and maintenance.

[0008] Breakdown of MS and life depletion of the components are characterized by breakdown and limiting state criteria. The operational safety and necessary lifetime are attained by reserves of working capacity and load-bearing capacity, diagnostic and prediction techniques that compensate for a scatter in external actions and a random nature thereof.

[0009] Over the past decades, the causes of failures in power engineering, chemical and petrochemical industry and transportation have been investigated in greater detail. This has demonstrated the complexity and diversity of the phenomena and cause-and-effect relations responsible for life depletion (degradation) and failures of MS. For example, investigations of failures in chemical reactors showed that through-wall cracks in heat exchange pipes developed due to the unfavorable combination of mechanical, physical and chemical effects. This was possible because of imperfect design norms and regulations, manufacturing and inspection techniques and operating conditions, as well as the violation thereof. Thus, the problem of strength and life of MS and components thereof is far from being solved, especially for unique external factors and small-scale MS and TS, whose failures result in significant economic and social consequences.

[0010] One way to address this problem is to combine the methods of material and structural mechanics with a theory of random processes. This is a basis for a MS reliability theory. The probability of degradation failures should be fairly small within limits of a predicted lifetime and is attained by appropriate maintenance system and life design allowing for a physical nature of degradation failures. Valid calculations of lifetime are possible here only based on the study of the mechano-physical-chemical nature of failures, i.e., with the availability of a design model adequate to a

failure nature, models of mechanism and kinetics of degradation processes, and a quality space (of operable conditions) for both MS as a whole and each component thereof.

[0011] However, operating experience of unique chemical-processing systems shows that more than 30% of failures are indeed due to imperfect design models under simultaneous action of mechano-physical-chemical factors that do not allow reliable life prediction, but result in design solutions which do not enable the technical condition and reparability of MS to be assessed.

[0012] Failures in this case are caused to a great extent because adequate experimental investigations are impossible due to non-repeatability of external factors under laboratory conditions (combined action of high pressures and temperatures, active and aggressive environments, including fast moving ones; low rate of many degradation processes, which cannot be accelerated, etc.). No doubt that insufficient experimental investigations and tests and hence, the lack of valid criteria of failures and limiting state entail inadequate maintenance.

[0013] A parametric reliability theory is based on calculating reliability parameters, including physico-mechanical failure models. This theory suggests that output parameters of a product change due to wear and damage of individual components. However, in many cases the output parameter is not susceptible to a damage value until some critical instant when functioning is terminated or safe operation conditions are violated. For example, cracking occurs in vessels, pipes and other components where functioning is terminated because of through-wall cracking or brittle or ductile fracture.

[0014] In this case, the parameters that characterize the danger of through crack formation or hydrogen embrittlement (crack depth or length, etc.) are specified. With current

controllability and diagnostic facilities of many MS, such parameters are often out of control or controlled insufficiently. Because of this, the reliability of such MS should be maintained by analysis and probabilistic assessment of possible and hypothetic damages. The results obtained govern the measures to prevent extension of failures and provide safety.

[0015] The breakdown of MS is a final stage preceded by failure of one or several components, which, in turn, is caused by the damaged material that reached the critical value. Various parameters are taken as a damaging measure, depending on the material properties and external factors. The damage parameters characterize the change in physical, chemical and mechanical properties of the material, as well as surface and structural conditions.

[0016] Basically, the current measurement techniques do not detect initial damage stages due to their local application or because the industry lacks the necessary technical means and this should be considered during MS development. This brings a problem of identifying direct and indirect diagnostic features and developing diagnostic means needed to evaluate and predict the state during testing and in service.

[0017] The relationships, describing the processes of changing the properties and state of the material under combined action of various factors, are substantially non-linear. These processes are studied and formalized chiefly empirically. There is also a problem associated with the evaluation and prediction of material damage kinetics under various combinations of external factors.

[0018] Multiple effects on MS and TS, especially in chemistry, petrochemistry, nuclear engineering, bioengineering and pipeline infrastructure, cause a great variety of degradation processes that are responsible for complex damage of the material, life depletion and breakdown of MS.

Identifying possible degradation processes is the most important objective during pre-design investigations and design work.

[0019] A great number of metallophysical, metallurgy, physicochemical, strength, endurance and other investigations and tests were carried out to study these processes. The main objective of such investigations is to identify the mechanism, kinetics and dynamics of changes in structures and properties depending on the initial parameters. The monograph edited by G.P. Karzov is one of the latest and most comprehensive efforts directed to combining various approaches to investigation of failure processes occurring in materials and structures.

[0020] In many cases, a widely used and well-studied reliability method such as structural redundancy is not applicable for MS where reliability cannot be provided or correctly assessed based on the strength and life criteria. For example, the main failure criterion for pipelines, tubular devices and pressure vessels is seal failures due to through-wall damages or component failures, leading to leakage or atmospheric injection.

[0021] Any damage process may be described by its mechanism, kinetics and dynamics. The mechanism of the damage process implies the combination and interaction of the factors determining the process; the kinetics implies damages such as micro and/or macroscopic events occurring as a result of summing or accumulating elementary motion events; and dynamics implies the process velocity change over time. Thus, the damage mechanism (degradation mechanism) is identified with a number of factors affecting the components material; kinetics and dynamics are identified with material response within micro- and submicrovolumes to a given effect in time; and damage parameters are identified with consequences of external effects within component volume. Each damage process is a

collective process that is accompanied by a complex of effects with special cause-and-effect relations. Any damage process has a minimum number of dominant factors that are typically taken as a basis to assign a class to the process.

[0022] Identifying the nature and causes of MS component material failure is fundamental as this presents the following: a basis for a design model to assess the strength and lifetime; a criterion of correct choice of test methods and conditions; the initial information to validate diagnostic, prediction and improvement methods for MS.

[0023] In terms of endurance and reliability of MS, the damage mechanisms, kinetics and parameters should be studied not only to rationally select the component or structure material considering the manufacturing technique, but chiefly to set criteria of failures and limiting states, periodicity and control and diagnostic means, prediction methodology for technical conditions, reliability and safety. Metallophysicists and metallurgists use the term "material failure," while strength and reliability experts use "component material damage" or just "component damage," which is used herein.

[0024] The chemical activity of materials increases under stress and this increase is even greater under cyclic stresses. Because of this, strength and life investigations should not be limited to mechanical criteria only. Corrosion-mechanical damages, which cause MS components failure, are mainly responsible for equipment failures at chemical, petrochemical, oil-processing plants, power installations, and gas and oil pipelines. This equipment is designed for heat-mass-transfer processes and transportation of media which are primary for chemical, petrochemical and power technologies.

[0025] The material damage is described as a multi-stage, statistical and large-scale process due to various damage micromechanisms, statistical relationships of heat

fluctuations in time and simultaneous phenomena at nuclear, dislocation, substructural and structural levels. The use of purely mechanical criteria to assess the strength and life under combined action of loads and media does not ensure accuracy nor allow improving these criteria and affecting the damage process.

[0026] Based on the results of experimental investigations, tests and controlled service, the physicomechanical essence of some of the most common component material damage processes, which are as yet little understood, such as corrosion cracking (CC), hydrogen embrittlement (HE), corrosion fatigue (CF), mechanical fatigue (MF), etc. are addressed. The most important factors responsible for one or the other of degradation processes were detected and the damage parameters describing each process identified. Table 1 shows the classification of major factors comprising various damage mechanisms and defining damage processes and parameters. The damage processes caused by major factors may be implemented under various quantitative relations between factors, individual components of each factor and additional factors initiating and accelerating the process.

Table 1 - Classification of Major Parameters, Mechanisms and Processes of Material Damage

Damage Parameters	Damage Mechanism (combination of factors)	Damage Process
Field of oriented and single cracks	Contact interaction with external environment; tensile static or intermittent static stresses; material susceptible to a given external environment	Corrosion cracking
	Contact interaction with hydrogenous environment; tensile stresses; periodic abrupt temperature fluctuations; welding heat affected zones	Hydrogen embrittle-ment
Single crack	Interaction with active external environment; cyclic stresses; susceptible material	Corrosion fatigue
	Low-cycle and high-cycle stresses	Mechanical fatigue
Local corrosion damage of surface (pits, pitting)	Contact interaction with electrolytes, as well as in stagnant and slot zones; electrolytic potential; electrochemical heterogeneity of alloys; non-regular stressed-deformed state	Electro-chemical corrosion
General uniform or non-uniform dissolution of material	Contact interaction with electrolytes; pH of environment; surface passivation character; thermodynamically unstable material	Electro-chemical corrosion
Scaling; sublimation or dissolution of material	Contact interaction with high-temperature gases or non-electrolytes; environment pressure	Chemical corrosion
Surface relief change	Separate or combined action of moving gas, liquid, abrasive; velocity and temperature of environment; magnitude and hardness of abrasive, wear and heat resistance of material	Erosion
Micro-cracking, porosity at grain and sub-structure boundaries	Long exposure to high temperatures and tensile stresses	Creep

Change in mechanical and physical properties	High temperatures and pressure of hydrogenous environment; susceptible material	Hydrogen corrosion
Increase in hardness of surface layers; formation of residual stresses	High temperature and high pressure of nitrogen-containing environment; presence of nitride-forming elements in ferritic low-alloy steels	Nitride corrosion
Intensification of thermo-fluctuating processes and diffusion of impurity elements	Neutron spectrum and neutron irradiation intensity; high temperature; ferritic steels; impurities, especially copper and phosphorous	Radiation embrittlement

Table 2 shows the classification results of the most common and hazardous type of damage parameters that have substantial effect on MS life and characterized by cracking.

Table 2 – Cracking Parameters Intensification

Classification Parameter					
Crack front shape in fracture	Crack surface structure in fracture	Crack development path	Branching type	Type of failure at microcrack tip	Type of failure at macrocrack tip
Semi-circular; semi-elliptic; linear	One-focus; multi-focus	Intra-granular; inter-granular; combined	Strongly branching; weakly branching; non-branching	Dislocation type; growth and coalescence of pores; dislocation type and local corrosion	Chip; fracture; cut

[0027] Also known is Accelerated Aging of Materials and Structures: The Effects of Long-Term Elevated-Temperature Exposure, (National Materials Advisory Board of USA (NMAB), 1996), which addresses the issue of developing testing procedures for various materials used in the aircraft industry, which allow a reliable prediction of their degradation in service and the life of new aircraft components. To predict the response of a materials system to long-term exposure in an aircraft structure service environment, a fundamental understanding of the physical phenomena associated with damage and failure must be developed. This can only be established by experimental materials characterization and development of the associated mathematical and computational models that describe the physical phenomena. In many cases, testing standards and codes are available to provide guidance on specific types of component design and test methodology. However, for some advanced materials, e.g., composites, different approaches to materials testing may be required, and there may be a lack of standardized methods. Although the requirement for the same basic material properties may be similar, users often develop their own test methods. The different testing methodologies can lead to ambiguities in the test data, resulting in uncertainties in materials selection, design, and production.

[0028] The evaluation of long-term aging responses of materials and structures using accelerated testing and analytical methods is very difficult, especially for the complex conditions encountered in aircraft service. Even the best techniques will probably not yield completely satisfactory predictions of materials performance. However, because new aircraft will be designed, and materials and structures evaluated over their entire life cycle, it is important to develop testing and analysis methods that provide the best possible understanding of materials and structures

performance to support materials selection and structural design decisions. It is better to have incomplete data available in time to influence key program decisions than to wait for the completely rigorous data to be developed.

[0029] Concerns over these issues have led the National Aeronautics and Space Administration (NASA) to request the National Research Council's National Materials Advisory Board (NMAB) to identify issues related to the aging of advanced materials and suggest accelerated evaluation approaches and analytical methods to characterize the durability of future aircraft materials and structures throughout their service lives. A NMAB study committee was established to (1) provide an overview of long-term exposure effects on future high-performance aircraft structures and materials; (2) recommend improvements to analytical methods and approaches to accelerate laboratory testing and analytical techniques to characterize and predict material responses to likely aircraft operating environments; and (3) identify research needed to develop and verify the required testing, predictive analytical capabilities, and evaluation criteria.

[0030] The general degradation mechanisms, i.e., the physical event or chain of events that underlie observed degradation effects, that must be considered include:

- microstructural and compositional changes,
- time-dependent deformation and resultant damage accumulation,
- environmental attack and the accelerating effects of elevated temperature, and
- synergistic effects among the above.

[0031] Historically, the chief damage mechanisms for aluminum alloys in aircraft applications are corrosion and fatigue, mechanisms generally associated with an aging fleet. Potential damage mechanisms include microstructural changes, fatigue, creep, and environmental effects.

[0032] Determination of the most critical degradation mechanisms depends on what properties are important in a particular application. For example, if strength is critical, coarsening of the matrix precipitates during elevated-temperature service will be important; if toughness is critical, grain-boundary precipitation or the development of a precipitate-free zone will be important; and if creep or fatigue are critical, the nucleation, growth, and coalescence of microcracks will be important. Potential damage mechanisms associated with high-temperature applications of aluminum alloys include microstructural changes, fatigue, creep, and environmental effects.

[0033] Elevated-temperature exposure under applied stress can introduce a number of microstructural changes including coarsening of the matrix precipitates (important in strength-critical applications) and grain-boundary precipitation or the development of a precipitate-free zone (important in toughness-critical applications). Fatigue resistance is degraded by the nucleation, growth, and coalescence of voids or microcracks. High-cycle fatigue resistance is sensitive to the nucleation of microcracks at microstructural inhomogeneities, while fatigue crack growth thresholds are affected by the level of residual stresses and crack tip shielding produced by variations in microstructure. Creep resistance appears to improve with increasing grain size. Also, cold work reduces creep resistance in precipitation-strengthened and dispersion-strengthened aluminum alloys. Degradation mechanisms due to service environmental interactions that need to be considered for aluminum alloys include corrosion, stress corrosion cracking, hydrogen embrittlement, solid-metal embrittlement, and liquid-metal embrittlement.

[0034] Three interrelated problems associated with the complexity of fracture processes in titanium alloys, and the

possibility of time-temperature-hydrogen-dependent failure modes, could hinder development of high-strength and high-toughness titanium alloys for high-speed civil transport (HSCT) applications. These problems include the effects of microstructural variations on deformation and local fracture, uncertainties in intermediate temperature deformation behavior, and hydrogen embrittlement.

[0035] The three primary factors that need to be considered in long-term, elevated-temperature applications of high-strength and high-toughness titanium alloys for HSCT applications, include:

- the effect of microstructural variations (e.g., variations in beta grain size, alpha volume fraction, grain-boundary alpha formation, alpha morphology on aging, and metastable phases) should be developed, analogous to what has been developed for aluminum alloys,

- the effects of moderate service temperatures and loading rates on alloy behavior, including the possibility for dynamic strain aging, thermally activated slip localization, time-temperature effects on hydrogen embrittlement, and deformation and fracture behavior at cryogenic temperatures, and

- the degradation of tensile ductility and fracture toughness due to dissolved hydrogen from aggressive environments such as airplane hydraulic fluid.

[0036] Also known is High Temperature Degradation in Power Plants and Refineries, by Heloisa Cunha Furtado and Iain Le May (Mat. Res. vol. 7, no.1. São Carlos. Jan./Mar.,2004), which discloses the mechanisms of degradation at high temperature and methods of assessment of such damage and of the remaining safe life for operation. The principal deterioration mechanisms in high temperature plant are creep damage, microstructural degradation, high temperature fatigue, creep-fatigue, embrittlement, carburization, hydrogen damage,

graphitization, thermal shock, erosion, liquid metal embrittlement, and high temperature corrosion of various types. Additionally, stress corrosion cracking and aqueous corrosion may be problems although these damage mechanisms are not generally expected in high temperature components. However, they may occur when components are cooled down and liquid is still present within or in contact with them. Aspects of each will be considered in turn.

[0037] Creep is one of the most serious high temperature damage mechanisms. Creep involves time-dependent deformation. High temperature creep cracking generally develops in an intercrystalline manner in components of engineering importance that fail over an extended time and includes boiler superheater and other components operating at high temperature, petrochemical furnace and reactor vessel components and gas turbine blades. At higher temperatures, as can occur with local overheating, deformation may be localized, with large plastic strains and local wall thinning. At somewhat lower temperatures and under correspondingly higher stress levels, fracture can be transgranular in nature.

[0038] Microstructural degradation is a damage mechanism that can lead to failure by some other process such as creep, fatigue or more rapid fracture. Microstructure degradation is a mechanism of damage as it can result in a significant loss in strength in a material.

[0039] Fatigue, involving repeated stressing, can lead to failure at high temperature as it does at low temperature. In components operating at high temperature, fatigue often arises through temperature changes that can lead to cyclic thermal stresses, which can lead to thermal fatigue cracking. The cracking tends to develop in areas of high constraint, and the detailed mechanism may be one of local creep deformation.

[0040] Creep-fatigue interaction is a complex process of damage involving creep deformation and cyclic stress and the

predominant damage mode can range from primarily fatigue crack growth at higher frequencies and lower temperatures to primarily creep damage where hold times are long and temperature is at the high end of the scale.

[0041] Embrittlement from precipitation can arise in a number of different ways. For example, sigma phase formation in austenitic stainless steels maintained at high temperature or cycled through the critical temperature range (approximately 565 to 980°C) causes loss of ductility and embrittlement. Ferritic stainless steels may be subject to an embrittlement phenomenon when held at or cooled over the temperature range 550 to 400°C. If the temperature conditions are considered likely to lead to such effects, metallographic checks are advisable after extended exposure prior to an unexpected rupture developing. In addition to the embrittlement of ferritic steels exposed to high temperature during service, and of austenitic stainless steels through the formation of sigma phase, carburization can produce brittle material when a component is exposed to a carburizing atmosphere for extended time at high temperature.

[0042] Hydrogen damage, arising particularly in petrochemical plant, can occur in carbon steels through diffusion of atomic hydrogen into the metal, where it combines with the carbon in the Fe_3C to form methane and to eliminate the pearlite constituent. This is a special case of microstructural degradation, and is much less common today than in the past because of the use of low-alloy steels containing elements that stabilize carbides.

[0043] Graphitization can take place in ferritic steels after exposure to high temperature for extended time, owing to reversion of the cementite in the pearlite to the more stable graphite phase. It is a particular form of microstructural degradation that was formerly observed relatively frequently in petrochemical components. With the development of more

stable CrMo steels, it is not often seen today, but occurs from time to time both in petrochemical plants and in steam generators in which the temperature is high and the material is not entirely stable.

[0044] Thermal shock involves rapid temperature change producing a steep temperature gradient and consequently high stresses. Such loading can produce cracking, particularly if the shock loading is repetitive. Cracks generated in this manner progress by a process of thermal fatigue. Such conditions are not encountered in thermal generating plants and refineries under normal operating conditions, but may arise during emergencies or with an excursion in the operating conditions. Brittle materials are much more susceptible to thermal shock and ceramic components, as are becoming more common in advanced gas turbines for example, are susceptible to such damage.

[0045] Erosion can occur in high temperature components when there are particles present in flowing gases. This is a not uncommon situation in coal-fired power plants in which erosion by fly-ash can lead to tube thinning and failure in economizers and reheaters, and soot blower erosion can produce thinning in superheaters and reheaters in those tubes that are in the paths of the blowers. The solution to fly ash erosion depends in part on improving boiler flue gas distribution, and cutting down on local excessively high gas velocities. The control of soot blower erosion depends on many factors including excessive blowing pressure, poor maintenance and the provision of effective tube protection where required.

[0046] Liquid metal embrittlement (LME) can occur with a number of liquid-solid metal combinations, and one that can have serious consequences for the refining industry is LME of austenitic stainless steel by zinc. Rapid embrittlement can occur at temperatures above 750°C, and has been observed to produce widespread cracking in stainless steel components

after a fire when there is a source of Zn present such as galvanized steel structural parts, or when there is contamination from Zn-based paints. This latter source led to considerable cracking at the time of the Flixborough disaster (Flixborough, North Lincolnshire, England; 1974). Cracking can be extremely rapid (m/s) and stress levels can be as low as 20 MPa for such cracking to take place.

[0047] Minimization of corrosion in alloys for high temperature applications depends on the formation of a protective oxide scale. Alternatively, for alloys with very high strength properties at high temperature, a protective coating may need to be applied. The oxides that are generally used to provide protective layers are Cr_2O_3 and Al_2O_3. Corrosion protection usually breaks down through mechanical failure of the protective layer involving spalling of the oxide as a result of thermal cycling or from erosion or impact.

[0048] The above are not damage mechanisms that are normally associated with components operating at high temperature. However, when shutdown of a plant occurs, fluid may condense and there may be water containing contaminants within pipes or vessels in the plant. The corrosion or stress corrosion cracking that occurs at low temperature may lead to preferential damage at high temperature during later operation of the plant.

[0049] Also known is Interaction of Structural Defect and Degradation of Structural Material Properties, by G.A. Filippov and O.V. Livanova (All-Russian Conference Structural Defects and Crystal Strength, Chernogolovka 2002), which discloses that degradation of pipe metal properties after prolonged service is manifested by reduced resistance to brittle fracture, including brittle delayed fracture, and results from strain aging of steel. The effect of pipeline prolonged service on the mechanical properties and crack

resistance and suggests the aging mechanism of pipe steels is also addressed. Investigations were carried out on pipe specimens of 19 main pipelines operated in various climatic conditions. The basic statistical analysis was conducted on 17MnSi type steel that represented up to 80% of all pipes. In order to evaluate the mechanical properties, specimens were taken from operating pipelines, emergency reels and emergency stock. The useful life was between 4 and 44 years. The metal used in current production of Orsko-Khalilovsk metallurgical works and pipes from emergency stock were taken as the initial condition.

[0050] The standard mechanical properties such as tensile strength, σ_{TS}, yield strength, σ_{YS}, elongation, δ, and reduction of area, ψ, do not virtually vary with service (see Table 3). Within scatter limits, experimental data are close to standards (σ_{TS} - at least 520 MPa; δ - at least 24%). In order to reveal the properties susceptible to structural changes, other tests are needed, including those on sharp stress raiser specimens and precracked specimens; crack nucleation and propagation should also be evaluated.

[0051] On testing pipes using sharp notch specimens (see Table 3), the impact strength was found to decrease. After 20-25 years of service, KCV (impact strength) value at +20°C (KCV^{+20}) dropped from 55-70 to 30-50 J/cm^2. Impact tests within the temperature range between -40 and +20°C showed that as the life increases, the critical temperature of pipe metal transformation into a brittle state (T_{50}) shifts to higher temperatures (See FIGURE 1). After 25-35 years of service, the temperature cold-shortness threshold passes into an above-zero temperature area. As pipes reach about 25 years of service, all values, characterizing pipe metal breaking strength, decrease as evidenced by the sharp notch static bending test. The plasticity is reduced about 1.5 times.

After 25 years of service, the total fracture energy of pipe metal, A_{Σ}, is reduced almost by half, chiefly due to reduction in crack nucleation work, A_n (see Table 3). The crack propagation work, A_p, is reduced to a lesser extent. Hence, the change in structural change of pipe metal during prolonged service has the greatest effect on crack nucleation work.

[0052] FIGURE 1 shows the effect of life on the brittle state (T_{50}) transformation temperature for pipe metal of steel 17MnSi (sign ↑ means that there are cases of brittle state transfer at above +20°C).

[0053] The critical crack opening, COD, reflecting the limiting deformation of crack initiation, are reduced dramatically after 20-25 years of service - about 1.5 times. This indicates that steel susceptibility to stress concentration increases, i.e., stress concentrations on pipe surface (scratches, scuffing, indents, etc.), which were not initially very hazardous, can become critical after prolonged service because of a structural state change in pipe metal.

[0054] Thus, during long service the pipe metal undergoes changes in structural state that results in reduction of the brittle fracture resistance. It may be suggested that this happens due to increase in microplastic deformation resistance and higher local microstresses under load.

Table 3 - Degradation of Mechanical Properties of Pipe Steel of 17MnSi Type during Prolonged Service

Life, years	σ_{TS}, MPa	σ_{YS}, MPa	δ, %	ψ, %	A_n, J/cm^2	A_p, J/cm^2	KCV^{-40}, J/cm^2	KCV^{+20} J/cm^2
0	594	411	27	59	14.7	28	53	57
20-25	584	419	27	58	14.4	29	51	55
30-44	572	407	26	56	11.5	23	47	46

[0055] The change in structural state of pipe metal may result from the process of defect accumulation due to stress effects, corrosion environment and hydrogen. Corrosion

processes change surface condition of pipe metal, saturating metal with hydrogen, which entails formation of internal microcrack-like defects. The process of accumulation of microcrack-like defects and fracture under static or quasistatic stress, which is lower than the ultimate fracture stress and yield stress of steel, is commonly termed the delayed fracture. The delayed fracture is the cause of the premature brittle fracture of critical high-strength steel details exposed to corrosion environment, for example, tighten bolts, strained reinforcing wire, etc.

[0056] Delayed fracture tests were carried out in accordance with a specially developed procedure under simultaneous exposure to stresses, corrosion environment and hydrogen. The delayed fracture has three phases: incubation period (crack nucleation phase), slow growth of a stable crack and quick fracture. To assess the reliable operation of a pipeline under conditions of a possible contact with corrosive environment, the most important assessment is to find the resistance to crack nucleation and propagation (not quick as in shock testing, but slow), which is why the level of impact strength does not reflect the crack formation resistance for pipes.

[0057] FIGURE 2 shows the relationship between time to fracture, t_f, and initial stress intensity coefficient, K_i, for pipes of steel 17MnSi: 1 - as-manufactured; 2 - working pipe; 3 - emergency pipe. The prolonged service affects the inclination of pipe metal to delayed fracture, moving the K_i-versus-t_f curve to the region of lower time to fracture. Thus, given the same K_i, the time to fracture for as-manufactured pipes is much greater than that for working and emergency pipes as shown in FIGURE 2.

[0058] The stable crack propagation rate also depends on lifetime. The metal of as-manufactured pipes has the lowest stable crack propagation rate of (1-3) x 10^{-4} mm/min. The

longer the service life of pipes, the higher the stable crack propagation rate that approaches about 80 x 10^{-4} mm/min.

[0059] In order to find out why the pipe metal brittle fracture resistance decreases under prolonged service conditions, the strain aging test was carried out. During prolonged service, the change in structural state of pipe metal affects the fracture resistance under the most severe conditions (sharp stress raiser or low temperatures) and apparently this is associated with strain aging processes. Hence, it is important that this process be studied to understand the mechanism of a fracture resistance change.

[0060] Strain aging of iron and low-carbon steels is observed only when a solid solution contains carbon and nitrogen atoms of certain concentration. Strain aging results in improved tensile strength, yield strength, hardness; a yield plateau on SN curve; increased critical brittle temperature in shock tests; and lower plasticity. The tendency to strain aging is an important property of metals.

[0061] To assess the above-mentioned metal property, specimens were subjected to tension at the yield portion (2%), held for one hour at 200°C and tensile tested. The tendency to strain aging, $\Delta\sigma_s$, was found by the yield strength growth upon termination of active deformation ($\Delta\sigma_s = \sigma_s - \sigma_{2\%}$). The higher $\Delta\sigma_s$, the greater the tendency to strain aging. In addition, the plasticity was evaluated by the reduction of area, ψ_s, of pipe metal in aged condition.

[0062] From FIGURE 3 follows that during prolonged service the tendency of steel to strain aging is reduced, i.e., the smaller growth of the yield strength, $\Delta\sigma_5$, and reduction of area in aged condition. This is the most intensive during the first 15-30 years of service. The effect of service on the

tendency to deformation aging, $\Delta\sigma_s$, is shown in FIGURE 3 and the reduction of area of aged pipes, ψ_s, is shown in FIGURE 4.

[0063] It is common knowledge that the tendency of iron and steel to strain aging depends on the content of impurities (carbon and nitrogen) in solid solution in a free condition, i.e., not bonded with dislocations. To study the aging mechanism of pipe metal under long service conditions, an internal friction measurement method was used as the most sensible to local changes in structural condition of steel.

[0064] The carbon and nitrogen content in solid solution was judged from the results of measuring the internal friction temperature dependence (IFTD). It is well known that the IFTD curve for steel, containing free carbon and nitrogen, has a Snoek maximum near 40°C caused by the movement of free interstitial atoms in the stress field. The more free carbon and nitrogen atoms in solid solution, the greater the Snoek maximum.

[0065] The IFTD curves for specimens cut out from pipes after long service of 30 years have two maximums at 60 and 200-220°C, as shown in FIGURES 5 and 6. The temperature dependence of internal friction, Q^{-1}, of pipe metal of 17MnSi steel after prolonged service of 30 years is shown in FIGURE 5 and in emergency stock is shown in FIGURE 6. In the case of IFTD curves for specimens cut out from emergency stock pipes, the maximum at 60°C is higher. The Snoek maximum in IFTD curves in known to be observed when interstitial impurity content is greater than $2\text{-}10^{-4}$%. Hence, it may be concluded that the carbon and nitrogen content in solid solution of the pipes, being in service for 30 years, approximates 2×10^{-4}%, i.e., under pipeline conditions the carbon and nitrogen content in a free solid solution tends to decrease. Under pipeline conditions, the carbon and nitrogen content decreases during pipe service due to plastic deformation that results in

fresh dislocations being fixed by carbon and nitrogen atoms, forming so-called "atmospheres" of impurity atoms on dislocations and reducing the mobility thereof. The tendency of developing deformation aging under pipeline conditions is also evidenced by the increase in IFTD curve maximum at 200-250°C which is observed only when the metal is subject to plastic deformation and subsequent aging.

[0066] Thus, during service, the pipes undergo pressure and temperature differences, as well as dynamic and static loads. The pipe service conditions make possible deformation aging in metal, resulting in increased dislocation movement resistance and increased hazard of local stress "peaks" in the metal. Because of this, the local stress relaxation in the notch or crack apex is reduced, increasing the steel tendency to brittle fracture. In order to decrease the hazard of brittle fracture of the pipelines, being in service for more than 20 years, especially at low temperatures in winter time after shutdown of a pipeline, during activation of pumping stations, one should take account of increased cold brittleness of the pipe metal caused by deformation aging.

[0067] Accordingly, the following conclusions were determined:

1. In order to assess the condition of main pipelines, the knowledge of the conventional mechanical properties is insufficient. The reliability assessment criteria should include the properties susceptible to local structural changes, for example, those obtained by delayed fracture tests and tests on cracked or sharp notched specimens at low temperatures.

2. All fracture resistance properties of the metal decrease after sharp notch bending tests were carried out on specimens after 25 years of service. The tendency of steel to delayed fracture, under simultaneous action of stresses,

corrosive environment and hydrogen, was found to be especially susceptible to structural changes.

3. During prolonged service, the pipe metal properties degrade because of deformation aging, the mechanism of which lies in reduction of the concentration of free carbon and nitrogen atoms and reduction in dislocation mobility.

[0068] Also known is Environmental Degradation of Metals (Corrosion Technology), by U.K. Chatterjee, S.K. Bose, S.K. Roy (Marcel Dekker, 2001), which discloses all types of environmental degradation a metallic component may undergo during its processing, storage, and service. Coverage includes fundamentals, forms, and prevention of such types of degradation as aqueous corrosion, tarnishing and scaling processes, alloy oxidation, liquid metal attack, hydrogen damage, and radiation damage.

[0069] Clarifying general and localized corrosion effects, the effects of atmospheric exposure, high-temperature gases, soil, water, weak and strong chemicals, liquid metals and nuclear radiation are disclosed. This disclosure also shows how improvements in component design can reduce corrosion; details of the high- and low-temperature effects of oxidizing agents, such as oxygen, sulfur and water vapor, the halogens and CO_2; investigates the instantaneous and delayed failure of solid metal in contact with liquid metal; highlights the influence of hydrogen on metal, including the loss of ductility and internal flaking, blistering, fissuring and cracking; profiles radiation effects on metal, such as irradiation growth, void swelling, and embrittlement and more.

[0070] In addition, the disclosure covers the following subjects: types and prevention of aqueous corrosion, tarnishing and scaling processes (thermodynamic aspects of metal-oxidant system; kinetic aspects and rate equations; defect chemistry of oxides and other inorganic compounds; mechanisms of tarnishing and scaling processes; scale growth

by lattice and grain boundary diffusion; formation of voids, porosities and other macrodefects in oxide scale and in the substrate; development of stresses and strains in the growing scales; dissolution and diffusion of oxidant in metals; effect of metal surface preparation and pretreatment), alloy oxidation, liquid metal attach, and hydrogen damage.

[0071] Also known is Accelerated Degradation, by Brigitte Battat (AMPTIAC, Rome, NY 2001), which discloses a brief description of materials degradation, and the methodology for accelerated degradation. Testing through accelerated degradation or aging measures product performance as a function of time, at overstress conditions.

[0072] Characterization of materials aging or degradation is difficult due to the inability to simulate service environment in the laboratory. Cyclic or changing loads, temperature, radiation, humidity, and other effects influencing environments, are interactive and impossible to reproduce, especially in the case of aircraft service. Nevertheless, new component designs are based on materials and structures that have been evaluated over an entire life cycle, so testing methodology and analysis can and must be generated for new designs.

[0073] Table 4 (based on a compilation of data from Nelson's book on acceleration testing (see Nelson, W., Accelerated Testing: Statistical Models, Test Plans and Data Analyses, Wiley Series in Probability and Mathematical Statistics, 1990, p.11-49)) provides a breakdown of the degradation mechanisms, the materials they affect, the accelerated stress factors used, and the measured properties that gauge the response. For example, fatigue occurs in metals, plastics, etc, and accelerated stress factors can be temperature, load, or chemical reactions. The measured properties are residual life and cumulative damage effect. This information helps to generate models that can be

extrapolated to determine residual life. As such, this is different from accelerated life testing which spans the full extent of the material or component life.

Table 4: Degradation Mechanisms, Materials and Definition of Failure

Degradation mechanisms	Material	Accelerated stress	Measured properties
Fatigue	Metals, plastics, glass, ceramics, composites	Load, temperature, chemicals (wage, hydrogen, oxygen)	Residual life, residual strength, cumulative damage
Corrosion/ oxidation	Metals, food & drugs	Concentration of the chemicals, activators, temperature, voltage, mechanical load (stress-corrosion)	Probabilistic degradation model based on physical mechanism
Creep	Metals, plastics	Temperature and mechanical load, load cycling, chemical contaminants (e.g., water, hydrogen, fluorine)	Plastic deformation under constant load
Cracking	Metals, plastics, glass, ceramics, composites	Mechanical stress, temperature, chemicals (humidity, hydrogen, alkalis, acids)	Degradation testing for stability & shelf life
Wear	Rubber, polymers, metals	Speed, load (magnitude, type), temperature, lubrication, chemicals (humidity)	Degradation testing of mechanical properties
Weathering	Metals, protective coating (e.g., paint, electro-plating, anodizing), plastics, rubbers	Solar radiation (wavelength and intensity), chemicals (humidity, salt, sulfur, ozone)	Corrosion, oxidation tarnishing, chemical reaction

[0074] Accelerated aging implies accelerated exposure to generate end-of-life microstructure or damage states for subsequent characterization tests. For example, the coarsening of metal alloy microstructure can accelerate exposure by lowering the strength and toughness of the material. When multiple damage mechanisms (e.g., thermomechanical fatigue) are involved, both accelerated aging and accelerated life testing may be required for validation. Accelerated aging can be achieved by: (1) increasing temperature and load; (2) damaging the product before performing the test; (3) increasing the number of hold times between exposures; and (4) increasing the concentration of the chemical agent causing degradation.

[0075] Accelerated degradation tests compared to accelerated life tests have the advantage of analyzing performance before the material or the component fails. Degradation tests determine how much life there is left in a material or in components, and such knowledge enables life extension. Extrapolating performance degradation to estimate when it reaches failure level enables analysis of degradation data. However, such analysis is correct only if a good model for extrapolation of performance degradation and a suitable performance failure have been established.

[0076] Accelerated aging for cases where multiple degradation mechanisms are involved, should be performed in series: the sample should be exposed incrementally to conditions that bring about the degradation mechanisms one at a time, until the end-of-life condition is reached.

[0077] Aging of commercial and military aircraft is a large concern to the U.S. Department of Defense, NASA, and the Federal Aviation Administration. These agencies all conduct monitoring of aging problems such as corrosion and fatigue. Due to their exposure to severe environments, candidate materials for advanced subsonic aircraft and supersonic

applications are of special interest, including airframe materials like aluminum alloys, aluminum-matrix composites, titanium alloys, and polymer-matrix composites. Among materials being used for supersonic engines are nickel-based superalloys and ceramic-matrix composites. Due to their extensive use, aluminum alloys have a large database of information.

[0078] Degradation mechanisms for aluminum alloys include: microstructural and compositional changes; time-dependent deformation and resultant damage accumulation Environmental attack and the accelerated effects of elevated temperature; and synergistic effects of the above mechanisms. Damage mechanisms associated with high-temperature applications of aluminum alloys (e.g., microstructural changes, fatigue, creep, environmental effects) are illustrated in FIGURE 7.

[0079] Knowledge of component life expectancy is needed from the outset, at time t = 0. Depending on the particular case, life may be of the order of millions of cycles, or several years. Life depends on degradation processes, such as corrosion, fatigue, creep, etc. Certain components, such as aircraft parts, are made for the life of the system, while others, subject to fatigue, have a much tighter life schedule. The object of accelerated testing is to determine the life for the dominant failure mode under normal operating conditions, using information and testing obtained from stressed operating conditions. To achieve this, a mechanistic understanding of the failure mode is needed. In the case of accelerated degradation, temperature, load and duty cycle determine the life models that predict failure modes. Life testing may be accelerated by increasing the temperature, or by increasing load and duty cycle, or by using a combination of all effects. Under stressed conditions, the model predicts failure within a few hours (or minutes). Once verified, the same model is used to predict the life under nominal conditions of operation.

[0080] At the early design stage of a component or a device, when hardware details have not been selected and materials choice has not been finalized, the preoccupation is to make the system "work." The next concern is with the optimization of performance, meaning how to make the system yield better results. The next step is identifying directions for product improvements to meet the specification.

[0081] Life on the other hand, relates to failure modes and to the maintenance of performance and robustness over the lifetime of the item, as prescribed by the specification. Failures can occur due to shortfall of performance, or due to hard and catastrophic breakdown, that necessitate replacement. In this connection, accelerated testing may be used to determine and extend life, but it may also be employed to identify directions for performance improvement.

[0082] Accordingly, accelerated testing is a methodology for predicting future material and component performance from testing procedures performed in the present time. This is obtained by using a test environment more severe than that experienced in the normal use environment.

[0083] Also known is Degradation of Metals in the Atmosphere, (ASTM Special Technical Publication// Stp) edited by Dean, Lee, 1988 papers from a symposium held in Philadelphia, PA., May 1986, which provides access to technical data from recent tests, long-term test programs, and field experience, including data on new materials of construction.

[0084] Also known is Environment Assisted Degradation Mechanisms in Aluminum-Lithium Alloys, by Gangloff, R.P.; Stoner, G.E.; Swanson, R.E. (Univ. of Virginia, Charlottesville School of Engineering and Applied Science, 1988), which provides an overview of the need for research on the mechanisms of environmental-mechanical degradation of advanced aerospace alloys based on aluminum and lithium.

Progress is reported on three tasks targeted at characterizing aqueous and gaseous environment corrosion fatigue crack propagation kinetics, microstructural paths and damage mechanisms for alloy 2090. A study is summarized with the goal of isolating and measuring localized processes which are hypothesized to control corrosion and embrittlement of aluminum-lithium alloys.

[0085] Also known is Atmospheric Exposure of Nonferrous Metals and Alloys - Aluminum: Seven-Year Data, by McGeary, F.L.; Summerson, T.J.; Ailor, W.H. (Metal Corrosion in the Atmosphere - 70th Annual Meeting, ASTM-STP-435, 1967, pp. 141-174), which discloses the results of weathering tests on 34 wrought aluminum alloys exposed seven years at four ASTM sites in the United States. Also, included, for comparison, are data on three additional aluminum alloys exposed six years at five sites in England. The British industrial atmosphere exposures at Sheffield and London were found to produce the most corrosion, particularly on the sheltered sides of these panels which were exposed at an angle of 30 degrees from the horizontal. The self-limiting corrosion characteristics were observed on weather surfaces at all test sites in both countries. The test will be continued and again reported after twenty years, as was the case in a previous ASTM B-3 test (ASTM-STP-175) on older aluminum alloys.

[0086] Also known is Environment Assisted Degradation Mechanisms in Advanced Light Metals, by Gangloff, R.P.; Stoner, G.E.; Swanson, R.E. (Univ. of Virginia, Charlottesville School of Engineering and Applied Science. 1989), which discloses the research program, the general goal of which is to characterize alloy behavior quantitatively and to develop predictive mechanisms for environmental failure modes. The current projects include: damage localization mechanisms in aqueous chloride corrosion fatigue of aluminum-lithium alloys; measurements and mechanisms of localized

aqueous corrosion in aluminum-lithium alloys; an investigation of the localized corrosion and stress corrosion cracking behavior of alloy 2090; deformation and fracture of aluminum-lithium alloys - the effect of dissolved hydrogen and the effect of cryogenic temperatures; and elevated temperature crack growth in advanced powder metallurgy aluminum alloys.

[0087] Also known is Microstructural Degradation of Plain and Platinum Aluminide Coatings on Superalloy CM247 During Isothermal Oxidation, by D.K. Das, Manish Roy, Vakil Singh, and S.V. Joshi, "Material Science and Technology", October 1999, Vol. 15, No. 10, pp. 1199-1208(10)), which discloses the experiment, involving isothermal oxidation at 1100°C of a high activity plain aluminide coating and a platinum aluminide coating, developed by the pack cementation technique, on cast nickel base superalloy CM247 with the primary objective of systematically understanding the coating degradation process during oxidation. While the weight gains during oxidation for both plain aluminide and platinum aluminide coatings follow parabolic kinetics from the very beginning of oxidation exposure, the bare alloy was seen to exhibit a considerably long initial transient oxidation period (~20 h), beyond which the parabolic law was followed. The parabolic rate constant for the platinum aluminide coating was found to be nearly two orders of magnitude lower than that for the plain aluminide coating. Alumina was identified as the only oxide phase that formed on both plain aluminide and platinum aluminide coatings during most of the oxidation exposure, although $NiAl_2O_4$ was also found in the case of the plain aluminide coating beyond ~200 h. The oxide layer on the bare alloy, however, was found to consist of Al_2O_3, Cr_2O_3, and $NiAl_2O_4$. The microstructural degradation of both the plain aluminide and platinum aluminide coatings during oxidation was seen to occur in three distinct stages which, however, differed for each coating. This

stagewise degradation, which involves final obliteration of the interdiffusion layer in each case, is disclosed therein in detail.

[0088] Also known is Oxidation-Induced Degradation of Coatings on High Temperature Materials: An Overview, by Jedlinskia, Jerzy, (Proceedings Symp. Elevated Temp Coatings: SCI & TECH, 1994, Vol. 1, pp. 75-83), which discloses that interaction between an aggressive environment and coated materials leads to the accelerated degradation of the latter. An understanding of the mechanisms of degradation plays a crucial role in the design of materials with improved service properties. The state-of-the-art in the field of coatings development for high temperature applications in oxidizing atmospheres is also disclosed. Deposition procedures and degradation mechanisms of the major types of coatings, as well as the routes used to improve the coating oxidation resistance, and the current problems relevant to the protection of Ti-based alloys and C/C composites are also disclosed.

[0089] Also known is Corrosion and Environmental Degradation, by Schtze, Michael; Editor: Robert W. Cahn; Peter Haasen (2000), which provides a sound and broad survey on the whole subject - from the fundamentals to the latest research results. Written by a team of international top experts it will become an indispensable reference for any materials scientist, physicist or chemist involved in corrosion science. Corrosion and corrosion protection is one of most important topics in applied materials science. Corrosion science is not only important from an economic point of view, but, due to its interdisciplinary nature combining metallurgy, materials physics and electrochemistry, it is also of high scientific interest. Nowadays corrosion science even gets new impetus from surface science and polymer chemistry.

[0090] Also known is Environmental Degradation of Materials and Corrosion Control in Metals, edited by M. Elboujdaini, E. Ghali (1999), which includes papers authored by specialists around the world and summarizes the recent progress in the field of corrosion and performance of aluminum alloys, magnesium alloys and steels. Inhibitions of metals and stress corrosion cracking are treated profoundly, as well as recent technologies in corrosion monitoring, coating application and testing. The detailed topics include: Corrosion Behavior of Aluminum Alloys, Inhibition and Protection of Aluminum and Magnesium Alloys; Inhibition and Protection of Metals in Process Industries; Assisted Cracking of Steels: Stress Corrosion Cracking, Corrosion Fatigue, and Hydrogen Damage; Electrochemical and Monitoring Techniques; Durability of Materials: Coatings and their Performance.

[0091] Also known is Role of Microstructural Degradation in the Heat-Affected Zone of 2.25Cr-1Mo Steel Weldments on Subscale Features during Steam Oxidation and Their Role in Weld Failures, by R.K. Singh Rama (Metallurgical and Materials Transactions, Volume 29A, No. 2, February 1998), which provides characterization of the microstructural degradation in the base metal adjacent to the weld pool, i.e., the heat-affected zone (HAZ), caused during welding of 2.25Cr-1Mo steel by electron and optical microscopy of different regions of the weldments. In order to study the influence of the microstructural degradations on scaling kinetics in steam and the resulting subscale features, samples of the base metal, the HAZ, and weld metal specimens were extracted from the weldment and oxidized in an environment of 35 pct steam 1 nitrogen at 873 K for 10 hours. Oxide scales formed in the three regions and the underlying subscales were characterized using scanning electron microscopy (SEM) and electron probe microanalysis (EPMA). Influence of the "free" chromium content in the three weldment regions on protective scale

formation and on the subscale features has been investigated. As the principal achievement, this study has clearly shown the occurrence of oxidation-induced void formation in the subscale zone and grain boundary cavitation in the neighboring area during steam oxidation of the HAZ. The possible role of oxidation-induced void formation and grain boundary cavitation in the inferior service life of welds in 2.25Cr-1Mo steel components is also disclosed.

[0092] Also known is Basic Types of Materials Corrosion That Designers Must Be Able to Competently Address, by Desi J. Kiss, M.S., P.E. (DJK Engineering, LLC, published at the Internet site http://djkeng.tripod.com/id3.html), which discloses that all materials that can be formed into usable implements, structures and conveyances are subject to corrosion. The various forms of corrosion can impact any material. Most of the materials that are used to carry or withstand heavy loads are either metal or metal containing, i.e., steel reinforced concrete. The eight forms of corrosion include: stress-corrosion cracking, erosion-corrosion, crevice corrosion, galvanic corrosion, intergranular attack corrosion, uniform attack, pitting, and selective leaching. Corrosion of stainless steels, corrosion of plastics, composites and ceramics, corrosion control and prevention is also disclosed.

[0093] Also known is Microstructural Changes in Austenitic Stainless Steels During Long-Term Aging, by Y. Minami, H. Kimura, Y. Ihara (Mater. Sci. Techn., 2:795-806, 1986), which discloses the study of the microstructural changes, precipitation behavior, and mechanical properties of typical austenitic stainless steels (304 h, 316 h, 321 h, 347 h, and tempaloy a-1) after long-term aging. The steels were aged statically in the temperature range 600-800°C for up to 50,000 hours. The microstructural changes were observed by optical

and transmission electron microscopy, and the extracted residue was identified using X-ray analysis. Time-temperature precipitation diagrams were made for each steel. The amount of sigma-phase was measured in samples aged at 700°C. The hardness and impact-value changes, and the tensile properties of aged samples were measured.

[0094] Also known is Decrease of Ductility in Al-10 PCT Mg Alloys During Long-Term Natural Aging, by Y. Kojima; T. Takahashi; and M. Kubo (1981), which provides the investigation of the changes in mechanical properties of Al-10pct Mg casting alloys during natural aging up to about L3 years. An elongation of more than 20pct in specimens naturally aged for less than 3 months fell to only 1 to 2 pct due to natural aging over ten years. By reversion experiments and electron microscopy, it was shown that this large decrease in ductility was caused by the formation of spherical coherent GP zones during the process of natural aging. Transmission electron microscopy (TEM) investigations also indicated that the structure of GP zone appears to be the L1 (sub 2) structure, in which Al and Mg atoms alternately align in three-dimensional periodicity along the (100) direction.

[0095] Also known is Degradation Due to Creep Deformation of 1CR-1MO-1/4V Steel at 550°C, by K. Kimura; T. Kisanuki; S. Komatsu (Journal of the Iron and Steel Institute of Japan, 1985, Vol. 71, No. 15, pp. 1803-1810), which describes the study of microstructural changes and the degradation of creep resistance due to creep damage on 1CR-1MO-1/4V steel crept for a duration of 9500 hours at 550°C. In particular, the effect of grain boundary void on the creep resistance has been examined on the creep damaged specimens, with and without a reheat treatment. Metallographic observations have shown three types of microstructural changes with creep deformation: coarsening of the carbide that usually occurs during

tempering, formation of voids and cracks, and remarkable recovery in the vicinity of prior austenite grain boundaries. The extent of carbide coarsening is slight even in the accelerating creep stage, and the effect of voids on the creep resistance is negligibly small. Progressive loss of the creep resistance is shown to be closely associated with the local recovery in the vicinity of prior austenite grain boundaries.

[0096] Also known is Role of Microstructural Instability in Long Time Creep Life Prediction, by J.W. Jones, S.F. Claeys (Pentagon Report D026031, 1984), which describes the influence of microstructural instability on long time creep life prediction using Al alloy 6061 as a model material. The effect of microstructural changes on lifetime during long time creep was determined by measuring the influence of microstructural degradation on steady state creep rate through the use of accelerated aging and short time creep tests. At intermediate stresses at 260°C and 288°C the creep life was strongly influenced by the rate of microstructural degradation and method proposed by other workers are effective in predicting creep life. At low stresses, creep lives for times approaching 100,000 hours are adequately predicted by performing short time creep tests on fully overaged specimens and using simple extrapolation techniques. The results indicate that knowledge of the aging response of alloys can be used to predict long time creep lives with reasonable accuracy.

[0097] Also known is Fatigue and Damage Tolerance Behaviour of Corroded 2024 T351 Aircraft Aluminum Alloy, by Al.Th. Kermanidis, P.V. Petroyiannis and Sp.G. Pantelakis, (Theoretical and Applied Fracture Mechanics, Volume 43, Issue 1, March 1, 2005, pp. 121-132), which describes the fatigue and damage tolerance behaviour of corroded aluminium 2024 T351 alloy specimens and comparison against the behaviour of the

uncorroded material. An experimental investigation was performed on specimens pre-corroded in exfoliation corrosion environment and included the derivation of S-N and fatigue crack growth curves, as well as measurements of fracture toughness. The fatigue crack growth tests were performed for different stress ratios R. All mechanical tests were repeated under same conditions for uncorroded specimens to obtain reference material behaviour. For the corroded material an appreciable decrease on fatigue resistance and damage tolerance was obtained. The results of the experimental investigation were discussed under the viewpoint of corrosion and corrosion-induced hydrogen embrittlement of the 2024 aluminum alloy. The need to account for the influence of pre-existing corrosion on the material's properties in fatigue and damage tolerance analyses of components involving corroded areas was demonstrated.

[0098] Aluminum aircraft structures are susceptible to corrosion and fatigue damage, which interact mainly at structural joints. Interactions between corrosion and fatigue may represent a serious threat for the structural integrity of the aircraft, especially as the aircrafts become older. Present day considerations of the corrosion induced structural degradation relate the presence of corrosion with a decrease of the load bearing capacity of the corroded structural member, as well as with the onset of fatigue cracks. In corrosion-pitting damage has been quantified and related to the decrease in fatigue life of 2024-T3 specimens corroded in alternate immersion corrosion process. In the effect of corrosion on multisite damage scenarios and aircraft structural integrity is considered such as to account for the onset of Multiple Site Damage (MSD) from corrosion pits. On the other hand, it was found that there is no significant effect of prior exfoliation corrosion on the fatigue crack growth rate of 2024-T351 specimens.

[0099] Corrosion attack of aluminum alloys has been classically attributed to the complex processes of oxidation. Yet, recent investigations performed on a series of aircraft alloys have provided evidence that corrosion is not limited to the well known surface damage process, which affects yield strength and fatigue life through the occurrence of corrosion notches, but it is also the cause for a diffusion controlled material hydrogen embrittlement.

[00100] For the Mg containing 6xxx series, additionally to the oxidation processes, hydrogen produced during the corrosion process may diffuse in the material and lead to hydrogen-metal interaction. Recent investigations have shown that corrosion may result to hydrogen embrittlement of the 2xxx, 7xxx and 8xxx aluminum alloy series as well. Although the mechanisms of the hydrogen embrittlement process are not yet sufficiently understood, different possible hydrogen trapping sites were identified which depend on the alloy system. This hydrogen embrittlement phenomenon is reflected into an appreciable reduction of tensile ductility of the corroded material areas. The obtained macroscopic hydrogen embrittlement is explained through a hydrogen induced local microplasticity. The process is formulated using the dislocation theory. Notice that, as both, corrosion and hydrogen embrittlement damage, are diffusion controlled processes, mentioned degradation of the material's mechanical performance is expected to occur locally. However, at present, there are no experimental data nor an established experimental nor theoretical methodology for assessing the values of the local material properties of the corroded areas of the material. Notice that the experimental investigations on the interaction of corrosion and fatigue usually refer to fatigue and fatigue crack growth tests which are performed in a certain corrosive environment and not to tests performed on precorroded material whereby, the latter represent a different

and, for a series of practical cases in older airplanes, more relevant situation.

[00101] The fatigue and damage tolerance behaviour of pre-corroded aluminum 2024 T351 alloy specimens have been investigated and discussed under the viewpoint of a synergistic effect of corrosion and corrosion-induced hydrogen embrittlement. The performed experiments included fatigue tests to obtain S-N curves, fatigue crack growth tests and fracture toughness tests. The fatigue crack growth tests were performed for different values of the stress ratio R. For comparison, all experiments were carried out also for the uncorroded material. The results have demonstrated the essential effect of existing corrosion on the fatigue and damage tolerance behaviour of the 2024 alloy as well as the need to account for the effect of corrosion on the mechanical properties in fatigue and damage tolerance analyses of the corroded areas of a structure.

[00102] A series of measurements of pitting density and the dimensions of pits for Al 2024 T351 subjected to exfoliation corrosion solution for 36 hours has shown an average pitting diameter of 2.586×10^{-3} mm and a pitting density of 920 samples per $100mm^2$. The measurements were made using the stereoscopic image analysis. Metallographic corrosion characterization has shown that for 36 hours of exposure to exfoliation corrosion, some intergranular corrosion may be expected as well. The presence of essential corrosion pitting and intergranular corrosion facilitates essentially the onset of fatigue cracks and, hence, reduces the fatigue life of the corroded specimens appreciably. As expected, the decrease on the fatigue life of the corroded specimens increases with the decrease of fatigue stress. The fatigue endurance limit drops from 175 MPa for the uncorroded material to 95 MPa for the pre-corroded specimens. Fitting curves for both, uncorroded and corroded material were derived using regression analysis.

[00103] In all cases investigated, with increasing crack length the fatigue crack growth resistance of the corroded specimens seems to degrade much faster than the fatigue crack growth resistance of the uncorroded specimens. It is reflected into appreciably lower fatigue life, significantly earlier entrance to the region of accelerated crack growth and steeper curves at this stage for the corroded specimens. The crack length at 3 seconds before failure, which is considered to represent a crack length measurement before the specimen failure which is still confident, is also smaller for the corroded specimens.

[00104] Crack growth may be interpreted to occur incrementally and to correspond to the failure of material elements ahead of an existing crack after a certain number of low cycle fatigue. By assuming corrosion induced embrittlement of the material, the fracture toughness value of the corroded material will be lower. The fracture toughness reduction of the corroded material was confirmed by fracture toughness measurements which will be discussed in a following paragraph. The above considerations may explain the higher crack growth rates and the steeper crack growth increase at the stage of accelerated crack growth. The reduced fracture toughness values for the corroded material explain the reduced crack length at failure and, with regard also to the higher crack growth rates at the stage of accelerated crack growth rate, the reduced fatigue lives for the corroded specimens.

[00105] The effect of corrosion and corrosion-induced hydrogen embrittlement on the fatigue and damage tolerance behaviour of 2024 aircraft aluminum alloy specimens has been investigated. The experimental results have shown an appreciable decrease in fatigue resistance and damage tolerance of the corroded material. The obtained results were discussed under the viewpoint of a synergistic effect of corrosion and corrosion-induced hydrogen embrittlement. The

results have demonstrated the need to account for the influence of pre-existing corrosion on the material's properties for the reliable fatigue and damage tolerance analyses of components involving corroded areas.

[00106] Also known is Corrosion-Induced Hydrogen Embrittlement of 2024 and 6013 Aluminum Alloys, by P.V. Petroyiannis, Al.Th. Kermanidis, P. Papanikos and Sp.G. Pantelakis, (Theoretical and Applied Fracture Mechanics, Volume 41, Issue 1-3, April 1, 2004, pp. 173-183), which discloses the effects of corrosion on the mechanical properties of typical aircraft aluminum alloys. The results showed that corrosion exposure leads to moderate reduction in the yield and ultimate tensile stress. In addition, dramatic reduction in elongation to failure and strain energy density was recorded even after short exposure times. Machining of the corroded surface was found to restore the yield and ultimate tensile stress, while, the ductility of the materials was not recovered. The latter, was stepwise restored to the values for the uncorroded materials after heat treatment at temperatures corresponding to thermal desorption of certain hydrogen trapping sites. The findings clearly suggest that corrosion of the above alloys is associated to volumetric hydrogen embrittlement. The dramatic reduction in tensile ductility was associated with the reduction in the residual strength of the corroded material. A model, based on a multiscaling concept, was used to relate the reduction of fracture toughness and residual strength to the reduction of the strain energy density obtained from tensile tests on corroded and uncorroded coupons. It has been shown that the strain energy density can be used to accurately predict the residual strength of corroded components.

[00107] For the evaluation of the structural integrity of ageing aircraft components the effect of corrosion has to be accounted for, since corrosion and the associated hydrogen

embrittlement of high strength aluminium alloys can lead to catastrophic failure. The effect of corrosion induced hydrogen embrittlement can be attenuated when corrosion interacts with other forms of damage such as a single fatigue crack or multiple site damage. Numerous committees and international conferences have been organized to ponder on the problem of material degradation in older aircraft and one important issue is corrosion. Yet, present day considerations of the corrosion-induced structural degradation relates the presence of corrosion with a decrease of the load bearing capacity of the corroded structural member. The significance of the corrosion-induced hydrogen embrittlement for the structural integrity has been not adequately recognized and remains clearly underestimated. Currently, corrosion and hydrogen damage mechanisms of aluminium alloys are far from being understood. The damage processes involved occur in atomic scale. Corrosion attack of aluminium alloys has been attributed to the complex process of oxidation. Yet, testing has revealed that in addition, hydrogen produced during the corrosion process may diffuse to the material interior and lead to concentration and trapping of hydrogen at preferable trapping sites, which depend on the alloy system.

[00108] Most of the investigations on hydrogen embrittlement of aluminium alloys have been made for the Al-Zn-Mg alloys of the 7xxx series. A metastable aluminium hydride has been considered responsible for the brittle intergranular fracture of Al-Zn-Mg alloys subjected to stress corrosion cracking in water vapor.

[00109] The preferential decohesion of grain boundaries containing segregated magnesium is a different explanation for the intergranular fracture of these alloys. Hydrogen embrittlement of different aluminium alloy series, i.e. 2xxx, 6xxx and 8xxx, is still underestimated and not adequately documented. Additionally, it has not been sufficiently

acknowledged that hydrogen embrittlement can take place even in the absence of mechanical loading, i.e., stress corrosion cracking is not necessary for hydrogen embrittlement. Evidence shows that corrosion-induced hydrogen embrittlement could be responsible for the dramatic degradation of toughness and ductility of the conventional 2024 and 6013 alloys, as well as, of the advanced 2091 and 8090 alloys. This degradation was explained by quantifying the hydrogen evolution in 2024 and 6013 alloys and identifying the different trapping sites. These results have been utilized by heat-treating corroded and uncorroded coupons at the temperatures corresponding to the hydrogen trapping sites for each of the examined alloys.

[00110] The fracture toughness of the corroded material decreases significantly and it is necessary to evaluate local fracture toughness values associated with the reduction of strain energy density. The involvement of multiscaling approaches is very efficient for facing the complex interactive corrosion hydrogen embrittlement process and it was suggested to examine the effect of corrosion-induced hydrogen embrittlement on multiple site damage (MSD) problems where the distance of the rivet holes is such that allows local volumetric embrittlement of the material.

[00111] A comprehensive experimental investigation was carried out in order to quantify the effects of corrosion and corrosion-induced hydrogen embrittlement on the mechanical properties of the aircraft aluminum alloys 2024 and 6013. In addition to tensile tests, residual strength tests were conducted using notched pre-fatigued (MSD) specimens containing a row of two holes. Both corroded and uncorroded specimens were tested. A multiscaling approach was used to relate the reduction of fracture toughness and residual strength to the reduction of the strain energy density obtained from tensile tests on corroded and un-corroded

coupons. Confirmation of the experimental findings was also achieved using an extensive fractographic analysis.

[00112] The effect of corrosion on the mechanical behaviour of the aircraft aluminum alloys 2024 and 6013 was investigated experimentally. The following conclusions were obtained:

- corrosion-induced degradation of mechanical properties occurs gradually with the exposure time. Tensile ductility decreases exponentially to extremely low final values;
- to interpret the results, a multi-scale approach is required to close the gap between the damage processes taking place at the micro-level and the resulting effect at the macroscopic mechanical properties of the material;
- mechanical removal of the corroded areas restored the yield and ultimate tensile stress but not the tensile ductility, wherein the latter was restored only after thermal treatment of the alloys at temperatures corresponding to hydrogen trapping, suggesting that corrosion of the examined alloys is associated to hydrogen embrittlement;
- the fracture toughness of the corroded material decreases significantly; it is necessary to evaluate a local fracture toughness associated with the reduction of strain energy density; and
- the use of the strain energy density reduction as measured from tensile tests can be used to evaluate the reduction of residual strength of structural components due to corrosion-induced hydrogen embrittlement.

[00113] Also known is Hydrogen Degradation of Ferrous Alloys, edited by Oriani, Richard A.; Hirth, John P.; Smialowski, Michael (William Andrew Publishing/Noyes, 1985, p. 900, ISBN 0-8155-1027-6), which provides a critical review of

the fundaments of hydrogen-metal interactions, mechanistic considerations, and the phenomenology of the degradation of mechanical properties. Hydrogen degradation of structural materials is a serious problem that has received increasing attention for the past fifty years. The ubiquity of the sources of hydrogen-corrosion in aqueous solutions, absorption into pipelines carrying humid and contaminated hydrocarbons, and contaminants in the melting processes contribute to the importance of the problem.

[00114] Also known is The Effect of Hydrogen on the Structure and Properties of Fe-Ni-Cr Austenite, by J. Burke; A. Jickels; P. Maulik (Proceedings of an International Conference. Moran, Wyoming, 1976, pp. 102-115), which addresses the loss of ductility in austenitic steels associated with the absorption of hydrogen either gaseously or electrolytically. Although the susceptibility of this type of material is much less than that of ferritic and martensitic steel, the deterioration in mechanical properties is nevertheless substantial under conditions where high hydrogen concentrations are absorbed. This has obvious implications regarding material utilization. Also, the clear link that has now been established between some types of stress corrosion cracking and hydrogen induced changes in structure and properties has further increased the interest in understanding the basic mechanisms of hydrogen embrittlement in these materials. Hydrogen embrittlement of austenitic steels can be divided into two broad types: (1) the combination of high hydrogen fugacity, low diffusivity (i.e., low temperature) and austenitic stability leads to severe internal strains, spontaneous transformation to alpha' and epsilon martensites and extensive intergranular and transgranular surface cracking, and (2) the combination of composition, temperature and fugacity are such that hydrogen is absorbed without accompanying gross structural changes.

[00115] Also known is Decomposition of Carbides in 2-1/4Cr-1Mo Steels During Hydrogen Attack, by Shimomura, J.; Imanada, T. (Scripta Metallurgica, 1985, Vol. 19, No. 12, pp. 1507-1511), which discloses that the resistance to hydrogen attack in 2.25Cr-1Mo steel is improved appreciably by reducing the Si content and have interpreted the effect of Si on hydrogen attack in terms of the carbide chemistry on the basis of the observation that the Si content influences greatly the composition and crystal structure of carbides. Clarification regarding the changes in carbide chemistry occurring during hydrogen attack and to relate them with the deterioration of mechanical properties in 2.25Cr-1Mo steel with different amounts of Si is also disclosed.

[00116] Also known is Hydrogen Attack, Detection, Assessment and Evaluation, by R. Kot (10th Asia-Pacific Conference on Non-Destructive Testing, 2001), which provides an overview of detection, assessment and evaluation methods of hydrogen attack in steels. Equipment in contact with H_2 at high temperature and pressure may suffer from hydrogen damage - hot hydrogen attack. Atomic hydrogen diffuses readily in steels and cracking may result from the formation of CH_4 or H_2 at high pressure and temperature in internal voids in the metal. This results in fissuring at grain boundaries and decarburization with loss of strength, which makes the material unreliable or dangerous. The sound attenuation in hydrogen-damaged steel can be used to quantify the level of degradation of the material's mechanical properties. Knowing this, the remaining life of an affected plant can be estimated.

[00117] Hydrogen has a diverse range of harmful effects on metals. Hydrogen induced degradation of metals is caused by exposure to atmosphere, where hydrogen is absorbed into the material and results in reduction of its mechanical performance. The severity and mode of the hydrogen damage

depends on: source of hydrogen - external (gaseous)/internal (dissolved), time of exposure, temperature and pressure, presence of solutions or solvents that may undergo some reaction with metals (e.g., acidic solutions), type of alloy and its production method, amount of discontinuities in the metal, treatment of exposed surfaces (barrier layers, e.g., oxide layers as hydrogen permeation barriers on metals), final treatment of the metal surface (e.g., galvanic nickel plating), method of heat treatment, and/or level of residual and applied stresses.

[00118] Depending on the combination and number of the above variables, the hydrogen damage may be classified as hydrogen embrittlement, hydride embrittlement, solid solution hardening, creation of internal defects, and can further be subdivided into various damaging processes as shown in FIGURE 8.

[00119] In the hydrogen attack mechanism and prevention, hydrogen forms methane bubbles within the material while reacting with the carbon of the steel. The methane bubbles form on the grain boundaries and in minute voids. Methane pressure build-up due to expansion and joining of such bubbles extends the voids into fissures. The growth of fissures and voids weakens the metal and the fissures develop into major cracks.

[00120] The degree of hydrogen attack depends on temperature, hydrogen partial pressure, stress level, exposure time, steel composition and structure. Hydrogen attack has been reported in plain carbon steel, low alloy steels and even some stainless steels operating above 473K. Hydrogen attack is one of the major problems in refineries, where hydrogen and hydrocarbon streams are handled up to 20 MPa and approximately 810K level. In order to prevent hydrogen attack from occurring at high temperature and/or pressure, a high alloy element content is required. Chromium (Cr), Molybdenum (Mo),

Tungsten (W), Vanadium (V), Titanium (Ti), Niobium (Nb), which are carbide forming elements, are used in steel to provide desired resistance.

[00121] API 941's Nelson Curves, based on industry experience, provide guidance universally used for alloy selection. The appropriate alloy to select is shown as the curve immediately to the right or above the temperature-hydrogen partial pressure coordinates, which represent anticipated parameters of operation.

[00122] Heat treatment influences steel resistance to hydrogen attack. For example, quenched and tempered 2-1/4Cr - 1Mo steel has increased susceptibility to hydrogen cracking due to low resistance of martensitic and bainitic structures to hydrogen damage. The heat treatments that would produce excessive yield strength levels should be avoided or used with caution.

[00123] Industry experience indicates that post-weld heat treatment of Cr-Mo steel is beneficial in resisting hydrogen attack in hydrogen service. It is a common practice to require a manufacturer of a hydrogen-hydrocarbon equipment to run embrittlement tests on weld consumables and store all "low hydrogen," electrodes in hot "boxes," before fabrication is begun. Preheat requirement on low chromium steel results in minimizing weld cracking caused by hydrogen during fabrication. Proper inspection, quality control, good design and a reputable manufacturer are all necessary to assure a finished vessel or reactor will be resistant to hydrogen attack.

[00124] Hydrogen attack is caused by exposure of steel to a hydrogen environment. The severity of the damage depends on the time of exposure, temperature, hydrogen partial pressure, stress level, steel composition and structure. To avoid/prevent hydrogen attack, steels with elements forming stable carbides should be used. A heat treatment should be

carefully applied to avoid producing structures with low resistance to hydrogen attack (martensite, bainite). Proper inspection and quality control systems are necessary during the manufacturing process of hydrogen and hydrocarbon handling equipment. Hydrogen undamaged and damaged samples of steel used in plant equipment should be available for the hydrogen attack testing purposes.

[00125] Also known is Influence of Dissolved Hydrogen on Structure of Oxide Film on Alloy 600 Formed in Primary Water of Pressurized Water Reactors, by Takumi Terachi, Nobuo Totsuka, Takuyo Yamada, Tomokazu Nakagawa, Hiroshi Deguchi, Masaki Horiuchi and Masato Oshitani (Journal of Nuclear Science and Technology, 2003, Vol. 40, No. 7, pp. 509-516), which discloses the results of the investigation of the relationship between the susceptibility of primary water stress corrosion cracking (PWSCC) in Alloy 600 and the content of dissolved hydrogen (DH) in the primary water of pressurized water reactors (PWR). To this end, structural analysis of oxide films formed under four different DH conditions in simulated primary water of PWR was carried out using a grazing incidence X-ray diffractometer (GIXRD), a scanning electron microscope (SEM) and a transmission electron microscope (TEM). In particular, to perform accurate analysis of the thin oxide films, the synchronotron radiation of Spring-8 was used for GIXRD. The oxide film is mainly composed of nickel oxide, under the condition without hydrogen. On the other hand, needle-like oxides are formed at 1.0 ppm of DH. In the environment of 2.75 ppm of DH, the oxide film has thin spinel structures. From these results and phase diagram considerations, the condition around 1.0 ppm of DH corresponds to the boundary between stable NiO and spinal oxides, and also to the peak range of PWSCC susceptibility. This suggests that the boundary between NiO and spinel oxides may affect the SCC susceptibility.

[00126] Also known is Internal Oxidation as a Possible Explanation of Intergranular Stress Corrosion Cracking of Alloy 600 in PWRs, by P.M. Scott (9th International Conference on Environmental Degradation of Materials in Nuclear Power Systems-Water Reactors, 1999), which provides an investigation of the internal oxidation mechanism in pressurized water reactors. Internal oxidation was first proposed as a plausible mechanism of intergranular stress corrosion cracking (IGSCC) in hydrogenated PWR primary water by Scott and Le Calvar in 1993. Since then several experimental studies have been undertaken to test the hypothesis. Some detailed microscopical examinations of both primary and secondary cracks in Alloy 600 using Secondary Ion Mass Spectrometry (SIMS) and Analytical Transmission Electron Microscopy (ATEM) have been carried out and preliminary results have already been published. Disclosed are some of the points of criticism which have arisen as to the applicability of the internal oxidation mechanism at typical PWR operating temperatures and corrosion potentials. This is the specific problem of reconciling the apparent rate of intergranular diffusion of oxygen in nickel base alloys with the observed rates of cracking and the thermodynamic requirement for internal oxidation that the corrosion potential be at or below the Ni/NiO redox potential. The latter point is of particular concern if this mechanism is invoked to explain the secondary side steam generator tube IGA/IGSCC. The second objective is to describe the morphology of known cases of intergranular internal oxidation cracking observed at higher temperatures in order to provide a point of reference for other papers in this conference concerned with detailed examinations of cracks in alloy 600 produced under actual or prototypical PWR conditions.

[00127] Also known is Corrosion and Protection of Aluminum Alloys, by V.S. Sinyavsky, V.D. Valkov and V.D. Kalinin

(Moscow, Metallurgia, 1986), which discloses that aluminum alloys are subject to various types of corrosion depending on service conditions, alloy composition, etc. These types of corrosion include corrosion cracking, intergranular corrosion and exfoliation corrosion. Some copper-containing aluminum alloys are prone to intergranular corrosion. This corrosion sometimes occurs in aluminum alloys containing magnesium and silicon.

[00128] Intergranular corrosion of aluminum alloys occurs because of incorrect heat treatment and sometimes due to a prolonged exposure to sunlight in many environments such as sea water, marine and industrial atmosphere. The intergranular corrosion theory holds that Al-Cu solid solution breaks down with precipitation primarily at grain boundaries during artificial aging of aluminum alloys or under other thermal effects produced during heat treatment in the temperature range between 90°C and 270°C. The composition of the precipitate is close to intermetallic compound $CuAl_2$. This results in a copper-depleted region near the boundaries. Within grains, intermetallic compounds precipitate to a lesser degree, hence the solid solution is less exhausted of copper in regions removed from boundaries. Upon heat effect in the above-mentioned temperature range, the surface of the aluminum alloy can no longer be considered homogeneous from the electrochemical standpoint. A potential difference between the grain boundaries and a grain may be up to 100 mV, which ultimately causes the electrochemical corrosion.

[00129] The aluminum alloys may generally be prevented from intergranular corrosion by subjecting to appropriate heat treatment that provides a favorable potential distribution over the surface. Correct heat treatment is to make the alloy more homogeneous and transfer as much copper as possible into a solid solution, which is fixed by a rapid quench process.

Duralumin has optimum corrosion resistance when quenched from 480-500°C in cold water (40°C) with further natural aging.

[00130] Corrosion cracking occurs when alloys are simultaneously affected by a corrosive environment and static tensile stresses. The stresses may be both external and internal. Some aluminum alloys are apt to stress corrosion cracking. The susceptibility of alloys to such hazardous corrosion damage depends upon the metal structure, the magnitude and nature of stresses and corrosive environment. The corrosive environments that selectively attack alloys contribute to corrosion cracking.

[00131] Exfoliation corrosion is a specific type of sub-surface corrosion that develops mainly parallel to the vector of deformation, produced in shaping a semi-finished article, and is attended by crack formation in this direction, exfoliation of individual metal particles or complete failure of samples or components. This corrosion may develop along grain boundaries or deformed boundaries of dendrite cells, as well as transgranularly. Exfoliation corrosion is substantially typical of deformed semi-finished articles. In some exceptional cases, this may be observed in conventional castings with directional liquation, for example, in Al-Mg-Li alloy with high manganese content.

[00132] Corrosion exfoliation is attributable to a specific structural state, orientation of the second phases and solid solution crystals in a direction of deformation, high content of alloy elements or impurities and the nonuniform distribution thereof, internal stresses, and certain physical-and-chemical state of the surface that depends on the nature of the corrosive environment.

[00133] Thus, the corrosion resistance of aluminum alloys in service is determined by the following criteria: surface finish, internal compressive (favorable) stresses, and specific structure of alloy near the surface, which is

produced by certain quenching conditions. Under optimum conditions, the ultrasonic treatment applied to the surface of aluminum alloys is very likely to combine all the above favorable factors.

[00134] Also known is Corrosion of Aluminum and Its Alloys, by V.V. Gerasimov (Moscow, Metallurgia, 1967), which discloses that the electrochemical properties and corrosion resistance of aluminum depend heavily on the metal purity. The resistance of aluminum alloys is governed by the nature and the number of alloy elements. At temperatures below 100°C, pure aluminum has the greatest corrosion resistance. In water and neutral environments containing no activating ions, e.g. haloids, a stationary potential of pure aluminum corresponds to a passive region. Hence, the aluminum resistance is fairly high under such conditions.

[00135] The alloying of aluminum changes the kinetics of the anodic process. A stationary potential of the alloy with 1% iron content corresponds to the passive region. This determines a fairly low corrosion rate of such an alloy, though this is higher than that of pure aluminum. In a 3% solution of sodium chloride the corrosion rate of the alloy increases proportionally to the iron content, starting from 0.004%.

[00136] The alloying of aluminum with copper affects the kinetics of the anodic process (solution of aluminum alloy) to a greater extent than in the case of iron. A slight increase in corrosion rate in a 3% sodium chloride solution is observed as the copper content increases up to 0.01%. The corrosion process intensifies significantly with further increase in copper content.

[00137] The alloying aluminum with nickel reduces the hydrogen and oxygen over. The acceleration of the cathodic process due to nickel introduction increases stationary potentials of alloys. A standard potential of the alloy

containing 0.2% nickel corresponds to the passive region; the corrosion rate in this case is low. With the nickel content more than 0.6%, the stationary potential corresponds to the overpassivation region; the corrosion rate is naturally increases.

[00138] Thus, for aluminum the content of an alloying element up to 1% has the largest effect on the kinetics of the electrode processes. When alloyed with iron, copper or nickel, the aluminum alloys contain intermetallides of these elements. The electrode potentials of intermetallides are more positive than the stationary potential of aluminum and work as cathodes in aluminum alloys.

[00139] Manganese, zinc, magnesium and silicon in amounts up to 1-2% do not intensify the corrosion process. As the zinc content increases up to 25%, the stationary potential of the alloy is shifted in the negative direction in neutral and acid environments. The stationary potential of the alloy is virtually unaffected by further increase in zinc content. The addition of 0.16% zinc to aluminum has little effect on the cathodic process rate. Hence, the alloying of aluminum with zinc up to 2.05% does not increase, but even decreases somewhat the corrosion rate.

[00140] Magnesium in amounts up to 5% does not increase aluminum corrosion significantly. In neutral or acid environments, the stationary potential decreases when aluminum is alloyed with magnesium. The same is the case with lithium.

[00141] In neutral environments, the stationary potential of aluminum is virtually unaffected by silicon; in acid environment, this is increased. Silicon in a solid solution has virtually no effect on aluminum corrosion, while silicon intermetallides may present local cathodes and speed up corrosion. Note that silicon appears to enhance significantly the protective properties of the oxide film at the aluminum surface, because the silumin-type alloys are very corrosion

resistant. In acid environment, the sodium content in the range from 0.035 to 0.078% is very detrimental to the resistance of aluminum. The maximum sodium content in aluminum containing 0.3-0.4% iron impurity should range between 0.02 and 0.03%. If present in aluminum, sodium intensifies intergranular corrosion.

[00142] The calcium content of 0.08% reduces somewhat the resistance of commercial aluminum in neutral environment; 0.5-1.0% sodium speeds up aluminum corrosion significantly in 0.5-n alkaline solution (n designates the normality of a solution). The calcium impurity is especially hazardous in the presence of silicon.

[00143] The alloying of aluminum with cadmium suppresses the adverse action of copper. Lead has little effect on the aluminum resistance. The titanium content above 0.01% intensifies corrosion in acid environments. Cerium, cobalt, platinum, silver, thorium and vanadium have an adverse effect. For example, aluminum alloy with 40% silver failed completely after a few days of testing in the atmosphere at 100% relative humidity (RH). A high corrosion rate is caused by effective operation of Ag_2Al intermetallides as cathodes. In some instances, chromium, tin and cadmium have no effect, but sometimes these intensify corrosion. Antimony improves the corrosion resistance of aluminum.

[00144] Even small amounts of mercury result in aluminum amalgamation, metal surface depassivation and increased rate of metal dissolving. A mercury-containing aluminum protector has sufficiently negative potential and is virtually not passivated with time.

[00145] The alloying affects the dependence of a stationary potential and corrosion resistance upon pH environment. In alkali environments, pure aluminum and most of aluminum alloys are not resistant. Under such conditions, the alloy doped with 0.5% magnesium has the smallest corrosion rate. When

aluminum is alloyed with magnesium, an oxide film develops at the metal surface. This film contains magnesium hydrate, which is insoluble in alkali. In diluted alkalis, the alloy resistance improves with increase in magnesium content. In concentrated alkalis, magnesium does not improve the aluminum resistance. The alloying with magnesium and manganese enhances the resistance in ammonia. In ammonia-containing coke waters, 99-99.5% aluminum and aluminum alloys with 1.25% manganese or 3% magnesium are resistant to corrosion.

[00146] In nonoxidizing acids, silicon intensifies and cadmium suppresses corrosion of aluminum. Zinc and manganese have an unfavorable effect. Magnesium and tin enhance the corrosion resistance. In homogeneous alloys, 1% silicon does not impair metal resistance in nitric acid; in heterogeneous alloys, 1% silicon impairs the resistance significantly in 65% nitric acid. Copper in amounts of 1%, even if this is not completely dissolved in aluminum, intensifies corrosion significantly in 25% acid.

[00147] In 5% and 10% hydrochloric acid, 99.996% aluminum and aluminum alloy containing 0.5% magnesium are fairly resistant to corrosion. The corrosion rate in these cases does not exceed 3-5 g/m^2day. In the same environments, the respective corrosion rates of 99.5% aluminum were 352 and 7780 g/m^2day.

[00148] Impurities and alloying elements have a significant effect upon pitting corrosion in aluminum and its alloys. In 99.99% aluminum, corrosion is very rarely observed in fresh water. However in 99.5-99.8% aluminum, the depth of corrosion may reach 0.3 mm within a week. A reduction in aluminum purity from 99.99% to 99% increases the cathodic process rate in the oxygen ionization area, as well as the rate of limiting diffusion current and hydrogen ion discharge. This intensifies pitting corrosion.

[00149] The work of local cathodes intensifies local corrosion. The higher the iron and copper content, the greater the number of corrosion pits and the depth thereof. Corrosion pits are usually oriented in the rolling direction which corresponds to the arrangement of intermetallides. Pitting corrosion is also observed in scratch areas where intermetallides appear.

[00150] When the aluminum surface is treated in boiling water, a protective film is recovered in areas where this was impaired for one reason or another. Such a treatment enhances the resistance of alloys to pitting corrosion.

[00151] Various surface treatments such as after-rolling degreasing, etching in 10% alkali, chemical polishing in a mixture of phosphoric acid and nitric acid virtually have no effect on the resistance of 110 alloy in distilled water at 53-70°C. In chloride solution, surface polishing reduces corrosion losses. In potassium sulfate solutions of 0.001-1.0-n concentration, polished aluminum does not virtually corrode. Chemical polishing reduces 20-fold corrosion of 99.5% aluminum in an atmosphere at 87% RH.

[00152] Surface treatment of aluminum alloys affects their tendency to pitting corrosion. As a result of preliminary etching, the depth of pitting on 2S and 3S alloys (wrought aluminum alloys used in the USA; new designations are 1100 and 3003 respectively) increases 10-50 times upon testing in fresh water.

[00153] Plastic deformation, which disrupts the integrity of the impure intergranular substance, improves the resistance of aluminum doped with iron and nickel to intergranular corrosion. A reduction in intergranular internal adsorption or breakdown of solid solution at grain boundaries is attained by using lower heating temperature before quenching and aging.

[00154] Under the combined effect of corrosive environment and mechanical stress, some aluminum alloys, for example alloys doped with magnesium or magnesium and zinc, suffer a specific form of attack typically termed corrosion cracking or stress corrosion. This form of attack is usually observed in environments containing chlorides. Corrosion cracking of aluminum alloys may be explained by precipitation of an intermetallic phase Mg_2Al_3 at grain boundaries. This intermetallide was found by metallographic and electron-microscopic investigations to exist at grain boundaries of magnesium-doped aluminum alloys that suffered corrosion cracking.

[00155] Mechanical stresses create submicroscopic notches and cracks in the intermetallide, promote corrosive environment penetration into a β-phase and intensify dissolution of this phase. In addition, tensile stresses promote precipitation of the β-phase along boundaries of crystallites.

[00156] The corrosion cracking process of magnesium-doped aluminum alloys is as follows. The β-phase at crystallite boundaries is not passivated in chloride solution and dissolves intensively. The intermetallide may precipitate either during manufacture and treatment of an alloy or under tensile stresses. The dissolution of the β-phase and formation of submicroscopic cracks result in formation of concentrators and precipitation of new intermetallides. Thus, the process propagates intensively deep into the metal.

[00157] Deaeration of the environment or cathodic polarization shifts the potential in the negative direction and diminishes the dissolution of the β-phase and hence the corrosion cracking process. The anodic polarization or contact with more precious metals (copper, stainless steel) increases the dissolution rate of the β-phase (that is not passivated in chlorides) and hence intensifies corrosion

cracking. The corrosion cracking process is the fastest when the surface of the alloy is etched in acid or alkali. Surface polishing increases the alloy life to failure. With pH increase from 0 to 6, the specimen life to failure increases. Aluminum alloys doped simultaneously with magnesium and copper are less apt to corrosion cracking than magnesium-copper binary alloys. The additional alloying with 0.5-1.5% zinc enhances the corrosion cracking resistance of the alloy containing 7-8% magnesium; the tempering temperature and degree of deformation increase to values when the alloy becomes susceptible to corrosion cracking.

[00158] Under simultaneous action of corrosive environment and alternate loads, alloys may fail due to corrosion fatigue. Chlorides speed up the failure of aluminum alloys because of corrosion fatigue. In 3% solution of sodium chloride, the fatigue limit of 2024 alloy is 3.5 kg/mm^2 at 10^7.

[00159] In closed systems, inhibitors are coming into wide use to protect metals and alloys against corrosion. Some oxidizing agents, for example chromates and dichromate, are used as corrosion inhibitors in neutral environments (passivators). Under low temperatures, chromates may be used to protect aluminum and its alloys against corrosion in neutral, alkali and weak-acid environments. If 0.5-1.0 g/l sodium chromate or potassium chromate is added to water containing at most 50-100 mg/l of salts, the corrosion rate of aluminum and its alloys will decrease greatly. With a greater salt concentration, especially copper, the chromate protective properties are reduced and pitting corrosion may occur.

[00160] Some other compounds are used as inhibitors to protect aluminum parts of cooling systems. Thus with addition of 3% sodium nitrate, 0.03% sodium phosphate and 3% acid phosphate sodium to river water containing 35 mg/l of chlorides at 80°C, the corrosion rate is reduced by 2-3 times;

with addition of 0.03% sodium nitrate and sodium silicate, 3% sodium benzoate, corrosion is reduced by 6-8 times.

[00161] The electrochemical protection of duralumin was demonstrated by G.V. Akimov. Visual observations showed that the 4 m long duralumin plate, secured at ends by zinc strips, did not have any corrosion damages after sea water testing. The cathodic polarization with potential -0.8 V across chloride-silver electrode protects duralumin in sea water during 6 months. In sea environments, duralumin ship hulls may be corrosion protected by protectors. Magnesium protectors are uniformly located over the ship bottom and fastened on vinyl-plastic pads by steel zinc-coated bolts.

[00162] Also known is Chemical and Electrolytic Treatment of Aluminum and Aluminum Alloys, by S. Vernik and R. Pinner, translation edited by B.A. Zelenova and N.I. Veselova (Sudostroyeniye, Leningrad, 1960), which discloses that the corrosion resistance of aluminum alloys may in some cases be significantly improved by applying protective coatings. For aluminum alloys, it is common practice to build up an oxide film by oxidizing or anodizing. Anodizing greatly improves the resistance of aluminum and its alloys in industrial atmosphere. The best oxide films for aluminum are those that have the thickness of 0.0025-0.015 mm and obtained by anodizing in sulfuric acid and oxalic acid. Such films withstand a one-year test under conditions of spraying with 20% sodium chloride.

[00163] A protective oxide film on the surface of aluminum alloys may be developed in treating the metal in water or aqueous solutions at high temperatures. The high resistance of aluminum alloys in sea water may be achieved by cladding with pure aluminum. The clad layer not only isolates the alloy from corrosive environment, but also protects it electrochemically. To protect aluminum alloys against corrosion, enameling may be used. Enamels are fairly durable

in water, acids, alkalescent detergents, and city air. Bituminous, polymeric and paint coatings, as well as greases are used for corrosion protection of aluminum and its alloys in the atmosphere and soil.

[00164] Also known is Corrosion Theory and Corrosion-resistant Structural Alloys, by N.D. Tomashov and G.P. Chernova (Moscow, Metallurgia, 1986), which discloses that a chemical corrosion mechanism is typical for failure of metals when metals are in contact with dry gases at high temperatures or with non-electrolytes. As this takes place, oxidation-reduction reaction occurs in one event compared to electrochemical corrosion. Gas corrosion is possible in metallurgical operations during heat treatment of metals, during operation of details and structures in turbojet and rocket engines, in power plants, etc.

[00165] The ability of metals to resist corrosion attack of gases at high temperatures is called heat resistance. Another important behavior of metals at high temperatures is high-temperature strength, which defines the ability of the material to retain good mechanical properties under such conditions. The metal may be heat resistant but may not have good high-temperature strength (for example, aluminum alloys at 400-450°C). At 600-700°C, high-speed tungsten steel is heat resistant but not high-temperature strong.

[00166] The interaction between the metal and oxygen (metal oxidation) occurs in accordance with the formula: $Me + O_2 = MeO_2$. The oxygen molecules that reached the metal are adsorbed, i.e., captured by its surface. The oxygen adsorption in metal is usually represented as follows. The physical adsorption occurs on a clean surface, weakening the bonds between oxygen atoms and molecules. The molecules dissociate and oxygen atoms draw electrons away from the metal atoms. A chemical adsorption stage occurs when the shift of

electrons toward oxygen with the formation of O^{-2} ions is equal to the nuclei formation of the metal-oxygen compound (oxide). The product of the oxygen-metal interaction (oxide) provides the surface with an oxide film which reduces its chemical activity. Depending on the thickness, the films on metals may be classified as thin (invisible) of thickness up to 40 nm, average (visible as temper colors) of thickness 40-500 nm, or thick (visible) of thickness more than 500 nm. For example, in the case of aluminum:

- In dry air, after several days the film is 10 nm thick;
- At 600°C and after 60 hours the film is 200 nm thick;
- Upon anodizing, the film is from 3 to 300 μm thick.

[00167] For metals and alloys, the gas corrosion rate is influenced by the external factors such as the composition, pressure and velocity of the gaseous environment, the temperature and heating condition, as well as the internal factors such as the nature, chemical and phase composition of alloys, mechanical stresses and deformations.

[00168] Protective properties of oxide films are substantially dependent upon the nature and composition of alloys. Chromium, aluminum and silicon considerably retard the steel oxidation process, which occurs due to the formation of films with high protective properties. Deformation of metals during heating may cause film discontinuity, increasing thereby the oxidation rate. Preliminary deformation has little effect on oxidation rate only at temperatures below recrystallization temperature.

[00169] For gas corrosion protection, heat-resistant alloying, protective atmospheres and protective coatings are used.

[00170] Also known is Corrosion and Corrosion Protection, by F. Todt (Khimiya, Leningrad, 1967), which discloses that the process of electrochemical corrosion is a combination of two coupled reactions:

- the anodic reaction (oxidation) $Me = Me^{z+} + ze$;
- the cathodic reaction (recovery) $D + ze = (Dze)$;

where D is depolarizer (oxidant) that attaches z-electrons (ze) released as a result of the anodic reaction (metal ionization). A schematic representation of electrochemical corrosion process is shown in FIGURE 9.

[00171] The surface of the actual alloy is always heterogeneous, i.e., has areas that substantially differ in electric potential. The metal surface may differ not only in structural microirregularity (grain boundaries, impurities), but also in submicroirregularity (imperfections of a crystalline structure, foreign atoms in a lattice, etc.). This localizes the anodic and cathodic processes and causes local corrosion to develop (for example, development of pitting) - the theory of work of micro-galvanic elements under electrochemical corrosion.

[00172] The modern electrochemical corrosion theory, termed kinetic theory of electrochemical corrosion, emphasizes that the electrochemical failure of metals may occur when the metal-electrolyte interphase is available. The fact of corrosion does not depend on the electrolyte nature, whether in the case of super-pure water or concentrated water solution. The amount of electrolyte also has little importance: this may be the moisture film several microns thick. The only condition for corrosion to occur is a possible combination on the metallic surface of the anodic reaction of metal ionization and the cathodic reaction of recovery of some or the other ions or molecules. This is the case if the equilibrium potential of the anodic reaction is more negative than that of at least one of the possible

cathodic reactions. The (stationary) potential produced in this case will take an intermediate position. This condition should be met regardless of the corrosion type.

[00173] When the metal is submerged into the electrolytic solution, there is a certain potential difference between the metal surface and the electrolyte, which occurs due to the formation of a double electric layer, i.e., the asymmetric position of particles at the metal-electrolyte interphase.

[00174] FIGURES 10 and 11 show the schematic representation of the double electrochemical layer formation. More particularly, FIGURE 10 shows a metal atom ion transforming into solution; FIGURE 11 shows a cation transforming from the solution to the metal surface.

[00175] When the ion hydration energy is sufficient to break the bond between the metal ion-atoms and the electrons and the metal ions transfer into solution, an equivalent number of electrons remains at the metal surface, imparting a negative charge to the metal surface. Further, these negative charges attract metal cations from the solution. This results in a double electric layer at the metal-electrolyte interface, causing a certain potential difference between the metal and electrolytic solution.

[00176] Another variation is possible. On the metal surface, the cations may be discharged from the electrolytic solution (the bonding energy in a lattice is greater than the hydration energy). As a result, the metal surface obtains a positive charge and forms a double electric layer with solution anions.

[00177] The electrode potential values substantially affect the nature of the corrosion process. The electric current flow during work of a corrosion microelement is caused by the initial potential difference between the cathode and anode. When the corrosion current flows after circuit closing, the

potential difference decreases. Such a change of potentials as a result of the current flow is termed polarization.

[00178] Depending on the electrode process on the cathode, electrochemical corrosion may be classified in the following types: with hydrogen polarization (recovery of hydrogen ions on the cathode) - in acids; with oxygen recovery - atmospheric, in water, in salt solutions, etc.; or with recovery of other oxidants.

[00179] Passivity is a relatively high corrosion resistance state caused by the retardation of the anodic reaction of metal ionization in a certain region of potentials. The passive state generally occurs when metals are in contact with strong oxidants. However, for some metals even water may be rather strong oxidant (e.g., for titanium). The film theory of passivity is still one of basic theories. There is an adsorption theory that holds that the passivity occurs as a result of the oxygen adsorption at the metal surface. It has been found that passivity occurs even when the amount of adsorbed oxygen is such that the surface cannot be even covered with a layer one molecule thick. This is explained by blocking the active surface areas, which are limited.

[00180] Also known is Corrosion Cracking and Protection of High-strength Steels, by F. Azhogin (Moscow, Metallurgia, 1974), which discloses that corrosion cracking is possible under combined action of the corrosive environment and tensile stresses. The cracks generally develop along the planes perpendicular to tensile stresses, along grain boundaries (which is typical for a less stressed state) and transgranularly, which is especially typical for corrosion cracking and fatigue. In corrosion cracking, ductile metals are subject to pronounced brittle fracture. The notions about the corrosion cracking mechanism are ambiguous.

[00181] The adsorption theory presents the adsorption of solution anions on movable dislocations and other structural

imperfections. This reduces the surface energy and facilitates the breakdown of atomic bonding of metals. The crack nucleation may occur as a result of a wedging action of surface-active substances in adsorption thereof in microcrevices on the metal surface (Rebinder effect). Some researchers believe that corrosion cracking of carbon and stainless steels, titanium and its alloys may be due to hydrogen absorption at the progressive crack tip, which results in local embrittlement of metal.

[00182] The electrochemical theory holds that the main factor of crack development is the accelerated anodic dissolution of a metal at the crack base. The primary stress concentrator (that cannot relax easily in high-strength material) occurring on the surface of the tensioned metal specimen, may cause, due to some structural imperfection, the passivity breakdown in this point and a greater speed of electrochemical dissolution. The cathode of such a pair is the crack side surface and partially the external surface of a specimen, the anode is a crack tip. A significantly localized dissolution process maintains the crack sharpness at atomic level and hence the maximum stress concentration at the crack tip. Atomic dissolution at the crack tip is supposedly a notch of a gain or structural block, which occurs with relatively low linear velocity. At some instant this notch is realized by the subsequent brittle breakdown of a block or grain with very high linear velocity, but with possible delay in movement on the next block or grain, and then again with a slower electrochemical notch thereof, etc. In microscale, the crack development will occur fairly uniformly until alternation of electrochemical notches and mechanical breakdowns is so frequent that this will go into the avalanche brittle fracture of the remaining section of a specimen.

[00183] No doubt that in so doing the accompanying processes that intensify the development of crack and corrosion cracking will be as follows:

- the hydrogen pickup in the metal surface at the crack tip and hydrogen embrittlement in the pre-failure zone,
- the adsorptive decrease in strength (wedging effect of Rebinder),
- the high strength and hence low ductility of the alloy, allowing no stress concentration reduction in the primary stress concentrator due to relaxation processes,
- the microstructural heterogeneity of the alloy (microinclusions, structural submicroimperfections) that promote the formation of stress concentrators and a primary crack,
- the nature of dislocations, microdeformations and breakdown of the atomic lattice at the crack tip.

If stresses are not too high and the alloy has less perfect passivation at grain boundaries (for example, due to segregation of impurities), the crack will develop intergranularly. Otherwise, intragranular crack development also occurs. Most cases of corrosion cracking may be interpreted in more detail on the basis of a combined mechanical-electrochemical mechanism.

[00184] Initially, the basic role in stress concentrator initiation and growing thereof in a primary crack is probably played by the chemisorptive interaction between the active environment ions at separate metal surface irregularities and non-uniform deformation (dislocation) distribution which results in local surface activation and stress concentrator of a stressed state.

[00185] Further, the crack grows with continuous activation of the anodic process by mechanically increasing tension of the lattice in the crack tip zone. This activation is especially high if the initial state of the metal corresponds

to the passive state and superposition of tensile forces results in local activation at the crack tip. At the final stage, macromechanical failures increase in avalanche fashion and the fracture occurs under conditions when a mechanical factor prevails.

[00186] In corrosion cracking, mechanical stresses and corrosion environment cause, by simultaneous action, by far greater loss of metal strength than when these factors affect separately. Corrosion cracking of metals in many environments has long been known in practice, for example, so-called seasonal cracking of brass products such as condenser tubing, brass boxes, rifle shells; and corrosion cracking of steel products such as propellers, rods, diesel engines, turbine blades, etc.

[00187] Low-carbon steels containing nitrogen are very susceptible to corrosion cracking. The effect of nitrogen on corrosion cracking of high-strength steels is obviously associated with the change in internal stresses. Nitrogen forms interstitial solid solutions with alpha-iron and gamma-iron. The introduction of titanium in steel promotes nitrogen bonding in strong nitrides and prevents the formation of the interstitial solid solution, reducing internal stresses and improving high-strength steel resistance to corrosion cracking.

[00188] Also known is Metal Fatigue (Symposium, Moscow, Inostr. Literatura, 1961), which discloses that fatigue is the process of progressive accumulation of damage in a material under repetitive or repetitive-variable stresses, culminating in cracks and complete fracture. The most important feature of this process is that it develops under stresses substantially lower (twice and more) than the tensile strength which is a strength measure under static loading. The ability of a metal to withstand repetitive-variable loads, which is termed endurance, is substantially lower than static strength.

The main characteristic of the metal fatigue resistance is fatigue limit. Under similar testing conditions, the fatigue strength is determined by the chemical composition and internal structure of the metal, which depends on the manufacturing technique. At various periods of the fatigue process, the nature of structural changes and metal properties is as follows:

(1) Fatigue incubation - In a micro-yield stage, dislocation sources begin to function in individual grains and mainly in a surface layer of a specimen. In a cyclic yield stage, the entire volume of a specimen is involved in plastic deformation. Dislocations begin to multiply intensively and interact with the formation of a cell structure. Slip bands appear on the specimen surface. Cyclic strengthening is a final stage in fatigue incubation. So-called stable slip bands appear on the specimen surface, which are shorter than the cross-section of a grain. These cannot be eliminated by removing the surface layer several microns thick, while the slip bands occurring under static deformation are removed by light polishing. Toward the end of the strengthening stage, these bands open and transform into submicrocracks.

(2) The submicrocrack development period - The dislocation density is saturated and the dislocation structure is transformed: many grains have, mainly near the surface, very elongated cells whose walls are comparable with the grain size. Such a structure was termed a band structure. Toward the end of the second period, the whole surface of a specimen is covered by a thick network of submicrocracks, which however do not go beyond the grain boundaries. The damage so far accumulated cannot be regarded as irreversible yet, since this does not dramatically reduce the resistance to brittle fracture, ductility, etc.

(3) The microcrack formation (when the microcrack goes beyond the grain boundaries), substantial deterioration

of the entire complex of mechanical properties - The crack growth is determined by the nature of the stressed state of a specimen. Plastic deformation is localized in a relatively narrow zone near the crack tip where an increase in dislocation density and the formation of very fine cells is observed.

(4) The complete fracture occurs when the crack reaches its critical length.

[00189] The crack nucleation under cyclic loading results from the interaction of dislocations:

- between each other (if two dislocations having opposite signs at the end are located in planes, the distance between which is not greater than about 10 A (1 Angstrom = 10^{-8} cm), these dislocations are interattracted with such a force that a crack develops and in doing so other dislocations, moving along the same planes, shift to the crack and expand it),
- with various barriers (boundaries) that prevent slipping and cause the formation of sufficiently strong dislocation clouds.

[00190] An important phase of fatigue failure is the stage of crack growth to a critical size. This critical size, defined by the fracture mechanics relations, is measured in many cases in millimeters or tens of millimeters, so the crack may be visible by a naked eye long before the ultimate break. In fatigue failure, the fracture consists of two zones: (1) the fatigue crack development portion has a distinctive smooth, sometimes bright appearance and the surface often has concentric contours of crack propagation front, which meet in a fracture nucleus; (2) the second is a break zone that occurs as a result of a quick ultimate failure. The fatigue limit is favorably influenced by such structural changes that simultaneously increase the strength and ductility of the material (grain refinement or formation of a developed

substructure), metal pureness along non-metallic inclusions (internal concentrators).

[00191] In the case of fatigue, the surface layers condition is of special importance. The most effective are the treatments that harden the surface and at the same time induce residual compressive stresses in the surface layers. In this case, the fatigue crack nucleation and propagation resistance is improved simultaneously. Hardening impedes the slip development and compressive stresses prevent surface crack opening, reducing the effect of the tensile component.

[00192] Also known is Corrosion-fatigue Strength of Steel, by A.V. Ryabchenkov (Moscow, Mashinostroeniye, 1953), which discloses that the process of corrosion fatigue of a metal may be described as follows. First, the lattice elastic distortions accumulate at some portions of the metal surface due to dislocation density increase. Then submicroscopic cracks appear in the metal volumes, where a critical dislocation density is attained during mass slipping of separate blocks. Finally, microcracks grow into macrocracks. As this takes place, a brittle fracture occurs along one microcrack that develops most intensively.

[00193] Adsorption of surface-active substances, causing wedging along a microcrevice, may accelerate the environmental attack. If hydrogen is formed in the corrosion process, it may be easily diffused into the metal. The metal embrittlement in the pre-fracture zone (deep in a crack) also accelerates the failure. In plastic deformation, the hydrogen diffusion into the metal along slip planes zones may accelerate. The metal embrittlement under hydrogen attack is explained by dislocation blocking by atomic hydrogen interstitial in the metal lattice.

[00194] Environmental aggression has a substantial effect on the corrosion-fatigue strength. For example, after testing the fatigue limit of wrought and high-strength aluminum

alloys, D16 and V95 respectively, is reduced by 3-45% in water and by 4-5 times in 3% sodium chloride solution.

[00195] The corrosion fatigue in electrolytes is a mechano-electrochemical process. Hence, the electrochemical protection such as a zinc protector and anodic metallic coatings (zinc, cadmium) is feasible. Cathodic metallic coatings (lead, copper) are quite effective only if these are continuous. The metal surface processing is also effective that results in compressive stresses in the surface layer.

[00196] Also known is Hydrogen Embrittlement of Metals, by B.A. Kolachev (Moscow, Metallurgia, 1985), which discloses that the change in mechanical properties as a result of hydrogen pickup is termed hydrogen embrittlement. Hydrogen pickup is especially detrimental to the properties of high-strength steels. During 2 hours of etching of high-performance steel 40 CrSiNi with strength of about 2000 MPa in 15% hydrochloric acid, the reduction of area is decreased from 47 to 0.63% and elongation from 10.1 to 1.65.

[00197] In predeforming, the long-term strength of the hydrogenated steel is reduced. Thus, for example with strength of 2000 MPa the hydrogenated steel may be subjected to delayed brittle fracture under stress of only 300 MPa. Delayed brittle fracture means the fracture of details or specimens awhile after applying static tensile stresses without further increase thereof. This is especially dangerous, since the fracture may begin without visible plastic deformation under stresses far below the tensile strength.

[00198] During hydrogen pickup of the stressed steel, a delayed brittle fracture, which was termed hydrogen cracking, may also take place. This is associated with increased embrittlement of steel due to the atomic hydrogen adsorption at its surface (Rebinder effect) or an increased hydrogen concentration in the region of maximum triaxial tensile

stresses. The time to cracking in hydrogen pickup depends on the level of applied tensile stresses: the greater the stresses, the shorter the time to cracking. The cracks forming during hydrogen cracking of high-strength steels are of a brittle nature and propagate along the boundaries of former austenite and their direction is almost perpendicular to tensile stresses.

[00199] In metals, hydrogen may be present: in lattice interstices, forming an interstitial solid solution; in pores, cracks and other irregularities in the form of molecules; in the form of chemical compounds with impurities; and/or in the form of chemical compounds with solvent metal - hydrides. The sources of hydrogen penetration in metals include original charge materials, environment where technical operations are carried out at all stages of metal obtaining and processing (melting, hot plastic deformation, welding, heat treatment); electrochemical processes such as metal deposition on the cathode, acid etching, etc. Molten metals absorb hydrogen very intensively. At elevated temperatures, hydrogen is absorbed by many metals even in solid state (e.g., titanium). Under hydrogen embrittlement conditions, the reduction in ductility may vary in a wide range: from percentages to almost complete loss of ductility. There is no unified hydrogen embrittlement mechanism. The steel susceptibility to hydrogen embrittlement depends on many factors such as the strength level and then the condition, composition and structure of steel, as well as properties of individual heats.

[00200] The hydrogen-induced change in properties is generally eliminated by hydrogen desorption from steel during maturing or annealing. However, in some cases, for example high-strength steels, as small as $5cm^3/100g$ content of hydrogen results in irreversible changes that remain upon removal of hydrogen.

[00201] The hydrogen embrittlement manifests itself as follows:

(1) Hydrogen corrosion - develops in carbon steels under long exposure to high-pressure hydrogen environment at high temperature. This is based on the interaction between hydrogen and carbon with methane formation. This reaction begins from the surface, resulting in decarburization and formation of cracks that gradually propagate into the metal, reducing the strength and ductility.

(2) Hydrogen disease - occurs as a result of the interaction between hydrogen diffused from the metal surface and oxygen or oxides dissolved in the metal. The resultant water vapors create microscopic discontinuities.

(3) Primary gas porosity - occurs due to hydrogen precipitates in molecular form in the melt or at the crystallization front.

(4) Secondary porosity - caused by decomposition of solid solutions oversaturated in relation to hydrogen with the formation of fine submicroscopic pores filled with hydrogen. These are smaller than the primary pores and have almost spherical shape.

(5) Reduction in impact strength and fracture toughness - occurs in metals wherein hydrates are formed.

(6) Delayed fracture - cracking resulting in premature failure typically of ductile steels when these are under constant loading which is less than the yield strength.

(7) Reduction in deformation resistance - for a number of metals, hydrogen causes the creep resistance to decrease at elevated temperatures. Under certain conditions this effect may facilitate the failure.

(8) Rupture cracks, flakes, "fish eye" - defects detected, in the main, in large forgings.

(9) Bubble nucleation - hydrogen penetrates into the metal from water-containing environments and accumulates

in a molecular form on defects, for example non-metallic inclusions, the metal continuity gradually deteriorating with increase in hydrogen pressure.

(10) Corrosion cracking - in many cases this is associated with atomic hydrogen release in corrosion reactions, its adsorption on the crack surface and dissolving in the metal with the development of hydrogen embrittlement.

[00202] Also known is Hydrogen Embrittlement of Metals, by L.S. Moroz and B.B. Chechulin (Moscow, Metallurgia, 1967), which discloses that the types of metal hydrogen embrittlement are very diverse. It is customary to distinguish two types of hydrogen embrittlement: (1) embrittlement of the first kind whose sources change in the original metal due to the increased hydrogen content until any application of stresses, and (2) embrittlement of the second kind caused by features that form in the metal with increasing hydrogen content during plastic deformation. There are many theories on hydrogen embrittlement. One theory holds that hydrogen embrittlement of steel is the result of the loss of the intercrystalline strength under pressure of hydrogen accumulated in submicroscopic and microscopic pores at grain boundaries.

[00203] Also known is Mechanical Properties of Metals, by M.L. Bernshtein and V.A. Zaimovsky (Moscow, Metallurgia, 1979), which discloses that creep is the property of the metal of being plastically deformed in slow and continuous fashion under some constant loading, chiefly at high temperature. Creep consists of two alternating processes - strengthening due to cold work and weakening due to recrystallization or rest at temperatures below recrystallization temperature. The following types of plastic deformation occur in metals at high temperature during creep: (1) sliding and slip (dislocation pattern), (2) twinning, (3) flexure mechanism, (4) lamellation, (5) rotation and relative movement of grains, (6) rotation and relative displacement of mosaic blocks, (7) cell

formation mechanism, (8) diffusion plasticity, and/or (9) recrystallization mechanism.

[00204] The hypothesis on the role of vacancies in the lattice during crack formation and propagation (vacancy migration and cloud) was widely accepted.

[00205] During creep, the intercrystalline fracture is observed when stresses are relatively small and the time to failure is long. Under such conditions, deformation accumulates chiefly at the expense of grain movements, i.e., intergranular plasticity. In that case the formation and accumulation of vacancies and eventually cracking should occur at grain boundaries.

[00206] The conditions for crack formation under high stresses and large creep rate are otherwise. In such cases, the time to failure is reduced and the dislocation-shear mechanism, developing in the grain body, acquires great efficiency. The resultant slip lines will play the same role as the grain boundaries in terms of vacancy accumulation and crack formation.

[00207] Thus, during creep the intercrystalline and transcrystalline failure of metals is caused by one and the same processes, namely, diffusion of vacancies, gathering thereof in clouds or close to pores, development of pores into a crack and finally the crack growth due to the influx of new vacancies.

[00208] The following microdefects are recognized:

(1) Mature pores and discontinuities formed during recrystallization.

(2) Pores nucleated by vacancy coagulation.

(3) Jog opening at grain boundaries as a result of slipping along the boundary. When the polygonization structure is present, in the formation of which the vacancy sink to dislocations is of considerable importance, pores are

not detected. If the substructure is hard to form, the pores are observed within a wide range of creep temperatures.

(4) Nucleation of pores and microcracks as a result of thermally activated breakdown of atomic bonds.
Under actual conditions of high-temperature failure, all defects referenced above, which promote pore nucleation and microcrack development, occur to a greater or lesser extent.

[00209] Erosive wear consists in detachment of solid particles from the body surface as a result of the body contact with a moving liquid or gaseous environment or particles entrained thereby or as a result of the impact of solid particles. The following types of erosion wear may be specified:

- in the flow of water without abrasive impurities and in the absence of cavitation, the wear may occur due to the liquid flow destruction of surface films developed on the metal because of the metal interaction with a liquid with oxygen dissolved therein;
- in the gas flow with abrasive particles; the gas environment may or may not interact with the metal - corrosion-mechanical wear or mechanical wear respectively;
- in the jet of solid particles.

[00210] Under volumetric loading, the plastic deformation processes are localized in a certain portion of the volume, where structural defects accumulate, the stress concentration occur and the fracture source nucleates. Under surface loading, the plastic deformation processes differ, preserving their dislocation nature, first of all by complex stress distribution over the entire contact zone. Throughout the surface layer and in any point thereof, the participation of all portions of metal in the contact zone in plastic deformation and fracture is equiprobable, resulting in stress deconcentration.

[00211] Another feature is that during wear, the plastic deformation and fracture cycles continuously overlap when the next cycles occur following the entrainment of the wear debris. During wear, the constitution and structure of a thin surface layer (possibility of film formation when interacted with external environment, high stress concentration and possible rise in temperature) may substantially differ from the structure of a metal in volume. Wear and tear is the process of the gradual change in body dimensions during friction, consisting of detachment of the material from the friction surface and/or residual deformation thereof.

[00212] Also known is Corrosion and Protection of Metals, by M.A. Shluger, F.F. Azhogin and E.A. Efimov (Moscow, Metallurgia, 1981), which discloses that radioactive emission (neutrons, protons, deuterons, alpha- and beta-particles and gamma radiation) has a significant effect on corrosion processes, which is felt in the nuclear and power industry. In most cases, radiation intensifies corrosion by 1.5-3 times.

[00213] A sharp increase in the corrosion rate can occur under radiation. The atmospheric corrosion rate of iron, copper, zinc, nickel and lead may increase by 10-100 times. Catastrophic corrosion, which is accompanied by cracking, develops in uranium alloys.

[00214] In water cooled reactors, hydrogen released during water oxidation of uranium diffuses into the metal. In a relatively short while, the crystalline structure breaks down due to the formation of local precipitations of uranium hydride. Hydrogen, which is added to water, may diffuse through a protective oxide film and interact with uranium. The resultant uranium hydride then reacts with slower diffusing water, producing, in its turn, more stable UO_2. Hydrogen being released may again react with the next portion of uranium. Uranium forms with water uranium dioxide $U+2H_2O = UO_2+2H_2$. Uranium forms with hydrogen uranium hydride $U+2/3H_2 =$

UH_3, which then reacts with water, producing uranium dioxide $UH_3+2H_2O = UO_2+3\ ½\ H_2$.

[00215] When a protective film is formed, hydrogen diffuses into the base metal, so the time during which the alloy cracks rather than the corrosion rate is of great importance in characterizing the corrosion resistance of materials. Based on the experimental data, radioactive emission has considerable effect on the kinetics of corrosion processes without a fundamental change in corrosion mechanism. The radiolysis effect is caused by irradiation on water and accelerates the cathodic process. This is observed in metals whose surface has no thick oxide films. The destructive effect consists in elastic and thermal interaction between the surface and radiating particles, resulting in defects in the metal surface layer and oxide film. This effect is hazardous for the metals whose corrosion resistance is governed by the formation of phase protective films (for example, for aluminum alloys). Also, this facilitates the anodic process and has the most profound effect on the corrosion rate.

[00216] Corrosion cracking and corrosion fatigue develop according to mechano-electrochemical mechanisms: crack development - electrochemical process, complete fracture - avalanche mechanical failure of the remaining section; in so doing the processes are accompanied by hydrogen embrittlement of the material at the crack tip. The difference is in load application: tensile loads during corrosion cracking and cyclic loads in the case of fatigue. The type of cracks on microsections and the type of rupture are different. Hydrogen embrittlement of a metal has many forms of manifestation - the effect of the porosity and hydrides on the impact strength prior to cracking at the expense of methane being formed or corrosion cracking and flakes (clouds of small cracks in forgings). Hydrogen may have an unfavorable effect on the creep process as well, causing premature failure of structures

operating under constant loading at elevated temperatures. During creep, the failure process is caused in most cases by crack formation due to vacancy diffusion and the growth of porosity into microcracks.

[00217] Thus, degradation of the material or structures provides the process of the irreversible change in properties thereof, resulting in cessation of functioning of a component or structure and safety violation of their further service. All multiple types of damage, occurring due to material degradation and resulting from various process mechanisms, are divided into the following groups: local and extensive corrosive damages, single and multiple cracks, microcracks, pores at grain boundaries and substructures, mechanical wear and change in surface relief, creation of residual stresses, and change in mechanical and physical properties.

[00218] The operational factors, which lead to degradation and have separate or combined effect, may be divided as follows: contact interaction with the external environment, static stresses, low- and high-cycle stresses, interaction with active external environment in non-electrolytes or electrolytes, constantly high (or low) or cyclically changing temperature, and exposure to radiation. Degradation mechanisms causing the above types of damage are grouped as follows: corrosion cracking, hydrogen embrittlement, corrosion fatigue, mechanical fatigue, chemical corrosion, electrochemical corrosion, erosion, creep, and radiation embrittlement.

[00219] All these mechanisms differ in nature (chemical interaction between the component material and external environment during corrosion, anodic dissolution of the component material in the process of electrochemical corrosion, penetration of the atomic hydrogen in a lattice of the component material and reduction in bonding energy between metal atoms during hydrogen embrittlement, intensive

dislocation multiplication with subsequent formation of slip bands and development of microcracks in the process of fatigue, sliding, dislocation slip, twinning, etc. during creep, metal atom ionization that weakens bonds in a lattice during radiation embrittlement, synergetic effects during erosion, corrosion cracking and corrosion fatigue), but one common thing is that the atomic bonds are weakened or disturbed in the original lattice of the material of a component or a structure and hence their performance are deteriorated.

[00220] Various means of prevention and suppression of degradation are known. For example, known in the art is Materials Degradation and Its Control by Surface Engineering, by Andrew William Batchelor, Loh Nee Lam & Margam Chandrasekaran (World Scientific Publishing Co., 1999, p. 408, ISBN 1-86094-083-8), which discloses the various forms of damage occurring in all significant engineering materials, and both traditional and modern technologies of surface engineering for combating materials degradation. Scientific concepts are illustrated graphically, wherever possible, by numerous diagrams in order to maximize understanding. Materials degradation studies – concerning corrosion, for example – have traditionally been divided into separate disciplines for each type of material. The control of materials degradation is usually studied as a separate topic, such as corrosion and paints.

[00221] Also known is Assessment of Service Induced Microstructural Damage and Its Rejuvenation in Turbine Blades, by Koul, A.K.; Castillo, R. (Metallurgical Transactions A. 1988, Vol. 19A, No. 8, pp. 2049-2066), which discloses correlations between service induced microstructural degradation and creep properties in investment cast IN738LC turbine blades. Microstructural degradation in the form of gamma prime coarsening, MC carbide degeneration, formation of

continuous networks of grain boundary $M_{23}C_6$ carbides, and the disappearance of serrated grain boundaries are considered in some detail. Results from mathematical relationships are able to reveal service induced degeneration effects and can therefore be used to qualify rejuvenated blades. A systematic strategy for designing a hipping rejuvenation cycle for Ni-base superalloys is disclosed. Once a rejuvenation cycle is designed, the mathematical relationships can then be used to analyze the extent of the rejuvenation of microstructure and creep properties in reheat-treated or hot isostatically pressed service exposed turbine blades. The influence of trace amounts of Zr on creep properties of service exposed IN738LC turbine blades is also disclosed.

[00222] Also known is Repair of Air-Cooled Turbine Vanes of High-Performance Aircraft Engines - Problems and Experience, by P. Brauny; M. Hammerschmidt; M. Malik (Materials Science and Technology, 1985, Vol. 1, No. 9, pp. 719-727), which describes the air cooled turbine vanes made from nickel-base and cobalt-base superalloys that undergo distortion, cracking, burning, and material degradation in operation. The complex geometry of the parts and the compositional and microstructural heterogeneity of cast alloys impose limitations on the selection of repair methods. Selective chemical stripping of the diffusion coatings; elimination of cracks and restoration of dimensions by joining processes involving both welding and brazing techniques; and formation of coatings by pack cementation are the major processes employed. These processes may give rise to defects that significantly diminish the integrity of the parts.

[00223] Also known is Integrating Real Time Age Degradation Into the Structural Integrity Process, by Craig L. Brooks and David Simpson (NATO RTO's Workshop 2 on Fatigue in the Presence of Corrosion, Corfu, Greece, 1998), which discloses a process for incorporating the "age degradation" aspects of

aircraft into the existing infrastructure of the design, manufacturing, and maintenance of aircraft systems. The tailoring of the structural integrity process enables the industry and the user communities to meet the needs, opportunities, and challenges being presented by the Aging Aircraft Fleet. The economic and safety impact of the continued use of some aircraft necessitates an enhancement to the existing system. The rationale, approaches, and techniques to evolve the structural integrity process to include the effects of corrosion, sustained stress corrosion cracking, and other age related degradation effects is also disclosed. A viable method of utilizing the proposed approach is presented in a fashion to realize benefits throughout the full life cycle of aircraft systems.

[00224] Also known is Evaluation of Degradation Degree of Metal in Gas Pipelines, by E.E. Zorin, G.A. Lanchakov and A.I. Stepanenko (Gas Industry, No. 4, 2003), which addresses the development of the express diagnostics of the metal degradation degree in main pipelines. A great number of scientific works is devoted to the investigation of the scattered fatigue failure of metals. However, the physical methods of studying a metal structure at the phase of main crack nucleation do not allow devising an engineering express diagnostic system that would make possible a reliable prediction of the limiting state instant based on the changes in structural state properties and hence the life of structures.

[00225] The methods of designing shell structures and evaluating life time under non-stationary loading, which are based on the linear fracture mechanics criteria, have made good showing in the case of items with a wall thickness of more than 80-100 mm under controlled loading conditions. However, most oil and gas pipeline systems are made of two-phase ferritic-pearlitic steels with a wall thickness of at

most 25 mm. The instant of limiting state cannot be predicted for such structures for a number of reasons. Thus, for example, during a reshaping process cycle the material is subjected to significant plastic deformation and thermomechanical effect that may not be completely controlled. Steel of one grade composition may have essentially different metallurgy. For laminated materials, it is difficult to find the crack initiation conditions in actual structures in accordance with the criteria of the linear fracture mechanics.

[00226] Under variable loading conditions, the technical examination of welded structures in low and average strength steels should constitute the process of registering the accumulated damage (defect, foreign inclusion, discontinuity) in the metal volume being examined with simultaneous obtaining of the failure resistance parameters. Under any type of variable loading, a plastic hysteresis loop in stress-deformation coordinates and cyclic creep are registered in the material. The availability of damage stimulates plastic deformation in local volumes of metal and increases the closed plastic hysteresis loop parameters. The area of the loop is equal to the energy dissipated in the material, while its width equals non-elastic deformation per cycle. The development of local plastic deformation gives rise to new discontinuities and hence the damage density within unit volume of metal increases.

[00227] In total damage, D_{Σ}, two levels may be arbitrarily noted: hereditary density of damage D^1_n stemming from the metal quality and acquired density of damage D^2_{Σ} which is the function of the hereditary damage occurred during metal reshaping in manufacturing a structure and its operating conditions. It is natural that the first level of damage will control the intensity of the second level increment.

[00228] Despite considerable achievements in studying crack development using fracture mechanics criteria, the entire

process of the main crack development cannot be described unambiguously. This is explained by that the fracture mechanics criteria are usable when the crack is large (in the field of the stresses of the first kind) with sizes hundreds of times greater than those of structural components of metals. To develop an engineering express diagnostic method, one had to develop a model of formation of defects of certain length at the main crack nucleation stage by the example of two-phase ferritic-pearlitic steels.

[00229] The actual materials feature the combination of typical linear scales linked with different levels of their structure, micro- and macrotexture. The need to take account of the material structure in describing the deformation and fracture processes is essential in the fracture mechanics. According to one classification, of highest interest are the defects of 7-10 categories, i.e., 10^{-5}-10^{-4} m long, which are comparable with sizes of structural components.

[00230] The necessity and sufficiency principle has been formulated to be used as a basis of the express diagnostic methods being developed for a structure during service: the structural material volume being diagnosed shall be sufficient to reflect how the reshaping and manufacturing technique, service conditions, which cause the main crack formation, affect the material. In this case, by the main crack is meant one of existing microcracks, which under given conditions develops at a greater rate compared to the remaining cracks and causes the controlled failure of the structure.

[00231] The structural element, i.e., the grain may present the necessary and sufficient volume of metal, while microhardness measurement on the surface of the object being diagnosed may be an instrument recording the changes in physical-and-mechanical properties of structural elements subjected to reshaping technology and loading conditions.

[00232] If a specimen rigidly fixed along the contour is taken as a structural element and the indenter impression process is represented as an external loading, the microhardness measuring results will objectively reflect the mechanical properties, the stressed-deformed state and the presence of damage (microcracks) in a structural element. The combination of the microhardness data, i.e., the completeness of the sufficiently large data selection will make it possible to characterize the condition of the metal volume being diagnosed.

[00233] Since the optical observation of the impression is not possible in field conditions, there are necessary and sufficient array and microhardness measuring pitch available (60-80 impressions with 0.02 mm pitch for ferritic-pearlitic steels). The load on the indenter is chosen from the range, wherein the Kirpichev-Kick-Davidenko's impression similarity condition is not available for steels of this structural category.

[00234] In order to interpret the results obtained, the following model has been suggested: each microhardness measuring result obtained from the unit surface is processed in accordance with the method of one of three variations:

(1) The indenter gets into the structural element that does not have microcracks along the contour; the adjoining structural elements of the first row are also not damaged. In this case, the basic microhardness value of the element is observed.

(2) The indenter gets into the structural element that does not have microcracks, which however are present in adjacent volumes. Then the stress and strain redistribution caused by the discontinuity in a unit volume results in contact strengthening of the element being diagnosed as a results of additional triaxial deformation. In this case,

recording is made of the increases microhardness value that increases with the level of local stresses and deformations.

(3) The indenter gets into the structural element that has microcracks at boundaries. When the diamond pyramid is impressed into the grain body, the microcracks have time to develop as the indenter movement speed is substantially lower than the microcrack development rate in a given volume under additional deformation from the indenter. The volume continuousness is broken and the microhardness drops abruptly.

[00235] When the microhardness is successively measured at certain service intervals in regions of one and the same processing or structural stress concentrators, an increase in percentage of new selection of "strengthened" and "weakened" structural elements is registered. Ferritic-pearlitic steels of low and average strength do not virtually have phase transformations that may result in an abrupt drop or increase in grain microhardness, if this is not caused by the transcrystalline failure or local strain hardening in the field of the stresses of the second kind. The percentage change dynamics for "strengthened" and "weakened" grains in a microhardness measurement sample on the surface of the object being diagnosed will indicate the reduction in macro-failure resistance of the metal of the structure in service.

[00236] The mechanism of the failure nucleation and development in the metal of the structure in service at the structural level may be presented as follows:

a) development of the existing "inherited" microcracks and structural defects up to sizes comparable to the grain length, appearance of new microcrack nuclei, development of general loosening of the structure;

b) variation and growth of the gradients of the field of stresses of the second kind (stresses equilibrated at the grain level) and formation of new high stress concentration regions;

c) nucleation of service microcracks (damage) in stress concentration regions with further growth, merging and transformation from micro to macrocracks when failure covers grain blocks. This failure development stage in the metal of the structure cannot be correctly reflected by the micro-impression process, since the further crack growth is governed to a greater extent by the field of stresses of the first kind, equilibrated within the structure (operating, welding stresses, etc.).

[00237] Hence, the completeness of the microhardness data selection may indicate the degree of reduction in load-carrying capacity of the material, i.e., record the onset of necessary and sufficient conditions for main crack formation in the metal volume under examination under current loading conditions. If the completeness of the microhardness measurement data selection is presented in the form of bar charts where data are distributed along the microhardness scale, then the bar charts for the current instant of service will be shifted relative to those for initial condition of the material.

[00238] Damage accumulation coefficient k_p is a quantitative criterion to compare microhardness distribution bar charts: $k_p = K_p/K_p^o$ where K_p, K_p^o are the reduced frequency of the microhardness distribution bar chart at the current instant of service and in initial condition. The reduced frequency is calculated from the bar chart as a sum of individual frequencies allowing for weighting coefficients, a_j, that allow uniform consideration of the contribution (value) of each interval of the microhardness data.

$K_p=\Sigma a_i f_j$ where $f_j = n_j/N_j$ - the frequency of an individual interval of the microhardness data. Herein, $N = \Sigma n_j$ - the total number of grains; n_j - the number of the results in a given interval of microhardness data.

[00239] The design method for weighting coefficients, a_j, is based on the linear approximation of the distribution diagram from 0.1 to 1.0. The weighting coefficients should be calculated preserving the numeration of intervals for initial condition bar chart.

Table 5

Specimen cut direction	Characteristic	Pipe metal		Change of Character-istics, %
		Emergency stock	20 years of service	
Across pipe (rolling)	σ_{TS}, MPa	560	650	+16
	σ_{YS}, MPa	450	570	+27
	Δ, %	22	18	-18
	KCV_{20}, MJ/m^2	1,8	1,4	-22
	KCV_{-40}, MJ/m^2	1,7	1,0	-41
	KCV_{-75}, MJ/m^2	0,19	0,04	-78
Along pipe (rolling)	σ_{TS}, MPa	600	650	+8
	σ_{YS}, MPa	470	550	+17
	δ, %	23	22	-4
	KCV_{20}, MJ/m^2	1,6	1,4	-12
	KCV_{-40}, MJ/m^2	1,5	0,8	-46
	KCV_{-75}, MJ/m^2	0,1	0,02	-80

Note: The scatter of σ_{TS} and σ_{YS} is 25 MPa, impact strength KCV - 0,2 MJ/m^2 at T_t = 20°C and 0.01-0.07 MJ/m at subzero temperatures.

[00240] The reduced frequency of the microhardness measurement bar chart of the in-service metal, K_p, increases on a constant basis, while the damage accumulation coefficient, k_p, is always greater than 1 and also increases.

[00241] The controlled rolled steel pipes from Urengoi gas-condensate field were selected for study. The mechanical properties of emergency stock pipes were compared to those of pipes after 20 years of service. The metal of the pipes was close in chemical composition and mechanical properties to the steel of strength grade Cr65. The metallographic analysis of specimens cut from portions of pipe after 20 years of service

showed that the metal has no cracks detectable by non-destructive examination methods.

[00242] During impact test of controlled rolled steels specimens after prolonged service within a wide temperature range (from +20 to -75°C), the failure resistance reduced significantly both in terms of energy, spent for nucleation of the main crack from the notch, and the distribution energy compared with the properties of the emergency pipe specimens as shown in Table 5. After prolonged service, the strength properties (yield strength and tensile strength) of the gap pipeline metal increased somewhat, while the plasticity and ductility properties (elongation and impact strength) decreased. Attention should be given to the pipe metal properties anisotropy along and across rolling. In the material after long service, the change rate of all mechanical properties across rolling is greater than those along rolling.

[00243] FIGURE 12 shows the completeness of the surface microhardness measurement selection for portions of emergency stock pipe and pipe after about 20 years of service. After 20 years of service, the array of the microhardness data shifts to the left, the lower data side. This is testimony to the severe damage of the pipe metal. Quantitatively, the changes in completeness of the selection of the microhardness data obtained on the surface of the pipe portion after prolonged service are characterized by the damage accumulation coefficient k_p= 3.604.

[00244] Note that under accumulating service damage conditions such a substantial microhardness shift to the lower data side is observed only in controlled rolled steels and this is not typical for other examined steels of this structural type (steel 3, 20, 10, 09Mn2Si). The latter (and the welded joints thereof) are characterized by a more uniform change in a selection completeness, i.e., the damage accumulation is accompanied by the simultaneous growth of the

percentage of the abnormally high and abnormally low microhardness data in a selection; the growth of the abnormally low data are recorded only at the final stage. This may be due to the manufacturing technique used for controlled rolled steels. As early as at the plate production stage, the metal matrix is subjected to substantial residual plastic deformation. The realization of a plastic hysteresis loop in a crystalline material under non-stationary conditions requires that the metal matrix be subjected to contact strain hardening to withstand the microcrack development. If the deformation capability of the material volume is exhausted and stress relaxation at the progressive crack tip is impossible, the crack breaks it and continues to grow, accumulating the potential energy. This process of prevalent loosening of controlled rolled steel is recorded, under prolonged service loading without substantial strain hardening, in processing the completeness of the selection of the microhardness data obtained on the surface of the object under examination.

[00245] A conclusion can be drawn from the studies that microhardness may be measured on the surface of the object being diagnosed in the area of the structural-processing and service stress concentrators in order to evaluate the metal degradation degree and establish the correlation relationships between the completeness of the microhardness data selection and the resistance properties of the macro-failure nucleation and development in a structure.

[00246] Also known is Effects of Mixed Metal Addition on Surface Film and Corrosion. Prevention of Stainless Steel in BWR Water, by Takeshi Sakai, Yoshiyuki Saitoh, Yuuji Midorikawa and Teruchika Kikuchi (9th International Conference on Environmental Degradation of Materials in Nuclear Power Systems-Water Reactors, 1999), which provides the results of the application of a mixed metal addition to the primary water reactor. As an alternative technique to zinc injection into

BWR water, mixed metal addition has been developed. Mixed metal addition uses a compound of manganese, nickel, magnesium and small amount of natural zinc. Zinc concentration is decreased to the permissible limit that does not increase the radiation buildup of activated Zn-64, i.e., less than 1ppb according to the analysis of reactor water at Onagawa-1, and a synergistic effect of mixed metal elements to reduce corrosion and radiation buildup on stainless steel surfaces is expected. In the current study, high temperature autoclave testing was performed to investigate the effects of mixed metal addition on the oxide film characteristics and the corrosion of stainless steel in the simulated BWR environments. The results suggest that the mixed metal addition could be an alternative technique to zinc single injection.

[00247] Also known is Microstructure and Evolution of Mechanically-Induced Ultrafine Grain in Surface Layer of Al-Alloy Subjected to USSP, by X. Wu, N. Tao, Y. Hong, B. Xu, J. Lu, K. Lu. (Acta Materialia, 2002, No. 50, pp. 2075-2084), which provides the results of the investigation of the ultrafine-grained (UFG) microstructures in the surface layer of an aluminum alloy 7075 heavily worked by ultrasonic shot peening (USSP) by means of high-resolution transmission electron microscopy (TEM) to understand the microstructural evolution and grain refinement mechanism associated with formation of structures.

[00248] Ultrafine-grained (UFG) materials have attracted significant scientific interest. These materials are structurally characterized by very fine grain size (nano- and submicron-order) and large amount of grain boundary area (and volume). UFG materials have unusual and extraordinary mechanical and physical properties that are fundamentally different from, and often far superior to those of their conventional coarse-grained polycrystalline counterparts. Severe plastic deformation (SPD) is an effective processing

method for the fabrication of various UFG structures by imposing intense plastic strains into metals and alloys. The production of UFG materials by SPD offers two significant advantages over other techniques such as inert gas condensation, high-energy ball milling, and sliding wear. First, it is possible to produce large bulk samples. Second, these samples are free from any residual porosity and contamination. The resultant microstructures introduced by SPD are substantially grain refined along with high internal stresses and high-energy nonequilibrium boundaries. Several techniques are now available for producing the requisite high plastic strain of the order of several hundreds of percent, including equal-channel angular pressing (ECAP), high pressure torsion (HPT), multipass-coinforge, multi-axis deformation, and repetitive corrugation and strengthening (RCS).

[00249] The understanding of the microstructural evolution mechanism involved in SPD is an essential issue of the research topic having great importance from academic and technological points of view. The mechanism should account not only for the grain refinement but also for the generation of high-angle boundaries with increasing strain. Previous investigations have demonstrated that during repetitive deformation, the grain size refinement is most pronounced at the initial stage of the process, for example low and medium strain, and remain virtually unchanged upon further straining. However, at large strains, boundary misorientations dominate. Exposure of deforming surfaces to random and multidirectional deformation could effectively enhance evolution of low-angle boundary misorientations into high-angle ones. Recent studies reported the grain refinement associated with the slip systems and their interactions. Ultrafine dislocation cells enclosed by planes are produced by operation of multi-slip systems during ECAP. The generation of ultrafine subgrains resulted from the piling-up of dislocations along the glide planes

during RCS. However, the mechanism underlying the grain refinement itself during SPD is less developed to date. Even though most investigations have described changes of the microstructures and mechanical properties, they could not reveal the microstructural response to the dynamic plastic straining and hence, could not clarify the relation of UFG structures to plastic straining.

[00250] The principle of the USSP technique was as follows. A high-energy ultrasonic generator of high frequency (20 kHz) vibrated the reflecting chamber where the stainless steel shots of 7.5 mm diameter resonated. The shots then performed repetitive, high-speed, and multi-directional impact onto the surface of materials. Resultantly, severe strains were imparted into the surface by contact loading. A strain gradient changing from zero far into the matrix to the maximum at the top surface will simultaneously be established. Details of the equipment were reported in previous articles. In the present investigation, the USSP processing was conducted under vacuum at room temperature for 15 minutes.

[00251] Microstructural investigations have revealed that the USSP process can introduce UFG structures in the surface layer of materials. The closer the distance from the top surface of the layer, the finer the grain size, due to the increment of strain over the whole deformed layer. Three levels of grain sizes are present: (1) parallel, extended microbands (MBs) with interior elongated subgrains and cell blocks (CBs) (first level), (2) equiaxed, submicro-grained structure (second level), and (3) equiaxed, nano-grained structure (third level). As the top surface is approached, the grains appear finer, more equiaxed, more misoriented, and more uniformly distributed.

[00252] Dislocation gliding, accumulation, interaction, tangling, and spatial rearrangement cause grain subdivision in

order to accommodate plastic strains during deformation in polycrystalline materials.

[00253] The repetitive USSP could impart high strains of high strain rates into the surface layer. Severe plastic straining could produce a high density of dislocations, which are effective at blocking slip at increasing strains and as a result, the mechanism responsible for accommodating large amounts of plastic straining is to subdivide original grains into subgrains with dislocations forming their boundaries. The subdivision of grains takes place on a macroscopic scale with the formation of MBs at low strains. With further straining, subgrains may further break up into smaller CBs. The submicro- and nano-sized subgrains could be produced under much larger strains.

[00254] By performing repetitive USSP, very high strains may be achieved. Note that dislocations of high density are always present in deformed structures of various grain sizes. Simultaneously, low angle boundaries are produced, which means new boundaries are being continuously formed during the deformation. With increasing strain, the microscopic subdivision takes place on a finer and finer scale. Resultantly, the process of structural refinement could conduct successively into submicro- and nano-meter regime.

[00255] The multi-directional peening may lead to the change of slip systems with the strain path even inside the same subgrain, much different from the deformation mode caused by other SPD processes. The dislocations not only interact with other dislocations in the current active slip systems, but also interact with inactive dislocations generated in previous deformation. This will promote the formation of subgrains. As a consequence, the effectiveness of grain refinement is enhanced.

[00256] The development of equiaxed, highly misoriented grains consists of two steps, i.e., the formation of subgrains

through grain subdivision and the subsequent evolution of boundary misorientations. The subgrains resulted from the grain subdivision, however, have a critical size before leveling off, relevant to a certain value of straining. The grain subdivision does not continue indefinitely, and eventually, after a given amount of deformation, the continued straining can no longer reduce the subgrain size. At this stage, since the dislocation movement is more strongly restricted, slip systems within adjacent subgrains will be activated in response to applied straining in order to rotate those subgrains into a more energetically favorable orientation. Shot peening provides the multi-directional strain path and high strain rate, which are especially effective at promoting subgrain rotation. The mechanism for the development of high misorientations should be the subgrain rotation. Therefore, the accumulated rotation of subgrains appears to be the primary mechanism as a means of accommodating further deformation, resulting in highly misoriented, equiaxed grains.

[00257] Deformation of subgrains is controlled by the activation of slip systems, where the critical resolved shear stress has been achieved. During plastic straining, different slip system combinations would be activated in each individual subgrain. Adjacent misoriented subgrains will have different activated slip systems because of their different orientations. Certain slip systems will be selectively activated to minimize the internal energy in the subgrain. The adjacent misoriented subgrains will rotate into coincidence to minimize the energy across the sub-boundaries under the driving force of the selectively activated slip systems. With increasing strain, subgrains can no longer accommodate deformation by dislocation glide along the same slip systems and, therefore, begin to rotate independently. The rotation angles increase, eventually becoming highly

misoriented grains. As compared with other SPD processing methods, USSP produces a high strain rate, which plays a significant role in lattice rotation during deformation. The high strain rate results in significantly higher flow stresses for an equivalent increment in strain relative to low strain rates. Computer simulation revealed that the higher strain rates promote lattice rotation in simple shear to a greater extent than lower strain rates due to the reduced plastic spin component and the great number of activated slip systems. It is observed that the average misorientation angle between the subgrains increased for the same strain, with an increase in strain rate from $6x10^{-6}$ to $6x10^{1}$ s^{-1} during tension of pure aluminum.

[00258] Accordingly, USSP provides a simple and effective procedure for producing a UFG structure on the surface layer of aluminum alloy 7075. The development of microstructures during the USSP process is characterized by the sequence of elongated microbands (MBs) with dislocation cells (DCs), equiaxed submicro- and nano-grains, respectively, with increasing straining. The grain refinement and microstructural evolution during the process of USSP is as follows. During plastic straining, the formation of subgrains through grain subdivision occurs in order to accommodate the strain. The highly misoriented boundaries are generated by the subgrain rotation for accommodating further deformation.

[00259] Also known is The Effect of Controlled Shot Peening and Laser Shock Peening on the Fatigue Performance of 2024-T351 Aluminium Alloy, by C.A. Rodopoulos, J.S. Romero, S.A. Curtis, E.R. de los Rios, P. Peyre (Journal of Materials Engineering and Performance, 2003, 12(4), pp. 414-419), which discloses the influence of shot peening, laser shock peening and dual (shot and laser peening) treatment on the fatigue behaviour of 2024-T351. Tests showed a fatigue life improvement in all three cases with laser shock peening and

dual treatment displaying superior fatigue performance than shot peening. Fractographic analysis showed that the relatively poor performance of the shot peening is caused by ductility loss.

[00260] The potential of using surface engineering techniques, such as controlled shot peening (CSP) and laser shock peening (LSP), to improve the fatigue resistance of monolithic materials has long been recognized by the automotive and the aerospace industry. The beneficial effect brought about by CSP and LSP derives mainly from the generation of a stable compressive residual stress profile and strain hardening in the near surface region. Compressive residual stresses are the more important of the two in the case of high strength materials. However, in softer materials, strain hardening dominates since partial or complete relaxation of the residual stresses may occur. Strain hardening has been reported to decelerate microcrack growth but to accelerate long crack propagation due to low residual ductility. In high strength materials however, the beneficial effect of the compressive residual stress can be compromised by the development of subsurface cracking, usually in the regions where tensile residual stress balances the compressive residual stress field. Subsurface cracking may even be detrimental in smooth fatigue specimens or in components where, surface initiation is not considered to be the critical nucleation site. Roughening of the surface is the major detrimental effect of CSP. Surface roughness, owing to the local intensification of the far-field stress, can account for the premature initiation and propagation of short fatigue cracks.

[00261] The latter indicates that the application of surface engineering to improve fatigue resistance is not straightforward and that there may be cases where surface engineering can even have the opposite effect. To establish

with certainty the conditions under which CSP and LSP would produce beneficial results, an investigation of these surface treatments in terms of the fatigue resistance of 2024-T351 aluminium alloy, was undertaken.

[00262] Controlled shot peening was performed using a Tealgate peening machine. The peening intensity was 4A and it was achieved using a S110 (diameter 0.279 mm and hardness 410.5-548.5 Hv) spherical cast steel shot, incidence angle of 45° and a coverage rate of 200%. These conditions were recommended in a study of maximum, near surface, residual stress profile to counterbalance the increased surface roughness profile.

[00263] Laser shock peening was performed in water confinement using a Continuum YAG Laser (Powerlite plus) operating in the green wavelength (0.532 μm) regime. The output energy was approximately 1.3 J with pulse duration in the 6-7ns regime. All specimens were protected from the thermal effects of LSP by a 70 μm aluminum coating. The laser intensity was set to 10GW/cm^2 (estimated pressure of 5 GPa) with a focal point of 2 mm. The specimens were treated using an overlapping rate of 50% (1 pass=4 local pulses) and charged with 2 to 3 passes.

[00264] The results indicate that the two LSPs and the dual treatment can significantly increase the fatigue life of the material independently of their original surface finish. The dual treatment, however showed an inferior performance compared to the single LSP treatment, which confirms findings made about low residual ductility. On the other hand, life improvement due to CSP is only realized when compared to the EDM finish. Compared to the mirror finish, CSP appears to have little effect on fatigue life. The poor performance of CSP is even more noticeable in the near 5M cycles mark. To explain this performance, a theoretical analysis suggested was

used. According to that work, part of the residual stress profile is used to counterbalance the increased roughening of the surface (amplified nominal stress). For the selected CSP treatment and the corresponding K_t, the analysis suggests a counterbalance residual stress between 90-125 MPa within the first 50 μm of depth for applied stress levels between 220-300 MPa. The above, indicates that the remaining part of the residual stress profile should give some fatigue life increase.

[00265] To assist in the interpretation of the test data, an extensive fractographic analysis was performed. Fracture surfaces were examined using a Camscan Mark 2 SEM. Prior to examination, the surfaces were ultrasonically cleaned in an alcohol based solution. FIGURES 13-18 show the crack nucleation site and early crack growth of all six test groups at a maximum stress of 300 MPa.

[00266] More particularly, FIGURE 13 shows surface crack initiation and crack growth of pristine material with mirror finish. The fractograph clearly indicates the faceted growth (shear mode growth). FIGURE 14 shows surface crack initiation and crack growth of pristine material with EDM finish. The near surface region shows evidence of multiple crack nuclei, possibly caused by the irregular surface. FIGURE 15 shows the site of corner crack initiation and crack growth morphology of a S110-200%-45° CSP specimen. The faceted area extends to a depth of approximately 150 μm. The faceted area is surrounded by cleavage like fatigue fracture. FIGURE 16 shows crack initiation and crack growth of LSP 10GW/cm^2 (2 passes). The fractograph indicates surface crack initiation and crack branching at 50 μm. The propagation path of Crack B is almost parallel to the direction of stress. FIGURE 17 shows crack initiation and early crack growth of LSP 10GW/cm^2 (3 passes). The fractograph indicates surface crack initiation and crack

branching at 90 μm. The propagation path of Crack A is almost parallel to the direction of stress. FIGURE 18 shows crack initiation and early crack growth of dual treatment. The fractograph indicates surface crack initiation from a typical shot peening dent. Crack branching is also evident.

[00267] The lack of surface stress concentration features in the specimen with the mirror like finish, leads to a single crack nucleus (possible at an inclusion) and to a surface crack of an almost semi-circular shape (see FIGURE 13). On the other hand, the rough surface of the EDM finish promotes multiple crack nucleation sites which join at an early stage and the crack adopts an elongated semi-elliptical shape (see FIGURE 14). The fracture surface of the 4A CSP shows limited faceted crack growth and extensive evidence of cleavage like fatigue growth which can not be explained by the faster growing corner crack. The above reinforces the initial assumption of ductility loss. Ductility loss can be attributed to a very high and irregular dislocation density in the near surface region caused by work hardening. In the case of LSP, the fracture surfaces indicate branching of the crack. In both cases (2 passes or 3 passes), a part of the crack was observed to propagate almost parallel to the direction of the stress indicating slow crack growth rate. Close examination of the crack paths and the corresponding residual stress profiles, indicates the tendency of the "parallel" crack to propagate along the minimum in the residual stress profile. On the other hand the "perpendicular" crack shows an extensive amount of faceted growth, especially in the case of 2 passes. The dual treatment shows evidence of fracture more similar to LSP (crack branching). In contrast to CSP, the dual treatment shows no evidence of cleavage like fracture.

[00268] Considering that, both the CSP and the dual treatment provided strain hardening of the near surface layer and also that only the CSP showed evidence of ductility loss,

it is assumed that in the case of the dual treatment the residual stresses, created by the LSP, compensated for the possible ductility loss by possible rearrangement of the near surface dislocations. This could imply that the poor fatigue performance of the CSP material is possibly due to the partial relaxation of the residual stresses. Herein, it is important to note that residual stress relaxation is time and stress level dependent. Thus, a better understanding could be obtained by relating the residual stress relaxation pattern to crack length.

[00269] Fatigue data showed that, even though all treatments (CSP, LSP and dual) improved fatigue life, the LSP and dual treatment had a far more superior performance. Fractographic analysis indicated that this was due to the phenomena of ductility loss and possible residual stress relaxation experienced by the CSP and not by the LSP and dual treated specimens.

[00270] In summary, the following conclusions can be drawn:

(1) CSP, LSP and dual treatments are expected to increase the fatigue life of poorly machined components and thus reduce the production cost;

(2) LSP was found to cause negligible strain hardening as in the case of CSP and dual treatment;

(3) LSP and dual treatments exhibit a far more superior fatigue improvement compared to CSP;

(4) Ductility loss due to strain hardening and possible residual stress relaxation is possible in CSP and requires further research; and

(5) Pre-stressing the material (dual treatment) can increase the magnitude of the residual stress profile while at the same time stabilizes the residual stresses.

[00271] Also known is Basic Metallurgy, by G.A. Kashenko (Moscow, Mashgiz, 1957), which discloses that the crystalline state of metal is defined by the ions arranged at known

distances from each other and bonded by free electrons. The atom positions represent so-called lattice points. The arranged points may form various geometric figures, providing a lattice with a specific configuration. The space that each lattice takes may vary and the lattice volume may be arbitrarily large. To characterize the lattice, its smallest portion may only be explained in the form of an elementary figure that, when duplicated, constitutes the entire lattice. This smallest lattice is termed a unit lattice or unit cell which generally defines the type of each lattice.

[00272] For crystals, the following crystal systems are established depending on the slope of the coordinate axis and relative length of parameters: cubic, tetragonal, rhombic, monoclinic, etc. Aluminum, for example, has face-centered cubic lattice (the metals with this type of lattice are generally well susceptible to plastic deformation), iron has face-centered cubic lattice and body-centered cubic lattice. The cubic lattice is characterized by that all the angles between axes are 90°, all parameters being the same. The typical figure of the polyhedron is cube. The variations of cubic lattice include space-centered (or body-centered) lattice, which differs from a simple cubic lattice by that in addition to atoms at corners of a cube, it has one atom in the center of the cube, as shown in FIGURES 19 and 20, and face-centered lattice, which has atoms located at each of the corners and the centers of all the cubic faces, i.e., presents the cube with centered faces, as shown in FIGURES 21 and 22. Additionally, FIGURES 19 and 20 show body-centered lattice in lattice form and in cell form, respectively. FIGURES 21 and 22 show face-centered lattice in lattice form and in cell form, respectively.

[00273] Thus, each metal-element is a crystalline body or crystal. The geometric regularity of the particles arrangement in crystalline bodies imparts some characteristics

thereto that distinguish them from non-crystalline or amorphous bodies. First, anisotropy or vectoriality implies the difference of properties according to the direction. Another characteristic of crystalline bodies is the existence of slip planes or cleavage, along which the particles slip or detach under mechanical action upon the crystal. This breaks the crystal (if brittle) or deforms it, i.e., changes the exterior form non-destructively.

[00274] In the first case, the fracture of metal piece has clear planes, along which the crystals break more easily. Such planes are termed cleavage planes, as shown in FIGURES 23-25. When no failures happen and the crystal is deformed only, this results from particles slipping along slip planes.

[00275] Metal crystallization from liquid always begins when this is overcooled and crystallization centers are available. This results in crystalline formations of different types. In some exceptional cases, a geometrically regular full-weight or full-face crystal may form. However, this requires certain favorable conditions. Typically, the crystals are formed of irregular exterior shape and therefore termed crystallites.

[00276] There are two types of crystals. In one case, the exterior shape, which approximates more or less to the geometric regularity of the polyhedron, takes a rounded shape. Such crystals are termed grains or granules. In another case, crystalline formations have a branching shape with unfilled spaces and are termed dendrites, which generally present the initial phase of a crystal being formed.

[00277] Any metal is a polycrystal comprising many grains. The neighboring grains have differently oriented lattices. The grain boundaries are called high-angle boundaries, since the crystallographic directions in neighboring grains form angles of up to tens of degrees.

[00278] Each grain consists of individual subgrains that form a so-called substructure. Substructures are off-oriented

relative to each other at angles ranging from fractions to units of degrees - low-angle boundaries. Subgrains are measured 0.1-1 microns, which is one-three orders less than grain sizes. The boundaries between individual crystals (grains) are generally a transition region of width up to 2-3 interatomic distances. Atoms in such a region are arranged differently than in grain volume. In addition, impurities tend to concentrate at grain boundaries of technical metals and this further disturbs a regular atomic arrangement. Somewhat lesser disturbances are observed at subgrain boundaries. The dislocation density in metal increases with increase in a subgrain off-orientation angle and decrease in subgrain size.

[00279] The grain size affects the metal properties substantially. Large grains are mainly accompanied by lower mechanical quality of metal. Also, the other properties may change which may be explained by more or less extension of boundaries between grain-crystals. On the whole, the effect of grain boundaries on metal properties is manifested first of all by that these boundaries are surfaces that divide grains, wherein the particles (atoms) of the metal itself are different in energy terms from the atoms located in the lattice inside the grain. The particles between grains are believed to have higher energy representing the surface energy that plays an important role in phenomena occurring in various bodies, including metals and their alloys. Thus, the interlayer between grains in the form of randomly arranged atoms, which is sometimes considered as an amorphous metal film, may affect the properties of the entire piece of metal as a whole.

[00280] However, in addition to such films, consisting of atoms of the metal itself, the metals used in practice always have impurities that may also be located in spaces between grains in the form of films or inclusions and influence the

metal properties. For example, if such films are weak (brittle), the bond between grains will be weakened and the metal will break under mechanical action at grain boundaries. In this case, intercrystalline fracture of metal will be observed. If fracture occurs inside grains, then intracrystalline fracture will happen.

[00281] Structural change in solid metals is disclosed hereafter. A fine grain may be obtained from a coarse grain thermally (by only heating and cooling in a solid state) only in metals that experience allotropic changes. Such changes constitute a transition from one lattice to another, i.e., atomic rearrangement from one location to another. Each type of lattice is an allotropic alteration or modification of the metal, which is often called a phase, while metals, existing in several modifications, are termed polymorphous metals. Each modification has its own region of temperatures, at which this is stable and hence at certain temperatures there should be a transition from one modification to another. In this manner the crystallization process occurs, which is termed secondary crystallization, in contrast to primary crystallization which occurs during solidification of a liquid.

[00282] Polymorphous metals include iron. In iron, there are several allotropic changes between a solidification point (1540°C) and a usual temperature. Of most practical value is a change at 910°C that is responsible for transition of a γ modification into an α modification during cooling (and vice versa during heating). The essence of this change is that the atoms of the γ-iron lattice, which constitutes a cube with centered faces, rearrange into a centered cubic lattice which is typical for α-iron. This change of internal structure is accompanied by the change in external shape of grain-crystals, i.e., recrystallization takes place. In recrystallization,

the grain size decreases significantly. The new crystals are closely adjacent to each other, increasing the metal strength.

[00283] Thus, by using the allotropic change in a metal, one may induce recrystallization and obtain fine grains from coarse grains. An example of such a microstructural change of the coarse-grain cast iron into the fine-grain, heat treated or annealed iron is shown in FIGURES 26-27. More particularly, FIGURE 26 shows a microstructure of cast (x20) iron and FIGURE 27 shows a microstructure annealed (x100) iron.

[00284] If no allotropic changes occur in a metal (for example, in aluminum), grains may not be refined in the manner described above (heat treatment only). In this case, the only method is the preliminary mechanical shaping that induces a so-called plastic deformation of a metal. Thereafter, grains of various sizes may be obtained by heating.

[00285] This method may be applied only to ductile metals, i.e., those capable of withstanding mechanical effect and changing their external shape (deformation) without failure. The metal may be mechanically shaped by various methods including rolling, drawing, forging, pressure forming, etc. Each case has some characteristic metal behavior depending on the method applied; however in all cases main process occurs, which is plastic deformation of the metal that consists of changing the exterior shape of the metal without the loss in integrity and strength.

[00286] Metal deformation is accompanied by an increase in its strength with reduction of ductility (i.e., the ability for further deformation). The metal hardness improves simultaneously with increased strength. In practice, the metal becomes "rigid." Such a state of the metal, obtained as a result of deformation, is usually termed cold work. The cold work state is induced chiefly by displacements or slips

of lattice particles that take place during mechanical effect upon grain crystals in a metal.

[00287] Deformation of the metal usually begins from slipping along easiest slip planes (atoms in these planes are very close to each other) and with a force, which is smaller when above-mentioned slip planes are more conveniently located relative to this force. Similar slips in tension of single-crystal round specimen are schematically shown in FIGURES 28-30, i.e., slips in single crystal zinc. Tension of the specimen lies in multiple slips of thin metal layers (termed packs or blocks) relative to each other. More particularly, FIGURE 28 shows the single crystal of zinc in the form of a hexagonal prism (the base (cross section)). This plane is an easiest slip plane and FIGURES 29 and 30 show the blocks of particles in the crystal-specimen slipped along this direction.

[00288] Simultaneously with slipping, thin metal layers (blocks) gradually change their direction relative to the tension force, tending to take, by their planes, the location which is less convenient for slipping, i.e., with the greatest resistance to slipping. Hence, as the crystal is deformed, the stress required for further deformation increases. Apart from rotation of the easiest slip planes into unfavorable position, an increased stress in metal during slipping may be caused by some other factors associated with irregular location of particles near slip sites (lattice distortion, plane warp, formation of the finest fragments, voids, etc.).

[00289] Thus, the resistance to slip along easiest slip planes reaches the value, wherein slips stop and begin along different directions or secondary slip planes that were less convenient and favorable directions for slipping. Slipping along these secondary directions does not reach such a great extent as in the case of primary slips and occurs with substantially increasing stresses until the latter causes a

separation of sliding layers from each other, which may result in specimen failure.

[00290] Thus, only simple slip (translation), i.e., relative displacements along the planes of separate blocks in a crystal, occurring within one crystal, may explain the essence of the changes occurring therein in plastic deformation and cause the cold work state. In reality, even in one crystal the deformation is not limited by only simple slipping (translation); twin displacements may also occur when groups of particles not only slip along planes, but also rotate through some angle. Hence, in deformation the structural changes pattern in only one grain-crystal is fairly complex.

[00291] The process becomes even more complicated when the multiple-grain (polycrystalline) metal, presenting multiple closely adjacent grains, is deformed. This adjacency of grains, which generally have various orientations (direction), should naturally impede free slipping in each grain and allegedly prevent deformation. The intercrystalline substance that often occurs at boundaries and impedes block slipping may have the same effect.

[00292] However, despite such inhibition, slipping occurs in grains and each grain elongates (or flattens in compression) and consists of multiple slip blocks, oriented predominantly in one direction and presenting "fragments" of the former integral grain.

[00293] Indeed, the structural examination of the deformed metal reveals similar elongated grains. FIGURE 31 shows the microstructure of deformed iron (x100) and FIGURE 32 shows the microstructure of non-deformed iron (x300). During intensive deformation the grains become so elongated that they more likely resemble fibers in shape and this is the reason why such a structure of the deformed metal is called fibrous. Thus, "fibers" in this structure are the same initial metal grains, only with changed configuration due to slipping and

lattice distortion. There is still no grain refinement as such. The structure has no distinctive individual fine grains and only elongated boundaries of former (initial) grains are visible. With low deformation extent, the structure may be little different from the initial one, since grain elongation is small and grain boundaries are not broken. In such cases, a structural indication of ongoing plastic deformation is slip lines occurring on the deformed metallographic section of the metal in the form of parallel or intersecting lines that spread throughout the grain section. An example of slip lines on non-etched metallographic section of iron (x300) is shown in FIGURE 33.

[00294] In a deformed state, there are essentially no grains and the state itself is not very stable thermodynamically, having an excess of free energy. For most metals at low temperatures, such an unstable state of cold worked metal may remain unchanged for a long time. However, this should gradually change into more stable state in heating, which is the case in reality.

[00295] At known temperatures, new grains with non-deformed (non-distorted) lattice develop in deformed grains. As in so doing a crystallization process occurs again, this is termed recrystallization. The beginning of this process, i.e., the temperature at which new finest grains with non-distorted lattice start to occur is called a recrystallization threshold or recrystallization temperature. For various pure metals, this temperature varies and may be approximately determined in relation to the metal melting temperature. Absolute recrystallization temperature has been shown to be about 0.4 of the absolute melting temperature. During recrystallization the grain size changes so demonstratively that the average grain size may be measured depending on various factors and the grain growth may be represented schematically. A recrystallization diagram, which is plotted in space, may

represent the relationship between grain size and the two factors such as the heating temperature and the extent of prior deformation. Thus, mechanical treatment (deformation) followed by heating (recrystallization) may refine grain in any ductile coarse-grain metal and recrystallization diagrams can help to consider the main factors accurately and obtain grains of desired size and hence various metal properties.

[00296] The metal may be plastically deformed by various methods such as ball and roller burnishing, shot peening, laser strengthening, and high-intensity ultrasound. Some of these methods are characterized below. Also, effects are discussed that accompany the influence of plastic deformation upon the structure of such metals as aluminum alloys and steel.

[00297] Also known is Aluminum Alloys: Structure and Properties, by L.F. Mondolfo (Butterworths, London, 1976), which discloses the fundamental characteristics of aluminum alloy vs. steel. Both metals are complex alloys. On cooling from melt, they may have a different structure depending on conditions (temperature, cooling rate). Impurities in alloys add complexity. They simultaneously precipitate in the form of various fine components mainly at boundaries of crystallites of the basic structure. Al-Cu alloy (duralumin) differs in that its strength and hardness, with a specific weight close to conventional aluminum, is not less than those of mild steel (up to about 45-50 kg/mm^2 of σ_{TS} and up to 130 H_B) with elongation, δ, about 20%. If a specific strength is taken into account, i.e., the strength (σ_{TS}) related to a unit weight, this is almost thrice that of mild steel. However, such strength in duralumin may be obtained only after appropriate heat treatment - hardening and aging (mainly artificial). Note that immediately after quenching (from

500°C) the alloy has the reduced hardness, tensile strength and elastic limit (H_B~80; σ_{TS}~32 kg/mm^2; σ_{EL} ~11 kg/mm^2).

[00298] During heating before quenching, $CuAl_2$ compounds dissolve, phase S (Al_2 Mg Cu). At room temperature, copper solubility is 0.2% and at 548°C this is 5.7%. During sharp cooling, the oversaturated solid solution is fixed. After a short while the following happens: Guinier-Preston zones begin to form (zones of high concentration of copper); the precipitates are coherent; no disruption in bonding with the lattice; thin lamellar disc-shaped formations appear (several atomic layers in thickness, 40-100 Å in length). This results in elastic distortion of the lattice and an increase in strength, hardness and yield strength.

[00299] The structure of the aged alloy consists of α solid solution and non-soluble ferric and manganic compounds. Natural aging takes 1400 hours and more. Hence, artificial aging at 150-170°C is used.

[00300] Despite fairly high mechanical characteristics, duralumin materials are characterized by low corrosion resistance - susceptible to pitting, intergranular corrosion (when $CuAl_2$ precipitates at grain boundaries), corrosion cracking, corrosion fatigue and crevice corrosion.

[00301] Also known is The Effect of High-intensity Ultrasound on Metal Interphase, Chapter 4, edited by A.I. Manokhin (Moscow, Nauka, 1986), which discloses that the ultrasonic surface strengthening of metals is based on such physical phenomena as the interphase movement and atomic diffusion. The kinetics of such phenomena is complex and generally defined by the nature of distribution and interaction of the lattice defects like dislocations, vacancies and interstitial atoms with each other and atoms of impurities. The dislocation structure formed as a result of ultrasonic treatment (1-100 Hz) differs in nature from the

dislocation structure formed upon plastic deformation of constant sign. This dislocation structure is mainly a cell structure of subgrains with tight walls.

[00302] In investigations, the ultrasonic energy was applied to specimens by direct contact or directly with an oscillator, or via a metal concentrator.

[00303] In the process of cyclic loading, a great number of dislocation loops were observed in aluminum. It is suggested that loops are formed by closing the vacancy discs. During deformation of constant sign, dislocation loops are observed, but in considerably less number. Ultrasonic treatment at a frequency of 20 kHz increases dislocation density in aluminum monocrystals by 1-2 orders of magnitude. As this takes place, a well-formed grain structure is observed. The sub-boundaries were elongated in oscillation direction; the average size of subgrains was 2x10 μm.

[00304] The dislocation structure of austenitic steel 1Cr8Ni9Ti was studied by transmission electron microscope using foil. A comparison was made at 20°C between the dislocation structure after ultrasonic treatment and after plastic deformation by tension and compression. In tensioned and compressed specimens, dislocations are smoother, while ultrasonically treated specimens had more twisting dislocations with a great number of thresholds and kinks. This is testimony to intersection, transverse slip and climb of dislocations under ultrasonic effect. As the temperature rises, the number of grains with higher dislocation density increases and there is a tendency to form a cell structure, a great number of dislocation jogs and kinks. The data evidence that the grain boundaries and carbide precipitates are the sources of dislocation.

[00305] In addition to dislocation rearrangement, ultrasound also causes atomic diffusion in metals. Self-diffusion of

iron was studied in steels having various lattices. In steels with body-centered cubic (bcc) and face-centered cubic (fcc) lattices, ultrasound accelerates self-diffusion of iron at deformation amplitudes exceeding some threshold values. Also, the ultrasonic effect results in accelerated self-diffusion of iron regardless of the lattice type.

[00306] The most promising technique is the surface treatment by ultrasonic tool, which is effected by impact action of the "deforming element" that receives the energy from the ultrasonically oscillating transducer. This technique provides significant surface microhardness, residual compressive stresses and sliding friction resistance. The surface is plastically deformed at impact with indenters ("deforming elements"). The deformation properties are defined by a quick ultrasonic action and simultaneous introduction into the material (via a plastic deformation saturation region) of high-power ultrasonic oscillations that initiate therein a high-intensity ultrasonic wave at the level of cyclic stresses in the intense creep region and relaxation of the material stressed state. As this takes place, the contact point (in the local area of ultrasonic impact action) experiences accelerated repeated plastic deformation and, as a result thereof, intense heating (sufficient for structural changes) and quick cooling (sufficient to stabilize transition phase states). As a result, a material is formed on a surface with new properties resulted from structural changes.

[00307] In order to ensure a reliable operation of the components and structures of engineering systems, their technical condition is monitored and the technical measures are taken that prolong their lifetime. When the technical conditions of complex systems and devices are monitored, one of the most actual tasks is to objectively and timely detect various defects and control their development because the components age during service. A systematic use of non-

destructive methods is one way of preventing undesirable consequences in service of defective components.

[00308] In order to extend life of components and recover their performance, the following basic methods are used depending on the degradation types they experience: heat treatment to alter the structure and improve the properties of the component material, thermal and vibrational treatment to relax residual stresses, removal of stress concentrations, protective coatings, inhibitors and protectors, surface hardening by chemical-thermal treatment methods, and/or surface hardening by surface plastic deformation (SPD) methods. SPD is one of the most simple and effective methods of strengthening welds and machinery components. They are effective because of the following positive effects: increase in the dislocation density and microhardness and hence improvement of the surface layer wear resistance, creation of residual compressive stresses in the surface layer of a component, and suppression of the effect of stress concentration on the fatigue limit reduction for welds and welded components.

[00309] Ultrasonic impact treatment (UIT) is one of the most promising SPD methods. In the process of UIT, the plastic deformation resistance of the material is temporarily reduced when ultrasonic oscillations are excited therein and a large depth of a strengthened layer is achieved. This results in high degree of plastic deformation and high level of residual compressive stresses induced by treatment. UIT is also accompanied by the effects of surface thermomechanical and subsurface relaxation in the material of a treated product.

[00310] Also known is Degradation, Repair and Rebuilding of Bridges, (Materials Information/Cambridge Scientific Abstracts, 2005, ISBN 0-88387-217-X), which discloses all forms of degradation and deterioration of highway and railroad bridges and bridge-building materials including structural,

high-strength, and reinforcing steels, reinforced concrete, polymer concretes and reinforced plastics. Repair and renovation techniques/efforts envisioned, underway, or completed, materials selection and substitution, and corrosion prevention and control are also disclosed.

[00311] Also known is Preliminary Study Into The Effect Of Exfoliation Corrosion On Aircraft Structural Integrity, by N.C. Bellinger, J.P. Komorowski, M. Liao, D. Carmody, T. Foland, D. Peeler (6th Joint FAA/DOD/NASA Aging Aircraft Conference, 2002), which presents the results from a study that is being carried out to determine the effect that exfoliation has on the remaining life of upper wing skins. A number of coupons have been cut from naturally exfoliated upper wing skins fabricated from 7178-T6 alloy. These coupons, some of which provided low load transfer through the fasteners, contained various levels of exfoliation. Each coupon was tested to failure using constant amplitude compression dominated loading. The fracture surfaces were then examined to determine the fracture origin. Specimen failure locations varied, as did the crack origin sites. Crack origins were attributed to several causes, including planar cracking (exfoliation), fretting, pitting and manufacturing discontinuities. The results to date have suggested that exfoliation may not be the critical factor governing the life of an upper wing skin for the levels of exfoliation tested.

[00312] Corrosion in aircraft structures is a significant economic and safety problem affecting military and civilian aircraft fleets. The United States Air Force alone estimates that direct corrosion costs exceed $800M/year. Corrosion has many forms and affects most structural alloys found in airframes today. One of the most common problems is exfoliation corrosion, which affects rolled plates and forged alloys. Exfoliation is commonly found in upper wing skins

around fastener holes where it originates at the exposed end grains in the countersink and hole bore surfaces.

[00313] In ASTM G15-97a, exfoliation corrosion, or exfoliation, is defined as corrosion that proceeds laterally from the sites of "initiation" along planes parallel to the surface, generally at grain boundaries, forming corrosion products that force metal away from the body of the material, giving rise to a layered appearance. In other words, exfoliation is a form of severe intergranular corrosion, which occurs at the boundaries of grains elongated in the rolling direction. This form of corrosion is associated with a marked directionality of the grain structure. In aircraft materials exfoliation corrosion is most common in the heat-treatable Al-Zn-Mg-Cu (7000 series), Al-Cu-Mg (2000 series), and Al-Mg alloys, but it has also been observed in Al-Mg-Si alloys. The generation of exfoliation corrosion products forces layers apart and causes the metal component to swell. Flakes of metal may be pushed up and may even peel from the surface.

[00314] A review of over 80 publications on exfoliation corrosion has found that only 11 attempted to deal with issues of exfoliation and fatigue. The main conclusions on prior exfoliation and fatigue interaction research can be summarized as follows:

(1) Prior exfoliation accelerates fatigue crack nucleation;

(2) Prior exfoliation enhances fatigue crack growth rate (FCGR);

(3) Prior exfoliation causes earlier onset of multiple site damage (MSD);

(4) Some reasons causing the above mechanical phenomena are: material loss (cross section reduction or thickness reduction); hydrogen embrittlement (reduced toughness, strength, and ductility of material); and other chemical effects; and

(5) Prior exfoliation and fatigue interaction is not only an economic issue but also is a safety issue. Quantitative relationships between exfoliation damage and residual fatigue life and residual strength are not yet established.

[00315] Some studies have shown that exfoliation, when present around a fastener, may reduce the strength and fatigue properties of the structure less than the grinding repair. Independently in Australia, some exfoliation damage in C-130 aircraft has been arrested with the application of corrosion preventive compounds (CPC) and the aircraft was returned to service without exfoliation removal. The decision to rely on CPC was based on indications from laboratory experiments that CPCs are very effective in arresting corrosion and the growth of cracks in a corrosive environment.

[00316] Also known is Fatigue Degradation and Failure of Rotating Composite Structures - Materials Characterisation and Underlying Mechanisms, by E. Kristofer Gamstedt, Svend Ib Andersen (Riso National Laboratory, Roskilde, Denmark, 2001), which discloses rotating composite structures, in which fatigue degradation is of key concern for in-service failure. Such applications are for instance rotor blades in wind turbines, helicopter rotor blades, flywheels for energy storage, marine and aeronautical propellers, and rolls for paper machines. The purpose is to identify areas where impending efforts should be made to make better use of composite materials in these applications. In order to obtain better design methodologies, which would allow more reliable and slender structures, improved test methods are necessary. Furthermore, the relation between structural, component and specimen test results should be better understood than what is presently the case. Improved predictive methods rely on a better understanding of the underlying damage mechanisms. With mechanism-based models, the component substructure or

even the material microstructure could be optimized for best possible fatigue resistance. These issues are addressed in the present report, with special emphasis on test methods, and scaling from damage mechanisms to relevant material properties.

[00317] Also known is Metal Properties Degradation in Main Pipelines After Prolonged Service, by G.A. Filippov, O.V. Livanova and V.F. Dmitriyev ("Steel", No. 2, 2003), which discloses the results of the first part of comprehensive investigations into the effect of the operating conditions on the pipe properties. In Russia, most of the main pipelines have been in service for more than 20 years. Affected by stresses, corrosion environment and hydrogen for such a long period of time, the pipes are subjected to the processes that change the physicomechanical properties of the metal. The actual properties of the pipe metal must be considered to analyze the condition, evaluate the residual life and schedule the overhaul of pipelines. The pipeline premature failure is mainly caused by stress concentrations of mechanical origin (scratches, notches, structural defects, etc.) and defects formed by metal contact with corrosive environment. A prolonged service leads to degradation of the pipe metal properties due to a change in metal structural state, and failure is possible even under stresses below the upper stress limit. A reduced damage resistance may be associated with metal aging processes, increase in hydrogen content and internal stresses and accumulation of defects such as microcracks.

[00318] The results of the analysis carried out on pipe samples taken from 19 main oil pipelines located in various climates is disclosed. The samples of steels 20, 17MnSi, 17Mn1Se, 19Mn, 14CrMnSi, 15MnSiTiAl, 10Mn2Si1, 14MnNi were tested at the experimental facility of Central Research Institute of Ferrous Metals. The percentage of steels of

approximate chemical composition among all pipes investigated was as follows: steels 17MnSi, 17Mn1Si and 19Mn - 81% (37%, 19% and 25% respectively), steels 20 and 14MnNi - 1% each, steels 15MnSiTiAl, 10Mn2Si1 and 14CrMnSi - 3%, 5% and 9% respectively. The grade composition of steels 17MnSi, 17Mn1Si and 19Mn differs by carbon and manganese content. However the chemical analysis of pipe samples showed that the actual composition of steels is often inconsistent with industrial certificates and hence the basic statistical analysis was conducted just for these steels, further called as steels of 17MnSi type. Altogether 106 samples were studied, 86 from pipes in operation, 9 from emergency stock, 7 from emergency pipes, 3 from backup lines and one sample was taken from the as-manufactured pipe. Also, a number of welded pipe specimens were studied, a majority of which were factory longitudinal welds. All field welds and eight factory longitudinal welds had defects.

[00319] The standard tensile characteristics are insufficient to evaluate the condition of main pipelines. The reliability evaluation criteria should include the properties susceptible to local structural changes, for example, those obtained from low temperature tests, delayed fracture tests and tests on cracked or sharp notched specimens. All failure resistance characteristics of metal were found to decrease upon sharp notch bending test of specimens after 25 years in service. The fracture energy is reduced by half chiefly due to the reduction in work of crack nucleation. Cold-shortness threshold shifts to the positive temperature area. The crack critical opening is reduced by 1.5 times. The tendency of steel to delayed fracture under simultaneous action of stresses, corrosion environment and hydrogen was found to be the most susceptible to structural changes. The reduction in fracture resistance of pipe metal during long service is

associated with the deformation aging process and accumulation of defects and internal microstresses.

[00320] Also known is Assessment of Age-Related Degradation of Structures and Passive Components for U.S. Nuclear Power Plants, by J.I. Braverman, C.H. Hofmayer, R.J. Morante, S. Shteyngart and P. Bezler (NUREG/CR-6679, BNL-NUREG-52587, 2000), which describes the results of the first phase of a multi-year research program to assess age-related degradation of structures and passive components for U.S. nuclear power plants. The purpose of this research program is to develop the technical basis for the validation and improvement of analytical methods and acceptance criteria which can be used to make risk-informed decisions and to address technical issues related to degradation of structures and passive components. The approach adopted for this research program consists of three phases. Phase I included collection and evaluation of plant degradation occurrences, an assessment of the available technical information on age-related degradation, and a scoping study to identify which structures and components should be studied in the subsequent phases of the research program. Based on the results of Phase I, selected structures and passive components are evaluated in Phase II to assess the effects of age-related degradation using existing and enhanced analytical methods. Phase III will utilize the results of the analyses to develop recommendations to the NRC staff for making risk-informed decisions related to degradation of structures and passive components. The results of Phase I of the research program are disclosed.

[00321] Also known is The History of Cracking the RCPB of Swedish BWR Plants, by Karen Gott (9th International Conference on Environmental Degradation of Materials in Nuclear Power Systems-Water Reactors, 1999), which presents the results of monitoring the technical condition of the

equipment used at Swedish nuclear power plants. The nuclear power plants in Sweden are required to report all cracks to the Swedish Nuclear Power Inspectorate (SKI). This rule applies to all the systems covered by SKIs regulations concerning the structural integrity of mechanical components. As a result, SKI has over the years gathered extensive information concerning the history of the various degradation mechanisms which have been observed in Swedish plants. In the last couple of years this information has been put into a database set up specifically for the purpose. The information in the database includes details of when and how the cracks were detected, their dimensions and cause, as well as system and component details. The database also has a comprehensive reference list of all the related documentation associated with a crack or group of cracks. The database is described and its use illustrated with the trends found in the reactor coolant pressure boundary (RCPB) of the Swedish boiling water reactors (BWR).

[00322] Also known is Degradation of Spacecraft Materials, by J. Dever, B. Banks, K. deGroh and S. Miller (NASA Glenn Research Center, 2004), which discloses descriptions of specific space environmental threats to exterior spacecraft materials but does not address environmental effects on interior spacecraft systems, such as electronics. Space exposure studies and laboratory simulations of individual and combined space environmental threats are summarized. A significant emphasis is placed on effects of Earth orbit environments, because the majority of space missions have been flown in Earth orbits which have provided a significant amount of data on materials effects. Issues associated with interpreting materials degradation results is also disclosed, and deficiencies of ground testing will be identified. Recommendations are provided on reducing or preventing space

environmental degradation through appropriate materials selection.

[00323] Thus, the components and structures used in almost all areas of engineering are susceptible to degradation. The degradation problem is most serious for engineering systems whose failures may result in catastrophic consequences such as death of people, ecological damage, and severe material losses. These include: transport (bridges, tunnels, railways, load-carrying structures of transportation and load lifting facilities); oil & gas and chemical plants (main pipeline systems, pumping stations, distillation and other chemical facilities); flying vehicles (aircrafts of various types and purpose); power systems (nuclear power installations of nuclear power plants and power supply systems thereof, heat power plants); space systems (space vehicles, launching and rocket systems); and large military facilities.

[00324] Accordingly, metal degradation is the process of breakdown of metallic materials due to the formation and development of microdefects and cracks, which results in macrocracks and the loss of the load-carrying capacity of a component. As a result, the whole structure, comprising such a component, may fail.

[00325] The issue of providing a maximum possible service life, retarding aging of such components and structures and extending their useful lives is one of the most actual problems for scientists and engineers worldwide. Occurrences of failures, malfunctions or defects in engineering systems may result in even tragic consequences such as global disasters, environmental degradation, human losses, and severe financial and material losses.

[00326] Investigations in this area are impossible without a system approach. Various measures and solution of tasks that may improve the condition of systems guarantee an appropriate

reliability and extension of their service life allowing for economic criteria and restrictions.

[00327] Previously, the failure was regarded as an inevitable event. Each material was believed to have a certain structural strength. However, at present there are methods and mechanisms that not only assess the degradation level and provide prediction, but also retard the breakdown process and even restore the product or component, thus extending their service life. That is, the material breakdown is the process that may be controlled.

[00328] One of promising directions to retard degradation of structural materials and recover their properties is UIT application. In addition to the conventional effects obtained by SPD methods such as high level of compressive stresses, increased microhardness and suppression of stress concentration effect, UIT is also accompanied by relaxation of residual stresses; ultrasonic diffusion in the material; recovery of the degraded material properties; and amorphization of the material structure under the action of the ultrasonic impact.

OBJECTS AND SUMMARY OF INVENTION

[00329] The invention relates to a method and algorithm of improving the performance of metal and protecting the metal against degradation and suppression thereof by ultrasonic impact. The method and algorithm address the problems of degradation of metal properties during prolonged service under external forces, thermodynamic fluctuations and negative environmental factors. The invention also relates to the technologies oriented to protect against (prevent) and to suppress the danger of materials failure due to unfavorable change in performance over time. These problems commonly occur because of the damage of the original structure of materials under known conditions that accompany the processes

of environmental degradation of metals. In each specific case, the well-known methods of "combating" metal degradation cover a wide range of technologies from metallurgical alloying during melting, casting, welding and application of coatings to various thermal treatments and effects on the surface.

[00330] The invention provides a new versatile method and algorithm of addressing degradation problems in all cases mentioned above. This method and algorithm of processing the object being affected are detailed hereafter.

[00331] The response of the metal boundary layer to the effect and the properties and condition thereof before and after the technical effect substantially influence the characteristics of the subsurface layer, which define, either singly or in the aggregate with the surface characteristics, the technical effectiveness of the method. The effectiveness of the method and/or algorithm means the degree of the effect on material performance due to the directed change in properties and structure of a material, the stress-deformed state of the structure and hence the ability of the material to resist external forces, temperature changes and environmental effects. Thus, the method and/or algorithm of the present invention address the surface and the material thereunder as two independent but interrelated substances and, in this context, provides the method of increasing the object's ability to resist the unfavorable factors that cause degradation of its performance. So, the requirements to the condition of the treated surface and subsurface material determine, as two related but independent technical effectiveness criteria of the method, the features of the technique of affecting the surface of the object being affected and the material therethrough. Accordingly, the method and/or algorithm of ultrasonic impact and the variations of its versatile and specific application in areas

of engineering with different causes of degradation in performance of the object's material is detailed hereafter.

[00332] The task of improving metal degradation resistance is also addressed by the method and/or algorithm of the invention. The method and/or algorithm initiates organizing and controlling, as defined by the task, of "soft" and force normalized phases of the ultrasonic impact and attains the technological effectiveness (which results therefrom) of practical application to suppress degradation (according to the method of the invention using ultrasonic impact control). "Soft" is in reference to the phase and parameters of the ultrasonic impact that correspond to the task and directly govern the predetermined or experimentally established state of the material at the time the impact resistance of the material is possible to be identified and when in the treated area of the material a certain minimum impact resistance occurs depending on the impact phase, resulting in maximum possible strengthening (plastic deformation) while retaining the treated material mesostructure integrity.

[00333] The main phases of organizing and controlling of "soft" and force normalized phases of the ultrasonic impact preferably include the following:

- assessing the dynamic strength of the material in the context of subsequent formation of the optimal mesostructure at the object's surface;

- selecting the parameters and depth of controlling soft or force phases of the ultrasonic impact in accordance with the method and/or algorithm;

- experimental or expert analysis of the material surface structure condition and definition of the task of its modification in the context of suppressing the started degradation process and preventing the possibility thereof;

- experimental or expert selection of the intensity and sequence of the effect of the normalized (in accordance

with the control method and algorithm) ultrasonic impact on the material structure on and under the surface as defined by the task;

- determining the parameters and sequence of the force effect on the subsurface material structure during ultrasonic impact after its "soft" phases that retain the integrity and provide specified strengthening of the material mesostructure at the surface;

- preparing and consistent implementation of the method and/or algorithm of the invention;

- experimental verification of the results to match the technical task on the first experimental series of samples or simulators;

- entering the results into a database; and/or

- implementing the degradation suppression method and/or algorithm based on using the level (selected by the method described above) of ultrasonic impact control at stages of forming the properties of the surface and the subsurface of the material.

BRIEF DESCRIPTION OF THE DRAWINGS

[00334] Referring to the drawings:

[00335] FIGURE 1 (Prior Art) shows the effect of life on the brittle state (T_{50}) transformation temperature for pipe metal of steel MnSi.

[00336] FIGURE 2 (Prior Art) shows the relationship between time to fracture, t_f, and initial stress intensity coefficient, K_i, for pipes of steel 17MnSi, (1) as-manufactured, (2) working pipe, and (3) emergency pipe.

[00337] FIGURE 3 (Prior Art) shows the effect of service on the tendency to deformation aging.

[00338] FIGURE 4 (Prior Art) shows the reduction of area of aged pipes.

[00339] FIGURE 5 (Prior Art) shows the temperature dependence of internal friction, Q^{-1}, of pipe metal of 17MnSi steel after prolonged service of 30 years.

[00340] FIGURE 6 (Prior Art) shows the temperature dependence of internal friction, Q^{-1}, of pipe metal of 17MnSi steel in emergency stock.

[00341] FIGURE 7 (Prior Art) shows the potential damage mechanism associated with high temperature applications of aluminum alloys.

[00342] FIGURE 8 (Prior Art) shows various classifications of hydrogen damage.

[00343] FIGURE 9 (Prior Art) shows a schematic representation of an electrochemical corrosion process.

[00344] FIGURE 10 (Prior Art) shows a schematic representation of a double electrochemical layer formation of a metal atom ion transforming into solution.

[00345] FIGURE 11 (Prior Art) shows a schematic representation of a double electrochemical layer formation of a cation transforming from a solution to a metal surface.

[00346] FIGURE 12 (Prior Art) shows the completeness of the surface microhardness data obtained on the surface of pipe portions (steel X65) of emergency stock pipe and pipe after 20 years of service.

[00347] FIGURE 13 (Prior Art) shows surface crack initiation and crack growth of pristine material with a mirror finish with the fractograph clearly indicating the faceted growth (shear mode growth).

[00348] FIGURE 14 (Prior Art) shows surface crack initiation and crack growth of pristine material with EDM finish with the near surface region showing evidence of multiple crack nuclei.

[00349] FIGURE 15 (Prior Art) shows a site of corner crack initiation and crack growth morphology of a S110-200%-45° CSO specimen with the faceted area extending to a depth of

approximately 150 μm and the faceted area surrounded by cleavage like fatigue fractures.

[00350] FIGURE 16 (Prior Art) shows crack initiation and early crack growth of LSP 10GW/cm^2 (2 passes) with the fractograph indicating surface crack initiation, crack branching, and propagation path.

[00351] FIGURE 17 (Prior Art) shows crack initiation and early crack growth of LSP 10GW/cm^2 (3 passes) with the fractograph indicating surface crack initiation, crack branching, and propagation path.

[00352] FIGURE 18 (Prior Art) shows crack initiation and early crack growth of dual treatment with the fractograph indicating surface crack initiation from a typical shot peening dent and crack branching.

[00353] FIGURES 19 and 20 (Prior Art) show space-centered or body-centered cube lattice.

[00354] FIGURES 21 and 22 (Prior Art) show face-centered cube lattice.

[00355] FIGURES 23-25 (Prior Art) show main slip cleavage planes in simple cubic lattice.

[00356] FIGURE 26 (Prior Art) shows a microstructure of cast iron.

[00357] FIGURE 27 (Prior Art) shows a microstructure of annealed iron.

[00358] FIGURES 28-30 (Prior Art) show slips in tension of single crystal round specimens of zinc.

[00359] FIGURE 31 (Prior Art) shows the microstructure of deformed iron.

[00360] FIGURE 32 (Prior Art) shows the microstructure of non-deformed iron.

[00361] FIGURE 33 (Prior Art) shows slip lines on non-etched metallographic section of iron.

[00362] FIGURES 34 and 35 show an oscillating system wherein ultrasonic impact is accompanied by the movement of an oscillating system under elastic recovering force caused by the rebound of the oscillating system off of a treated surface and ultrasonic oscillations of the oscillating system end connected to an indenter.

[00363] FIGURE 36 shows plastic deformation distribution during ultrasonic impact of the invention.

[00364] FIGURE 37 shows a frequency diagram of ultrasonic impact.

[00365] FIGURE 38 shows stochastic ultrasonic impacts arbitrarily aligned.

[00366] FIGURE 39 shows a fragment of a diagram of an oscillating system movement in time.

[00367] FIGURES 40a-40c show the advance, soft contact and lag/soft impact of vectors of the velocities of the oscillating system at the oscillating system end reduced to an indenter butt.

[00368] FIGURE 41 shows vector diagrams of the velocities of the oscillating system of FIGURES 40a-40c.

[00369] FIGURE 42 shows oscilloscope pictures of ultrasonic impacts arbitrarily aligned.

[00370] FIGURE 43 shows the traditional area of UIT of a welded joint before groove formation by UIT.

[00371] FIGURE 44 shows mesodefect at the groove edge due to local overstrengthening under random impact conditions during UIT.

[00372] FIGURE 45 shows mesodefect in the center of a groove due to local overstrengthening under random impact conditions during UIT.

[00373] FIGURE 46 shows the mesostructural defect after conventional strengthening peening.

[00374] FIGURE 47 shows the state of groove mesostructure after UIT in accordance with the method of the invention.

[00375] FIGURE 48 shows independent and specified uniform (in time) distribution of a 30 μm amplitude.

[00376] FIGURE 49 shows specified distribution of ultrasonic amplitude over a convex parabola.

[00377] FIGURE 50 shows specified distribution of ultrasonic amplitude over a concave parabola.

[00378] FIGURE 51 shows specified increase in amplitude from 0 μm in accordance with a linear law.

[00379] FIGURE 52 shows a graph of microhardness distribution for cast iron.

[00380] FIGURE 53 shows a graph of residual stress distribution for cast iron.

[00381] FIGURE 54 shows corrosion strength of a cast iron structure of an untreated specimen at a depth of 100 μm.

[00382] FIGURE 55 shows improved corrosion strength of a cast iron structure of a UIT treated specimen at a depth of 100 μm.

[00383] FIGURE 56 shows a comparison of specimens treated and not treated by UIT and tested in tap water regarding corrosion.

[00384] FIGURE 57 shows a graph of improved fatigue resistance of welded specimens of steel as welded, after UIT using 5 mm pins, after hammer peening, after shot peening, after TIG dressing, after TIG dressing followed by UIT, and after UIT using 3 mm pins.

[00385] FIGURE 58 shows a graph of improved fatigue resistance of welded specimens of steel.

[00386] FIGURE 59 shows a graph of improved corrosion fatigue strength of steel.

[00387] FIGURE 60 shows a graph of test results of improved impact strength of steel.

[00388] FIGURE 61 shows a subdivided structure of high strength steels showing grain reduction range.

[00389] FIGURES 62 and 63 show a white layer in 10Mn2VNb steel weld joint of a main pipe line and in specimens of high strength steel SUJ2.

[00390] FIGURES 64 and 65 show the effect of UIT on weld metal crystallization in weld carbon ship building steel.

[00391] FIGURES 66 and 67 show improved mechanical properties of steel specimens.

[00392] FIGURE 68 shows a graph of S-N curves for 8 mm butt welds showing the fatigue limit of specimens made of aluminum alloy.

[00393] FIGURE 69 shows a graph of S-N curves for 8 mm specimens with longitudinal attachments showing improvement in high cycle fatigue strength of welds in aluminum alloys.

[00394] FIGURE 70 shows S-N curves for 8 mm specimens of lap joints showing improvement in high cycle fatigue strength of welds in aluminum alloys.

[00395] FIGURES 71 and 72 show suppression of porosity to a depth of up to 2.5 mm and a life extension of cast wheels made of aluminum alloys.

[00396] FIGURES 73 and 74 show maintained impact strength in treatment of cast wheels made of aluminum alloys.

[00397] FIGURES 75 and 76 show precipitation of silicon in aluminum alloys.

[00398] FIGURE 77 shows a graph of microhardness distribution of precipitation of silicon in aluminum alloys.

[00399] FIGURES 78 and 79 show improvement in strength properties of aluminum alloys after corrosion exfoliation.

[00400] FIGURE 80 shows the effect of UIT in accordance with the invention on fatigue resistance of specimens with different degree of corrosion.

[00401] FIGURES 81 and 82 show refined structure of aluminum alloys.

[00402] FIGURE 83 shows a graph of microhardness distribution during precipitate migration and occurrence of microbands in aluminum alloys.

[00403] FIGURES 84 and 85 show precipitate migration and occurrence of microbands in aluminum alloys.

[00404] FIGURES 86 and 87 show an increase in corrosion fatigue strength in bronze.

[00405] FIGURE 88 shows a chart of environmental degradation of metals.

DETAILED DESCRIPTION OF THE PREFERRED EMBODIMENTS

[00406] The invention relates to a method of improving the performance of metal and protecting the metal against degradation and suppression thereof by ultrasonic impact. The method addresses the problems of degradation of metal properties during prolonged service under external forces, thermodynamic fluctuations and negative environmental factors. The invention also relates to the technologies oriented to protect against (prevent) and suppress the danger of materials failure due to unfavorable change in performance over time. These problems commonly occur because of damage to the original structure of materials under known conditions that accompany the processes of environmental degradation of metals.

[00407] Various types of environmental degradation of metals are shown in FIGURE 88. Environmental degradation of metals includes corrosion, hydrogen damage, liquid-metal attack and radiation damage. Corrosion includes aqueous corrosion and high temperature corrosion. Aqueous corrosion may be a general attack or a localized attack of corrosion. A localized attack of aqueous corrosion may include galvanic corrosion, crevice corrosion, pitting, intergranular corrosion, selective leaching, erosion corrosion, or corrosion cracking. High temperature corrosion includes oxidation of

metals and hot corrosion. Oxidation of metals may include hydrogen embrittlement, hydrogen blistering, flakes, fish-eyes and shatter cracks, or hydrogen attack. Hydrogen embrittlement may include loss in tensile ductility, hydrogen stress cracking, hydrogen environment embrittlement, or embrittlement due to hydride formation. Liquid metal attack may include liquid metal embrittlement, grain boundary penetration, and/or liquid metal corrosion. Radiation damage may include radiation growth, void swelling, radiation enhanced creep, and/or radiation strengthening and embrittlement.

[00408] In each specific case, the well-known methods of "combating" metal degradation cover a wide range of technologies from metallurgical alloying during melting, casting, welding and application of coatings to various thermal treatments and effects on the surface. The invention provides a new method of addressing degradation problems in all cases mentioned above. This method of processing the object being affected is detailed hereafter.

[00409] The response of the metal boundary layer to the effect and the properties and condition thereof before and after the technical effect substantially influence the characteristics of the subsurface layer, which define, either singly or in the aggregate with the surface characteristics, the technical effectiveness of the treatment method. The effectiveness of the treatment method means the degree of the effect on material performance due to the directed change in properties and structure of a material, the stress-deformed state of the structure and hence the ability of the material to resist external forces, temperature changes and environmental effects. Thus, the method of the present invention addresses the surface and the material thereunder as two independent but interrelated substances and, in this context, provides the method of increasing the object's

ability to resist the unfavorable factors that cause degradation of its performance. The requirements to the condition of the treated surface and subsurface material determine, as two related but independent technical effectiveness criteria of the method, the features of the technique of affecting the surface of the object being affected and the material therethrough. Accordingly, the method of ultrasonic impact and the variations of its versatile and specific application in areas of engineering with different causes of degradation in performance of the object's material is detailed hereafter.

[00410] The task of improving metal degradation resistance is addressed by the method of the invention. The method initiates organizing and controlling, as defined by the task, of "soft" and force normalized phases of the ultrasonic impact and attains the technological effectiveness (which results therefrom) of practical application to suppress degradation (according to the method of the invention using ultrasonic impact control). "Soft" is in reference to the phase and parameters of the ultrasonic impact that correspond to the task and directly govern the predetermined or experimentally established state of the material at the time the impact resistance of the material is possible to be identified and when in the treated area of the material a certain minimum impact resistance occurs depending on the impact phase, resulting in maximum possible strengthening (plastic deformation) while retaining the treated material mesostructure integrity.

[00411] The main phases of organizing and controlling of "soft" and force normalized phases of the ultrasonic impact preferably include the following:

- assessing the dynamic strength of the material in the context of subsequent formation of the optimal mesostructure at the object's surface;

- selecting the parameters and depth of controlling soft or force phases of the ultrasonic impact in accordance with the method;

- experimental or expert analysis of the material surface structure condition and definition of the task of its modification in the context of suppressing the started degradation process and preventing the possibility thereof;

- experimental or expert selection of the intensity and sequence of the effect of the normalized (in accordance with the control method) ultrasonic impact on the material structure on and under the surface as defined by the task;

- determining the parameters and sequence of the force effect on the subsurface material structure during ultrasonic impact after its "soft" phases that retain the integrity and provide specified strengthening of the material mesostructure at the surface;

- preparing and consistent implementation of the method of the invention;

- experimental verification of the results to match the technical task on the first experimental series of samples or simulators;

- entering the results into a database; and/or

- implementing the degradation suppression method based on using the level (selected by the method described above) of ultrasonic impact control at stages of forming the properties of the surface and the subsurface of the material.

[00412] Ultrasonic impact is accompanied by two types of motions: (1) the movement of an oscillating system under elastic recovering force caused by the rebound of the oscillating system off of a treated surface, and (2) ultrasonic oscillations of the oscillating system end connected to an indenter, as shown for example in FIGURES 34 and 35. As shown therein, a basic tool comprises at least one indenter 103, a waveguide 102, a magnetostrictive transducer

101 with a casing 107 which may be a water cooled casing, a spring 106, and a tool case 105 with a handle. The magnetostrictive transducer 101, waveguide 102, indenter 103, tool casing 105, spring 106 and casing 107 of the transducer form the oscillating system (OS) with a processing setup structurally fixed thereto.

[00413] The following is a key of abbreviations as used throughout the following description of the invention and in the figures:

OS - oscillating system;

OSE - oscillating system end attached to the indenter butt;

TS - treated surface;

UI - ultrasonic impact

V_{os} - oscillating velocity of oscillating system;

V_{ose} - oscillating velocity of OSE at ultrasonic frequency;

V_r - resultant oscillating velocity of OSE in summation of V_{os} and V_{ose} at a certain period;

M_{os} - mass of oscillating system;

P_{imp} - impulse of force of ultrasonic impact;

f_{os} - frequency of oscillating movement of OS (200 Hz);

f_{ose} - frequency of oscillating movement of OSE (27000 Hz);

A_{os} - displacement amplitude in oscillating movement of OS (0.3 mm);

A_{ose} - displacement amplitude in oscillating movement of OSE (0.03 mm);

Ψ - phase of ultrasonic oscillations;

F - pressing force of OS against TS.

[00414] FIGURE 36 shows plastic deformation distribution during ultrasonic impact of the invention. The average

statistical ultrasonic impact comprises three time intervals (denoted in FIGURE 36 as a, b, and c) of the effect on the object, which define the intensity of the plastic deformation distribution in the treated material during each impact event. These intervals include: (a) oscillations of the indenter at increasing frequency above the carrier frequency of the ultrasonic transducer in a narrowing gap between the treated surface and the end of the oscillating system; (b) synchronous and in-phase uninterrupted oscillations in a system "oscillating system-indenter-treated surface"; (c) damped oscillations of the indenter in an increasing gap between the treated surface and the end of the oscillating system as a result of the oscillating system rebound from the treated surface as shown in FIGURE 37.

[00415] As this takes place, the events of rebounds and impacts of the oscillating system occur randomly relative to the ultrasonic oscillations of the output end of the oscillating system (carrier oscillations of the ultrasonic transducer) and form a stochastic pattern of phases, as shown for example in FIGURE 38, representing the start and the end of the events of each ultrasonic impact and the three time intervals thereof, namely (a), (b) and (c).

[00416] The oscillating system movement velocity and the velocity of ultrasonic oscillations of the oscillating system end with an indenter are added stochastically, creating a problem of dynamic overloads at the surface affected by the ultrasonic impact beyond the dynamic strength limits of the treated surface material mesostructure. This in turn causes the following: (a) dissipation of the impact energy on surface damages caused by mesostructural disruption, and unfavorable development of these damages at subsequent impacts; (b) reduction in intensity and depth of plastic deformations induced in the surface material and favorable compressive stresses caused thereby; and (c) reduction in

ultrasonic oscillation energy and hence ultrasonic stress waves in the material of the object being affected. These factors make ultrasonic impact treatment quality control difficult and reduce its technological effectiveness, i.e., the ability to consistently reproduce the predetermined structure, condition and properties of a treated material at and under the surface at a specified depth.

[00417] The degradation of metals is accompanied by disruption of their mesostructure, primarily in the surface layer. The dynamic strength of the surface material is defined by the surface deformation rate in accordance with a relation: $V = 2\sigma/\rho C$, wherein σ is the dynamic tensile strength at a specified loading rate, ρ is the material density, C is the sound of speed or deformation propagation in a material, V is the velocity of action before or after surface damage, and ρC is the resistance to the action (dynamic, acoustic, quasistatic).

[00418] Calculations show that within the ultrasonic frequency range there are substantial reserves for increasing ultrasonic impact intensity. Thus, at ultrasonic oscillation amplitude of 30 μm and frequency of 27 kHz, the oscillating velocity is 5.5 m/sec and the critical velocity under dynamic action on the steel with yield strength of 700 MPa is 34 m/sec. This makes it possible to change to more practically feasible higher carrier frequencies of the ultrasonic impact of up to 80 kHz. Yet, this reserve is very susceptible to external factors and environment that initiate material properties degradation during long service. Hence, the use of the control method developed is actual in construction and maintenance of critical highly-loaded metal structures.

[00419] Thus, we have to solve a three-fold technical task consisting of: (a) controlling the material mesostructure during ultrasonic impact to maintain the integrity thereof on

the treated surface; (b) recovering the degraded material mesostructure; and (c) directly affecting the structural state and properties of a material during ultrasonic impact upon and under the treated surface.

[00420] This technical task in turn requires that the ultrasonic oscillation conditions be independently formed (a) when the oscillating system approaches the treated surface, (b) directly during ultrasonic impact and, if additional correction is needed, (c) at the end of an experimentally found period of the effect of the ultrasonic impact upon the treated surface during periods (a) and (b).

[00421] As shown above, the ultrasonic impact treatment process is accompanied by two oscillation modes: (a) low-frequency oscillations of the oscillating system lumped mass and (b) ultrasonic frequency oscillations of coupled resonance elements, namely transducer-waveguide-indenter of the oscillating system. The portion of the diagram of these movements and a specific calculation of the relationships of the amplitude velocities thereof are shown for example in FIGURE 39.

[00422] Positive amplitude corresponds to the OS approach to TS. The formulas to calculate the displacement, velocity and acceleration of a point at any given instant of time, t, are:

$x(t) = A \cos \omega t$; $v(t) = -A\omega \sin \omega t$; $a(t) = -A\omega^2 \cos \omega t$.

The maximum velocity is $A\omega$. Thus, the maximum velocities of OS and OSE are as follows:

$V_{os} = 2A_{os}\pi f_{os} = 0.38$ m/sec (maximum); and

$V_{ose} = 2A_{ose}\pi f_{ose} = 5.09$ m/sec (maximum).

As can be seen, the oscillating system movement is accompanied by two frequency categories of oscillating velocities, wherein the carrier ultrasonic oscillating velocity is ahead, by at least an order of magnitude, of the reactive oscillating

velocity, at which the oscillating system approaches to the treated surface.

[00423] Thus, the method of the invention comprises the following two main conditions:

(a) substantial excess of the ultrasonic oscillation velocity over the velocity of the oscillating system approach to the treated surface before the impact (in particular, by at least 10 times at a frequency of 27 kHz with an ultrasonic oscillation amplitude of 30 microns and a rebound frequency of 200 Hz at an amplitude of 0.3 mm, as shown above); and

(b) quick change in oscillating system oscillation mode at the instant corresponding to the time interval (more precisely, the number of oscillation periods at a specified energy of a drive pulse, including the compensation for transient processes), which is sufficient to attain a specified reduction, compensation or increase in sum between the approach velocity and the ultrasonic oscillation velocity at the onset of impact to protect the mesostructure against unfavorable damages and during impact to directly affect, through the treated surface, the structure and characteristics of the treated material.

[00424] The conditions, under which the method of impact control is formed in phase of the effect upon the material mesostructure, i.e., impact phases, are shown in FIGURES 40a-40c. More particularly, FIGURE 40a shows the "advance" wherein the vectors of oscillating velocities of OS and OSE have one direction and the resultant velocity of OSE, V_r, is maximum. When OSE contacts TS, the maximum impact impulse, P_{imp}, is transferred thereto. FIGURE 40b shows the "soft contact" wherein the vectors of oscillating velocities of OS and OSE are opposite and the resultant velocity, V_r, is "0" at the instant of contacting TS. More particularly, at the instant of contact, the ultrasonic component of the impact impulse is "0." FIGURE 40c shows the "lag/soft impact"

wherein the vectors of oscillating velocities of OS and OSE are opposite. The resultant velocity of OSE (in the contact region) is minimum. The impact impulse is minimum.

[00425] Thus, the change in ultrasonic oscillating velocity at the end of the oscillating system creates, in a phase matched with OSE, initial prerequisites for controlling impulse of force at the point of impact: from "rigid," when the oscillating velocities are added, to "soft" contact or impact, when the oscillating velocities are equal or when the ultrasonic oscillation velocity exceeds the oscillating system approach velocity at ultrasonic frequency, respectively. The vector diagrams of such states of the oscillating system according to the method are shown for example in FIGURE 41.

[00426] The diagrams in FIGURE 41 clearly reflect the "soft" impact formation mechanism at a point of the first contact between the oscillating system and the treated surface. The superposition of this mechanism on actual oscilloscope pictures of actual impacts is shown for example in FIGURE 42. At soft contact, the resultant of ultrasonic oscillation velocities of the OS and the tool at the onset of impact is zero (0). At soft impact, the resultant ultrasonic oscillation velocities of the OS and the tool at the onset of impact are negative. At rigid impact, the resultant ultrasonic oscillation velocities of the OS and the tool at the onset of impact are maximum.

[00427] FIGURE 43 shows the traditional area of UIT of a welded joint before groove formation by UIT (x10). FIGURES 44 and 45 show the types of mesostructural defects after UIT under random impact conditions, wherein FIGURE 44 shows the mesodefect at the groove edge due to local overstrengthening under random impact conditions during UIT (x40) and FIGURE 45 shows the mesodefect in the center of the groove due to local overstrengthening under random impact conditions during UIT (x160). FIGURE 46 shows the mesostructural defect after

conventional strengthening peening, i.e., surface mesodefect after hammer peening (x160). FIGURE 47 shows the state of mesostructure, i.e. groove mesostructure, after UIT (x160) in accordance with the method of the invention.

[00428] As follows from FIGURE 47, by controlling the ultrasonic impact parameters in accordance with the method described above, the surface and mesostructure of the treated surface are formed without damages that may initiate the propagation of degradation effects in service of a given welded joint. Also, at the depth of at least 1.5 mm, the region of intense plastic deformation is visible and, in turn, creates a sound physical barrier against the occurrence of such damages in the geometrical stress concentrator region under service loads during long period of time. These effects are described below in more detail. The task of formation of the strengthened layer, after "soft contact" or "soft ultrasonic impact," is solved by a method that constitutes a part of the method of the invention and involves the reverse task of excitation, in the surface layer and material, of the wave (which is maximum for a given material) of ultrasonic stresses initiated by the ultrasonic impact through the area (with optimal mesostructure) of saturation of plastic deformations caused by the soft ultrasonic impact of maximum (in terms of the treated surface strength) power.

[00429] The control parameters of high-power controlled ultrasonic impact during treatment of subsurface layer are defined by the task. As described and shown hereinabove, the "soft" phases of the ultrasonic impact are necessary to protect the treated surface against mesostructural damages and create plastic deformations in the saturation area for optimum continuation of the UIT process with minimum scattering losses at the surface and as a result thereof: (a) effective ultrasonic oscillations of the indenter of the oscillating system with detachment from the surface and synchronously

therewith; and (b) excitation under the surface of high-power ultrasonic stress waves which are sufficient, in combination with the protective properties of the modified treatment surface, to suppress the occurrence or propagation of the started process of material properties degradation.

[00430] FIGURES 48-51 show the results of varying the conditions of treated material plastic deformation under the surface at various ultrasonic impact amplitude change laws after the "soft" onset of the ultrasonic impact. In particular, the integrated oscilloscope pictures show the relation between the residual surface plastic deformation and the conditions of the change in the amplitude of 1 ms long ultrasonic impacts after "soft" phases thereof. All the results are given in comparison with the actual free dropping distribution of the amplitude within the range of the actual values thereof as shown in FIGURE 48 that also illustrates the same dependence from the specified and actually used amplitude of 30 μm, which is uniformly distributed in time. Specifically, FIGURE 48 shows independent and specified uniform (in time) distribution of the 30 μm amplitude. FIGURE 49 shows specified distribution of the ultrasonic amplitude over a convex parabola. FIGURE 50 shows specified distribution of ultrasonic amplitude over a concave parabola. FIGURE 51 shows specified increase in amplitude from 0 μm in accordance with a linear law.

[00431] The analysis of the above integrated oscilloscope pictures of ultrasonic impacts (after their "soft" phase), related to plastic deformation produced thereby, shows that plastic deformation may be controlled within a wide range during each impact event as defined by the task of affecting the material to suppress metal degradation or the conditions of its occurrence. The physical sequence of the ultrasonic impact effect on the metal structure is defined first of all

by a specific task. Some generic steps of this sequence involving the transfer from the original condition of a material to that initiated by the method of the invention are:

(1) deformation of the surface material at a rate sufficient to fill intergranular defective voids, maintaining the integrity and mesostructure of the surface material during plastic deformation initiated by "soft" impact phases;

(2) closing of structural defect boundaries under forces occurring during plastic deformation of the surface material during "soft" and force phases of the ultrasonic impact;

(3) activation of the defect boundaries closing surfaces under elastic residual stresses caused by plastic deformation of the treated surface material by means of the normalized ultrasonic impact, including periods of "soft" and force phases;

(4) activation of the defect boundary closing surfaces under impulses of force caused by impacts at a repetition rate thereof;

(5) activation of the defect boundary closing surfaces under the action of the ultrasonic impact, wherein the vector sum of the oscillating velocity is determined by the relation between the velocities of the movement of the oscillating system lumped mass and distributed masses, reduced to the oscillating system end (with an indenter), during ultrasonic oscillations of the oscillating system end in a phase specified by the control method of the resultant oscillating velocity and hence the impulse of force initiated by the ultrasonic impact;

(6) activation of the defect boundary closing surfaces under friction forces caused by the displacement of the defect boundaries during action of impact pulses and ultrasound;

(7) activation of the defect boundary closing surfaces under ultrasonic oscillations and waves of ultrasonic stresses going through a closing boundary during impulse of force caused by the ultrasonic impact;

(8) activation of the defect boundary closing surfaces in the area of elevated temperature caused by plastic deformation and friction at boundaries of structural defects and fragments during impulse action, recurring at a repetition rate of ultrasonic impacts in a phase specified by the control method as determined by the material properties and the task of action;

(9) ultrasonic self-diffusion and annihilation of closing boundaries under static pressure, impulses of force, friction, heating and ultrasonic oscillations;

(10) activation of precipitation of alloying phases, such as silicon precipitates in Al alloys, responsible for improvement in material strength in controlling the ultrasonic impact in accordance with the method of the invention;

(11) fixation of unstable phases, similar to copper in Al alloys, at the stage of "soft" ultrasonic contacts and accompanying impacts to protect against precipitation in solid solutions and prevent degradation development;

(12) activation of "reverse" self-diffusion of the precipitate in solid solutions, similar to copper in Al alloys, responsible for weakening structural bonds and creation of hidden structural stress concentrators under external forces as nuclei of subsequent metal degradation; reverse self-diffusion in this case is a means of recovering lost strength and ductility of an alloy under normalized ultrasonic impact during and after a "soft" phase thereof;

(13) activation of phase migration as a result of normalized ultrasonic impact during and after "soft" onset thereof in accordance with the control method of the invention

during, for example, increase of the fatigue resistance due to the reduction in density of distribution of potential concentrators of internal stresses at nanostructural level;

(14) activation of material structure self-control under ultrasonic impact, wherein "soft" phases of the ultrasonic impact and normalizing the ultrasonic impact parameters are in accordance with specified favorable changes in the structure of the treated surface and treated material in rotation, bending, twinning, recrystallization, flow, gliding, yielding and aging adequate to the task at the level of fragments of nano-, micro- and macrostructure of the treated material;

(15) activation of subdivision, uniformization and arrangement of the metal structure at microlevel as a means of increasing degradation resistance under normalized ultrasonic impact, wherein "soft" phases are controlled as defined by the task and thereafter, the ultrasonic impact parameters are normalized;

(16) activation of amorphization under the influence of processes initiated by organizing "soft" phases and normalizing the ultrasonic impact parameters as defined by the task - as a means of final optimization of the surface metal structure at nanolevel;

(17) using the method of controlling "soft" and force phases of the ultrasonic impact for metal protection against degradation nucleation in the original condition, prevention and suppression of degradation in the material of objects during or after long service thereof;

(18) using "soft" and force phases of the stochastic ultrasonic impact to protect a material against degradation initiation in original condition, preventing and suppressing degradation in the material during or after long service based on experimental or expert data obtained by any method referenced above.

[00432] Each technical task, the solution of which involves controlling "soft" phases of the ultrasonic impact and the parameters of the impact itself during synchronous and in-phase ultrasonic oscillations in the acoustic series "oscillating system-indenter-treated surface," may, depending on the treated material structure susceptibility, set up different requirements to the degree of controlling and matching the approach velocities and the oscillating velocity at the output of the ultrasonic oscillating system. The only criterion of the effective engineering solution of a given task is attaining a desired technical effect of degradation suppression with minimum energy consumption. This condition alone determines the requirements to the necessary degree of controlling the velocities of the action upon the material prior to and during ultrasonic impact.

[00433] A method of the invention protects metals against degradation and suppresses degradation by ultrasonic impact comprises providing impact energy, specified in accordance with a task of affecting at least one property and a state of a material and based on a dynamic strength of the material, predetermining a moment of a drive pulse initiation, predetermining phase and an amplitude of ultrasonic oscillations of an ultrasonic oscillating system, during approach of the oscillating system to a treated surface. To accomplish this aim, the method also provides surface mesostructure integrity by setting the above-mentioned adjustable parameters of the ultrasonic impact, within a range, including maximum, minimum and compensated value of a resultant of a velocity vector at an onset of the impact, setting and changing oscillating amplitude during ultrasonic impact following the oscillating system contacting the treated surface in accordance with affecting the material structure under the treated surface and based on requirements to rebound

of the oscillating system from the treated surface until termination of the ultrasonic impact.

[00434] The amplitude and the phase of ultrasonic oscillations are set, before the oscillating system contacts the treated surface during approach therebetween, such that at an onset of the impact, the velocity and energy of the impact correspond to the conditions of maintaining mesostructure integrity of the material in a surface layer and creating treated surface plastic deformation not exceeding the saturation level but sufficient to transfer an ultrasonic stress wave into the treated material, with acoustic losses remaining within a range from a level necessary for specified subsequent plastic deformation to a level determined by a Q-factor of the material.

[00435] The method of the invention further comprises setting a degree of controlling oscillating velocities in phase of the oscillating system approach to the treated surface thereby providing integrity of the material and surface layer mesostructure, based on dynamic strength reserve of the surface material in relation with an allowable rate of deformation thereof; setting ultrasonic oscillation intensity distribution during ultrasonic impacts thereby attaining at least one property and/or state of the structure and material under the treated surface, based on susceptibility of the treated material to an action of ultrasonic impacts in transition to a specified state, wherein the degree of controlling oscillating velocities and ultrasonic oscillation intensity distribution are preliminary determined based on experimental data or expertise as defined by the task.

[00436] In the method of the invention, the surface material is deformed at a rate sufficient to fill intergranular defective voids while maintaining the integrity of the surface material and mesostructure thereof during plastic deformation initiated by soft phases of the impact. Structural defect

boundaries are closed under forces occurring during plastic deformation of the surface material caused by an action of soft and force phases of the ultrasonic impact. Defect boundary closing surfaces may be activated under elastic residual stresses caused by plastic deformation of the treated surface material. Defect boundary closing surfaces also may be activated under impulses of force caused by impacts at a predetermined repetition rate.

[00437] Activation of defect boundary closing surfaces may be accompanied by an action of a vector sum of oscillating velocities of movement of the oscillating system lumped mass and oscillating system distributed mass, reduced to an oscillating system end, during ultrasonic oscillations of the ultrasonic system end in a phase, which is set by the program of controlling resultant oscillating velocity, and impulse of force caused by the ultrasonic impact. Activation of defect boundary closing surfaces under friction forces, which are caused by defect boundary displacement during an action of impact impulses and ultrasound.

[00438] Activation of defect boundary closing surfaces is accompanied by an action of ultrasonic oscillations and waves going through a closing boundary during an action of the impulse of force caused by the ultrasonic impact. In the method of the invention, defect boundary closing is also activated in an area of elevated temperature caused by plastic deformation and friction at boundaries of structural defects and fragments during impulse action, recurring at a repetition rate of ultrasonic impacts in a phase, which corresponds to material properties and task of action.

[00439] Ultrasonic self-diffusion and annihilation of closing boundaries occur under static pressure of the oscillating system, impulses of force, friction at boundaries, heating, ultrasonic oscillations and ultrasonic stress waves, which are set by conditions of forming and controlling "soft"

and force phases of the ultrasonic impact as defined by the task.

[00440] In a preferred embodiment of the invention, precipitation of alloying phases, including silicon precipitates in Al alloys, provides increased material strength which is attained by controlling the ultrasonic impact. Unstable phases, similar to copper in Al alloys, are fixed at a stage of soft ultrasonic contacts and impacts for protection against precipitation in solid solutions and prevention of degradation development.

[00441] To suppress degradation or protect metals thereagainst, activation of reverse self-diffusion of unfavorable precipitates in solid solutions, similar to copper in Al alloys, wherein the unfavorable precipitates cause weakening of structural bonds, creation of hidden structural stress concentrators caused by external forces and initiation of subsequent metal degradation, is attained by normalizing the ultrasonic impact intensity in time after a soft phase thereof and is accompanied by recovery of lost strength and ductility of an alloy.

[00442] Activation of phase migration preferably occurs as a result of normalized ultrasonic impact after soft onset thereof in accordance with a predetermined change in ultrasonic impact intensity with time. The activation is preferably accompanied by increased fatigue resistance due to redistribution and reduction in density of distribution of potential concentrators of internal stresses at a nanostructural level.

[00443] In a preferred embodiment of the invention, self-control of the material structure in rotation, bending, twinning, recrystallization, flow, gliding, yielding and aging is activated by the ultrasonic impact during normalized "soft" phases and subsequent force phases of the ultrasonic impact at a level of fragments of nanostructure, microstructure and

macrostructure of metals. Activation of subdivision, uniformization and arrangement of material structure at a microlevel, as a means of increasing degradation resistance, occurs under the effect of the ultrasonic impact during "soft" and subsequent force phases, wherein the parameters are normalized as defined by a task. The activation of amorphization, as a means of final optimization of surface material structure at a nanolevel, occurs as a result of processes initiated by the ultrasonic impact during "soft" and subsequent force phases, wherein the parameters are normalized based on experimental or expert data as defined by a task allowing for rapid local heating and cooling of a metal in the area of plastic deformation thereof. Controlling soft and force phases of the ultrasonic impact protects the material against degradation nucleation in an original condition, as well as prevents and suppresses degradation in the material of a structure during or after long service thereof.

[00444] In preferred embodiments, (1) aluminum alloys are protected against corrosion exfoliation and/or (2) properties of an aluminum alloy, which have been damaged by exfoliation, are recovered and/or repaired.

[00445] As described hereafter, the action of the method of the invention in comparison with the known methods of "combating" degradation is illustrated and provides a spectrum of engineering solutions and techniques of degradation suppression based on using "soft" phases of the ultrasonic impact of high power in affecting the surface mesostructure and controlling the ultrasonic impact parameters after a "soft" phase in affecting the properties and condition of the treated material under the treated surface.

[00446] The following are examples of types of degradation, the symptoms of the degradation, the physics of the degradation, the area of occurrence of the degradation and the application and transformation of the methods of affecting the

treated surface and treated material in accordance with the present invention to suppress the degradation.

[00447] One type of degradation is mechanical fatigue. The symptoms of mechanical fatigue include fatigue cracks. The fatigue process includes the following phases: at first, accumulation of elastic distortions of a lattice because of the increased dislocation density; thereafter, appearance of submicrocracks in the metal volumes, where a critical dislocation density is attained during mass slipping of separate blocks; and finally, microcracks growing into macrocracks. As this takes place, a brittle fracture occurs along one microcrack that develops most intensively. Mechanical fatigue occurs most often in bridges, tunnels, railways, load-carrying structures of transportation and load lifting facilities, aviation, and transport (loaded welds, stress concentration regions). The method of the invention provides creation of a compensation protective barrier and recovery of the properties of the damaged material by high-power "soft ultrasonic impact" (PSUI) with adaptive on-off time ratio modulation (O/OTRM) of drive pulses synchronized with the high-power soft ultrasonic impact. To implement such a control of drive pulse on-off time ratio, pulse width and amplitude modulation are used, which is initiated when an increase in frequency of synchronized ultrasonic impacts is needed with a small (i.e., insufficient for independent predetermined oscillation suppression) pause therebetween or the length of the transient process that is insufficient for independent recovery of oscillations. In such a manner, the following is achieved: control of plastic deformation intensity distribution in time and space during each ultrasonic impact; control of surface parameters at scales of mesostructure and crystalline structure, its stressed-deformed state and the depth of penetration in the area of existing or possible damage; and stabilization of phases, homogeneity of

structure and properties of a material in the area of instability thereof under external conditions (heating, loading, environment).

[00448] Another type of degradation is corrosion fatigue. The symptoms of corrosion fatigue include fatigue cracks that propagate from the surface. The fatigue failure process, accelerated by corrosion mechanisms is initiated by: adsorption of surface-active substances, producing a wedging effect at a microcrevice; and hydrogen diffusion, causing metal embrittlement. Corrosion fatigue occurs most often in bridges, pipelines, tunnels, sea transport, and equipment in the chemical industry (loaded welds and stress concentration regions subjected to environmental aggressive action). The invention provides protection from adsorption and prevention of adsorbing inclusions from contact with structural fragments; an increase in mobility and loss of bonding of adsorbing inclusions and surface-active substances with adsorbing surfaces, as well as in the damaged area of a material or its structure; and optimization of the surface, its mesostructure and roughness, residual stresses in the surface layer and hence the surface material resistance to adsorption (increase in material density in the surface layer).

[00449] Another type of degradation is thermal and thermal-mechanical fatigue. The symptoms of thermal and thermal-mechanical fatigue include fatigue cracks. In the fatigue failure process, a component is cyclically deformed due to low- or high-cycle temperature effect and mechanical fluctuating stresses caused thereby. As this takes place, heating may be caused by inherent basic processes of energy obtaining and spending, as well as accompanying causes during service of machinery. Thermal and thermal-mechanical fatigue occurs most often in heat and nuclear power plants, metallurgical plants (boilers, furnaces), motor and railway

transport, and handling of machinery (components of braking devices). The invention provides increased resistance to thermal and thermal-mechanical damages in the original condition and in service; maintenance and recovery of the material properties based on creating a compensation barrier of distributed residual stresses, relaxation of the stress and deformation gradient in the areas of accumulated thermal and thermal-mechanical damages, filling of the intergranular space in the areas of structural defects by grain material, and ultrasonic diffusion at grain boundaries; and optimizing the friction couples surface as a means of reducing time and heat losses in braking.

[00450] Another type of degradation is chemical corrosion. The symptoms of chemical corrosion include uniform dissolution of a material, pitting and pinpoint corrosion, flaws, crevice corrosion, and corrosion exfoliation. The physics of chemical corrosion include metal-environment chemical interaction (gas or liquid), formation of new chemical compounds on the surface, reduction in material strength and formation of stress concentrators. The negative effects of chemical corrosion occur most often in chemical plants, nuclear power engineering, pipeline transportation (tanks, pipelines, reactors), aviation, and sea, railway and motor transport (skin, hull plating). The invention provides protection of the original surface being affected and recovery of the material properties; modification of meso and crystalline structures, amorphization of the surface material, creation of the compensation barrier of residual compressive stresses in the surface material based on formulating a function of oscillating amplitude changing in the "transducer-indenter-surface" system (TIS) during PSUI; pulse and ultrasonic diffusion at grain boundaries in the region of structural failures caused by intercrystalline corrosion; and plastic deformation of a material, increase in grain size uniformity,

filling an intergranular space by grain material, pulse ultrasonic diffusion at grain boundaries.

[00451] Another type of degradation is electrochemical corrosion. The symptoms of electrochemical corrosion include local (pitting) and extensive surface corrosive damages accompanied by metal dissolution. The mechanism of metal-environment electrochemical interaction includes: anodic process - metal atom ionization with formation of ions aquated in solution and uncompensated electrons in a metal; the process of electron transfer from anodic reaction zones to regions where a cathodic process is feasible in thermodynamic and kinetic terms; the process of oxidant-depolarizer application to cathodic zones (reaction of metal ions and electrolyte ions); the cathodic process - assimilation of excess electrons by the depolarizer and in cathodic zones, the thermodynamic conditions of the recovery process is provided for the depolarizer; and dissolution and disturbance of the surface geometrical homogeneity, weakening of structural bonds and reduction in material strength in this area.

Electrochemical corrosion occurs most often in sea transport (hull plating, propellers), the chemical industry (tanks, reactors), pipelines, subsurface and subsea lines. The means of suppressing the negative effects of electrochemical corrosion in accordance with the invention include: creation of an electrochemical corrosion compensation barrier in the original condition of a material and recovery of the properties thereof; optimization of the micro- and macro-geometry of the surface, homogeneity of the surface material crystalline structure, nano crystallization and amorphization of the surface material as a means of retardation of the anodic processes; surface plastic deformation, creation of the area of compressive stress and increased material density to retard the localization of electrochemical corrosion of surface defects; and using the PSUI mechanism to form the

above surface conditions in the case of optimum surface mesostructure.

[00452] Another type of degradation is thermal corrosion. The symptoms of thermal corrosion include material dissolution and evaporation, and scale formation. The physics of thermal corrosion include high temperature induced metal-environment chemical interaction. Thermal corrosion occurs most often in thermal and nuclear power plants, metallurgical plants (boilers, furnaces), and chemical plants (reactors). The invention provides creation of a chemical corrosion compensation barrier in the original condition of a material and recovery of the properties thereof through the use of the PSUI mechanism to optimize the quality and increase the surface alloying depth in application of protective heat-resistant coatings and in repetition of these operations, if needed, on a scale layer and if the surface material properties need to be repaired.

[00453] Another type of degradation is radiation corrosion. The symptoms of radiation corrosion include corrosion pits and cracks. The mechanisms of the radiation emission effect on the kinetics of corrosion processes include: a radiolysis effect which is caused by irradiation on water and accelerates the cathodic process due to water ionization; and the destructive effect which consists of elastic and thermal metal surface-radiating particles interaction, resulting in defects in the metal surface layer and oxide film. These defects facilitate the anodic process and have the most profound effect on the corrosion rate. The negative effects of radiation corrosion occur most often in nuclear power engineering, military facilities, and space systems. The method of affecting the treated surface and treated material of the present invention provides creation of a radiation corrosion compensation protective barrier in the original condition of a material being affected and recovery of the

properties thereof using the PSUI mechanism to: optimize the quality and increase the surface alloying depth in application of protective heat- and radiation-resistant coatings; optimize the surface condition in terms of its roughness, mesostructure, micro-grain structure and material amorphization; and create the favorable compressive stress field and increase the surface material density. Repetition of these operations on a damaged layer provides recovery of the radiation resistance of the surface material at a level of an original material being affected.

[00454] Another type of degradation is corrosion cracking. The symptom of corrosion cracking includes corrosion cracks. The mechanisms of corrosion cracking include: adsorption of solution anions on movable dislocations and other structural imperfections which reduces the surface energy and facilitates the breakdown of atomic bonding of metals; occurrence of crack nucleation as a result of a wedging action of surface-active substances in adsorption thereof in microcrevices on the metal surface. A high crack development rate in this case is caused by the accelerated anodic dissolution of the metal at the crack base, where the stressed-deformed state is generally determined by a tensile stress concentration. Corrosion cracking occurs most often in chemical plants, nuclear power engineering, and pipeline transportation (tanks, pipelines, pumping facilities, reactors). The method of protection against corrosion cracking in accordance with the present invention provides creation of a compensation protective barrier against the formation of corrosion cracks in the original condition of a material and in recovery of the properties thereof by using the PSUI mechanism to: optimize the quality, adhesion or to increase the alloying depth of protective coatings applied to potentially or actually damaged surface, as well as to induce favorable compressive stresses into the surface in strengthening or modification thereof to a

predetermined depth in optimal or specified condition of the mesostructure; modify the structure and create the stressed-deformed state of the material structure that makes impossible absorption of solution anions on movable dislocations and other structural imperfections that reduce the surface energy and weaken atomic bonds; optimize the surface mesostructure and prevent crack nucleation as a result of a wedging action of surface-active substances in adsorption thereof in microcrevices on the metal surface; create a compressive stress field on the surface with optimal mesostructure, the magnitude and depth of which is sufficient for protection against high crack propagation rate caused by accelerated anodic dissolution of a metal at the crack base, where the stressed-deformed state is generally determined by tensile stress concentration.

[00455] Another type of degradation is hydrogen embrittlement. The symptoms of hydrogen embrittlement include reduction in strength properties and brittle cracks. The mechanisms of hydrogen embrittlement include: penetration of atomic hydrogen in voids, pores and other lattice defects; hydrogen transformation into molecular gas that creates high pressure; adsorption of atomic hydrogen on surfaces of a component and internal defects with formation of chemical compounds with metal and impurities; and reducing the surface energy and the brittle fracture resistance of a metal. Hydrogen embrittlement occurs most often in metallurgical and engineering plants, pipelines (welded structures, galvanic plants), petrochemical plants (reactors), and aviation (skin). The method of protection against hydrogen embrittlement in accordance with the present invention provides using the PSUI mechanism to: strengthen the surface alloying quality, adhesion strength and density of galvanic coatings; create a compressive stress field on the surface with optimal mesostructure, the magnitude and depth of which is sufficient

for protection against reduction in strength properties and formation of brittle cracks that may be caused by penetration of atomic hydrogen in voids, pores and other lattice defects; hydrogen transformation into molecular gas that creates high interfragmentary pressure; adsorption of atomic hydrogen on surfaces of a material and internal defects with formation of chemical compounds with metal and impurities that reduce the surface energy of a metal and the brittle fracture resistance.

[00456] Another type of degradation is liquid-metal embrittlement. The symptoms of liquid-metal embrittlement include reducing strength properties and brittle cracks. The physics of liquid-metal embrittlement includes: adsorption penetration of the molten metal in the solid metal pre-failure zone; and reduction in surface energy and metal rupture resistance in the damaged area. Liquid-metal embrittlement occurs most often in metallurgical plants (galvanic manufacture). The method of prevention or "healing" against liquid-metal embrittlement in accordance with the present invention provides using PSUI to create an optimal mesostructure and compressive stress field on a surface, the magnitude and depth of which is sufficient for protection against the strength properties reduction, formation of brittle cracks, adsorption penetration of the molten metal in a solid metal pre-failure zone, reduction in surface energy and metal rupture resistance.

[00457] Another type of degradation is erosion. The symptom of erosion includes surface relief change. The physics of erosion include detaching solid particles from the body surface being affected as a result of the body contact with a moving liquid, gaseous environment or particles entrained thereby as a result of the impact of solid particles with the surface being affected. Erosion occurs most often in pipeline transportation (pipes, pumping facilities), aviation (turbines), sea transport (propellers), rockets and missiles

(skin). The method of prevention or recovery of eroded surfaces in accordance with the present invention provides using PSUI to create an optimum density, roughness, mesostructure and compressive stress field at the surface, the magnitude and depth of which is sufficient for protection against the detachment of solid particles from the body surface as a result of the body contact with a moving liquid, gaseous environment or particles entrained thereby or as a result of the impact of solid particles upon the surface being affected.

[00458] Another type of degradation is creep. The symptoms of creep include formation of microcracks and pores (microvoids) at grain boundaries and substructure formation. The mechanisms of creep include: gliding and slip (dislocation diagram); twinning; bending of slip planes; lamellation; rotation and relative movement of grains; rotation and relative shift of mosaic blocks; poligonization; diffusion plasticity; recrystallization mechanism; and combining defects and structural damage at micro and macro levels. Creep occurs most often in heat and nuclear power plants, petrochemical industry, and aviation (structures, reactor bodies and turbine blades operating at high temperature). The method of preventing and "healing" creep in accordance with the present invention provides using PSUI to attain an optimal density, mesostructure condition and grain in a packing size and the field of compressive macrostress and microstress at and under the surface, the magnitude and depth of which is sufficient to protect against formation of microcracks and pores (microvoids) at grain boundaries and substructure, gliding and slip (based on dislocation diagram), twinning, bending of slip planes, lamellation, rotation and relative movement of gains, rotation and relative shift of mosaic blocks, polygonization, diffusion plasticity,

recrystallization, and combining defects and structural damage at micro and macro levels.

[00459] Another type of degradation is microstructural degradation. The symptom of microstructural degradation includes reduction in strength properties of a material. The mechanisms of microstructural degradation include absorption of molecules from the environment by micro-surfaces developing in a deformed body (Rebinder effect) and stabilizing the unfavorable metal phase condition in time at the expense of transforming unstable phases without a considerable change in microstructure (aging). Microstructural degradation occurs most often in power plants, refineries (frame structures), pipelines, sea transport, and aviation (body, skin). The method of preventing and "healing" microstructural degradation in accordance with the present invention is based on using PSUI in creating optimum density of a material, mesostructure on the material surface, and normalizing plastic deformations and compressive stress field at the surface, the magnitude and depth of which is sufficient to prevent reduction in material strength properties caused by microstructural degradation that may include absorption of molecules from the environment by micro-surfaces developing in a deformed body (Rebinder effect); and/or stabilizing the unfavorable metal phase condition in time at the expense of transforming unstable phases without a considerable change in microstructure (aging).

[00460] Another type of degradation is radiation embrittlement. A symptom of radiation embrittlement includes brittle cracking with an abrupt increase in yield strength. The physics of radiation embrittlement include a neutron stream shifting the atoms or producing a shift cascade in a metal lattice depending on the amount of the energy the neutron transfers to the metal atom which results in the volumes with high vacancy concentration, which are surrounded

along the periphery by zones with increased density of interstitial atoms. Radiation embrittlement occurs most often in nuclear power engineering (reactors), space systems, and military facilities (missile body skin). The method of preventing or "healing" radiation embrittlement in accordance with the present invention provides using PSUI to attain the optimal density and mesostructure of the treated material through normalization of plastic deformations and compressive stress field on and under the surface, the magnitude and depth of which is sufficient to prevent the formation, in the case of an abrupt increase in yield strength of brittle cracks caused by atomic shift or a shift cascade (under neutron stream) in a metal lattice depending on the amount of the energy the neutron transfers to the metal atom and thereafter the formation of high concentration of vacancies surrounded along the periphery by zones with increased density of interstitial atoms.

[00461] Another type of degradation is exfoliation. The symptoms of exfoliation include surface corrosion exfoliation of a metal with formation of stress concentrators and loss of strength. The physics of exfoliation include synergetic effect of corrosion and hydrogen embrittlement. Exfoliation occurs most often in aviation. The method of preventing or suppressing ongoing corrosion exfoliation in accordance with the present invention is based on using PSUI with a level and time parameters corresponding to the experimentally found requirements for attaining the optimum density of a treated material with a guaranteed integrity of its mesostructure, and for the conditions of formation and normalization of local point heating and the rate of heat rejection from this plastic deformation region, plastic deformations themselves and a compressive stress field on and under the treated surface, the magnitude and depth of which is sufficient to:

- prevent surface corrosion exfoliation of a metal with formation of stress concentrators and the loss of strength or recovery of metal properties in the area of these damages caused, in particular, by the synergetic effect of corrosion and hydrogen embrittlement,

- prevent formation of unstable phases that cause the components to precipitate, resulting in a reduced level of structural bonds and strength of a material, e.g., Cu,

- provide activation of self-diffusion at boundaries of structural fragments and elimination of corrosion cracking at grain boundaries,

- eliminate structural macro and micro defects such as pores or other types of intergranular discontinuities in closing their boundaries, and activating self-diffusion processes,

- provide reverse diffusion of precipitates and recovery of stable phases,

- provide precipitation of alloying elements, increase in their concentration density and the strength of a material in this region,

- ensure compensation, redistribution or relaxation of structural mechanical stresses in the area of their concentration, caused by precipitates from solid solutions of unstable phases,

- form hyper fine-grain structure, its amorphization, increase in strength of a material and its corrosion resistance on this basis.

[00462] The specific engineering solutions detailed above enable transfer to specific examples of application of the method of metal degradation suppression of the invention. The attained technical effects produced by the action of the developed method of using ultrasonic impact on various materials are detailed below. The results of the experimental investigation of this action and its conditions and the

effects attained are also detailed below. More particularly, the effect of ultrasonic impact on suppression of degradation phenomena in metals according to the method of the invention is detailed below.

[00463] Thus, in cast iron, a material effect attained is extended life of automotive brake drums and discs made of cast iron. The outcome is shown in FIGURES 52-53. FIGURE 52 shows microhardness distribution and FIGURE 53 shows residual stress distribution. The UIT conditions to attain this material effect are preferably as follows: f - 27 kHz; A - 30 μm; Pressure - 21 kg; Indenter - 6.35x25 mm, R5.5 mm; Dia. - 419 mm; Rot. - 190 RPM; Pass 1: Feed - 0.8 mm/min.; Pass 2: Feed - 0.4 mm/min. This material effect is attained by introduction of compressive stresses of high level, an increase in microhardness of a surface layer, and protection of mesostructure against service and process-induced damages.

[00464] Another material effect in cast iron by UIT in accordance with the invention is increased corrosion strength, in particular, of water cast iron pipes ANSI/AWWA C151/A21.51-96 made of cast iron of VCh45-5 type. The outcome is shown in FIGURES 54-56. More particularly, FIGURE 54 shows a structure of an untreated specimen at a depth of 100 μm, FIGURE 55 shows a structure of a UIT treated specimen at the depth of 100 μm and FIGURE 56 shows a comparison of specimens treated and not treated by UIT and tested in tap water. The UIT conditions for this material effect are preferably as follows: f - 44 kHz; A - 18 μm; Pressure - 5 kg; Indenter - 5x25 mm, R5 mm; Dia. - 230 mm; Rot. - 16 RPM; Feed - 0.25 mm/min. This material effect is attained by modification of the surface layer structure by intense normalized plastic deformation thereof, creation of the compressive stress region, and suppression of surface defects that initiate mesostructural damage during service.

[00465] In steel, a material effect attained is increased fatigue resistance of welded specimens in Weldox 420 steel. The outcome is shown in FIGURE 57. The UIT conditions to attain this material effect are preferably as follows: f - 27 kHz; P - up to 900 W; A - 30 μm; Pressure - 5 kg; Ultrasonic impact duration - 1.2-2 msec. This material effect is attained by introduction of compressive stresses of high level, stress concentration reduction, ultrasonic plastic deformation and structural modification of the treated material in the stress concentration area. The preferable relationship has been experimentally established between the conditions of ultrasonic oscillations, the pressure and indenter sizes that ensure protection of mesostructure against process-induced and operational damage during service and preparation of a surface with the use of PSUI.

[00466] Another material effect attained in steel is increased fatigue resistance of welded specimens in Weldox 700 steel. The outcome is shown in FIGURE 58. The UIT conditions to attain this material effect are preferably as follows: f - 27 kHz; P - up to 900 W; A - 30 μm; Pressure - 5 kg; Ultrasonic impact duration - 0.8-1.2 msec. This material effect is attained by introduction of compressive stresses of high level, stress concentration reduction, ultrasonic plastic deformation and structural modification of the treated material in the stress concentration area. The relationship has been experimentally established between the conditions of ultrasonic oscillations, the pressure and indenter sizes that ensure protection of mesostructure against process-induced and operational damage during service and preparation of a surface with the use of PSUI.

[00467] Another material effect attained in steel is increased corrosion-fatigue strength of 45Mn17Al3 steel. The outcome is shown in FIGURE 59. The UIT conditions to attain

this material effect are preferably as follows: f - 27 kHz; P - up to 900 W; A - 30 μm; Pressure - 5 kg; Ultrasonic impact duration - 1.5-2 msec. This material effect is attained by introduction of compressive stresses of high level into the treated surface and treated material and modification of their structure. The relationship has been experimentally established between the conditions of ultrasonic oscillations, the pressure and indenter sizes that ensure protection of mesostructure during service and treatment of a surface with the use of the ultrasonic impact in accordance with the invention.

[00468] Another material effect attained in steel is increased impact strength of bridge steel 10CrSiNiCu. The outcome is shown in FIGURE 60. The UIT conditions to attain this material effect are preferably as follows: f - 27 kHz; P - up to 900 W; A - 30 μm; Pressure - 5 kg; Ultrasonic impact duration - 1.2-1.7 msec. This material effect is attained by arrangement of a block structure at nanolevel and creation of regions of compressive stresses sufficient to retard mesostructural damage during effect upon the treated material by quasistatic and dynamic loads initiated by the ultrasonic impact normalized as defined by the task and thereafter by operation forces.

[00469] Another material effect attained in steel is a grain refinement in high-strength steels SUJ2 and S33C. The outcome is shown in FIGURE 61. The UIT conditions to attain this material effect are preferably as follows: f - 27 kHz; A - 25, 30 and 33 μm; NI80; Pressure - 20 kg; Indenter - 6.35x25 mm; Dia. - 5 mm; Rot. - 500 RPM; Ultrasonic impact duration - 1.5-1.6 msec. This material effect is attained by intense ultrasonic plastic deformation of the treated material and arrangement of microstructure at nanolevel and suppression of mesostructural damage.

[00470] Another material effect attained in steel is obtaining a "white layer" in 10Mn2VNb steel welded joint of a main pipeline and in specimens of high-strength steel SUJ2. The outcome is shown in FIGURES 62-63. More particularly, FIGURE 62 shows a welded joint of 10Mn2VNb steel and FIGURE 63 shows a specimen of SUJ2 steel. The UIT conditions to attain this material effect are preferably as follows:

For 10Mn2VNb steel: f - 27 kHz; P - up to 900 W; A - 30 μm; Ultrasonic impact duration - 0.8-12 msec.

For SUJ2 steel: f - 27 kHz; A - 25, 30 and 33 μm; NI80; Pressure - 20 kg; Indenter - 6.35x25 mm; Dia. - 5 mm; Rot. - 500 RPM. This material effect is attained by intense ultrasonic plastic deformation of the surface material under normalized ultrasonic impact at high deformation loading rate, local warming-up in the phase transformation region and quick heat removal from the impact region.

[00471] Another material effect in steel is attained by the effect of UIT on weld metal crystallization in welding carbon ship building steel 10CrSiNiCu which includes: (1) the dendritic structure in the untreated weld (before UIT) being much coarser than that in the treated weld (after UIT); (2) the grain structure, preferably with finer grain, prevailing in the UIT treated weld; and (3) dendrites in the untreated weld before UIT being longer and wider in the thicker intergranular layer than after UIT. This effect is shown in FIGURES 64-65. More particularly, FIGURE 64 shows welding without UIT and FIGURE 65 shows welding with UIT. The UIT conditions to attain this material effect are preferably as follows: f - 27 kHz; A - 30 μm; Pressure - 20 kg; Indenter - 6.35x25 mm; Ultrasonic impact duration - 1.5-2 msec. This material effect is attained by intensification of diffusion processes and metal recrystallization under the action of ultrasonic wave, acoustic flows, sound pressure and

cavitation, which are initiated by indenter ultrasonic oscillations synchronously with carrier oscillations of the ultrasonic oscillating system during ultrasonic impact.

[00472] Another material effect of affecting the structure and condition of a material is attained by UIT of sintered powder steel. This provides strengthened mechanical properties of steel specimens containing 0.4% C, 0.85% Mo, the remainder Fe, including: (1) up to 4.9% increase in density; and (2) up to 32% increase in strength. The structural condition of the sintered specimens before UIT and after UIT is shown in FIGURES 66-67, respectively. The UIT conditions to attain this are preferably as follows: f - 27 kHz; A - 28 μm; NI64; Pressure - 17 kg; Indenter - 6.35x25 mm; Feed - 400 mm/min.; Cross feed - 0.5 mm/travel; Static pressing at a level of 0.5 YS; Ultrasonic impact duration - 1.2-2 msec. This material effect is attained by intense ultrasonic plastic deformation of the surface material and activation therethrough of diffusion processes caused by ultrasonic wave during ultrasonic impact.

[00473] A material effect attained in aluminum alloys by UIT of the invention is the fatigue limit of specimens made of 6061 T6 alloy increased by 21% and the fatigue limit of the structure, which is equivalent to the type of a welded joint, increased by 32%. The outcome is shown in FIGURE 68. The UIT conditions to attain this material effect are preferably as follows: f - 27 kHz; P - up to 900 W; A - up to 30 μm; Treatment speed - 1.2 sec./cm per 2 passes, i.e., 0.6 sec./cm per pass for lap welds; Ultrasonic impact duration - 1.2-1.7 msec. This material effect is attained by introduction of compressive stresses of high level, stress concentration reduction, and creation of a physical barrier against mesostructural defect formation in the region of directed

plastic deformation and compressive stresses corresponding to the level of defects.

[00474] Another material effect attained in aluminum alloys is increased high-cycle fatigue strength in particular of welds in aluminum alloy AA5083 (or AlMg4.5Mn) was about 80% for 8 mm lap joints and specimens with longitudinal attachments. The outcome is shown in FIGURES 69-70. More particularly, FIGURE 69 shows S-N curves for 8 mm specimens with longitudinal attachments and FIGURE 70 shows S-N curves for 8 mm specimens of lap joints. The UIT conditions to attain this material effect are preferably as follows: f - 27 kHz; P - up to 900 W; A - up to 30 μm; Ultrasonic impact duration - 1.2-1.7 msec. This material effect is attained by introduction of compressive stresses of high level, stress concentration reduction, and suppression of possible mesostructural damages by means of ultrasonic recrystallization in solid solution and activation of ultrasonic diffusion at grain boundaries during ultrasonic impact in accordance with the invention.

[00475] Another material effect attained in aluminum alloys is suppression of near-surface, specifically casting porosity at a depth of up to 2.5 mm and as a result of this life extension of cast wheels, specifically automobile wheels, made of alloys AlSi7Mg, AlSi9Mg and AlSi11Mg. The outcome is shown in FIGURES 71-72. The UIT conditions to attain this material effect are preferably as follows: f - 27 kHz; Feed - 400 mm/min.; Cross feed - 0.5 mm/travel; Pressure - 15 kg; A - 30 μm; Pass 1: Indenter - 6.35x25 mm, R5.5 mm; Pass 2: Pin-9.05x25 mm, R10 mm; Ultrasonic impact duration - 1.2-1.7 msec. This material effect is attained by intense plastic deformation of the treated material near-surface layer, ultrasonic diffusion at defect boundaries, closed under ultrasonic impact, in the form of pores or discontinuities in

a material and suppression of mesostructural defects in the region of normalized plastic deformation and compressive stresses, corresponding to the level of plastic deformations, under normalized ultrasonic impact of the invention and effects accompanying its influence on the structure, which are caused, in particularly, by reduced deformation resistance during propagation of the ultrasonic stress wave in the material being deformed by the ultrasonic impact.

[00476] In addition to increased strength of the treated material, another material effect attained in aluminum alloys by UIT in accordance with the invention is maintained impact strength of the treated material, in particular, in treatment of cast wheels made of alloys AlSi7Mg, AlSi9Mg and AlSi11Mg. The outcome is shown in FIGURES 73-74. More particularly, FIGURE 73 shows impact strength on specimens with a strengthened notch and FIGURE 74 shows impact strength on specimens cut out from a strengthened wheel. The UIT and ultrasonic impact machining (UIM) conditions made it possible to fix the impact strength in the region of intense plastic deformation caused by impact loading at the level of original material. In the area of action of the wave of ultrasonic stresses initiated by the ultrasonic impact, the impact strength increases by 12%. The UIT conditions to attain this material effect are preferably as follows: f - 27 kHz; Feed - 400 mm/min.; Pressure - 15 kg; Pin- 9.05x25 mm, R0.25 mm; Wedge 44°; Condition 1: A - 10 μm; Condition 2: A - 20 μm; Condition 3: A - 30 μm; Ultrasonic impact duration - 1.2-1.7 msec. Additional UIT conditions are: f - 27 kHz; Indenter - 6.35x25 mm, R25 mm; UIT conditions: Pass 1: A - 20 μm and Pass 2: A - 12 μm; UIM conditions: V - 18 m/min.; Feed - 0.5 mm/rev.; Indenter - 6.35x33 mm, R25 mm; Pass 1: Pressure - 15 kg and A - 22 μm; Pass 2: Pressure - 7 kg and A - 12 μm; Ultrasonic impact duration - 1.2-1.7 msec. Since during UIM

and UIT, the structural distortion may occur under intense plastic deformation, which may therefore cause retardation of dislocations and formation of other defects in the treated material on a grain scale, having defined, in accordance with the invention, the conditions wherein after UIT of a stress concentrator, the impact strength of Charpy specimens directly depends on the specimen size, i.e., the relation between volumes of the deformed and non-deformed material. For terms of explanation, a Charpy Test is a pendulum-type single-blow impact test in which the specimen, which is usually notched, is supported at both ends as a simple beam and broken at the notch, a dynamic stress concentrator, by an impact of a falling pendulum. The energy absorbed is taken as a measure of impact strength or notch toughness calculated by the subsequent rise of the pendulum (following the impact upon the specimen being broken). In addition, the Charpy value is directly affected by the condition of the notch mesostructure, which according to the invention is controlled by normalizing plastic deformation during the action of the ultrasonic impact of the present invention and ultrasonic stress waves initiated thereby.

[00477] Another material effect attained in aluminum alloys by UIT in accordance with the present invention is specifically precipitation of silicon inclusions from solid solution of $AlSi_{11}Mg$ alloy, which are alloying inclusions and increase the material strength. This effect is shown in FIGURES 75-77. More particularly, FIGURE 75 shows an untreated specimen structure; FIGURE 76 shows silicon precipitates on a UIT treated specimen and FIGURE 77 shows microhardness distribution in depth of untreated specimens and UIM specimens, which clearly demonstrates the increase of, in particular, microstrength of the treated surface and treated material at the depth of at least 2 mm due to precipitation of silicon inclusions in the layer. The UIT conditions to attain

this material effect are preferably as follows: f - 27 kHz; V - 18 m/min.; Feed - 0.5 mm/rev.; Indenter - 6.35x25 mm, R25 mm; Pass 1: Press - 15 kg and A - 22 μm; Pass 2: Press - 7 kg and A - 12 μm; Ultrasonic impact duration - 1.2-1.7 msec. This material effect is attained by UIM in accordance with the present invention by strengthening a surface layer due to structural changes occurring therein. In the surface layer, a more solid eutectic structure (α+Si)+Si forms out of two-phase condition of the original structure (α+eutectic (α+Si)+Si). This process is also accompanied by migration of silicon inclusions to the surface under ultrasonic impacts and substantially reflects the objective ability of Al-Si alloys to be strengthened due to silicon precipitation in the near-surface layer.

[00478] Another material effect attained in aluminum alloys by UIT/UIM in accordance with the invention is a recovery of properties of 2024-T351 alloy after corrosion exfoliation. After UIT in accordance with the invention, the yield strength of exfoliated specimens increased by 33% (19% increase as against the untreated non-exfoliated material), the ultimate strength increase by 24% (as against the untreated non-exfoliated material, after UIT/UIM an increase is up to typical strength of the material within measuring accuracy). The outcome is shown in FIGURES 78-79. The UIT conditions to attain this material effect are preferably as follows: f - 36 kHz; Indenter - 5x17 mm, R25 mm; A - 18 μm; NI64; Pressure - 3 kg; Feed - 400 mm/min.; Cross feed - 0.5 mm/travel; Ultrasonic impact duration - 1.0-1.3 msec. This material effect is attained by ultrasonic impact diffusion at grain boundaries.

[00479] Another material effect attained in aluminum alloys by UIT in accordance with the invention is an increase in cyclic life of specimens made of 7075-T6 alloy cut from aircraft wing skin panels by a factor of 3.2 in a lightly

corroded specimen and 2.9 in a severely corroded specimen. FIGURE 80 shows the effect of UIT in accordance with the invention on fatigue resistance of specimens with different degree of corrosion. The UIT conditions to attain this material effect are preferably as follows: F - 36 kHz; Indenter - 5x17 mm, R25 mm; A - 20 μm; NI64; Press - 3 kg; Feed - 400 mm/min; Cross feed - 0.5 mm/travel; Ultrasonic impact duration - 1.0-1.3 msec. UIT of the invention changes the crack nucleation mechanism. Thus, for corroded specimens without UIT, cracks nucleate from intergranular cracking on the interface of the corrosion region and substrate; and for lightly corroded specimens with UIT of these portions in accordance with the invention, cracks do not nucleate. This effect is explained by mechanical closing of the grain boundaries followed by ultrasonic diffusion therebetween in the area of intergranular corrosive damage under intense ultrasonic plastic deformation.

[00480] Another material effect attained in aluminum alloys by UIT in accordance with the invention is more refined structure of cold-rolled plate of 2024-T351 alloy (on average from 16.52 nm to 8-10 nm) as against the original state. The outcome is shown in FIGURES 81-82. More particularly, FIGURE 81 shows a structure in a surface layer before UIT treatment and FIGURE 82 shows a finer grain structure refined by UIT. The UIT conditions to attain this material effect are preferably as follows: f - 36 kHz; Indenter - 5x17 mm, R25 mm; A - 15 μm; NI64; Press - 3 kg; Feed - 1000 mm/min.; Cross feed - 0.5 mm/travel; Ultrasonic impact duration - 0.9-1.2 msec. This material effect of grain refinement occurs due to: formation of high dislocation density and twinning structure because of additional deformation; formation of microband structure; subdivision of microband structure into submicron grains; and further breakdown of the subgrains to be equiaxed.

[00481] Another material effect attained in aluminum alloys by UIT in accordance with the invention, specifically cold-rolled plate of 2024-T351 alloy, is precipitate migration and occurrence of microbands 10-15 nm wide. This accompanies the process of subfinegrain structure self-arrangement and increases the resistance of the mesostructure to mechanical and corrosive damage in the surface layer at nanolevel. Thus, two effects that occur due to UIT of the invention are an increase in microhardness in the surface layer and hence an increase in static strength of the material, and creation of conditions for fatigue strength improvement through the reduction of distribution density of precipitates, i.e., structural stress concentrators, as well as an increase in structural homogeneity in the surface layer. This effect is shown in FIGURES 83-85. More particularly, FIGURE 83 shows microhardness distribution, FIGURE 84 shows a surface layer structure before UIT treatment of the invention and FIGURE 85 shows microbands in a UIT specimen. Examination of the precipitates using energy dispersive spectroscopy (EDS) identified that the precipitates were rich in Al, Cu, Fe, Mn and Si. However, the density of the precipitates was found to exhibit a minimum at the surface and near surface of the UIT samples. Comparison with the "as-rolled" state reveals that the size of the precipitates after the UIT exhibits a reduced scale while their density shows maxima within the band. By integrated comparison of the above observations, the potential stress concentration distribution density is generally reduced at structural level. This may be considered as a necessary condition for increasing the material ability to resist the fatigue damage formation. The UIT conditions to attain this material effect are preferably as follows: f - 36 kHz; Pin-5x17 mm, R25 mm; A - 18 μm; NI64; Pressure - 3 kg; Feed - 400 mm/min.; Cross feed - 0.5 mm/travel; Ultrasonic impact

duration - 1.0-1.3 msec. This material effect is attained by a geometric dynamic recrystallization process in which the high energy and high temperature may achieve a critical level and hence cause the precipices to migrate. In any case, this effect is accompanied by a normalized action of the ultrasonic impact, local heating, heat removal, distribution of a normalized ultrasonic stress wave and, as a result thereof, normalization of metal plastic deformation.

[00482] A material effect attained in bronze by UIT in accordance with the invention is an increase in corrosion-fatigue strength, in particular of Cu_3 bronze propellers ($BrAl_9Fe_4Ni_4$). The outcome is shown in FIGURES 86-87. More particularly, FIGURE 86 shows corrosion damage on an untreated sample surface and FIGURE 87 shows a surface of a sample after UIT. The UIT conditions to attain this material effect are preferably as follows: f - 27 kHz; P - 900 W; A - up to 30 μm; Pins- 3x20 mm, R3 mm. This material effect is attained by introduction of compressive stresses of high level, modification of the surface layer structure, ultrasonic diffusion at boundary closing of structural defects such as pores, protection against damages and suppression of mesostructural damages at micro and macro levels.

[00483] Since cracks of different nature present the most prevailing final evidence of major types of metal degradation, specific methods of the UIT effect on the kinetics of crack initiation and development include:

(a) a "very" smooth surface with a roughness of, e.g., not greater than 0.5 μm and residual compressive stresses induced to a relatively small depth of up to 0.7 mm, wherein such a surface will allow a "long" delay in crack initiation with a possible rather rapid crack development after starting, and suppression by the techniques of UIT of the present invention described hereinabove;

(b) a smooth surface with a roughness of 0.5 μm and more, an intact mesostructure and compressive stresses induced to a medium depth of up to 1.5 mm, which together will allow a longer material resistance to crack initiation and development after starting in the high compressive stress field to a rather significant depth, but not less than 0.7-1.5 mm;

(c) a smooth surface with an intact subsurface mesostructure (minor surface damage is possible to the depth of no greater than 0.003 mm), fine grain in the subsurface layer and compressive stresses induced to a greater depth of up to 2.5 mm, which result in higher material resistance to crack initiation and damp the crack development after starting in the area of a fine grain structure and a compressive stress field;

(d) a smooth surface with an intact subsurface mesostructure (minor surface damage is possible to the depth of no greater than 0.008 mm), fine grain and amorphous structure in the near-surface layer, as well as compressive stresses induced to a maximum depth for a given material (up to 4.0 mm) using controlled ultrasonic impact, which will result in higher material resistance to crack initiation, damp the crack development after starting in the area of fine grain and/or amorphous structure and continue the crack retardation in the field of compressive stresses that are substantial as against the yield strength of the treated material.

[00484] In addition, starting cracks are "cured" and developing fatigue cracks are retarded by the following effects of UIT of the present invention:

(a) diffusion joining of crack boundaries;

(b) submersion of the crack development zone into residual compressive stress area (crack preservation);

(c) removal of a cracked metal surface layer (similar to abrasive grinding) to the undamaged metal.

[00485] The material effects described above are attained by controlling ultrasonic impact parameters during its soft and force phases. Also, the major criterion of setting ultrasonic impact parameters is a specific engineering task that governs the requirements to the depth of controlling thereof. In addition, the ultrasonic impact parameters are set based on experimental or expert data. Thus, in accordance with the invention, the depth of controlling ultrasonic impact parameters, specifically a resultant velocity at the onset of impact, impact energy, repetition rate and time of impact, amplitude and phase of impact, is defined by a specific task based on experimental or expert data, wherein these parameters are set with a scatter from 5% to random values based on specific technical requirements and practical results.

[00486] The results detailed above confirm the high technological effectiveness of the techniques (developed in accordance with the present method) of using the ultrasonic impact of the invention to suppress phenomena initiating metal degradation and degradation as such if this occurs during service of machinery and structures.

[00487] It is to be understood that any of the above described types or symptoms of degradation can be prevented or suppressed by the described engineering solution on the material either individually or in combination to provide at least one desired material effect to achieve any desired technical effect or task. For example, degradation based on corrosion cracking can be addressed individually to achieve one technical effect or can be addressed in combination, for example, with thermal cracking and/or erosion to achieve a further technical effect. Thus, different data elements are interchangeable to achieve different results or technical effects for different tasks.

[00488] As will be apparent to one skilled in the art, various modifications can be made within the scope of the aforesaid description. Such modifications being within the ability of one skilled in the art form a part of the present invention and are embraced by the appended claims.

WHAT IS CLAIMED:

1. A method of protecting metals against degradation and suppressing degradation by ultrasonic impact under impact energy defined by a task of affecting at least one property or condition of a material and based on a dynamic strength of the material, comprising:

predetermining a moment of a drive pulse initiation, a phase and an amplitude of ultrasonic oscillations of an ultrasonic oscillating system end, during approach of an oscillating system to a surface to be treated to provide surface mesostructure integrity, within a range, including maximum value, minimum value and compensated value of a resultant velocity vector at an onset of an impact; and

setting and changing an oscillating amplitude during ultrasonic impact following the oscillating system contacting the surface in accordance with affecting a material structure under a treated surface and based on requirements to rebound the oscillating system from the treated surface until termination of the ultrasonic impact.

2. The method according to claim 1, wherein the amplitude and the phase of ultrasonic oscillations are set, before the oscillating system contacts the surface during approach therebetween, such that at an onset of a contact, a velocity and energy of the impact correspond to a condition of maintaining mesostructure integrity of the material in a surface layer at a level of treated surface plastic deformation not exceeding saturation thereof but sufficient to transfer an ultrasonic stress wave into the material with acoustic losses remaining within a range sufficient for specified subsequent plastic deformation but not greater than that determined by a Q-factor of the material.

3. The method according to claim 1, further comprising:

setting a degree of controlling oscillating velocities in phase of the oscillating system approach to the surface thereby providing integrity of the material and surface layer mesostructure, based on dynamic strength reserve of a surface material in relation with an allowable rate of deformation thereof; and

setting ultrasonic oscillation intensity distribution during ultrasonic impacts, which is sufficient to attain said at least one property of the material structure and material under the surface, based on susceptibility of the material treated to an action of ultrasonic impacts in transition to a specified state,

wherein said degree of controlling oscillating velocities and ultrasonic oscillation intensity distribution are preliminarily determined based on experimental data or expertise as defined by the task.

4. The method according to claim 2, further comprising:

setting a degree of controlling oscillating velocities in phase of the oscillating system approach to the surface thereby providing integrity of the material and surface layer mesostructure, based on dynamic strength reserve of a surface material in relation with an allowable rate of deformation thereof; and

setting ultrasonic oscillation intensity distribution during ultrasonic impacts, which is sufficient to attain said at least one property of the material structure and material under the surface, based on susceptibility of the material treated to an action of ultrasonic impacts in transition to a specified state,

wherein said degree of controlling oscillating velocities and ultrasonic oscillation intensity distribution are preliminarily determined based on experimental data or expertise as defined by the task.

5. The method according to claim 1, 2, 3 or 4, wherein the surface of the material is deformed at a rate and energy sufficient to fill intergranular defective voids while maintaining integrity of the surface of the material and mesostructure thereof during plastic deformation during soft impact phases predetermined in accordance with the task.

6. The method according to claim 1, 2, 3 or 4, wherein structural defect boundaries are closed under forces occurring during plastic deformation of the surface of the material caused by an action of soft and force phases of the ultrasonic impact.

7. The method according to claim 1, 2, 3 or 4, wherein defect boundary closing surfaces are activated under elastic residual stresses caused by plastic deformation of the surface of the material.

8. The method according to claim 1, 2, 3 or 4, wherein defect boundary closing surfaces are activated under impulses of force caused by impacts at a predetermined repetition rate.

9. The method according to claim 1, 2, 3 or 4, wherein activation of defect boundary closing surfaces is accompanied by an action of a vector sum of oscillating velocities of movement of oscillating system lumped mass and oscillating system distributed mass, reduced to said oscillating system end, during ultrasonic oscillations of said

ultrasonic oscillating system end in a phase, which corresponds to attaining resultant oscillating velocity, and impulse of force caused by the ultrasonic impact, wherein said resultant oscillating velocity and impulse of force are predetermined in accordance with the task.

10. The method according to claim 1, 2, 3 or 4, wherein activation of defect boundary closing surfaces occurs under friction forces caused by defect boundary displacement during an action of impact impulses and ultrasound.

11. The method according to claim 1, 2, 3 or 4, wherein activation of defect boundary closing surfaces is accompanied by an action of ultrasonic oscillations and waves going through a closing boundary during an action of impulse of force caused by the ultrasonic impact.

12. The method according to claim 1, 2, 3 or 4, wherein defect boundary closing is activated in an area of elevated temperature caused by plastic deformation and friction at boundaries of structural defects and fragments during impulse action, recurring at a repetition rate of ultrasonic impacts in a controlled phase, specified by material properties and the task.

13. The method according to claim 1, 2, 3 or 4, wherein ultrasonic self-diffusion and annihilation of closing boundaries occur under static pressure of the oscillating system, impulses of force, friction at boundaries, heating, ultrasonic oscillations and ultrasonic stress waves.

14. The method according to claim 1, 2, 3 or 4, wherein precipitation of alloying phases, including silicon precipitates in aluminum alloys, provides increased material

strength and is activated as a result of controlling the ultrasonic impact.

15. The method according to claim 1, 2, 3 or 4, wherein unstable phases, including copper in aluminum alloys, are fixed at a stage of soft ultrasonic contacts and impacts for protection against precipitation in solid solutions and prevention of degradation development.

16. The method according to claim 1, 2, 3 or 4, wherein activation of reverse self-diffusion of a precipitate in solid solutions, including copper in aluminum alloys, which results in weakening of structural bonds, creation of hidden structural stress concentrators caused by external forces and initiation of subsequent metal degradation, occurs due to normalizing the ultrasonic impact after a soft phase thereof and is accompanied by recovery of lost strength and ductility of an alloy.

17. The method according to claim 1, 2, 3 or 4, wherein activation of phase migration occurs as a result of normalizing the ultrasonic impact after soft phase onset thereof, said activation is accompanied by increased fatigue resistance due to reduction in density of distribution of potential concentrators of internal stresses at a nanostructural level.

18. The method according to claim 1, 2, 3 or 4, wherein self-control of the material structure in rotation, bending, twinning, recrystallization, flow, gliding, yielding and aging is activated at a level of fragments of nanostructure, microstructure and macrostructure of metals as a result of controlling formation of soft phases and subsequent normalizing of ultrasonic impact parameters.

19. The method according to claim 1, 2, 3 or 4, wherein activation of subdivision, uniformization and arrangement of material structure at a microlevel, as a means of increasing degradation resistance, occurs under ultrasonic impact as a result of normalizing, as defined by the task, parameters of soft phases and subsequent force phases of the ultrasonic impact.

20. The method according to claim 1, 2, 3 or 4, wherein activation of amorphization, as a means of final optimization of surface material structure at a nanolevel, occurs as a result of processes initiated by a dynamic model, as defined by the task, of controlling soft phases and normalizing parameters of ultrasonic impact.

21. The method according to claim 1, 2, 3 or 4, wherein controlling soft and force phases of the ultrasonic impact is used to protect the material against degradation nucleation in an original condition, as well as prevents and suppresses degradation in the material of a structure during or after long service thereof.

22. The method according to claim 1, 2, 3 or 4, wherein aluminum alloys are protected against corrosion exfoliation and/or properties of aluminum alloys, which have been damaged by exfoliation, are recovered and/or repaired.

23. The method according to claim 1, 2, 3 or 4, wherein at least one technical effect is attained including:

creation of a compensation protective barrier and recovery of properties of a damaged material by high-power soft ultrasonic impact (PSUI) with adaptive on-off time ratio modulation (O/OTRM) of drive pulses synchronized with the high-power soft ultrasonic impact, wherein to implement such a

control of drive pulse on-off time ratio, pulse-width and amplitude modulation are used, which are initiated when an increase in frequency of synchronized ultrasonic impacts is needed with a pause insufficient for independent predetermined oscillation suppression therebetween or a length of a transient process that is insufficient for independent recovery of oscillations, thereby achieving:

control of plastic deformation intensity distribution in time and space during each ultrasonic impact;

control of surface parameters at scales of mesostructure and crystalline structure, stressed-deformed state of the material and depth of penetration in an area of existing or potential damage; and/or

stabilization of phases, homogeneity of structure and properties of the material in an area of instability thereof under external conditions of heating, loading, and/or environment.

24. The method according to claim 1, 2, 3 or 4, wherein at least one technical effect is attained including:

protection from adsorption and prevention of adsorbing inclusions from contact with structural fragments;

an increase in mobility and loss of bonding of adsorbing inclusions and surface active substances with adsorbing surfaces, a damaged area of the material or the material structure; and/or

optimization of the surface treated, mesostructure and roughness of the surface, and residual stresses in a layer of the surface and surface material resistance to adsorption by an increase in material density in a layer of the surface.

25. The method according to claim 1, 2, 3 or 4, wherein at least one technical effect is attained including:

increased resistance to thermal and thermal-mechanical damages in an original condition and in service;

maintaining and recovery of material properties based on at least one of creation of a compensation barrier of distributed residual stresses, relaxation of stress and deformation gradient in areas of accumulated thermal and thermal-mechanical damages, filling of intergranular space in areas of structural defects by grain material, and ultrasonic diffusion at grain boundaries; and/or

optimization of friction couples surface as a means of reducing time and heat losses in braking.

26. The method according to claim 1, 2, 3 or 4, wherein at least one technical effect is attained including:

protection of an original surface being affected and recovery of material properties;

modification of meso and crystalline structures, amorphization of a surface material, creation of a compensation barrier of residual compressive stresses in the surface material based on formulating a function of oscillating amplitude changing in a "transducer-indenter-surface" system during high-power soft ultrasonic impact;

pulse and ultrasonic diffusion at grain boundaries in a region of structural failures caused by intercrystalline corrosion; and/or

plastic deformation of the material, increase in grain size uniformity, filling an intergranular space by grain material, or pulse ultrasonic diffusion at grain boundaries.

27. The method according to claim 1, 2, 3 or 4, wherein at least one technical effect is attained including:

creation of an electrochemical corrosion compensation barrier in an original condition of the material and recovery of the at least one property thereof;

strengthening micro- and macro-geometry of the surface, homogeneity of a crystalline structure of the surface of the material, nano-crystallization and amorphization of the surface of the material as a means of retardation of anodic processes;

surface plastic deformation, creation of an area of compressive stress and increased material density to retard localization of electrochemical corrosion of surface defects; and/or

use of a high-power soft ultrasonic impact mechanism to form strengthened surface conditions and surface mesostructure.

28. The method according to claim 1, 2, 3 or 4, wherein at least one technical effect is attained including:

creation of a chemical corrosion compensation barrier in an original condition of the material and recovery of said at least one property thereof through use of a high-power soft ultrasonic impact mechanism to strengthen quality and increase surface alloying depth in application of protective heat-resistant coatings and in repetition of these operations, if needed, on a scale layer and if properties of the material need to be repaired.

29. The method according to claim 1, 2, 3 or 4, wherein at least one technical effect is attained including:

creation of a radiation corrosion compensation protective barrier in an original condition of the material being affected and recovery of the at least one property thereof using a high-power soft ultrasonic impact mechanism to:

strengthen quality and increase surface alloying depth in application of protective heat- and radiation-resistant coatings;

strengthen surface condition in terms of its roughness, mesostructure, micro-grain structure and material amorphization; and

create a favorable compressive stress field and increase surface material density, wherein repetition of these operations on a damaged layer provides recovery of radiation resistance of the surface material at a level of an original material being affected.

30. The method according to claim 1, 2, 3 or 4, wherein at least one technical effect is attained including:

creation of a compensation protective barrier against formation of corrosion cracks in an original condition of the material and in recovery of the at least one property thereof by using a high-power soft ultrasonic impact (PSUI) mechanism to:

strengthen quality, adhesion or to increase an alloying depth of protective coatings applied to potentially or actually damaged surface to induce favorable compressive stresses into the surface of the material in strengthening or modification thereof to a predetermined depth in strengthened or specified condition of mesostructure;

modify the material structure and create a stressed-deformed state of the material structure that makes impossible absorption of solution anions on movable dislocations and other structural imperfections that reduce surface energy and weaken atomic bonds;

strengthen surface mesostructure and prevent crack nucleation as a result of a wedging action of surface-active substances in adsorption thereof in microcrevices on the surface of the material; and/or

create a compressive stress field on the treated surface with strengthened mesostructure, a magnitude and depth of which is sufficient for protection against high crack

propagation rate caused by accelerated anodic dissolution of a metal at a crack base, wherein a stressed-deformed state is generally determined by tensile stress concentration.

31. The method according to claim 1, 2, 3 or 4, wherein at least one technical effect is attained including:

use of a high-power soft ultrasonic impact (PSUI) mechanism to:

strengthen surface alloying quality, adhesion strength and density of galvanic coatings; and/or

create a compressive stress field on the treated surface with strengthened mesostructure, a magnitude and depth of which is sufficient for protection against reduction in strength properties and formation of brittle cracks that may be caused by at least one of penetration of atomic hydrogen in voids, pores and other lattice defects, hydrogen transformation into molecular gas that creates high interfragmentary pressure, and/or adsorption of atomic hydrogen on surfaces of a component and internal defects with formation of chemical compounds with metal and impurities that reduce surface energy of the material and brittle fracture resistance.

32. The method according to claim 1, 2, 3 or 4, wherein at least one technical effect is attained including:

use of high-power soft ultrasonic impacts to create a strengthened mesostructure and compressive stress field on the surface, a magnitude and depth of which is sufficient for protection against strength properties reduction, formation of brittle cracks, adsorption penetration of molten metal in a solid metal pre-failure zone, reduction in surface energy and metal rupture resistance.

33. The method according to claim 1, 2, 3 or 4, wherein at least one technical effect is attained including:

use of high-power soft ultrasonic impacts to create a strengthened density, roughness, mesostructure and compressive stress field at the surface, a magnitude and depth of which is sufficient for protection against detachment of solid particles from the material structure as a result of material contact with a moving liquid, gaseous environment or solid particles entrained thereby or as a result of an impact of solid particles upon the surface being affected.

34. The method according to claim 1, 2, 3 or 4, wherein at least one technical effect is attained including:

use of high-power soft ultrasonic impacts to create a strengthened density, mesostructure condition and a grain packing size and a field of compressive macrostresses and microstresses at and under the surface, a magnitude and depth of which is sufficient to protect against formation of microcracks and pores (microvoids) at grain boundaries and substructure, gliding and slip, twinning, bending of slip planes, lamellation, rotation and relative movement of grains, rotation and relative shift of mosaic blocks, polygonization, diffusion plasticity, recrystallization, and/or combining defects and structural damage at micro and micro levels.

35. The method according to claim 1, 2, 3 or 4, wherein at least one technical effect is attained including:

use of high-power soft ultrasonic impacts in creating strengthened density of a material, mesostructure on the material surface, and normalizing plastic deformations and compressive stress field at the surface, a magnitude and depth of which is sufficient to prevent reduction in material strength properties caused by microstructural degradation including at least one of absorption of molecules from

environment by micro-surfaces developing in a deformed body, and/or unfavorable stabilization of a metal phase condition in time at an expense of transformation of unstable phases without a considerable change in microstructure.

36. The method according to claim 1, 2, 3 or 4, wherein at least one technical effect is attained including:

use of high-power soft ultrasonic impacts to attain strengthened density and mesostructure of the treated material through normalization of plastic deformations and compressive stress field on and under the surface, a magnitude and depth of which is sufficient to prevent formation of an abrupt increase in yield strength of brittle cracks caused by atomic shift or a shift cascade under neutron stream in a metal lattice depending on an amount of energy a neutron transfers to a metal atom and thereafter formation of high concentration of vacancies surrounded along a periphery by zones with increased density of interstitial atoms.

37. The method according to claim 1, 2, 3 or 4, wherein at least one technical effect is attained including:

use of high-power soft ultrasonic impacts with level and time parameters corresponding to experimentally found requirements for attaining strengthened density of a treated material with a guaranteed integrity of a mesostructure thereof and for conditions of formation and normalization of local point heating and a rate of heat rejection from a plastic deformation region, plastic deformations themselves and a compressive stress field on and under the treated surface, a magnitude and depth of which is sufficient to:

- prevent surface corrosion exfoliation of a metal with formation of stress concentrators and loss of strength or recovery of metal properties in an area of these damages

caused by synergetic effect of corrosion and hydrogen embrittlement,

- prevent formation of unstable phases that cause the material to precipitate, resulting in a reduced level of structural bonds and strength of a material and intergranular corrosion,

- eliminate structural micro and macro defects, including optionally porosity or other intergranular discontinuities in closing boundaries thereof and activating self-diffusion processes,

- provide activation of self-diffusion at boundaries of structural fragments and elimination of corrosion cracking at grain boundaries,

- provide reverse diffusion of precipitates and recovery of stable phases,

- provide precipitation of alloying elements, increase in concentration density and strength of the treated material,

- ensure compensation, redistribution or relaxation of structural mechanical stresses in an area of concentration, caused by precipitates from solid solutions of unstable phases, and/or

- form hyper fine-grain structure, amorphization, increase in strength of the material and corrosion resistance.

38. The method according to claim 1, 2, 3 or 4, wherein at least one result is attained including:

introduction of compressive stresses of a substantial level, an increase in microhardness of a surface layer, and/or protection of mesostructure against service and process-induced damages in cast iron brake drums and discs.

39. The method according to claim 1, 2, 3 or 4, wherein at least one result is attained including:

modification of surface layer structure by intense normalized plastic deformation thereof, creation of a compressive stress region, and/or suppression of surface defects that initiate mesostructural damage during service to increase corrosion strength in cast iron pipes.

40. The method according to claim 1, 2, 3 or 4, wherein at least one result is attained including:

introduction of compressive stresses of a substantial level, stress concentration reduction, ultrasonic plastic deformation and structural modification of the treated material in a stress concentration area, wherein conditions of ultrasonic oscillations, pressure and indenter size ensure protection of mesostructure against process-induced and operational damage during service and preparation of the surface with use of high-power soft ultrasonic impact to increase fatigue resistance of welded steel.

41. The method according to claim 1, 2, 3 or 4, wherein at least one result is attained including:

introduction of compressive stresses of a substantial level into the treated surface and treated material and modification of a structure thereof, wherein conditions of ultrasonic oscillations, pressure and indenter size ensure protection of mesostructure during service and treatment of a surface with use of said ultrasonic impact to strengthen corrosion fatigue strength of steel.

42. The method according to claim 1, 2, 3 or 4, wherein at least one result is attained including:

an arrangement of a block structure at nanolevel and creation of regions of compressive stresses sufficient to retard mesostructural damage during effect upon a treated material by quasistatic and dynamic loads initiated by the

ultrasonic impact normalized as defined by the task and thereafter by operation forces to strengthen impact strength of steel.

43. The method according to claim 1, 2, 3 or 4, wherein at least one result is attained including:

intense ultrasonic plastic deformation of a treated material, arrangement of microstructure at a nanolevel and/or suppression of mesostructural damage of steel.

44. The method according to claim 1, 2, 3 or 4, wherein at least one result is attained including:

intense ultrasonic plastic deformation of a surface material under normalized ultrasonic impact at a substantial deformation loading rate, local warming-up in a phase transformation region and/or quick heat removal from an impact region to obtain a white layer in steel.

45. The method according to claim 1, 2, 3 or 4, wherein at least one result is attained including:

intensification of diffusion processes and metal recrystallization under an action of ultrasonic wave, acoustic flows, sound pressure and cavitation, which are initiated by indenter ultrasonic oscillations synchronously with carrier oscillations of the ultrasonic oscillating system during ultrasonic impact to strengthen metal crystallization of steel.

46. The method according to claim 1, 2, 3 or 4, wherein at least one result is attained including:

intense ultrasonic plastic deformation of a surface material and/or activation therethrough of diffusion processes caused by ultrasonic wave during ultrasonic impact to strengthen mechanical properties of steel.

47. The method according to claim 1, 2, 3 or 4, wherein at least one result is attained including:

introduction of compressive stresses of a substantial level, stress concentration reduction, and/or creation of a physical barrier against mesostructural defect formation in a region of directed plastic deformation and compressive stresses corresponding to a level of defects to strengthen a fatigue limit of aluminum alloys.

48. The method according to claim 1, 2, 3 or 4, wherein at least one result is attained including:

introduction of compressive stresses of a substantial level, stress concentration reduction, and/or suppression of possible mesostructural damages by means of ultrasonic recrystallization in solid solution and activation of ultrasonic diffusion at grain boundaries during said ultrasonic impact to strengthen high-cycle fatigue strength of aluminum alloys.

49. The method according to claim 1, 2, 3 or 4, wherein at least one result is attained including:

intense plastic deformation of a treated material near-surface layer, ultrasonic diffusion at defect boundaries, closed under ultrasonic impact in a form of pores or discontinuities in the material and/or suppression of mesostructural defects in a region of normalized plastic deformation and compressive stresses, corresponding to a level of plastic deformation, under normalized ultrasonic impact and effects accompanying an influence of said ultrasonic impact on the material, wherein said effects are caused, in particular, by reduced deformation resistance during propagation of an ultrasonic stress wave in the material being deformed by said ultrasonic impact to suppress porosity to a predetermined depth and extend life of aluminum alloys.

50. The method according to claim 1, 2, 3 or 4, wherein at least one result is attained including:

maintaining or increasing, as a result of ultrasonic plastic deformation, an impact strength in metals, including steels and aluminum alloys, wherein the impact strength may decrease under conventional plastic deformation, resulting in a reduced reserve of material plasticity, due to retardation of dislocations and other structural defects in plastically deformed structures.

51. The method according to claim 1, 2, 3 or 4, wherein at least one result is attained including:

a strengthened surface layer during ultrasonic impact machining, specifically steels, due to structural changes caused by predetermined controlling of ultrasonic impact parameters;

transformation of two-phase condition of an original structure in a surface layer, specifically in aluminum alloys, and formation of a more solid eutectic structure; and/or

migration of alloying inclusions to the treated surface, in particular silicon inclusions in aluminum alloys, and thereby strengthening the surface being affected.

52. The method according to claim 1, 2, 3 or 4, wherein at least one result is attained including:

ultrasonic impact diffusion at grain boundaries to recover properties of aluminum alloys after corrosion exfoliation.

53. The method according to claim 1, 2, 3 or 4, wherein at least one result is attained including:

providing a grain refinement, specifically in aluminum alloys, and increase in strength thereof which occurs due to formation of increased dislocation density and twinning

structure because of additional deformation, formation of microband structure, subdivision of microband structure into submicron grains, and/or further breakdown of subgrains to be equiaxed.

54. The method according to claim 1, 2, 3 or 4, wherein at least one result is attained including:

providing a geometric dynamic recrystallization of grains at nano-scale and micro-scale, wherein impact energy and temperature of local heating achieve a level which is critical relative to favorable structural conditions of the material and cause favorable migration of precipitates in occurrence of microbands, in particular, in aluminum alloys, as a result of normalizing the ultrasonic impact, local heating, heat removal, conditions of distribution of an ultrasonic stress wave, and as a result, normalization of metal plastic deformation, which is accompanied by an increase in metal strength and resistance to degradation of properties.

55. The method according to claim 1, 2, 3 or 4, wherein at least one result is attained including:

introduction of compressive stresses of a substantial level, modification of a surface layer structure, ultrasonic diffusion at a boundary closing of structural defects including optionally pores, protection against damages and suppression of mesostructural damages at micro and macro levels to strengthen corrosion fatigue strength in bronze.

56. The method according to claim 1, 2, 3 or 4, wherein controlling soft and force phases of ultrasonic impact, on condition that a mesostructure integrity is recovered, changes a service crack nucleation mechanism in corroded specimens, including aluminum alloys, wherein crack nucleation and development in an area of intergranular

corrosive damage is prevented by closing and subsequent elimination of boundaries thereof, which occur under intense plastic deformation followed by ultrasonic diffusion, thereby increasing a resistance of the material to corrosive and fatigue damage.

57. The method according to claim 1, 2, 3 or 4, wherein kinetics of nucleation and development of cracks of different nature, as a prevailing final evidence of major types of metal degradation, is affected for prevention and suppression thereof by controlling soft and force phases of the ultrasonic impact and obtaining:

- a smooth surface with a roughness of not greater than about 0.5 μm and residual compressive stresses induced to a depth of up to about 0.7 mm, wherein such a surface will delay crack initiation;

- a smooth surface with a roughness of about 0.5 μm or more, an intact mesostructure and compressive stresses induced to a depth of up to about 1.5 mm, which together allows a longer material resistance to crack initiation and development after starting in a substantial compressive stress field to a predetermined depth, but not less than about 1.5 mm;

- a smooth surface with an intact subsurface mesostructure, wherein minor surface damage is possible to a depth of no greater than about 0.003 mm, fine grain in a subsurface layer and compressive stresses induced to a depth of up to about 2.5 mm, which result in higher material resistance to crack initiation and dampen crack development after starting in an area of a fine grain structure and a compressive stress field; and/or

- a smooth surface with an intact subsurface mesostructure, wherein minor surface damage is possible to a depth of no greater than about 0.008 mm, fine grain and

amorphous structure in a near-surface layer, as well as compressive stresses induced to a maximum depth for a given material of up to about 4.0 mm using controlled ultrasonic impact, which results in higher material resistance to crack initiation, dampen crack development after starting in an area of fine grain and/or amorphous structure and continue crack retardation in a field of compressive stresses that are substantial as against a yield strength of the treated material;

wherein starting cracks are cured and developing fatigue cracks are retarded by diffusion joining of crack boundaries;

submersion of a crack development zone into a residual compressive stress area and crack preservation; and

removal of a cracked metal surface layer from an undamaged metal by force phases of the ultrasonic impact.

58. The method according to claim 1, 2, 3 or 4, wherein controlling at least one ultrasonic impact parameter of a resultant velocity at an onset of impact, impact energy, repetition rate and time of impact, and/or amplitude and phase of impact, is defined by a specific task based on predetermined data, wherein said at least one parameter is set with a scatter from about 5% to random values based on predetermined technical requirements and predetermined end results to be produced.

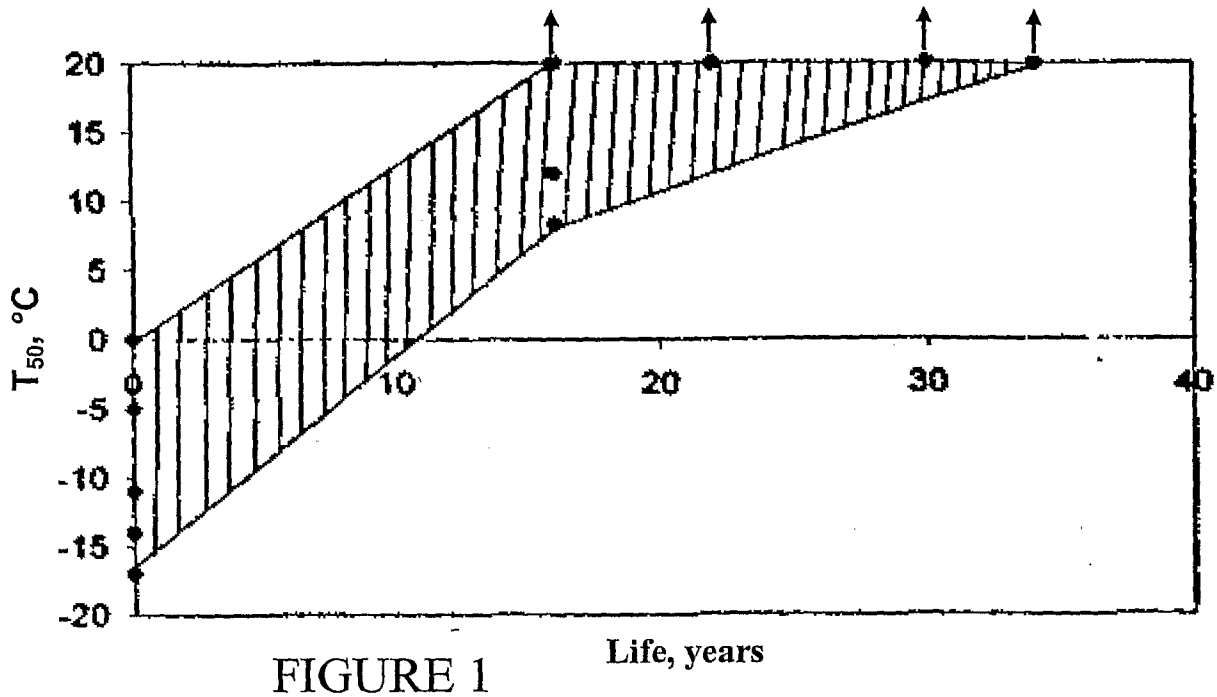

FIGURE 1
Prior Art

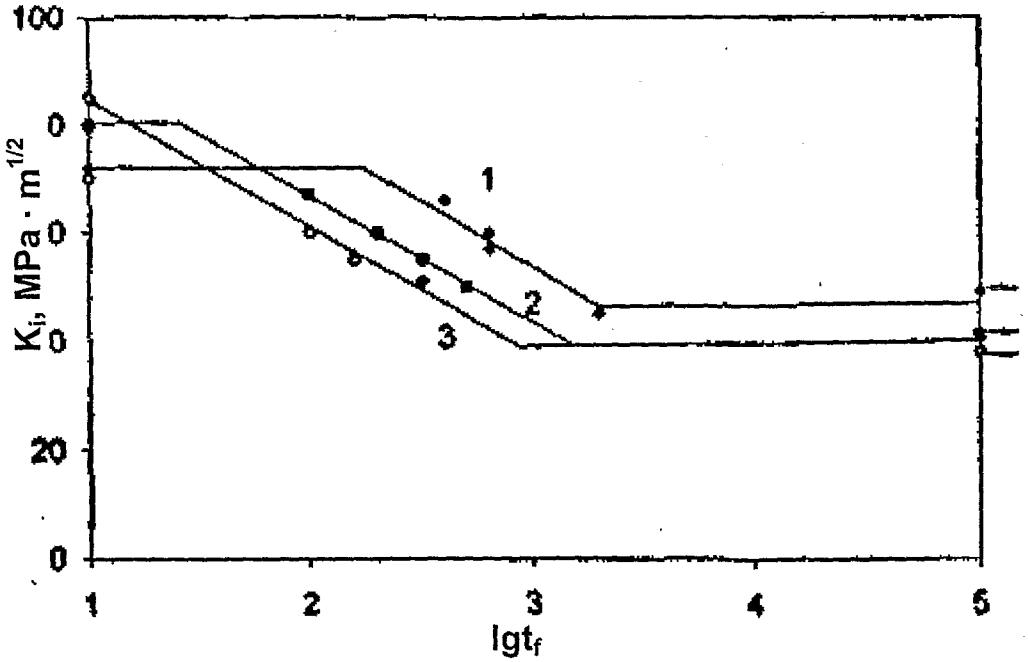

FIGURE 2
Prior Art

FIGURE 3
Prior Art

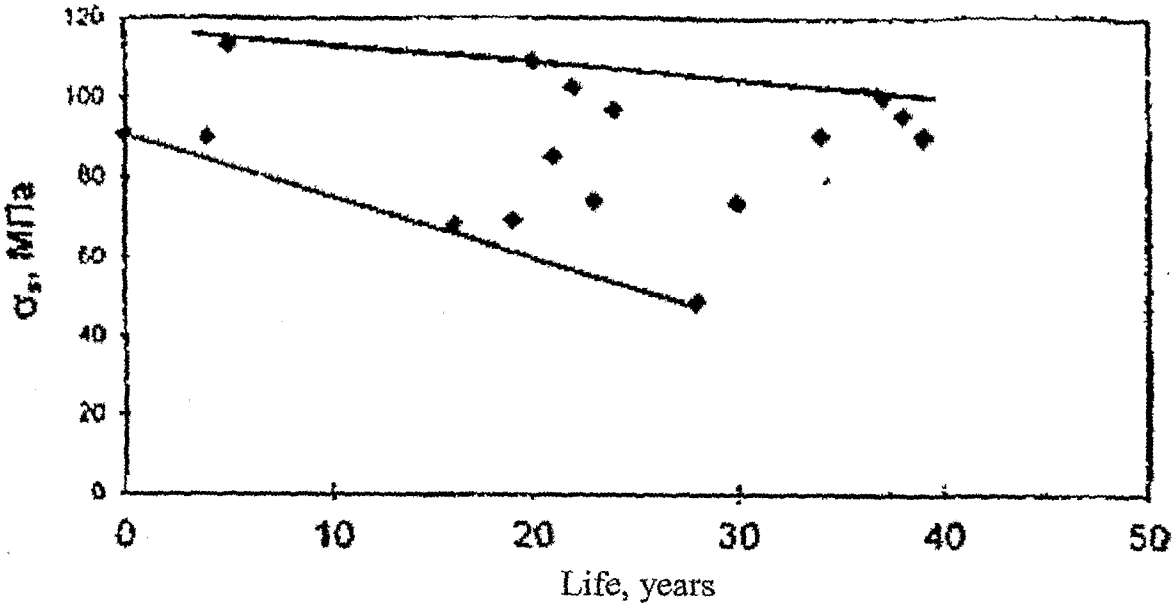

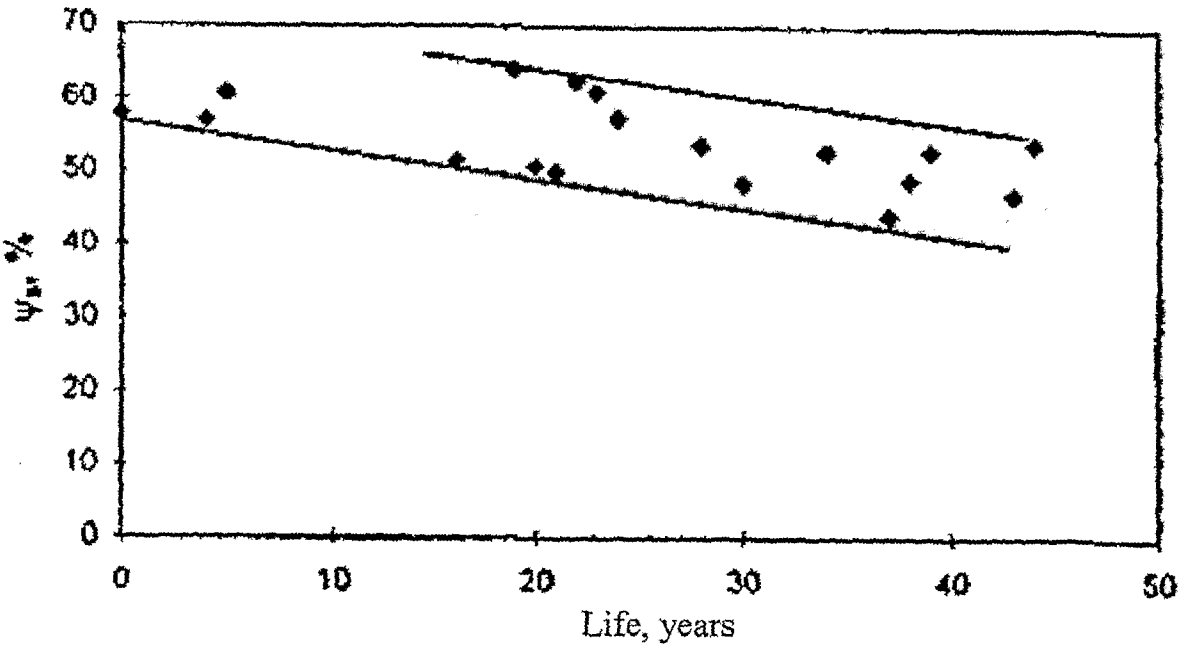

FIGURE 4
Prior Art

FIGURE 5
Prior Art

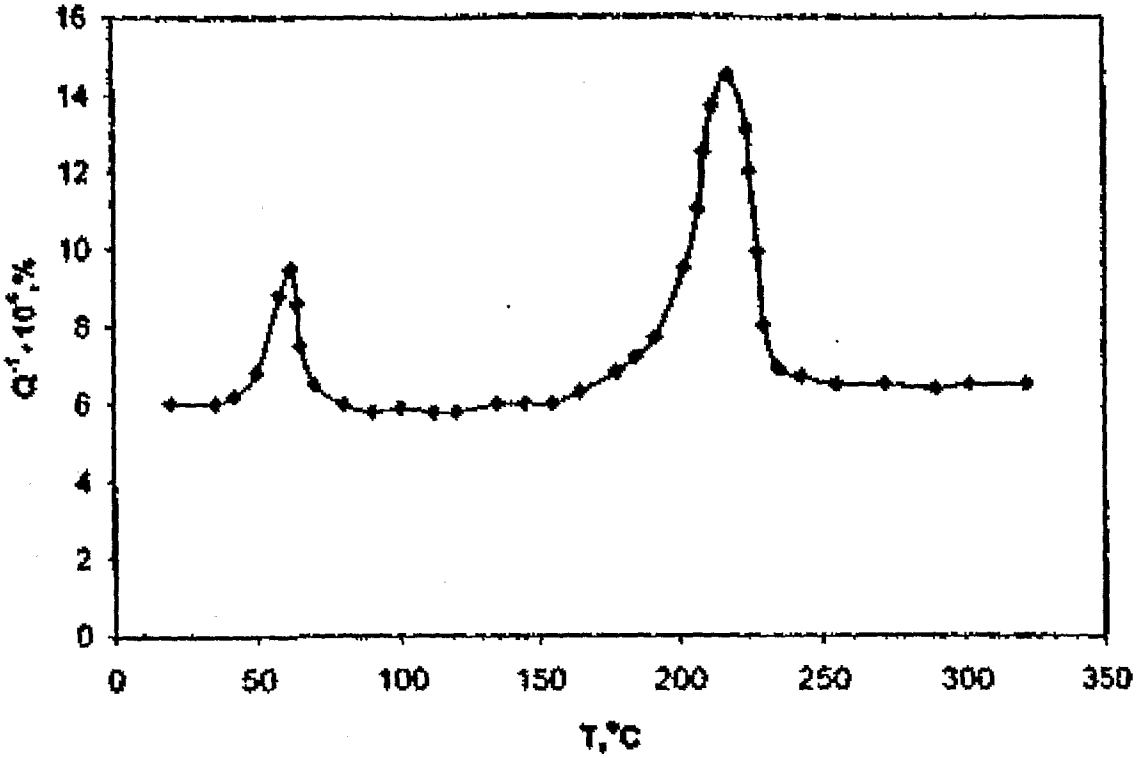

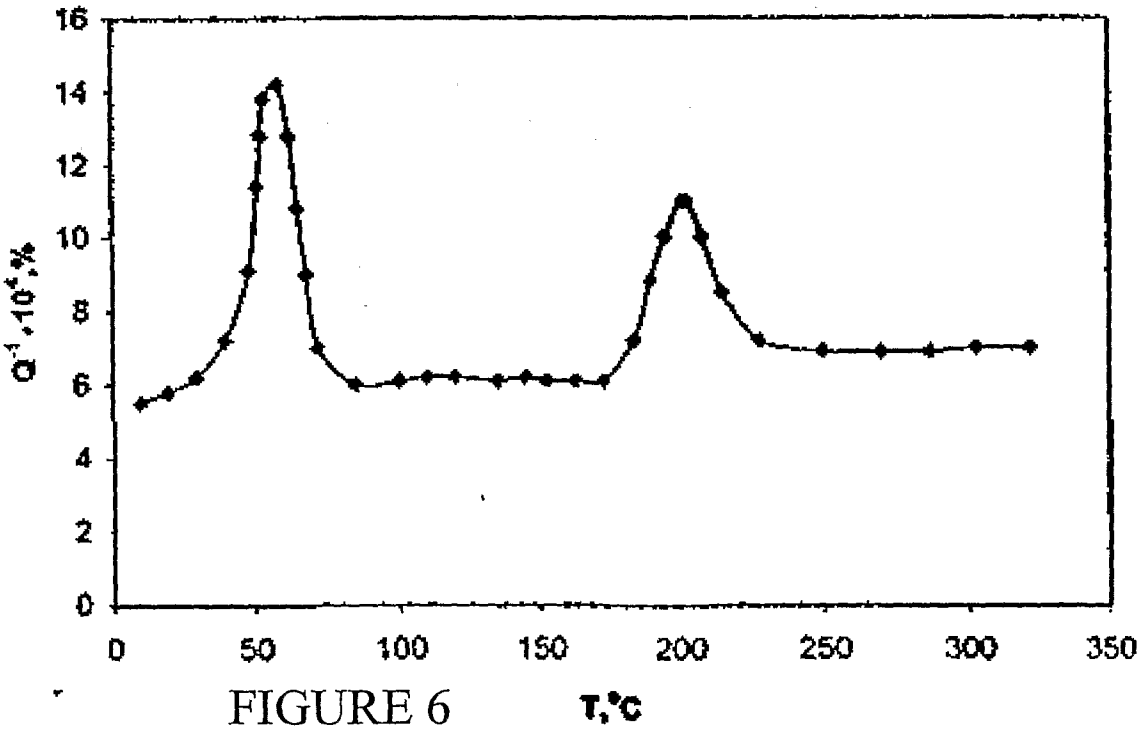

FIGURE 6
Prior Art

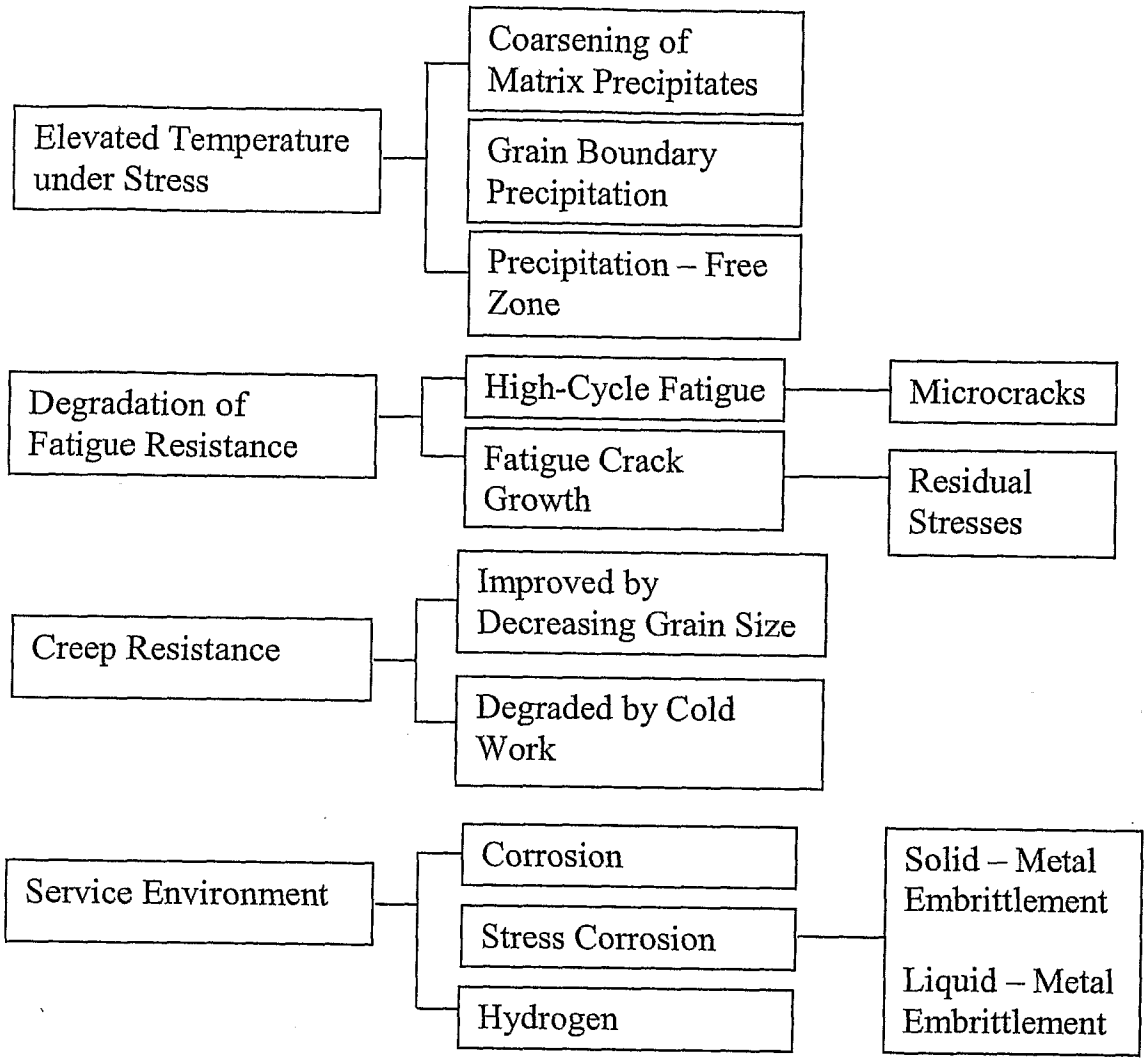

FIGURE 7
Prior Art

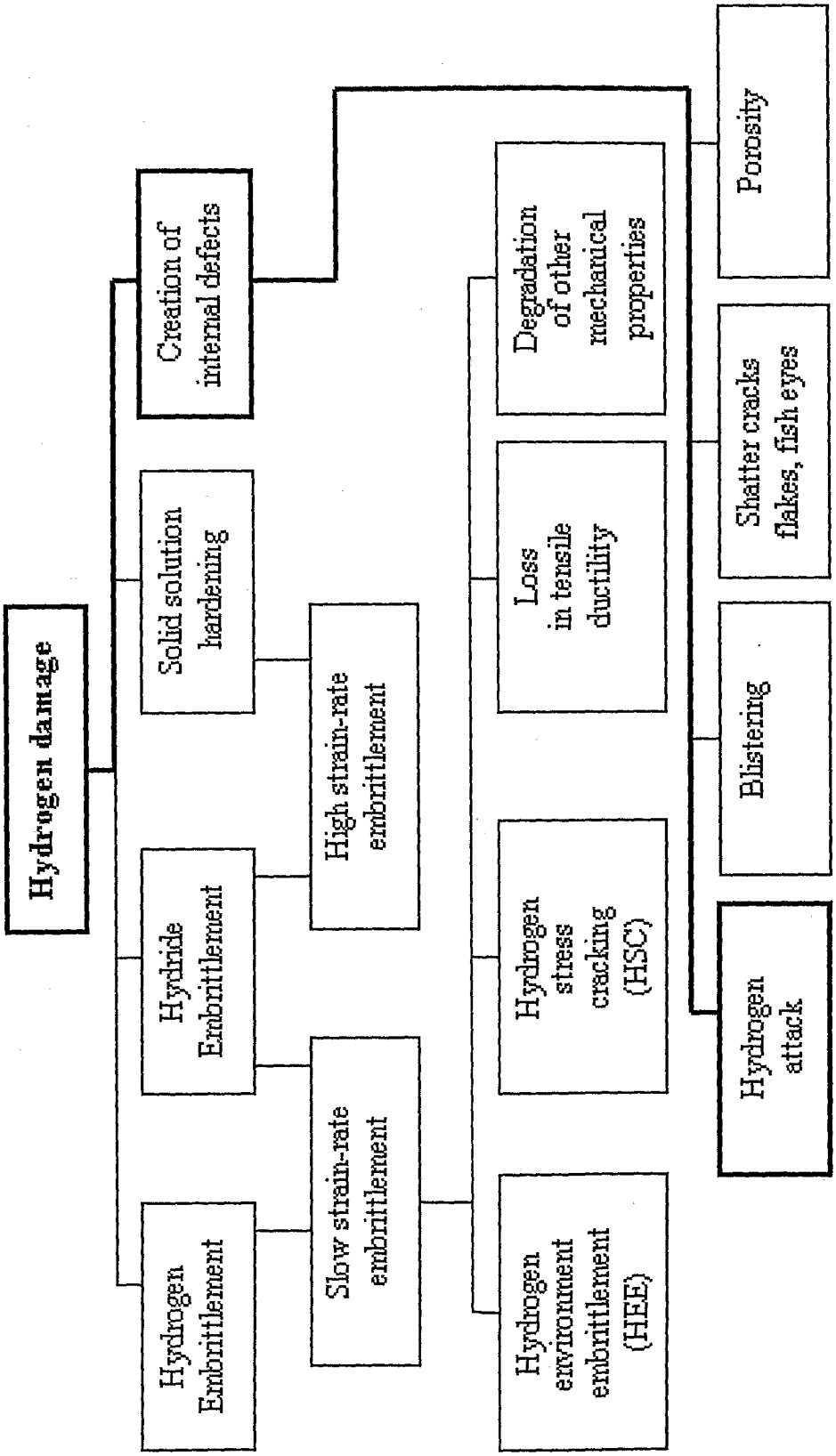

FIGURE 8
Prior Art

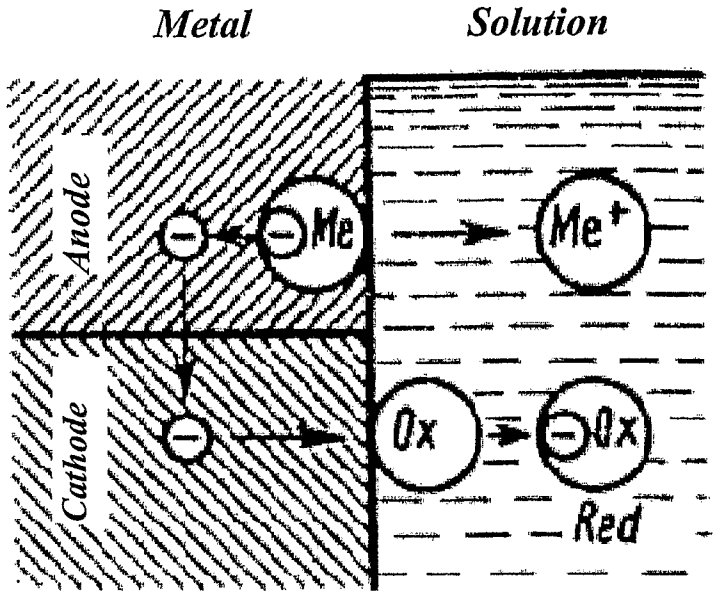

FIGURE 9
Prior Art

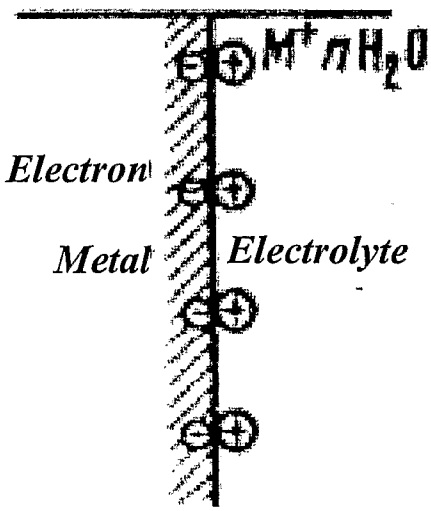

FIGURE 10
Prior Art

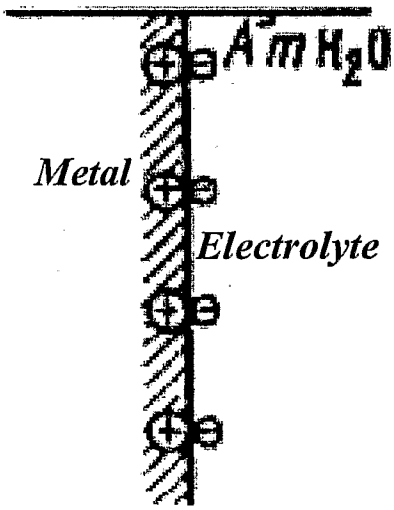

FIGURE 11
Prior Art

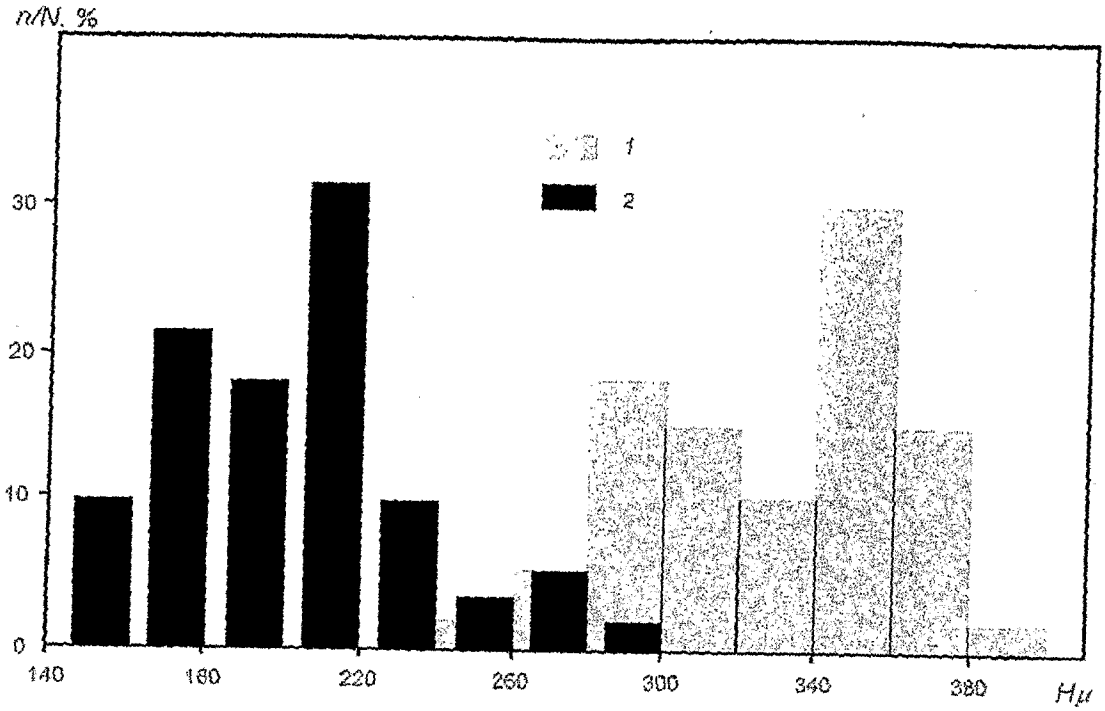

FIGURE 12
Prior Art

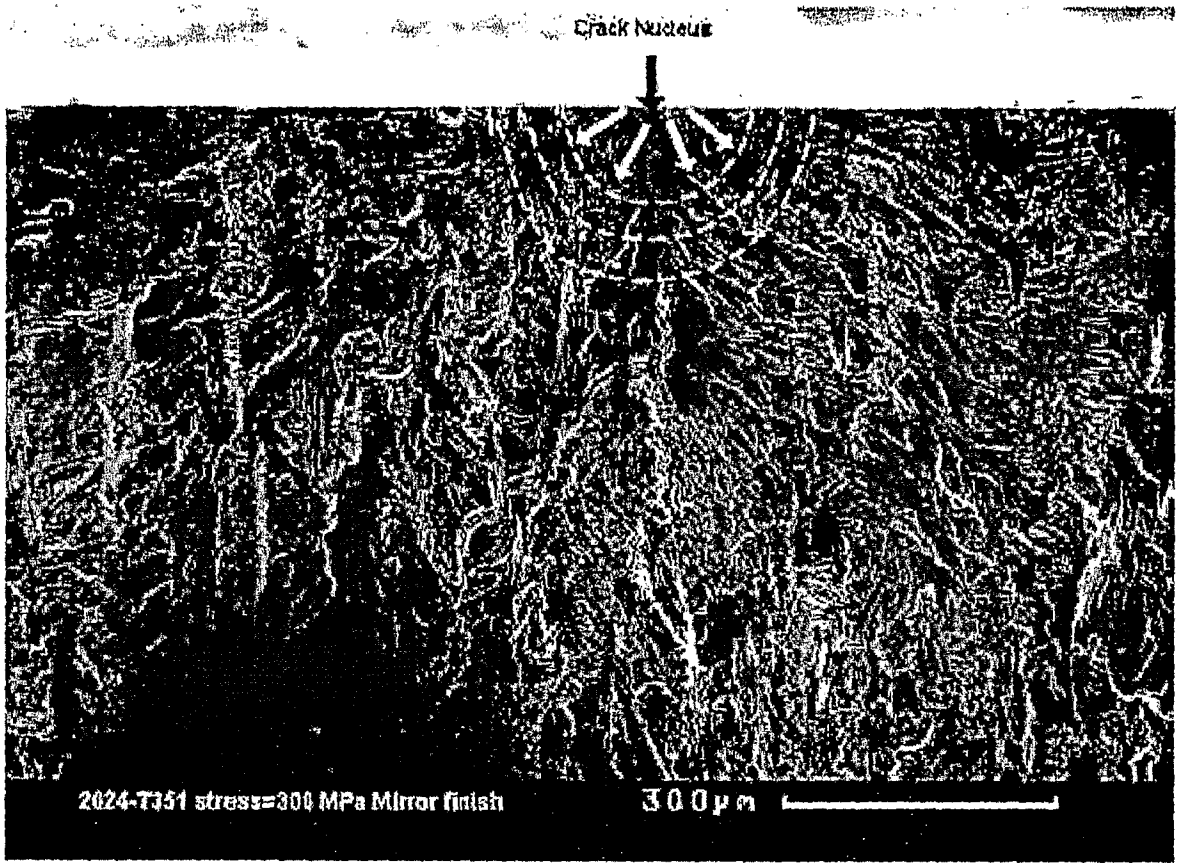

FIGURE 13
Prior Art

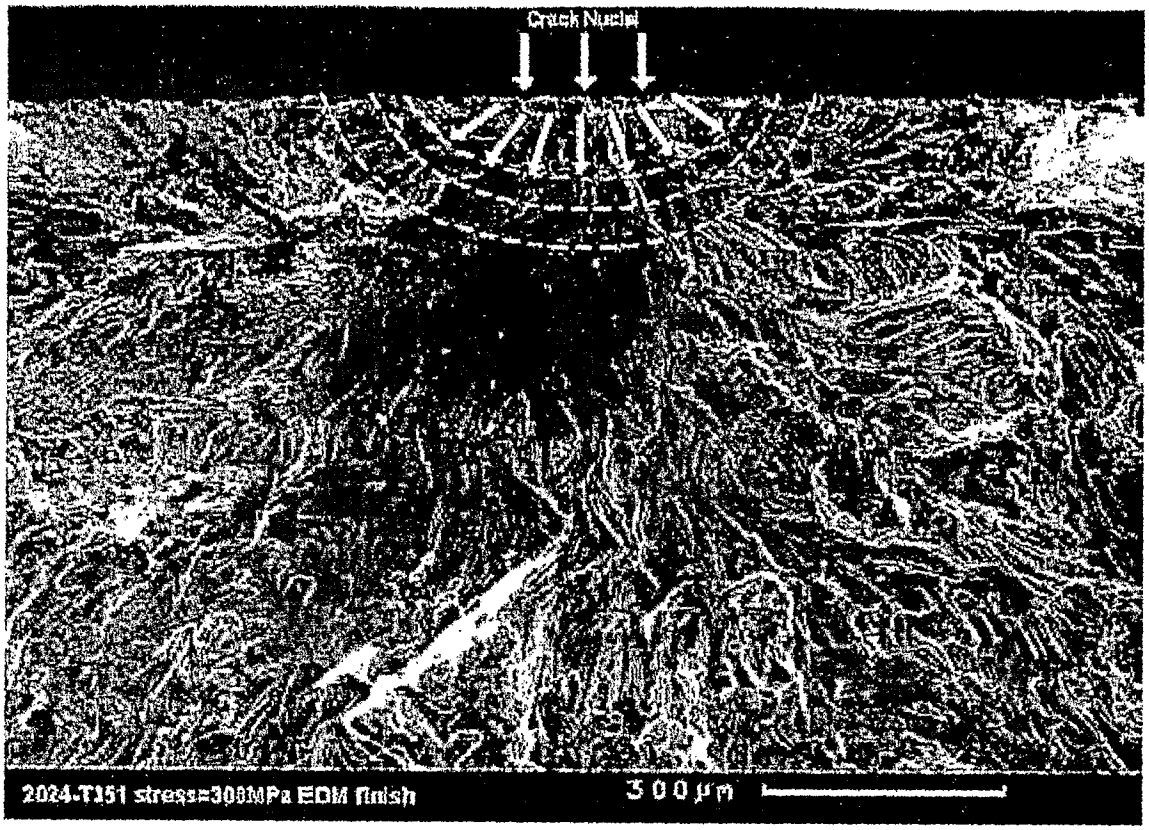

FIGURE 14
Prior Art

FIGURE 15
Prior Art

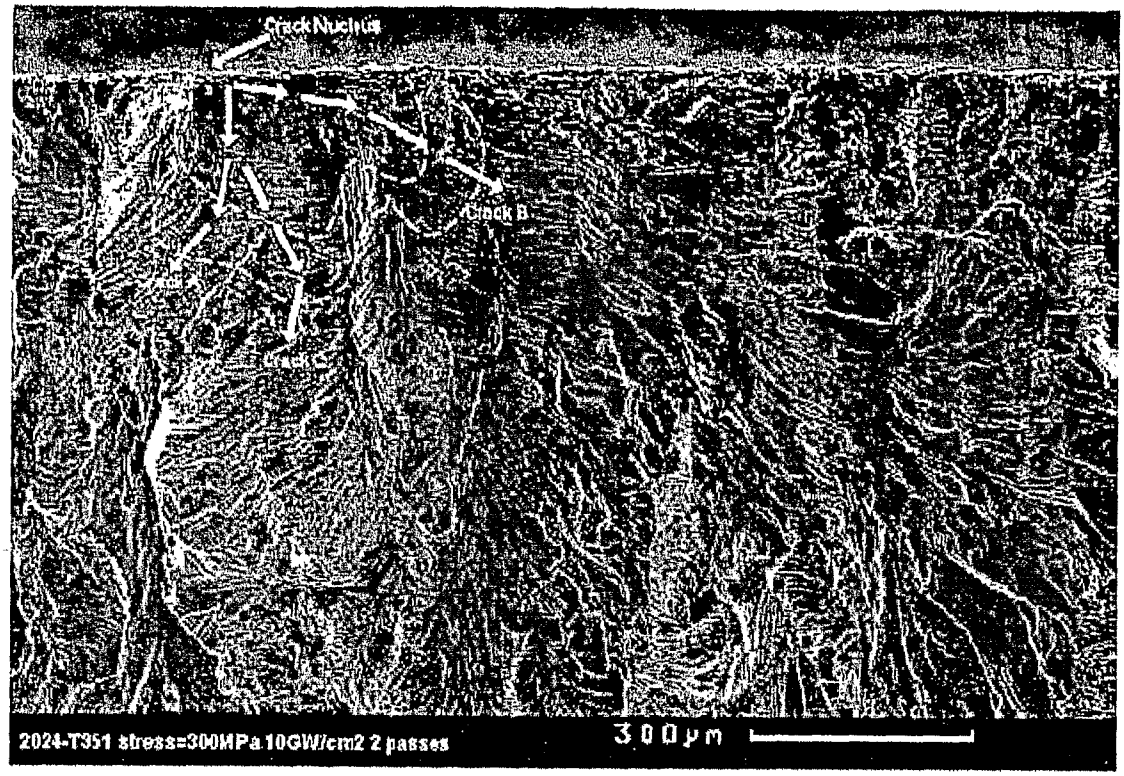

FIGURE 16
Prior Art

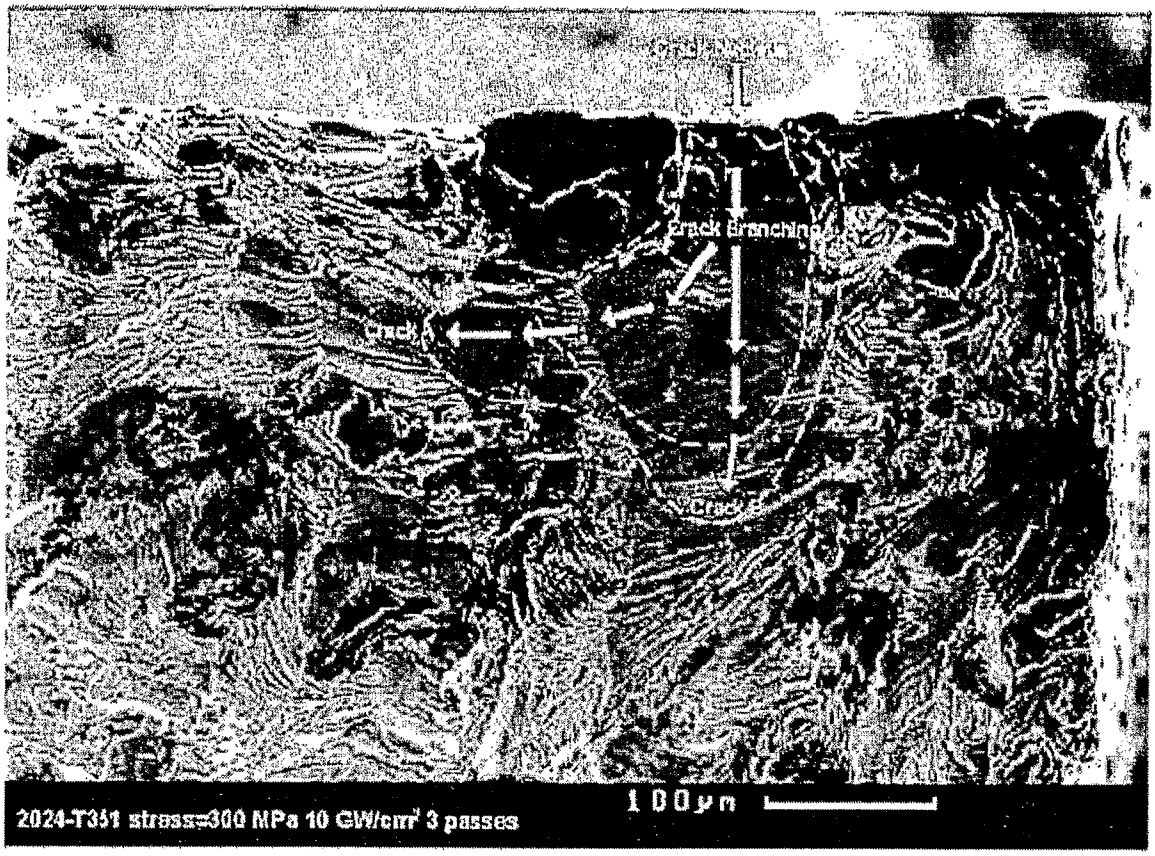

FIGURE 17
Prior Art

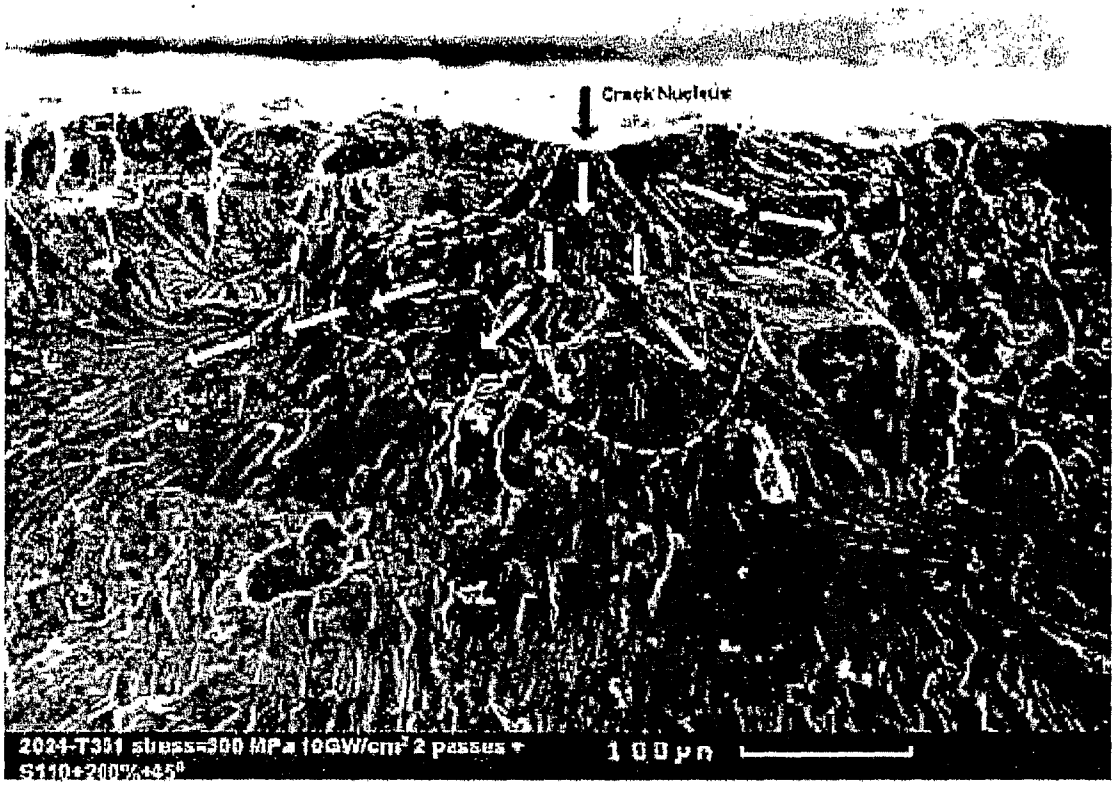

FIGURE 18
Prior Art

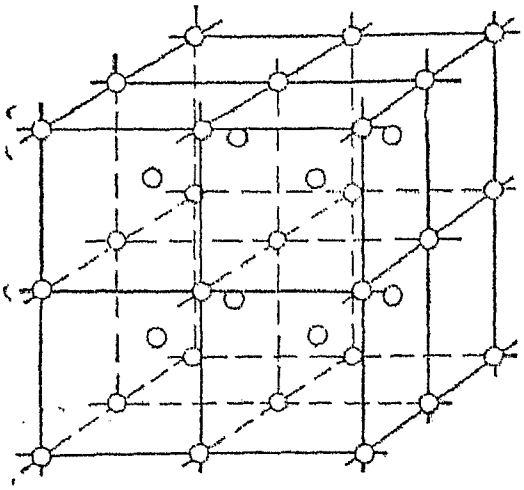

FIGURE 19
Prior Art

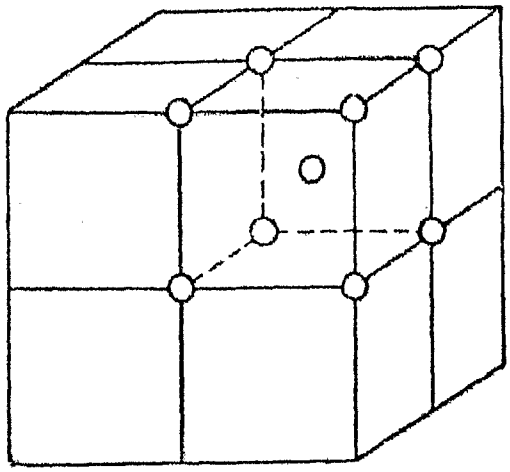

FIGURE 20
Prior Art

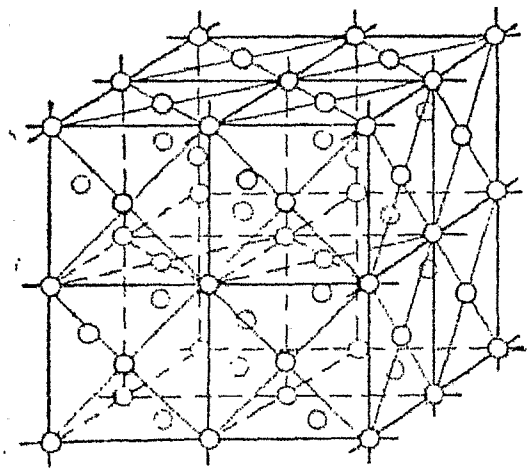

FIGURE 21
Prior Art

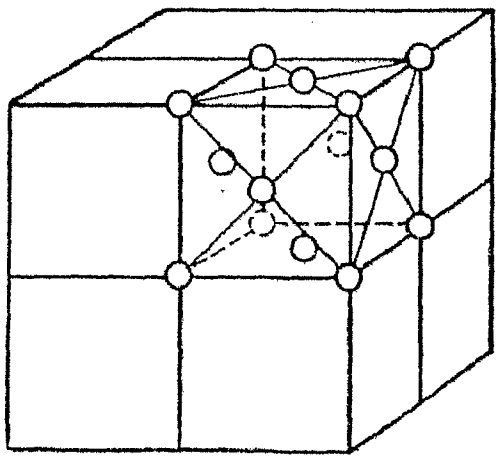

FIGURE 22
Prior Art

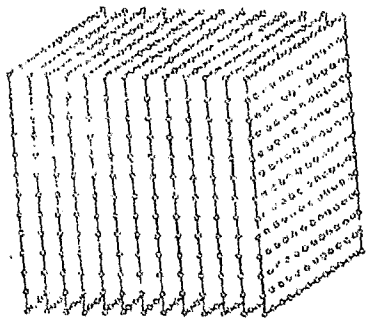

FIGURE 23
Prior Art

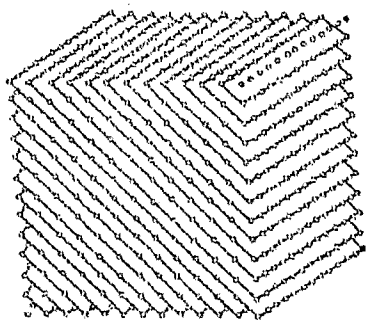

FIGURE 24
Prior Art

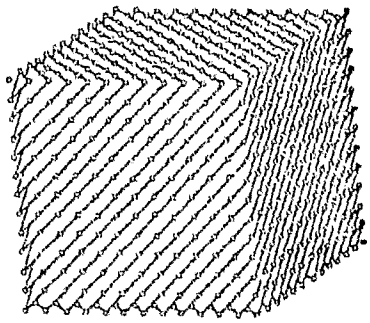

FIGURE 25
Prior Art

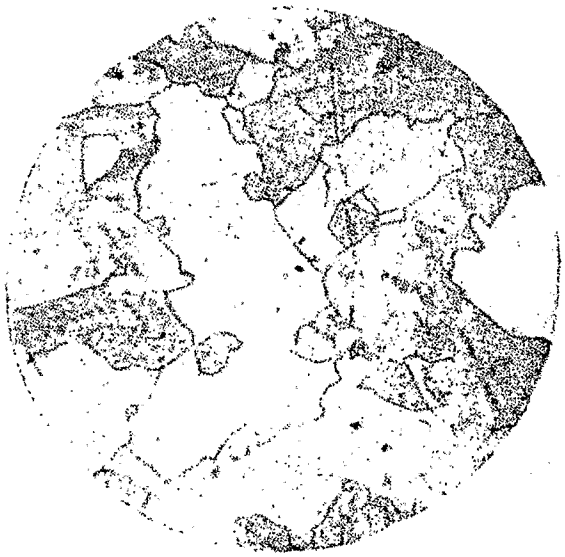

FIGURE 26
Prior Art

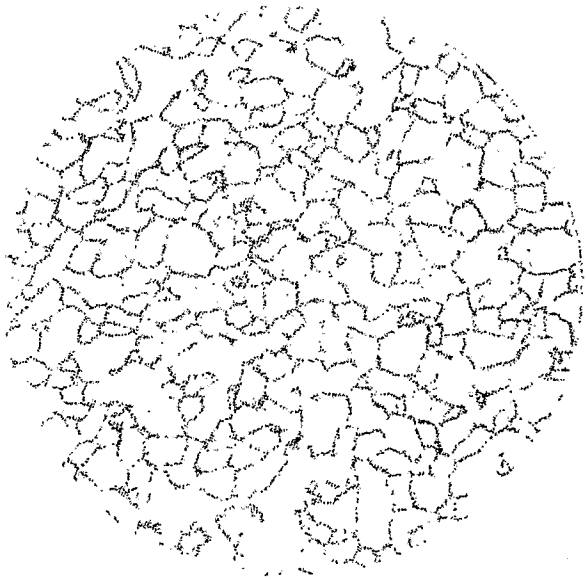

FIGURE 27
Prior Art

FIGURE 28
Prior Art

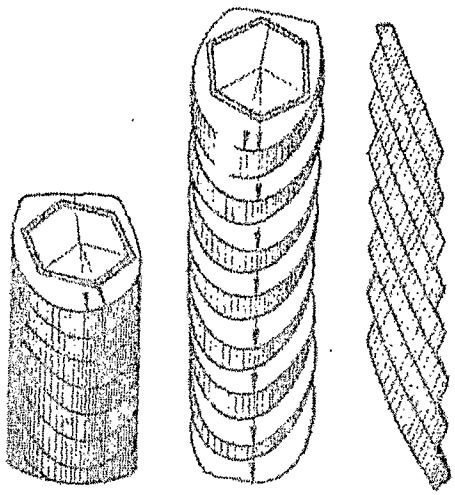

FIGURE 30
Prior Art

FIGURE 29
Prior Art

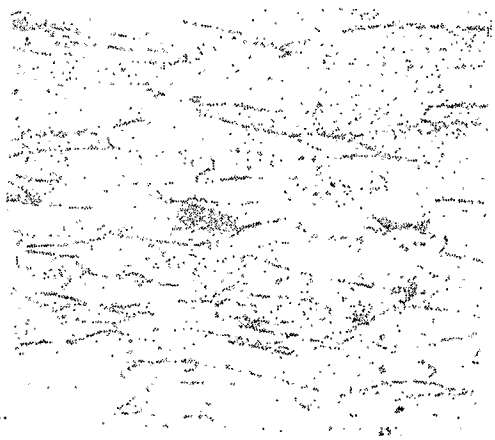

FIGURE 31
Prior Art

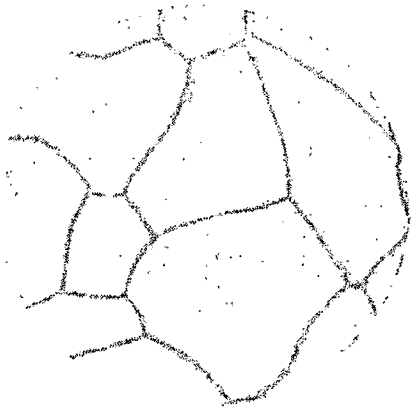

FIGURE 32
Prior Art

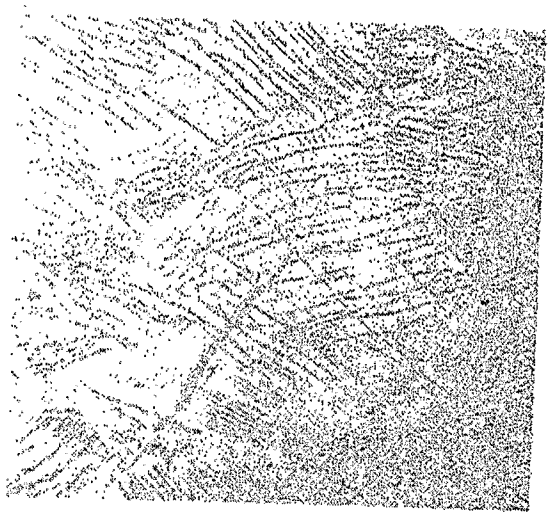

FIGURE 33
Prior Art

FIGURE 34

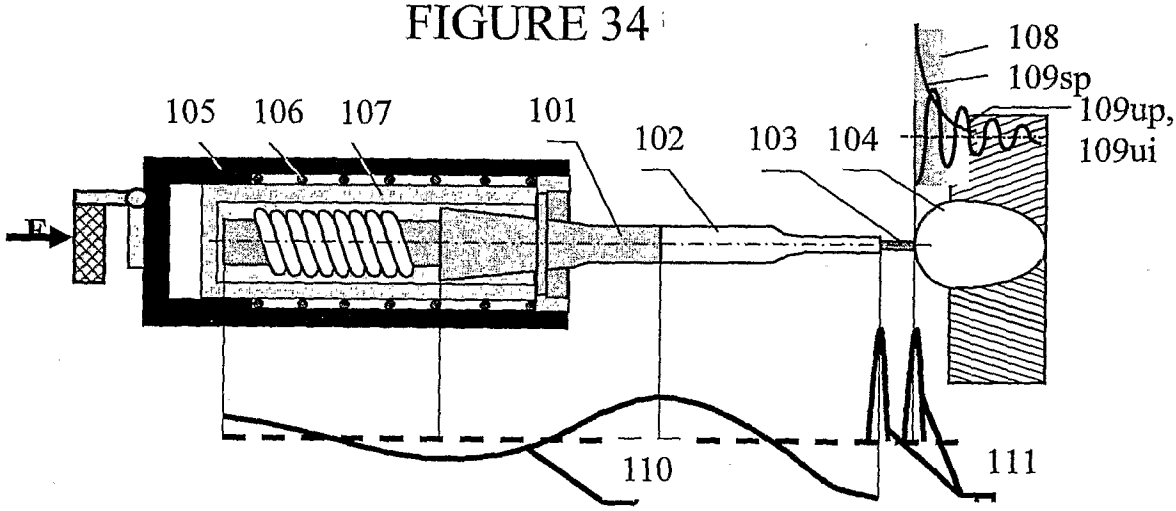

101 – MAGNETOSTRICTIVE TRANSDUCER
102 – WAVEGUIDE
103 – INDENTER
104 – TREATED SURFACE
105 – CASE (FIXED) WITH A HANDLE
106 – SPRING
107 – WATER-COOLED CASING OF TRANSDUCER
108 – PLASTIC DEFORMATION OF MATERIAL
109sp – SINGLE STRESS PULSES
109up– ULTRASONIC PERIODIC STRESS WAVE
109ui – ULTRASONIC (APERIODIC) IMPULSE STRESSES
110 – ULTRASONIC OSCILLATIONS
111 – IMPACT IMPULSES
F – PRESSING FORCE OF OS AGAINST TS

101, 102, 103 105, 106, 107 – FORM THE OSCILLATING SYSTEM (OS) WITH A RIGIDLY FIXED PROCESSING SETUP

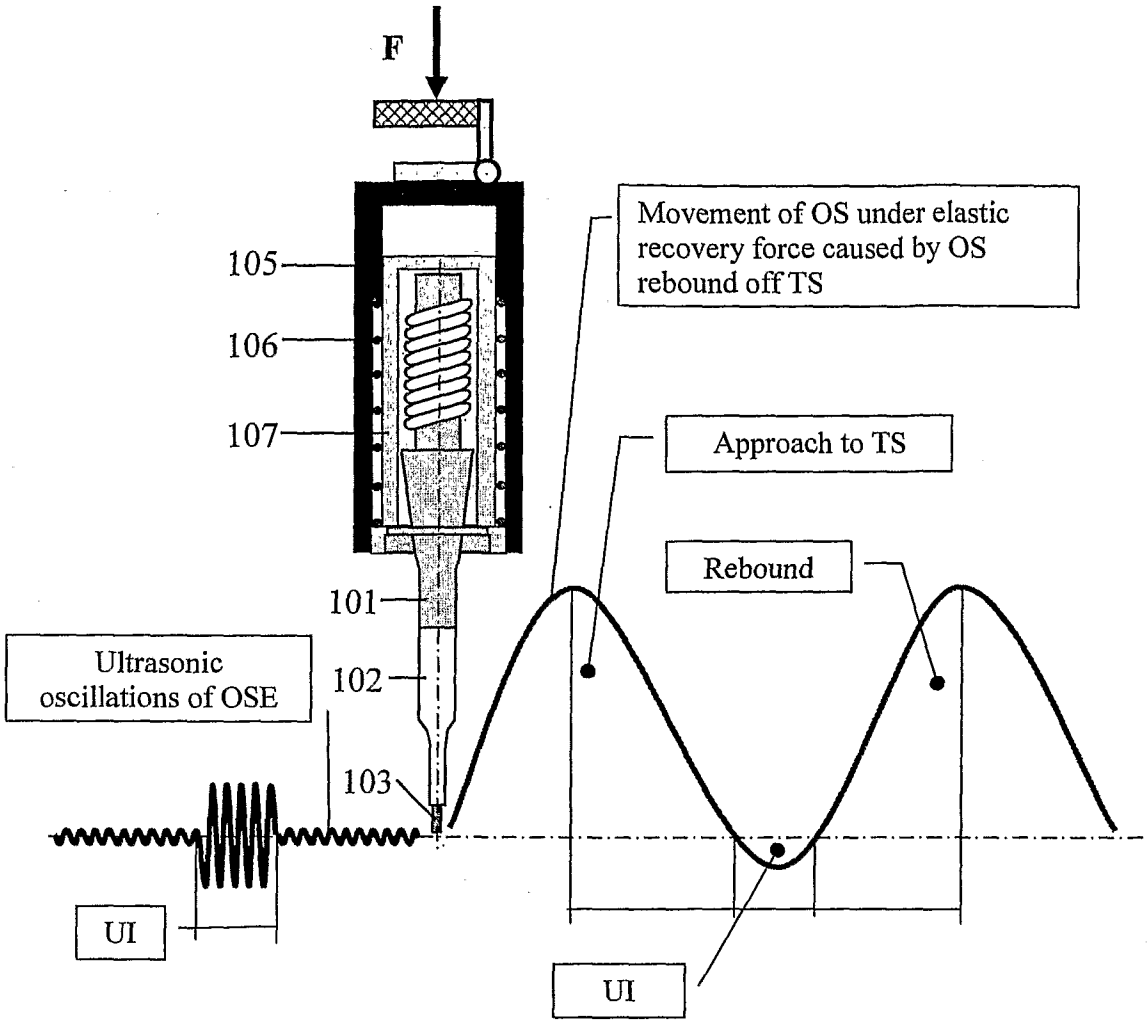

FIGURE 35

OS – OSCILLATING SYSTEM
OSE – OSCILLATING SYSTEM END ATTACHED TO THE INDENTER BUTT (SEE FIGURE 34)
TS – TREATED SURFACE
UI – ULTRASONIC IMPACT

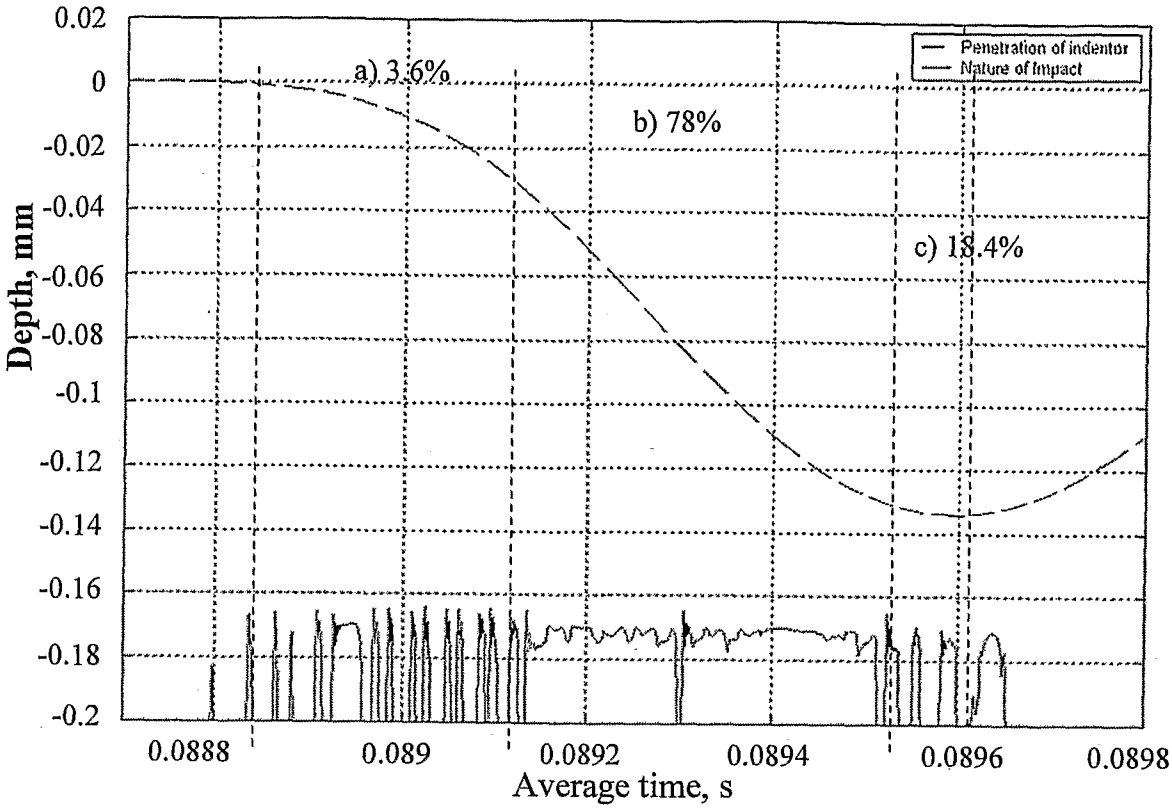
Penetration of indentor
Nature of Impact
a) 3.6%
b) 78%
c) 18.4%
Depth, mm
0.02
0
-0.02
-0.04
-0.06
-0.08
-0.1
-0.12
-0.14
-0.16
-0.18
-0.2
0.0888
0.089
0.0892
0.0894
0.0896
0.0898
Average time, s

FIGURE 36

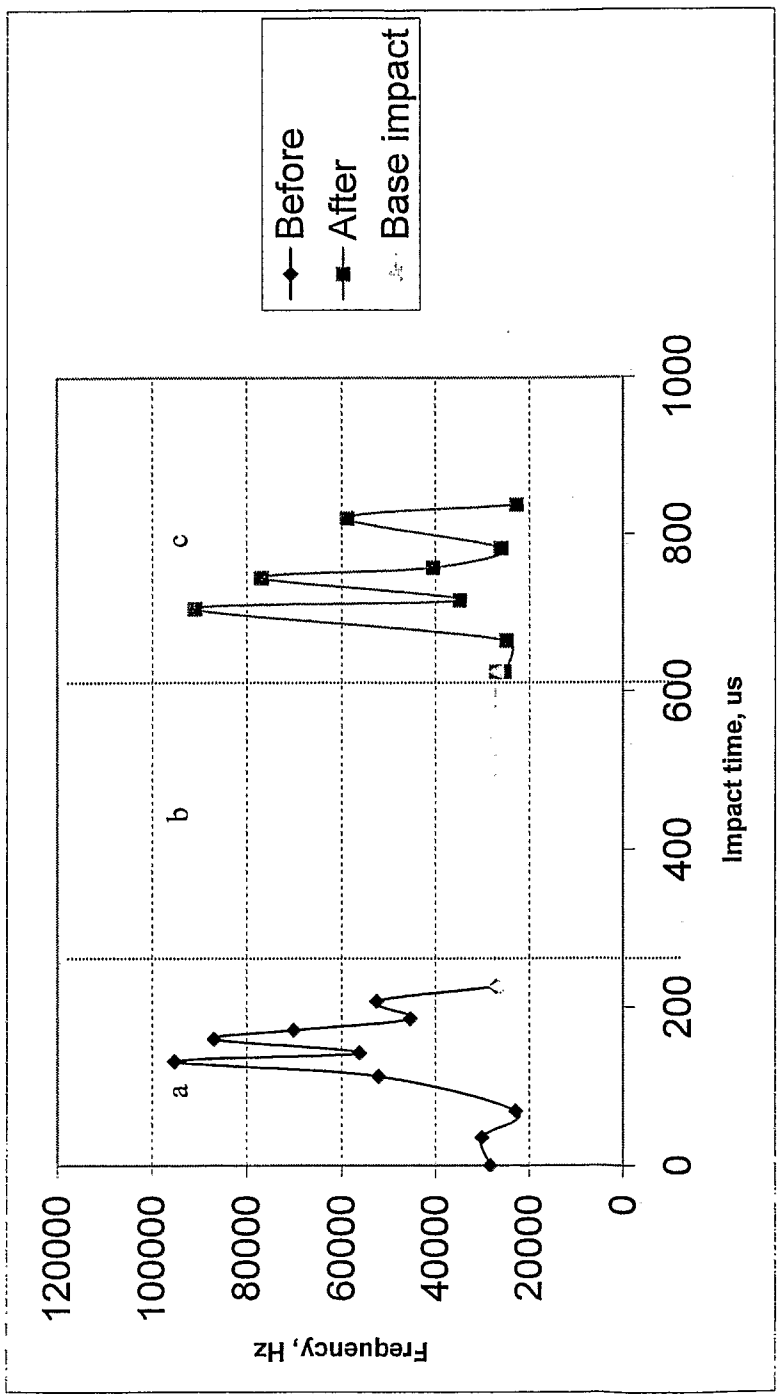
Before
After
Base impact
Frequency, Hz
120000
100000
80000
60000
40000
20000
0
0
200
400
600
800
1000
Impact time, us
a
b
c

FIGURE 37

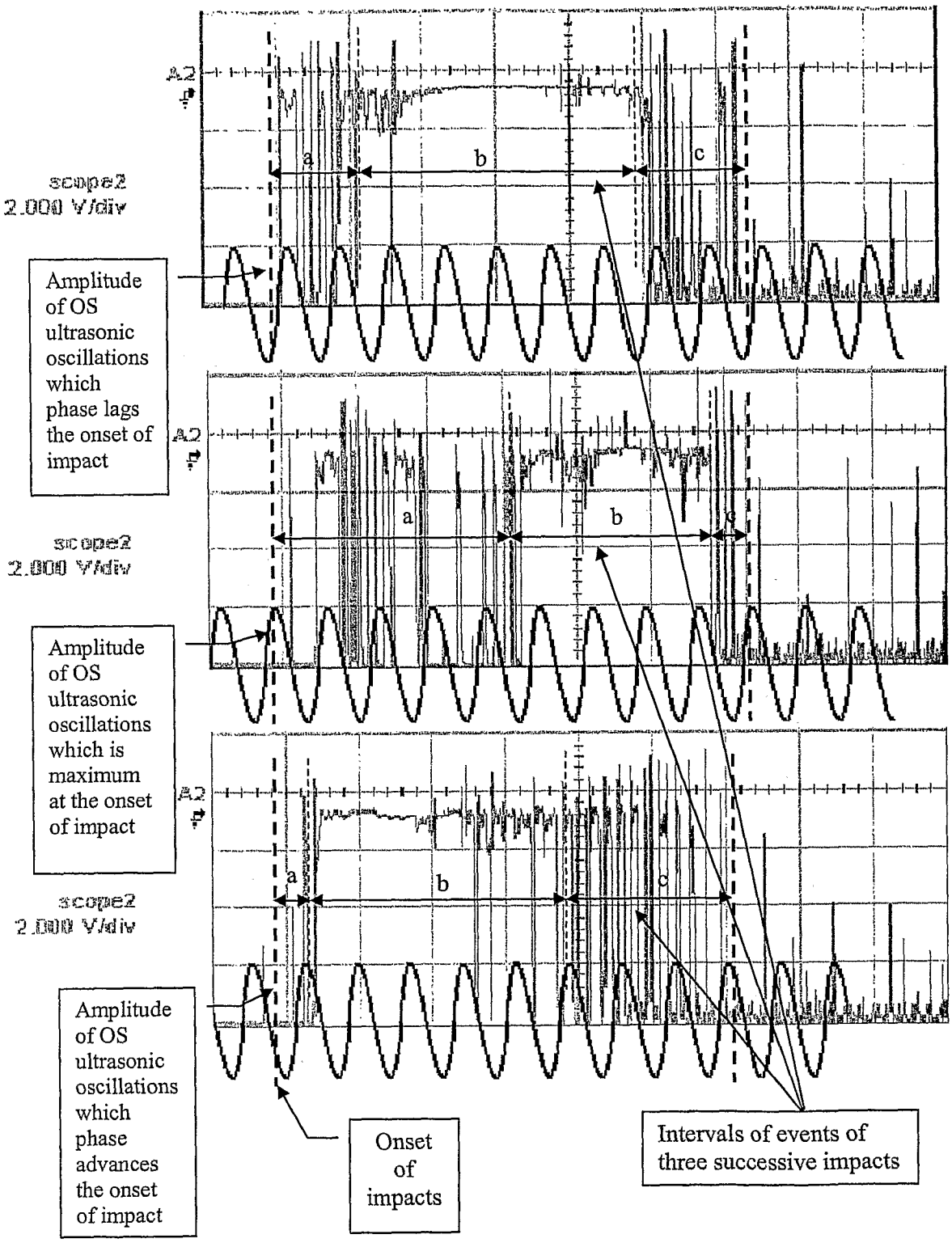
A2
a
b
c
scope2
2.000 V/div
Amplitude of OS ultrasonic oscillations which phase lags the onset of impact
A2
a
b
c
scope2
2.000 V/div
Amplitude of OS ultrasonic oscillations which is maximum at the onset of impact
A2
a
b
c
scope2
2.000 V/div
Amplitude of OS ultrasonic oscillations which phase advances the onset of impact
Onset of impacts
Intervals of events of three successive impacts

FIGURE 38

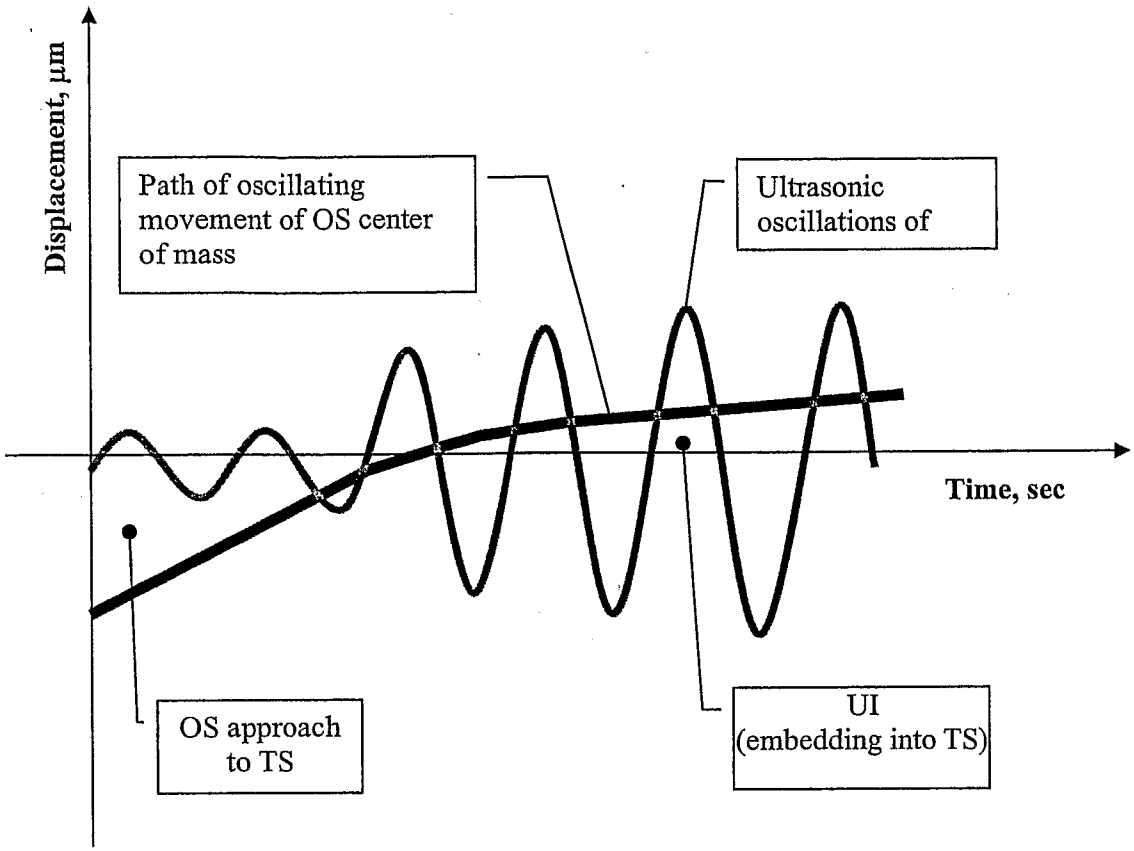

Initial data:

Frequency	f_{os} – frequency of oscillating movement of OS = 200 Hz
	f_{ose} – frequency of oscillating movement of OSE = 27000 Hz
Amplitude	A_{os} – displacement amplitude in oscillating movement of OS = 0.3 mm
	A_{ose} – displacement amplitude in oscillating movement of OSE = 0.03 mm

FIGURE 39

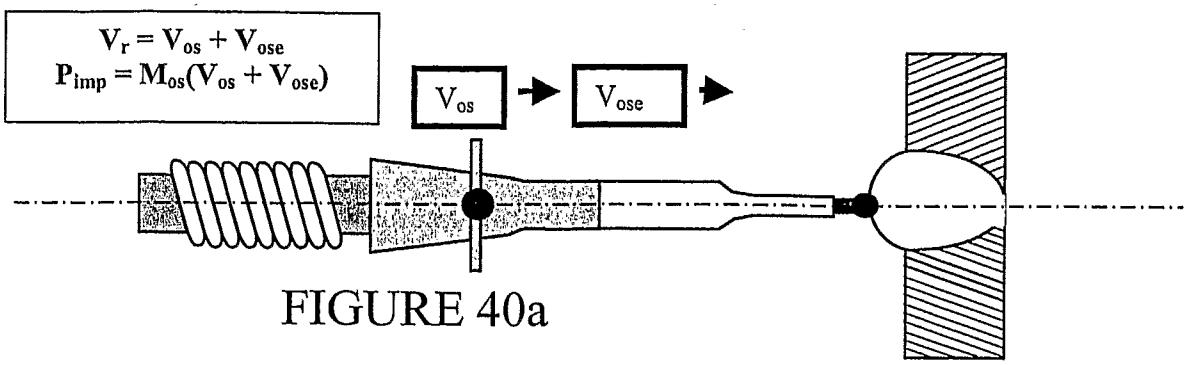

FIGURE 40a

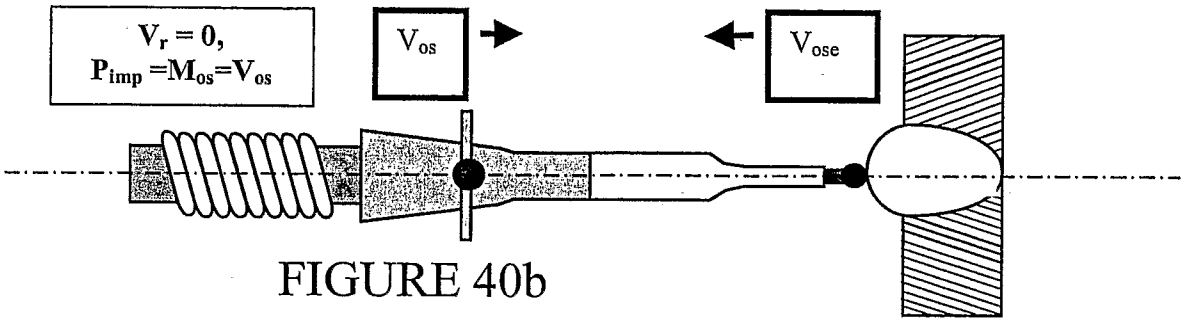

FIGURE 40b

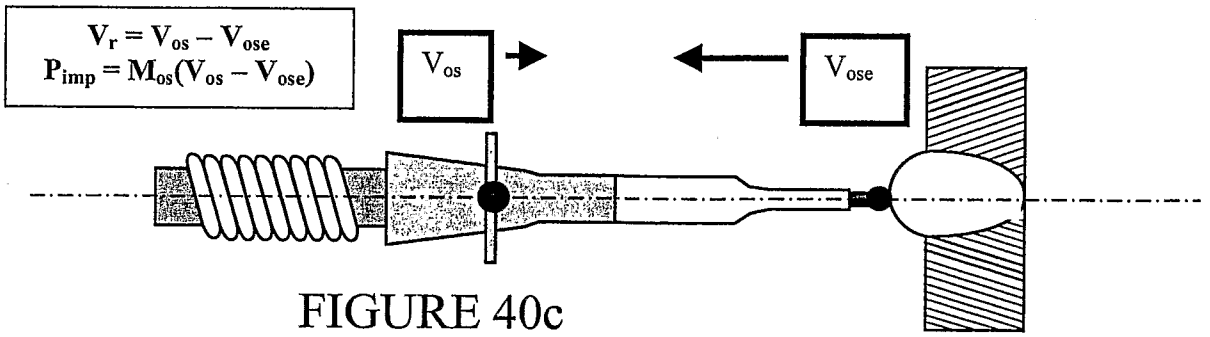

FIGURE 40c

V_{os} - oscillating velocity of the oscillating system (OS)
V_{ose} – oscillating velocity of the oscillating system end (OSE) at ultrasonic frequency
V_r – resultant oscillating velocity of OSE in summation of V_{os} and V_{ose}
M_{os} – oscillating system mass
P_{imp} – impulse of force of ultrasonic impact

FIGURE 41

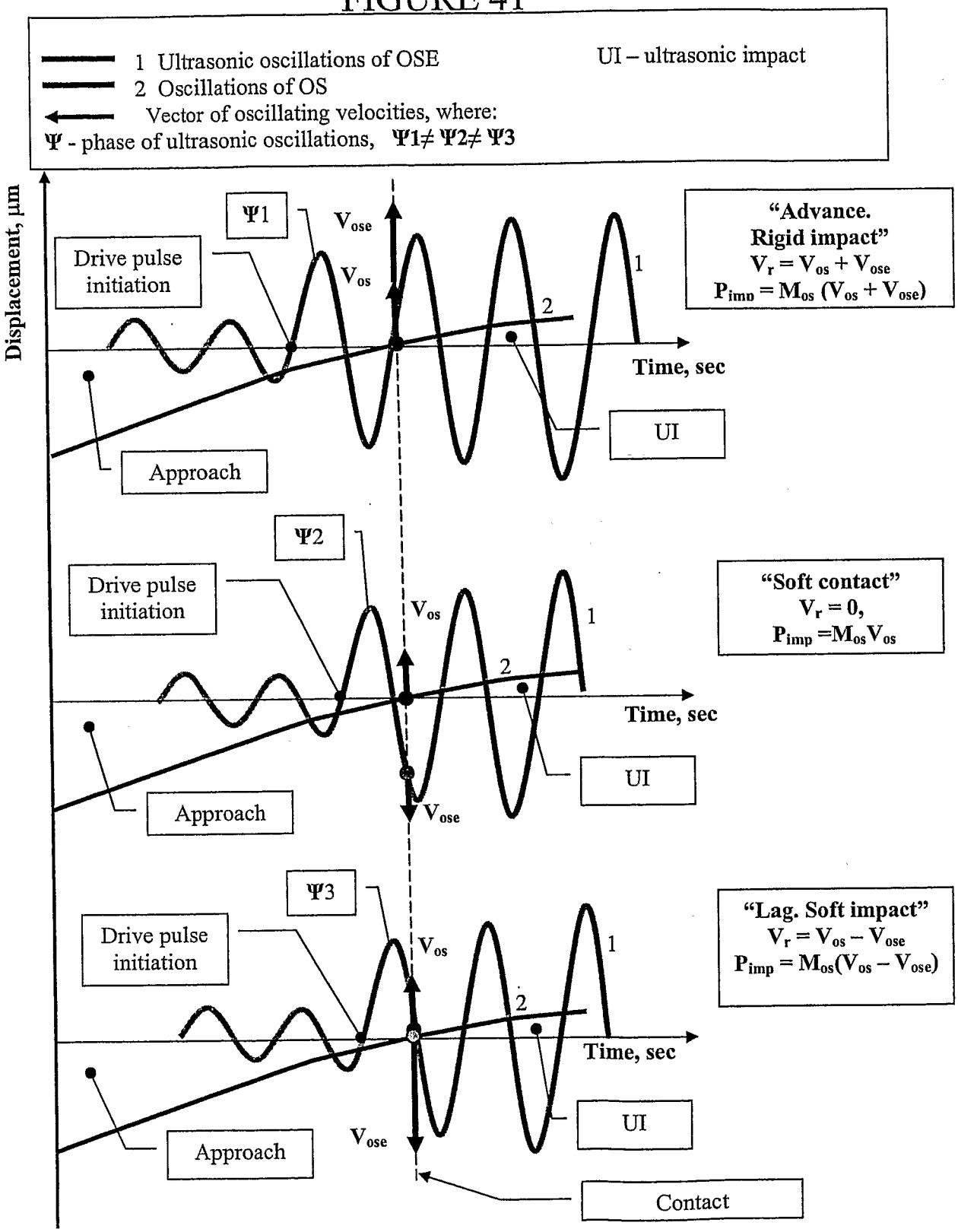
1 Ultrasonic oscillations of OSE
2 Oscillations of OS
Vector of oscillating velocities, where:
Ψ - phase of ultrasonic oscillations, Ψ1≠ Ψ2≠ Ψ3
UI – ultrasonic impact
Displacement, μm
Ψ1
Drive pulse initiation
Vose
Vos
1
2
Time, sec
UI
Approach
"Advance. Rigid impact"
Vr = Vos + Vose
Pimp = Mos (Vos + Vose)
Ψ2
Drive pulse initiation
Vos
1
2
Time, sec
UI
Approach
Vose
"Soft contact"
Vr = 0,
Pimp =MosVos
Ψ3
Drive pulse initiation
Vos
1
2
Time, sec
UI
Approach
Vose
Contact
"Lag. Soft impact"
Vr = Vos – Vose
Pimp = Mos(Vos – Vose)

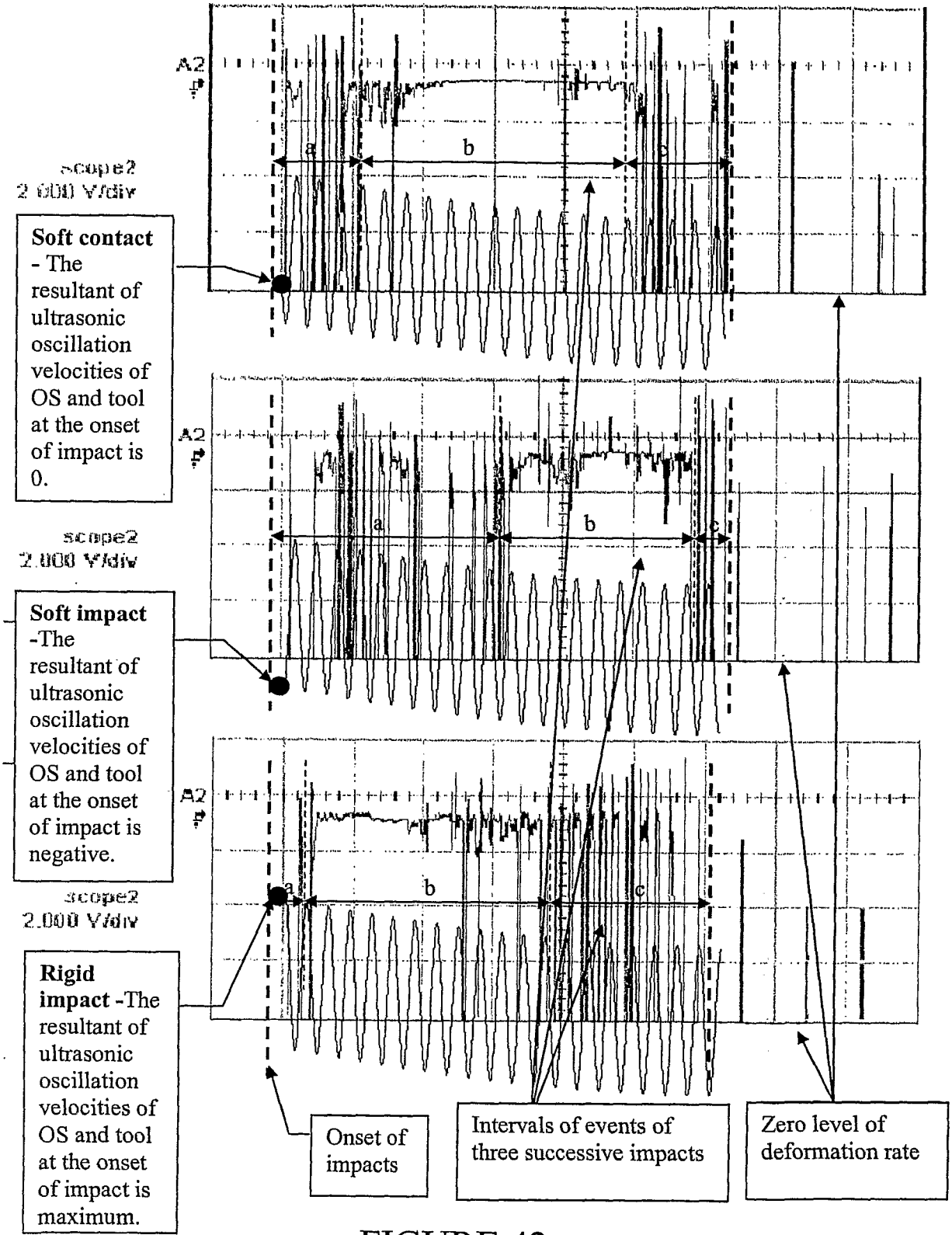
A2
a
b
c
scope2
2.000 V/div
Soft contact - The resultant of ultrasonic oscillation velocities of OS and tool at the onset of impact is 0.
Soft impact -The resultant of ultrasonic oscillation velocities of OS and tool at the onset of impact is negative.
Rigid impact -The resultant of ultrasonic oscillation velocities of OS and tool at the onset of impact is maximum.
Onset of impacts
Intervals of events of three successive impacts
Zero level of deformation rate

FIGURE 42

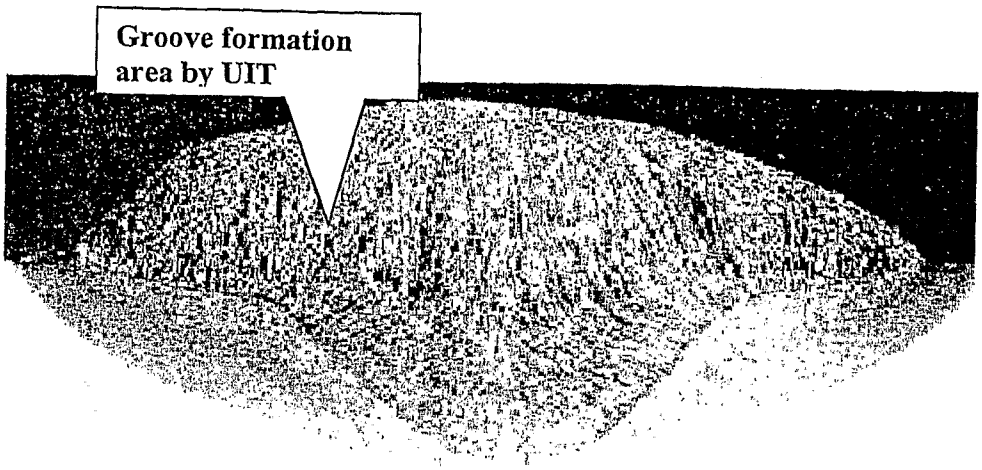

FIGURE 43

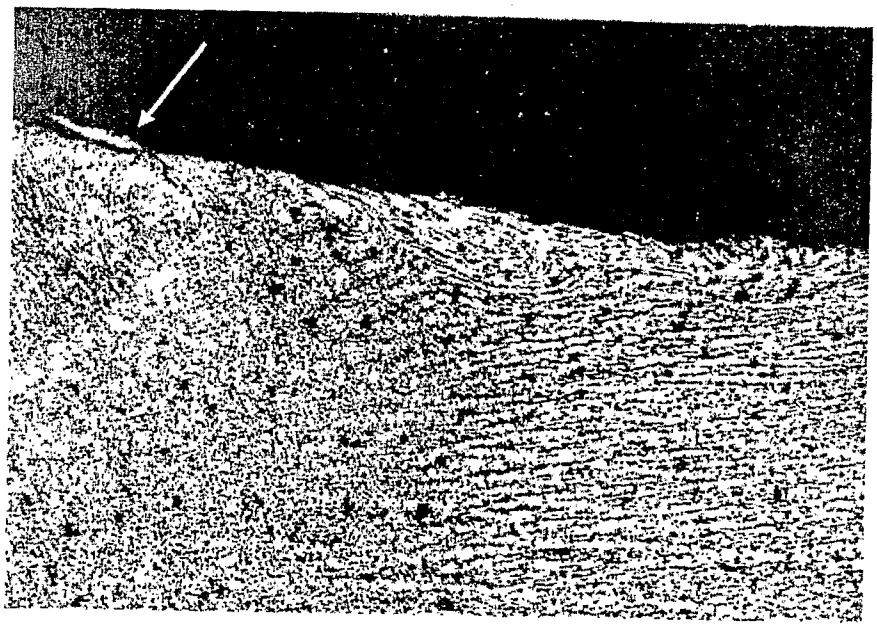

FIGURE 44

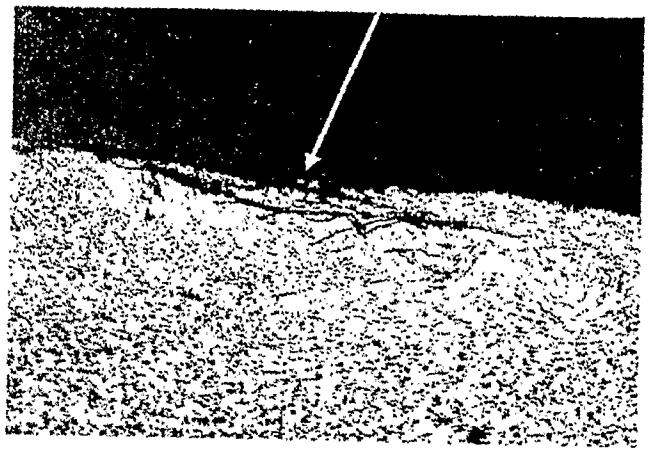

FIGURE 45

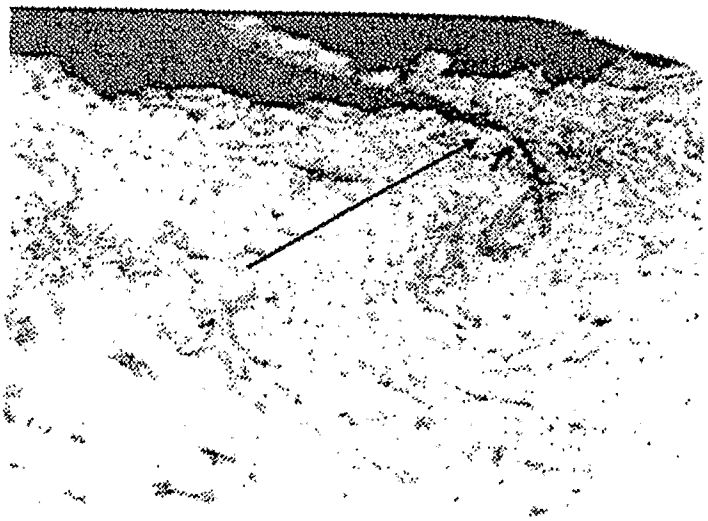

FIGURE 46

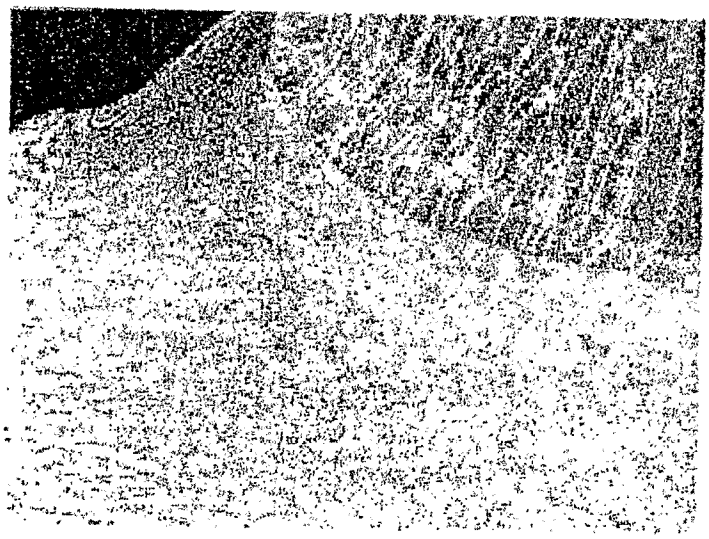

FIGURE 47

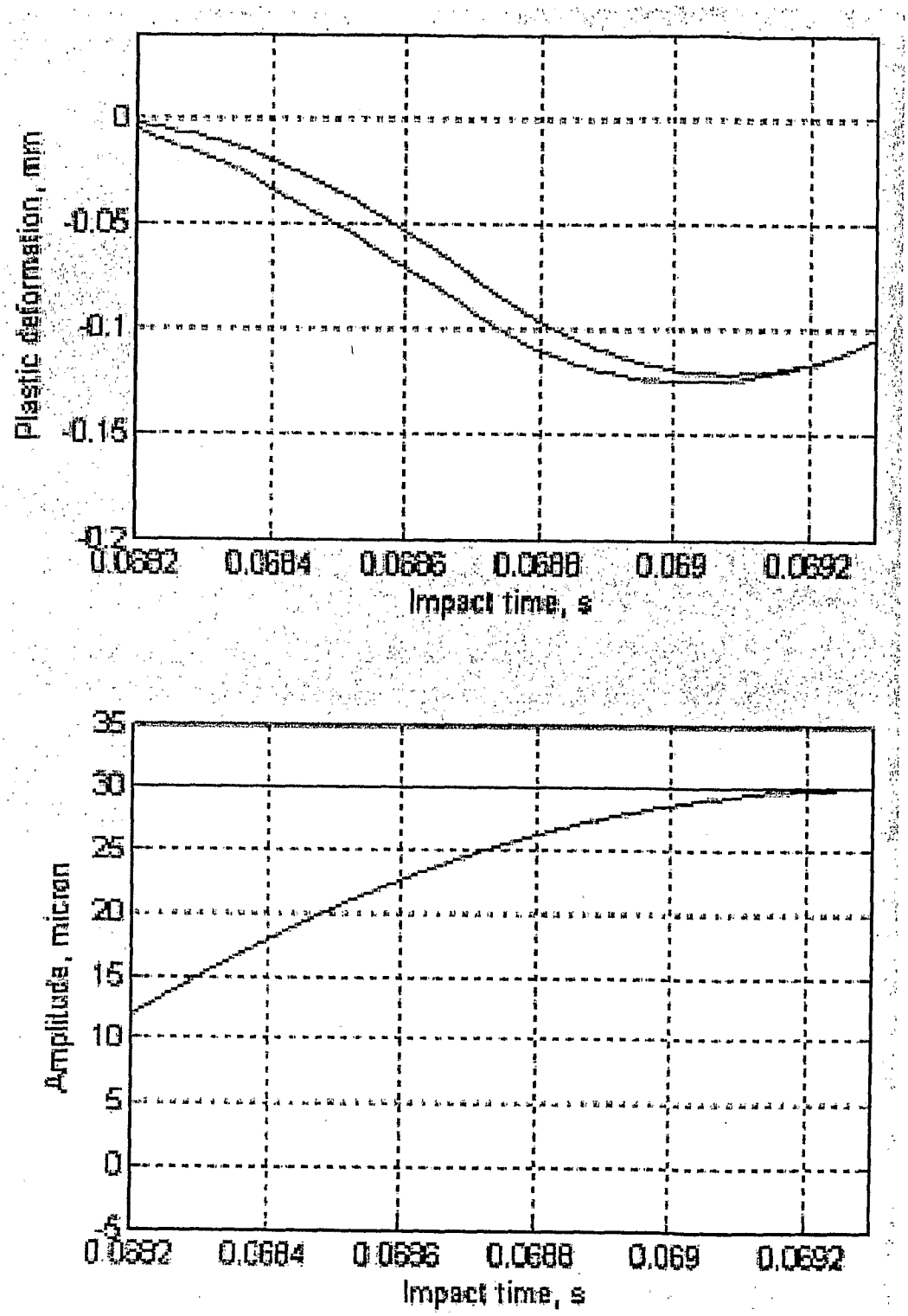
Plastic deformation, mm
0
-0.05
-0.1
-0.15
-0.2
0.0682
0.0684
0.0686
0.0688
0.069
0.0692
Impact time, s
Amplitude, micron
35
30
25
20
15
10
5
0
-5
0.0682
0.0684
0.0686
0.0688
0.069
0.0692
Impact time, s

FIGURE 48

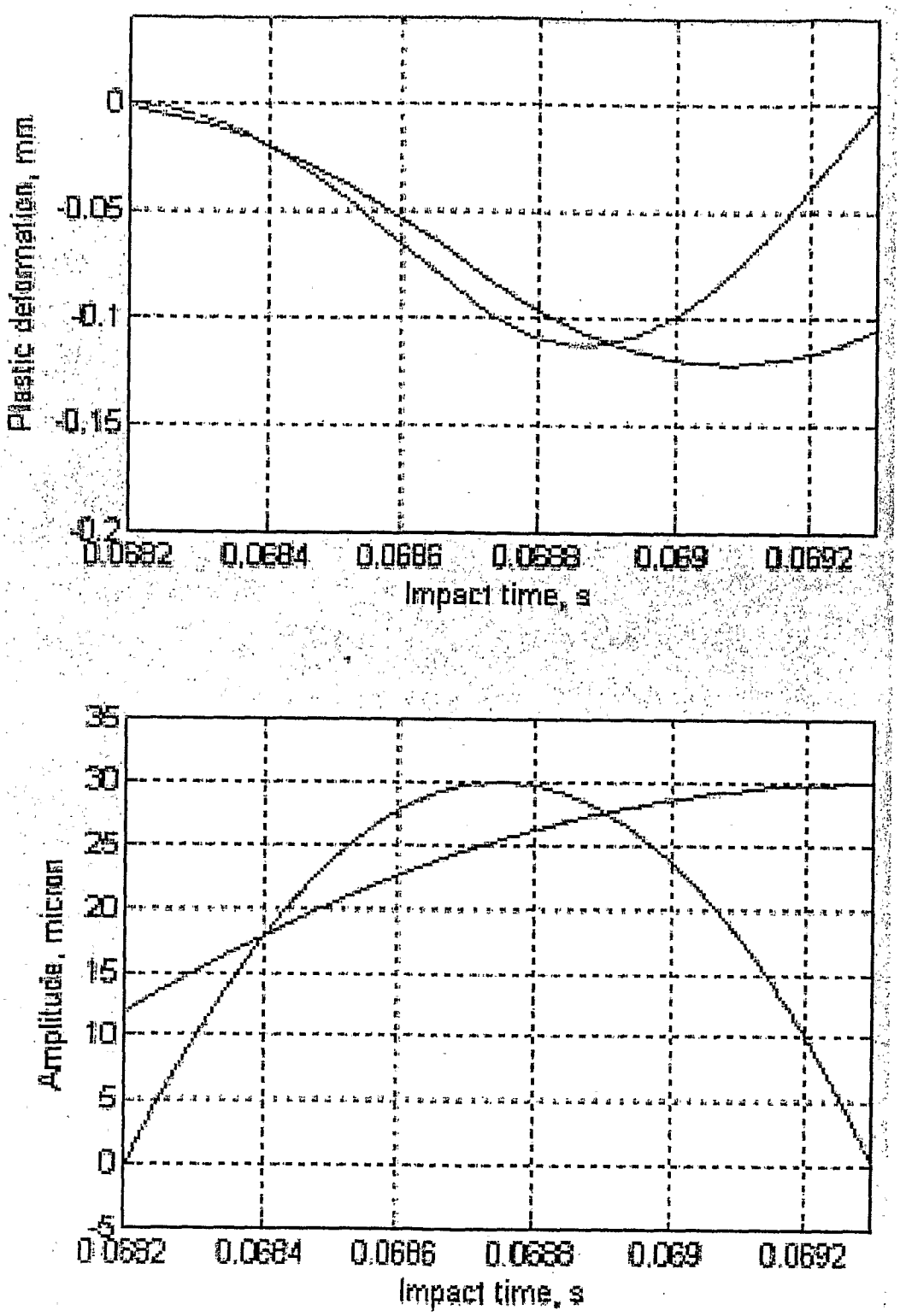
Plastic deformation, mm
0
-0.05
-0.1
-0.15
-0.2
0.0682
0.0684
0.0686
0.0688
0.069
0.0692
Impact time, s
Amplitude, micron
35
30
25
20
15
10
5
0
-5
0.0682
0.0684
0.0686
0.0688
0.069
0.0692
Impact time, s

FIGURE 49

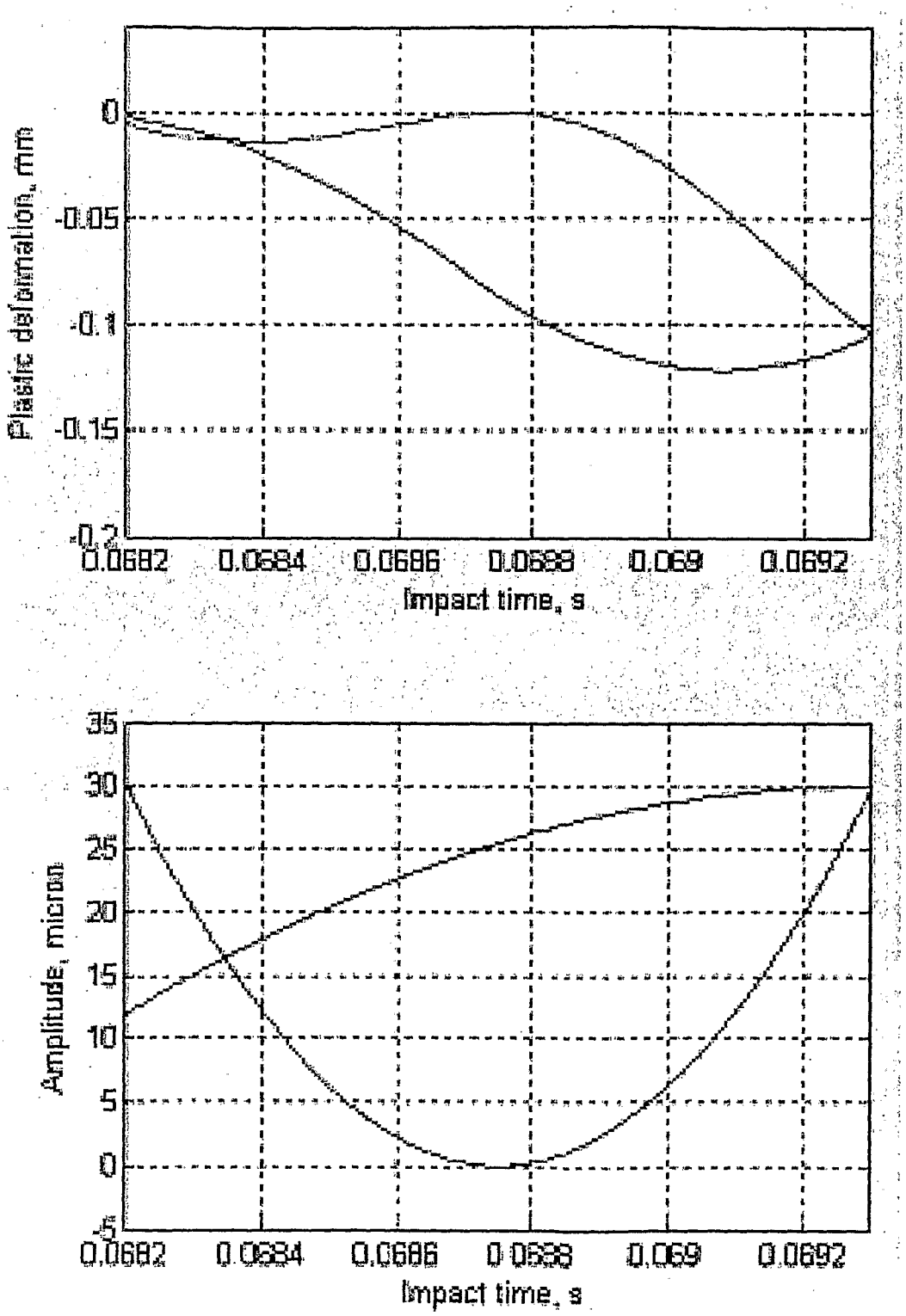
Plastic deformation, mm
0
-0.05
-0.1
-0.15
-0.2
0.0682
0.0684
0.0686
0.0688
0.069
0.0692
Impact time, s
Amplitude, micron
35
30
25
20
15
10
5
0
-5
0.0682
0.0684
0.0686
0.0688
0.069
0.0692
Impact time, s

FIGURE 50

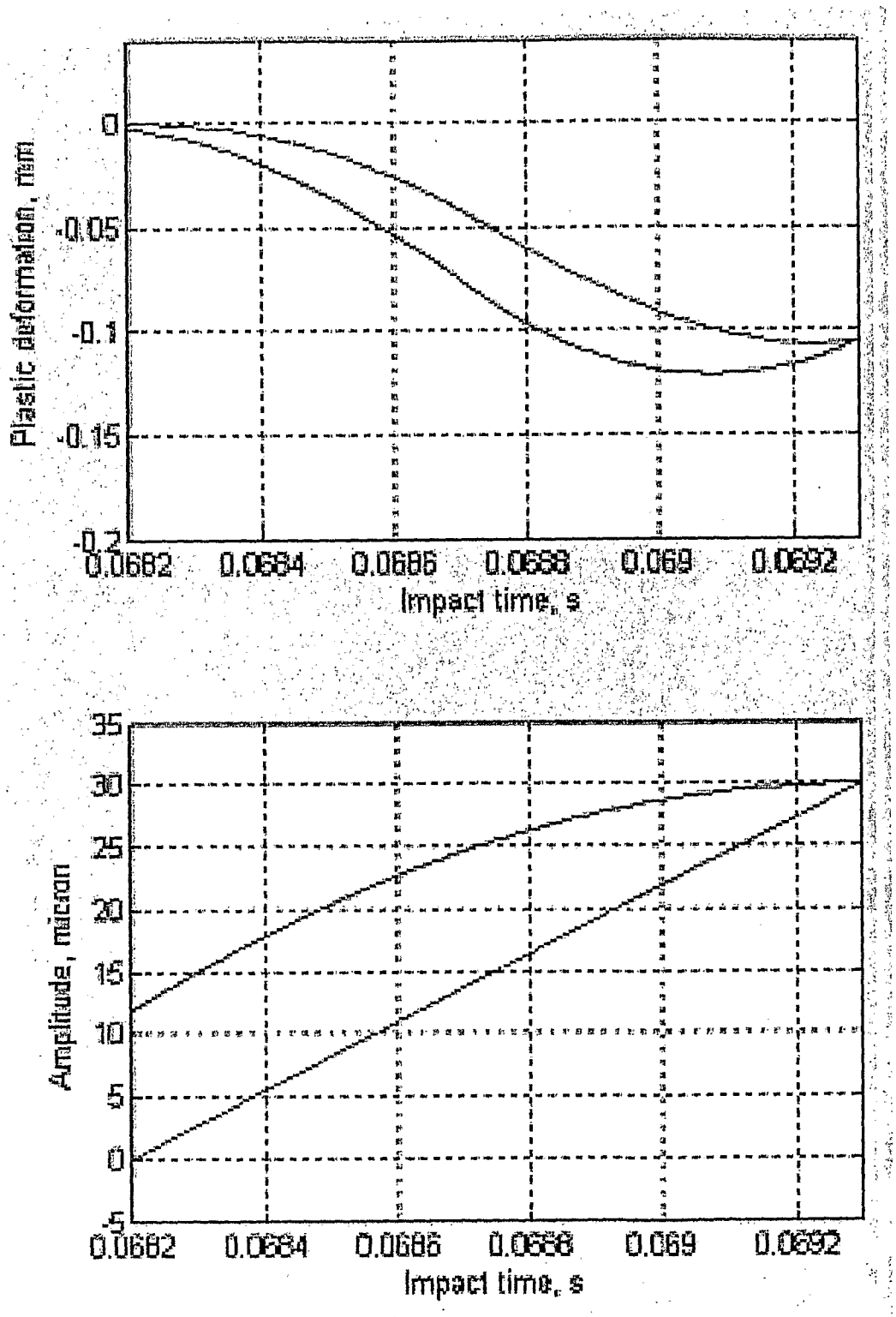
Plastic deformation, mm
0
-0.05
-0.1
-0.15
-0.2
0.0682
0.0684
0.0686
0.0688
0.069
0.0692
Impact time, s
Amplitude, micron
35
30
25
20
15
10
5
0
-5
0.0682
0.0684
0.0686
0.0688
0.069
0.0692
Impact time, s

FIGURE 51

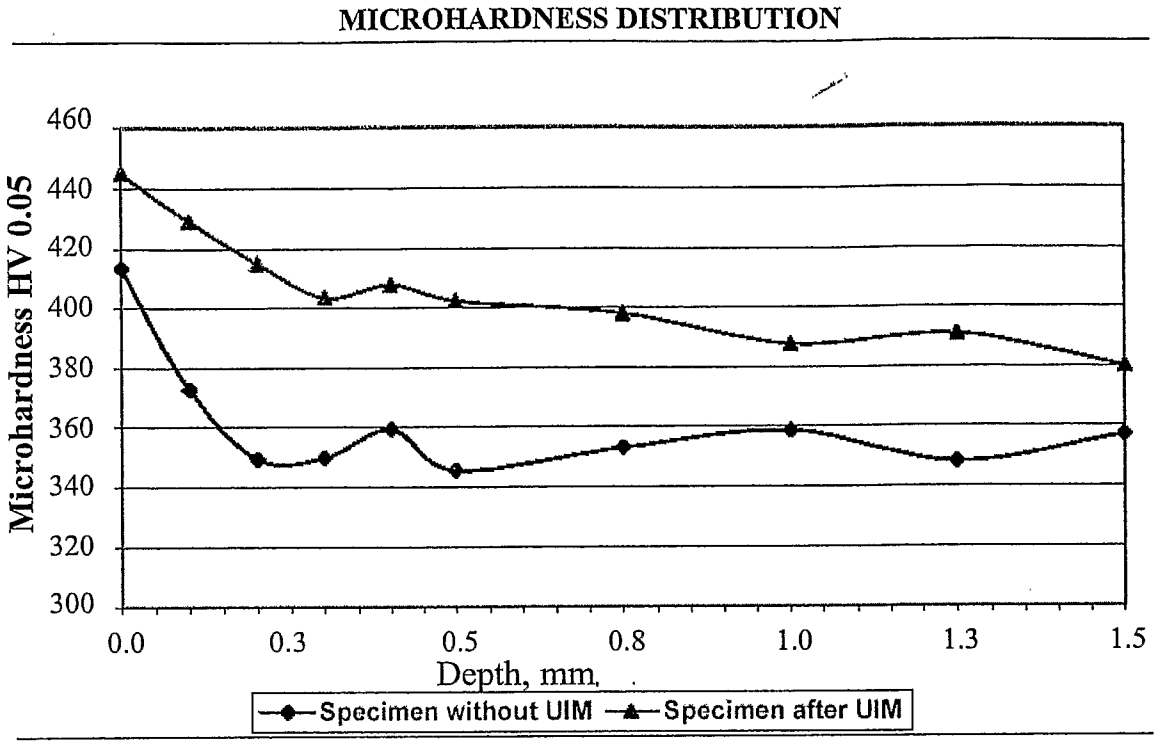

FIGURE 52

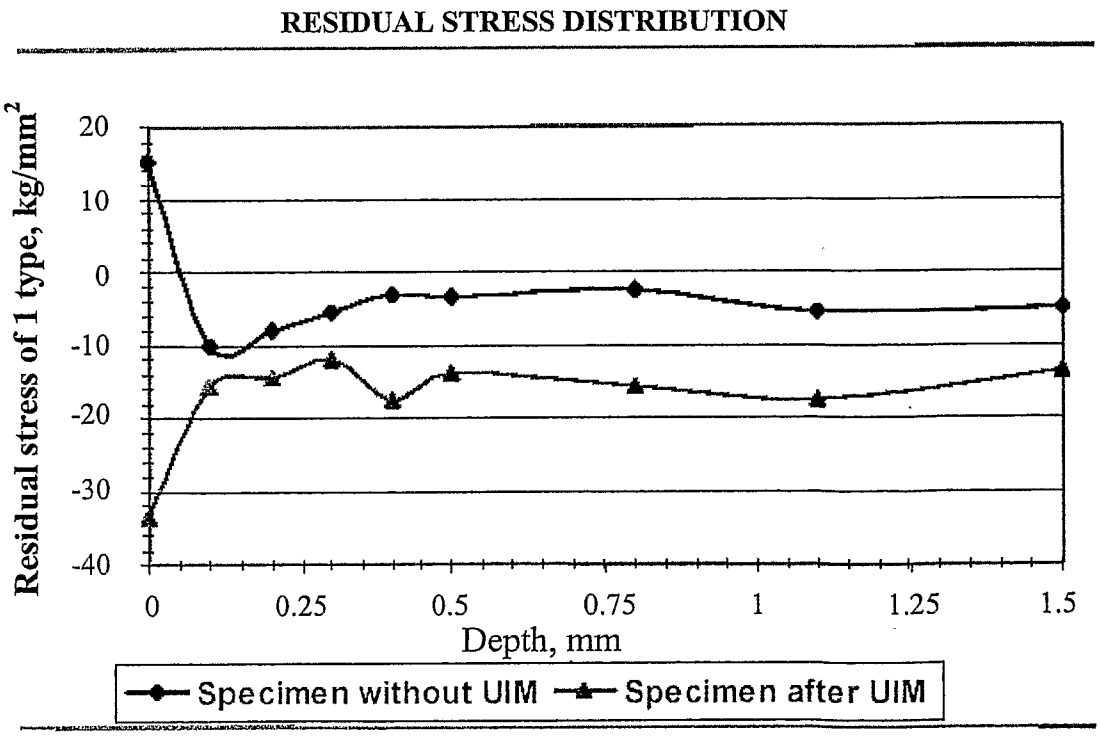

FIGURE 53

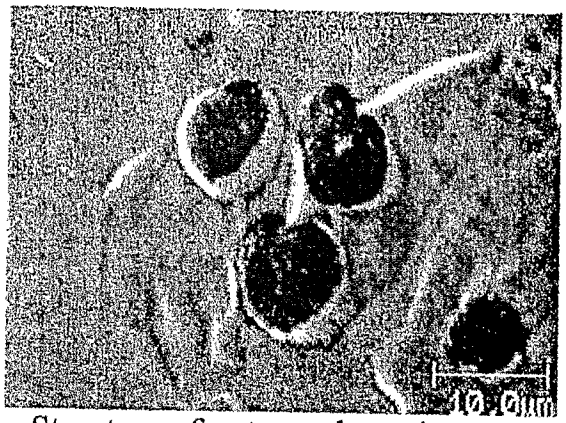

Structure of untreated specimen at the depth of 100 μm

FIGURE 54

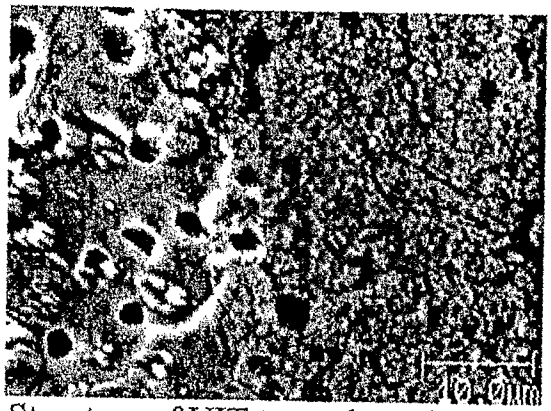

Structure of UIT treated specimen at the depth of 100 μm

FIGURE 55

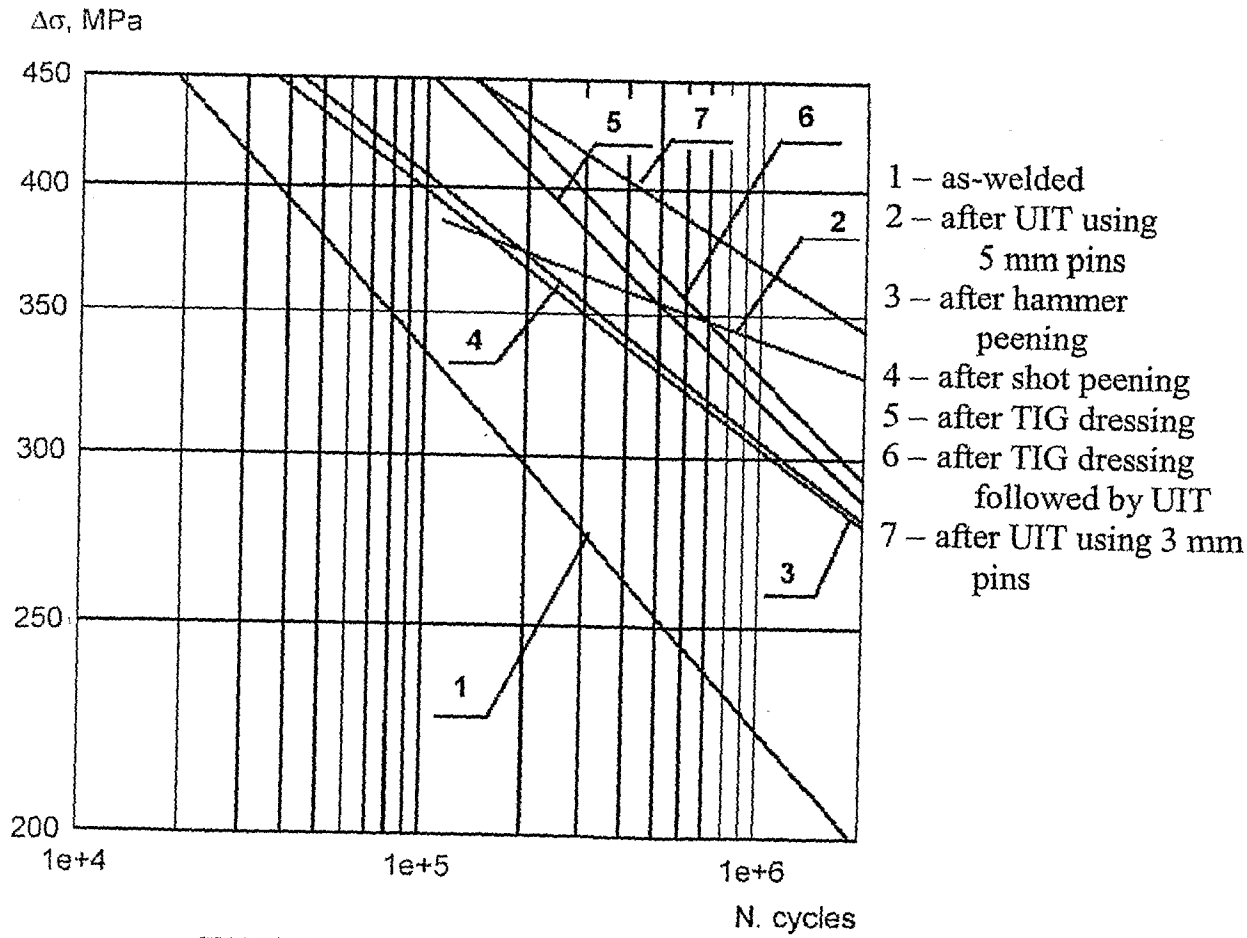

FIGURE 57

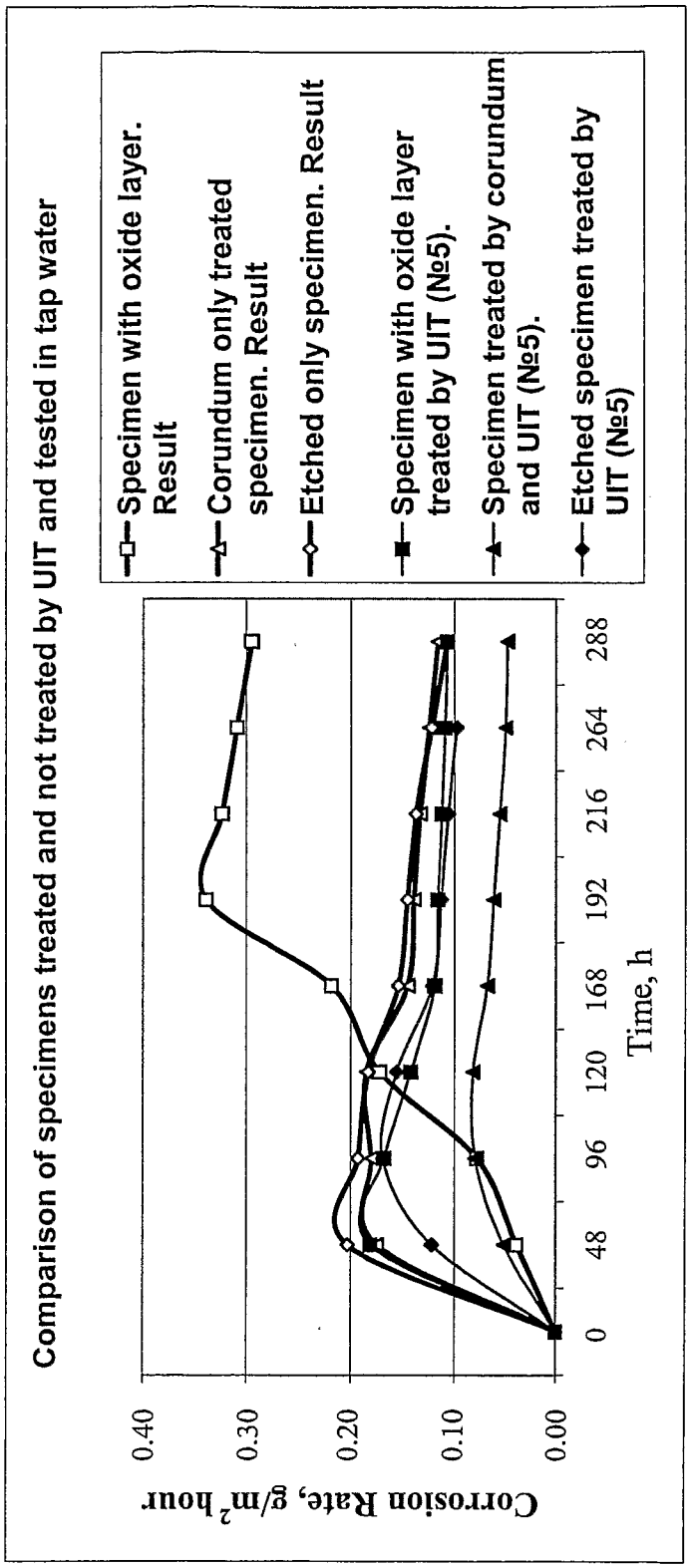
Comparison of specimens treated and not treated by UIT and tested in tap water
Corrosion Rate, g/m2 hour
0.40
0.30
0.20
0.10
0.00
0
48
96
120
168
192
216
264
288
Time, h
Specimen with oxide layer. Result
Corundum only treated specimen. Result
Etched only specimen. Result
Specimen with oxide layer treated by UIT (№5).
Specimen treated by corundum and UIT (№5).
Etched specimen treated by UIT (№5)

FIGURE 56

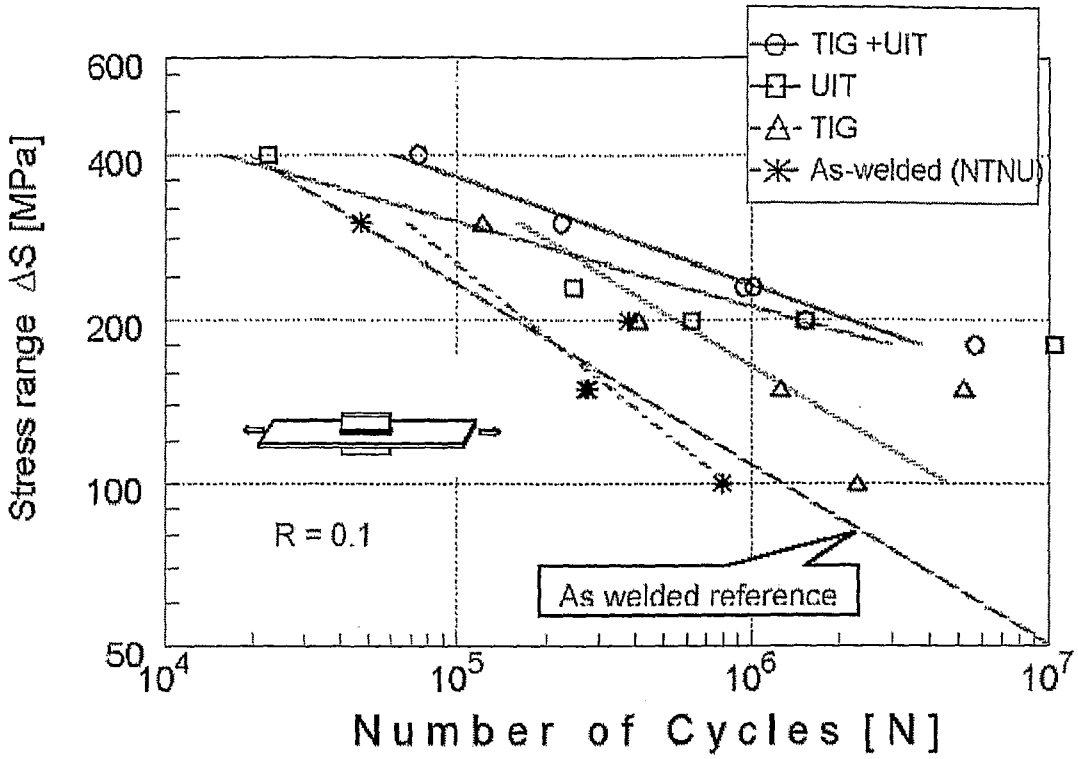

FIGURE 58

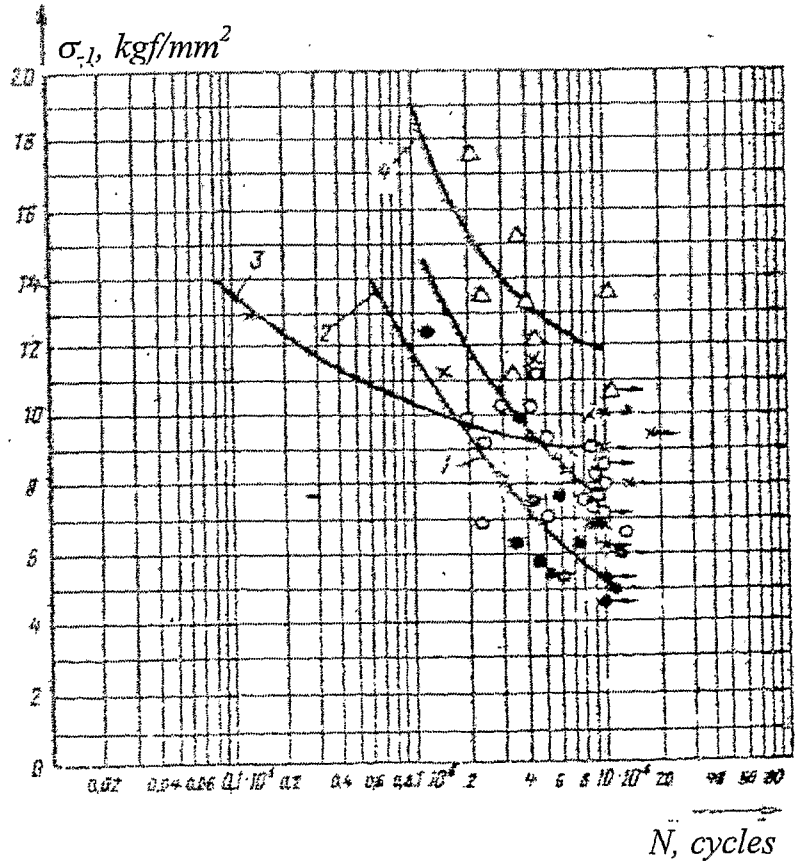

1 – untreated
2 – treated on smooth side
3 – treated on the weld side
4 – treated on two sides

FIGURE 59

Test results [kgs-m/cm^2]

Test Result	Weld Axis				Fusion line			
	h = 2 mm		h = 1 mm		h = 2 mm		h = 1 mm	
	As welded	After UIT	As welded	After UIT	As welded	After UIT	As welded	After UIT
	10.4	9.8	9.0	9.0	4.8	4.2	7.2	11.8
	8.6	11.2	9.2	10.0	6.2	8.6	10.4	12.4
	9.2	10.4	10.4	9.8	5.4	3.4	11.0	11.2
	7.8	8.0	11.2	10.2	3.8	6.0	8.8	9.4
	11.4	7.8	9.8	9.4	4.6	4.8	6.8	12.8
	8.8	9.4	8.8	8.8	7.0	5.2	8.0	10.4
Average	9.4	9.4	9.7	9.5	5.3	5.4	8.7	11.3

FIGURE 60

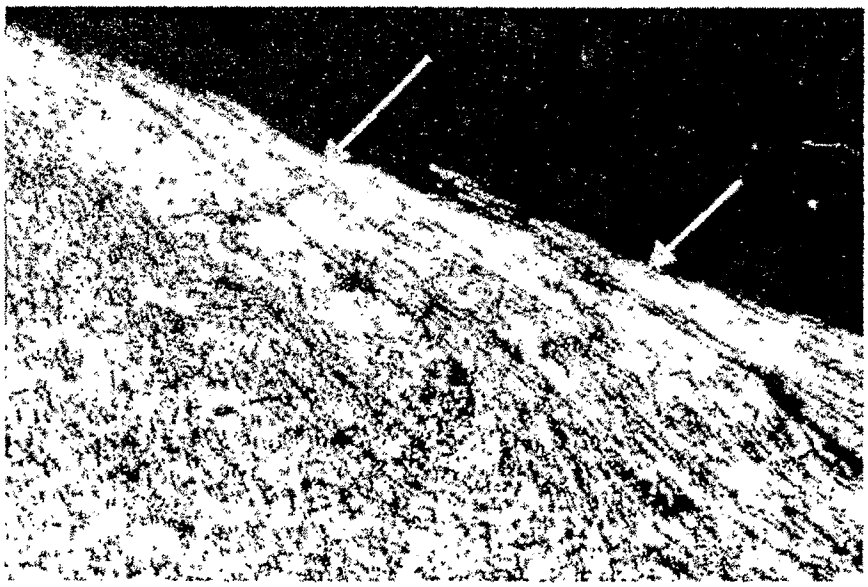

Welded joint of 10Mn2VNb steel

FIGURE 62

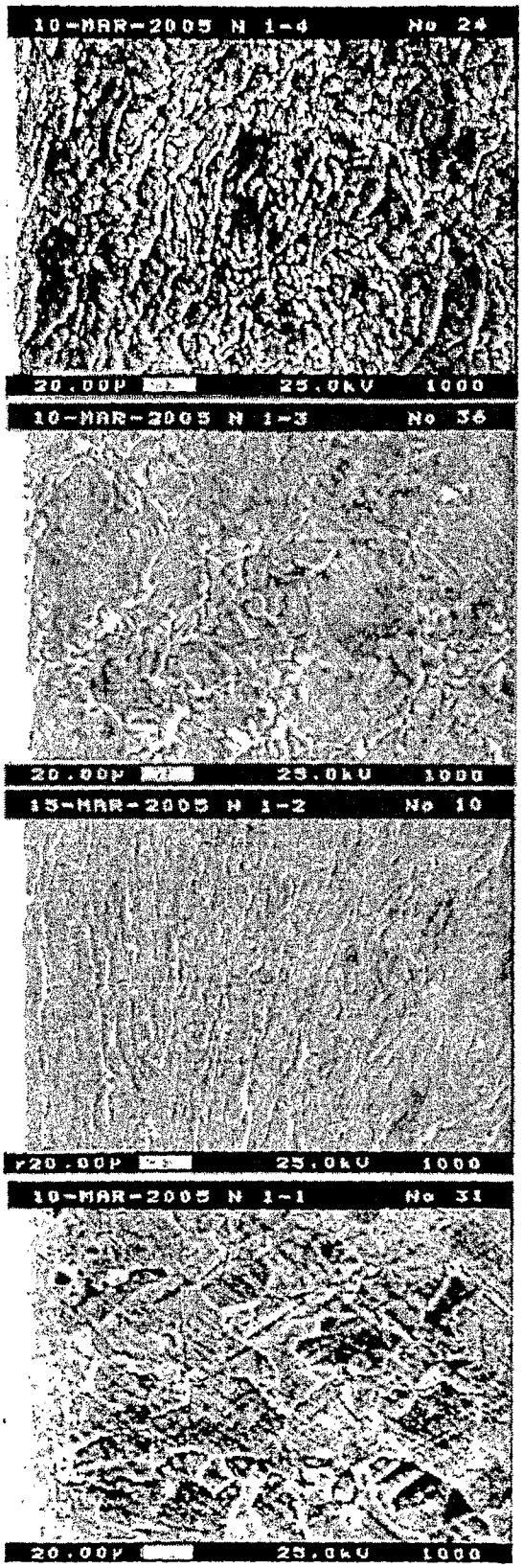

Grain size, micron (Grain Reduction Range)

At depth up to 50 mm		
7-21	4-15 (1.8)	3-8 (2.8)
		3-5 (3.2)
At depth up to 200...250 mm		
7-21	7-15 (1.1)	4-12 (1.6)
		7-9 (2.0)

FIGURE 61

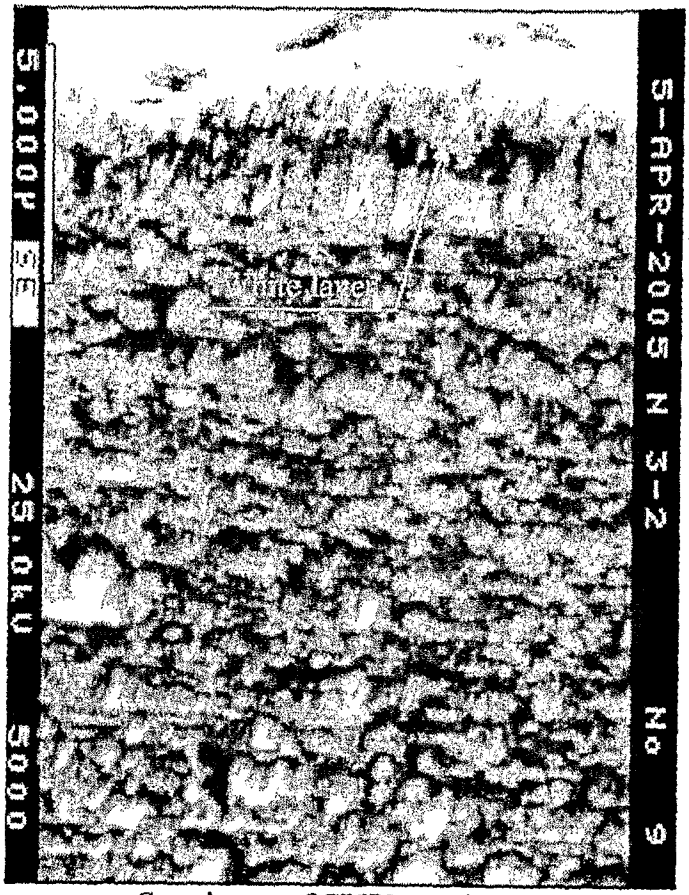

Specimen of SUJ2 steel

FIGURE 63

Welding without UIT

FIGURE 64

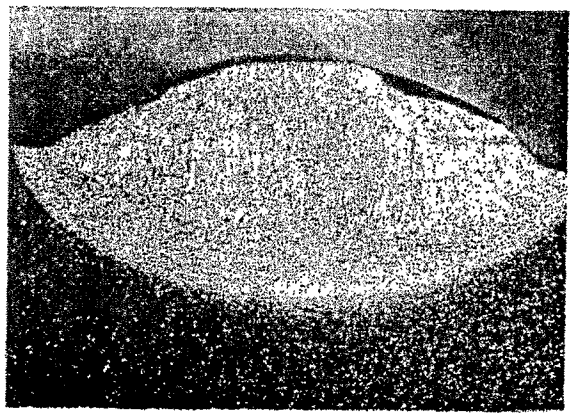

Welding with UIT

FIGURE 65

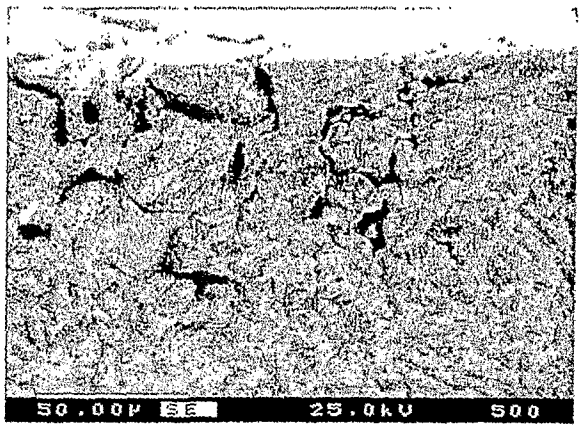

Without UIT

FIGURE 66

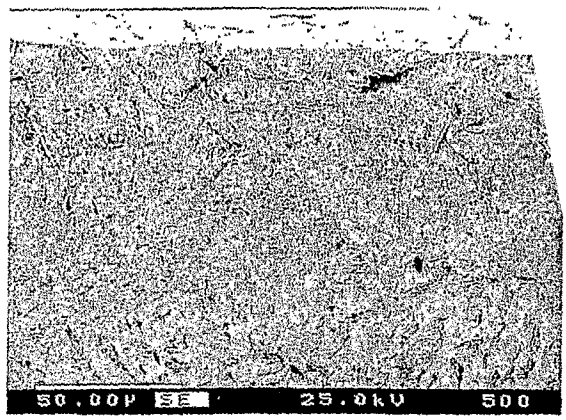

After UIT

FIGURE 67

S-N curves for 8 mm butt welds

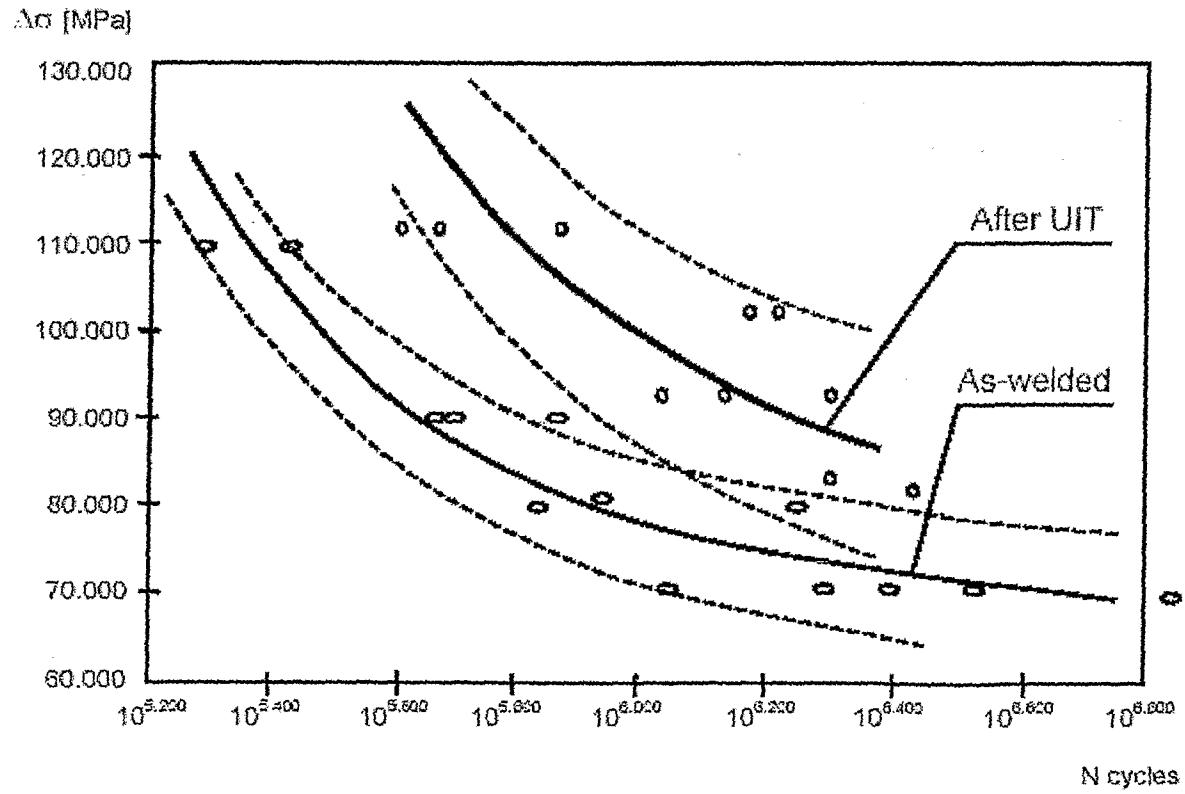

FIGURE 68

S-N curves for 8 mm specimens with longitudinal attachments

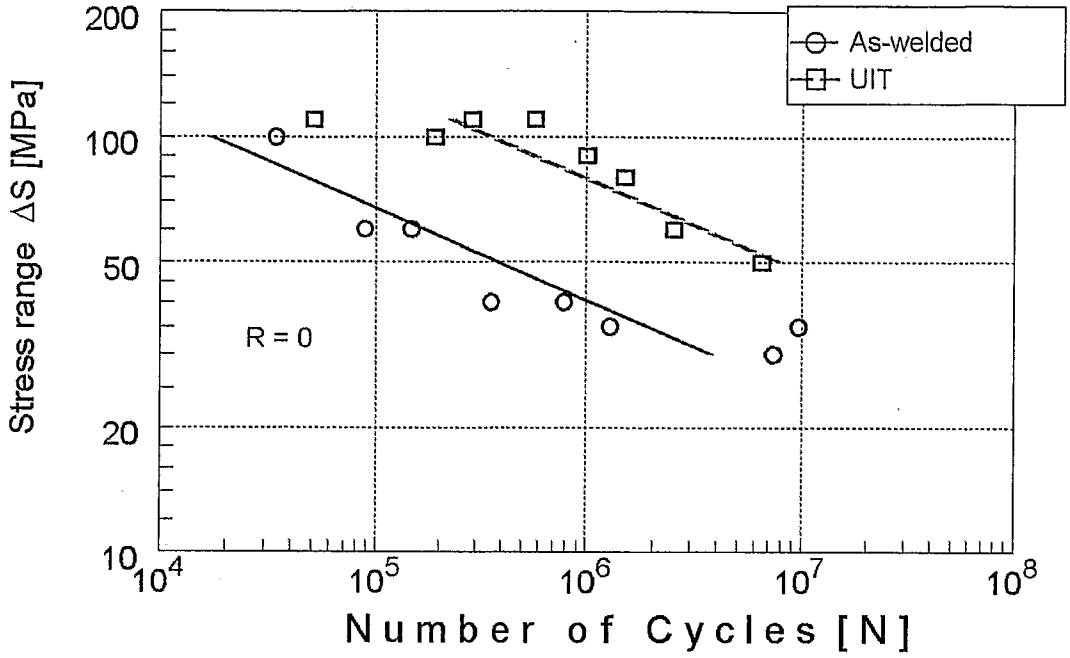

FIGURE 69

S-N curves for 8 mm specimens of lap joints

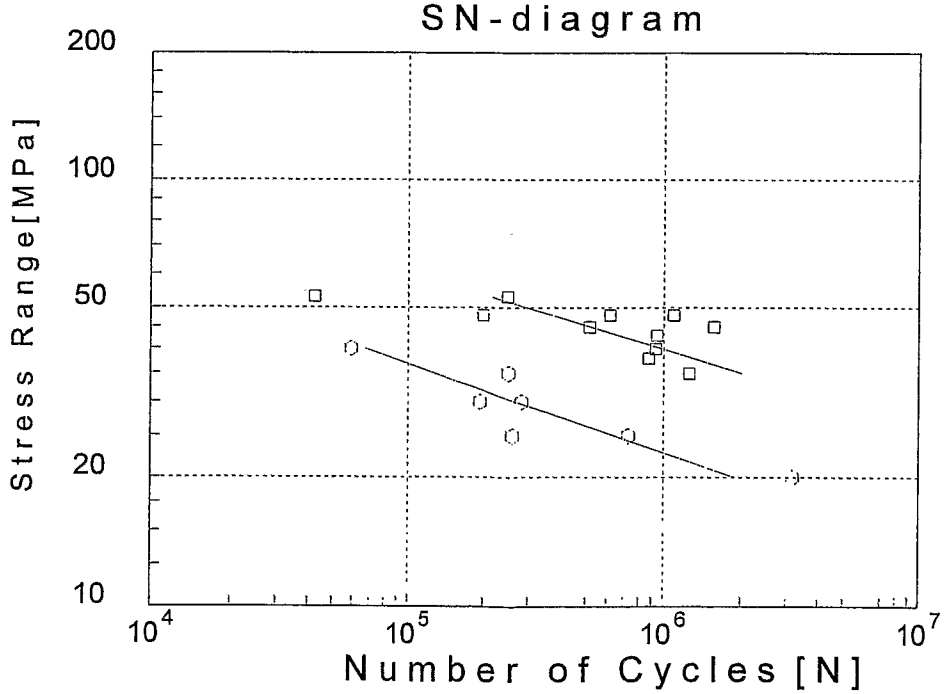

FIGURE 70

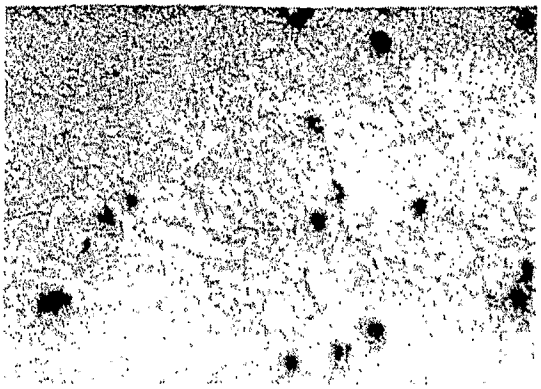

Without UIT

FIGURE 71

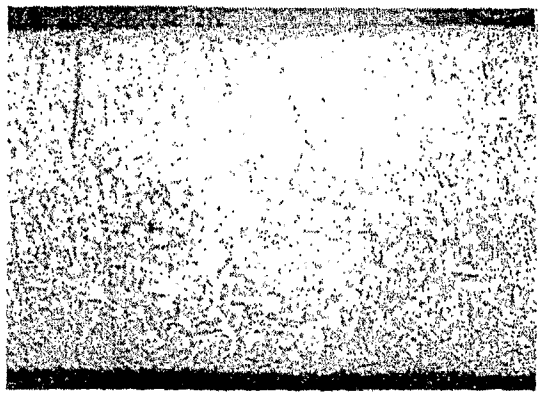

After UIT

FIGURE 72

Impact strength on specimens with a strengthened notch

Impact strength, J/cm^2		**Series 1** Machining	**Series 3** Machining + UIM (condition 1) + etching	**Series 4** Machining + UIM (condition 2) + etching
H=10 mm	Average	**4.25**	**4.0**	**3.2**
H=15 mm	Average	**7.0**	**6.0**	**4.6**
H=20 mm	Average	**8.4**	**8.0**	**8.4**

FIGURE 73

Impact strength on specimens cut out from a strengthened wheel

Measuring No.	Untreated		After UIT		After UIM		After VUT	
	#1	**#2**	**#1**	**#2**	**#1**	**#2**	**#1**	**#2**
1.	2.7	2.7	2.58	2.95	2.83	2.7	3.32	3.2
2.	2.45	2.7	2.39	2.7	2.45	2.45	3.08	3.57
3.	3.57	3.44	3.2	3.2	2.94	3.44	3.69	2.82
Average for sample	**2.9**	**2.94**	**2.72**	**2.95**	**2.74**	**2.86**	**3.36**	**3.19**
Average for wheel	**2.92**		**2.84**		**2.8**		**3.28**	

FIGURE 74

Untreated specimen structure

FIGURE 75

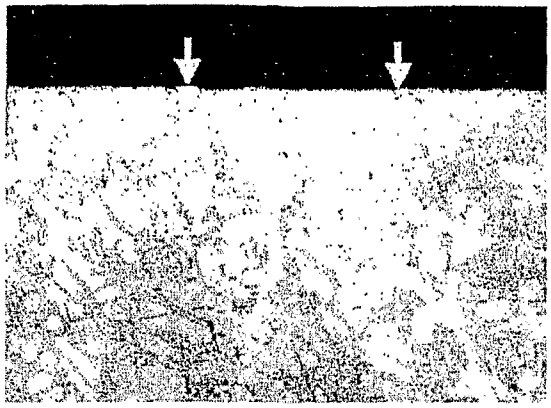

Silicon precipitates on UIT treated specimen

FIGURE 76

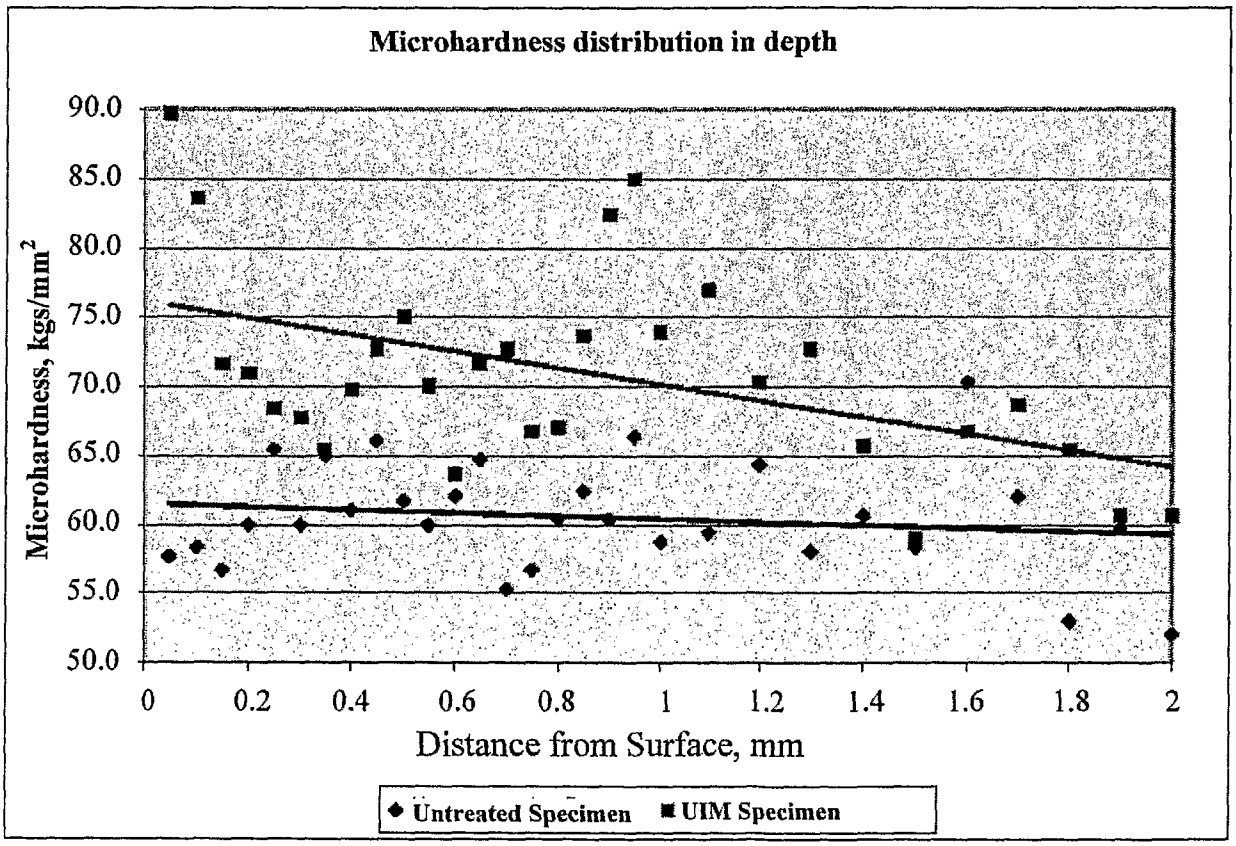

FIGURE 77

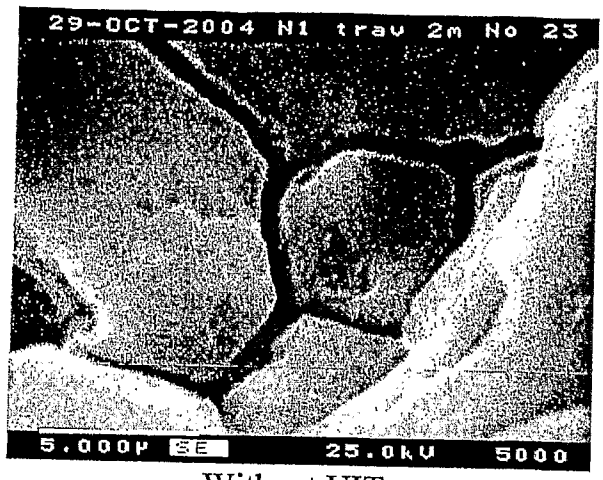

Without UIT

FIGURE 78

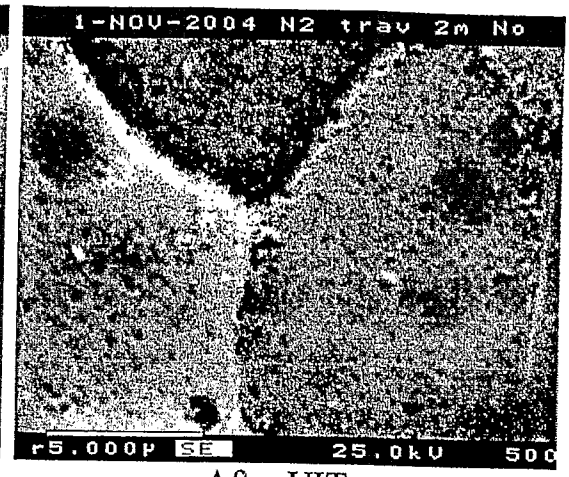

After UIT

FIGURE 79

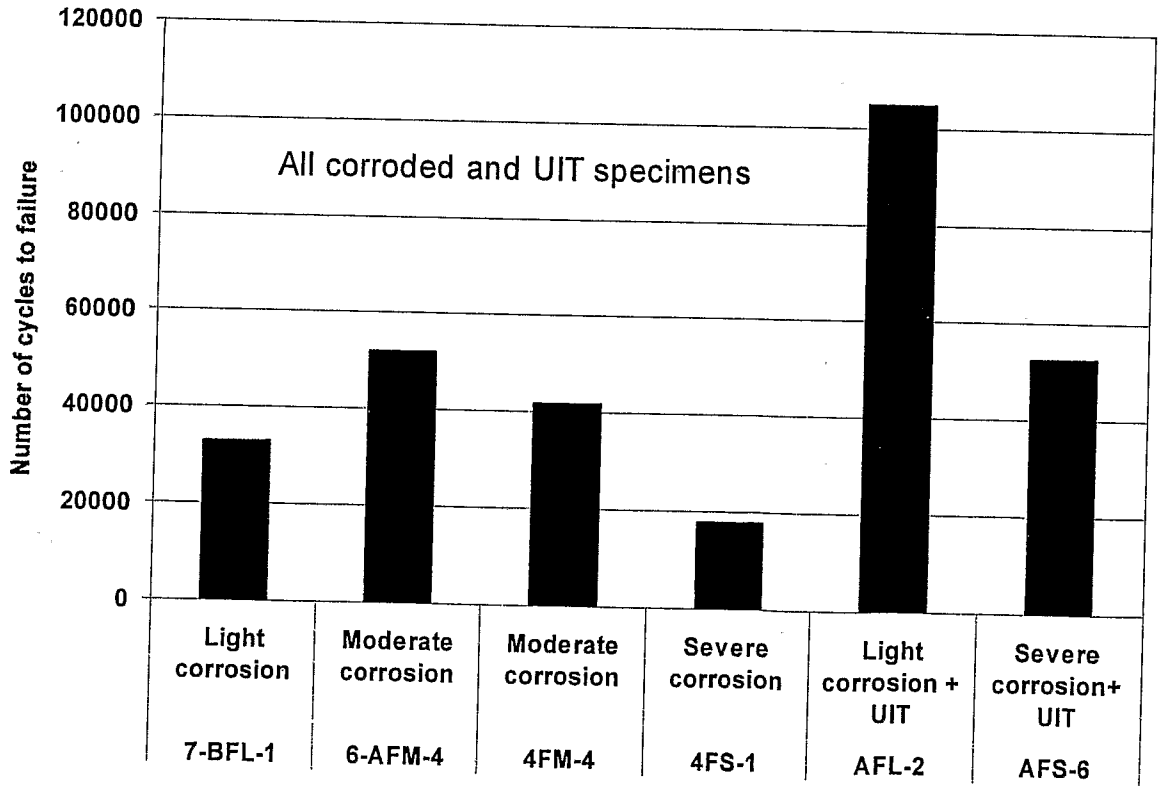

FIGURE 80

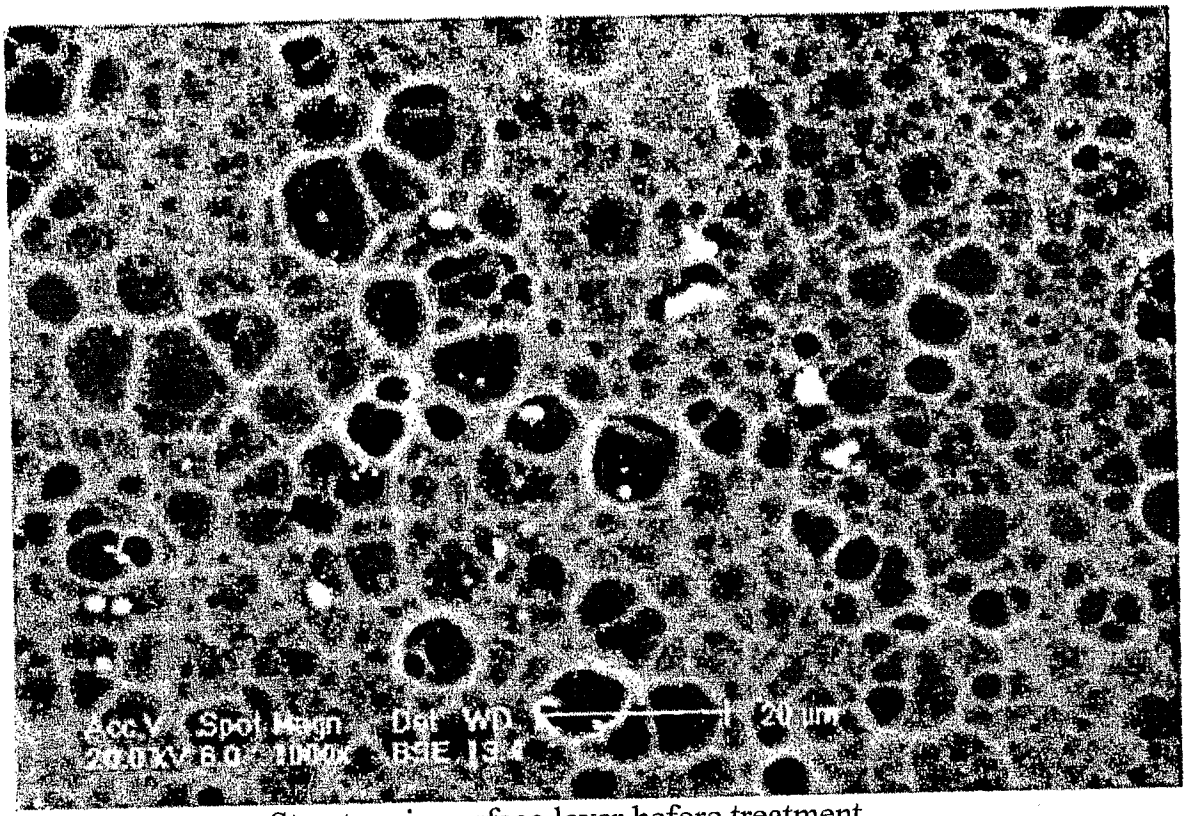

Structure in surface layer before treatment

FIGURE 81

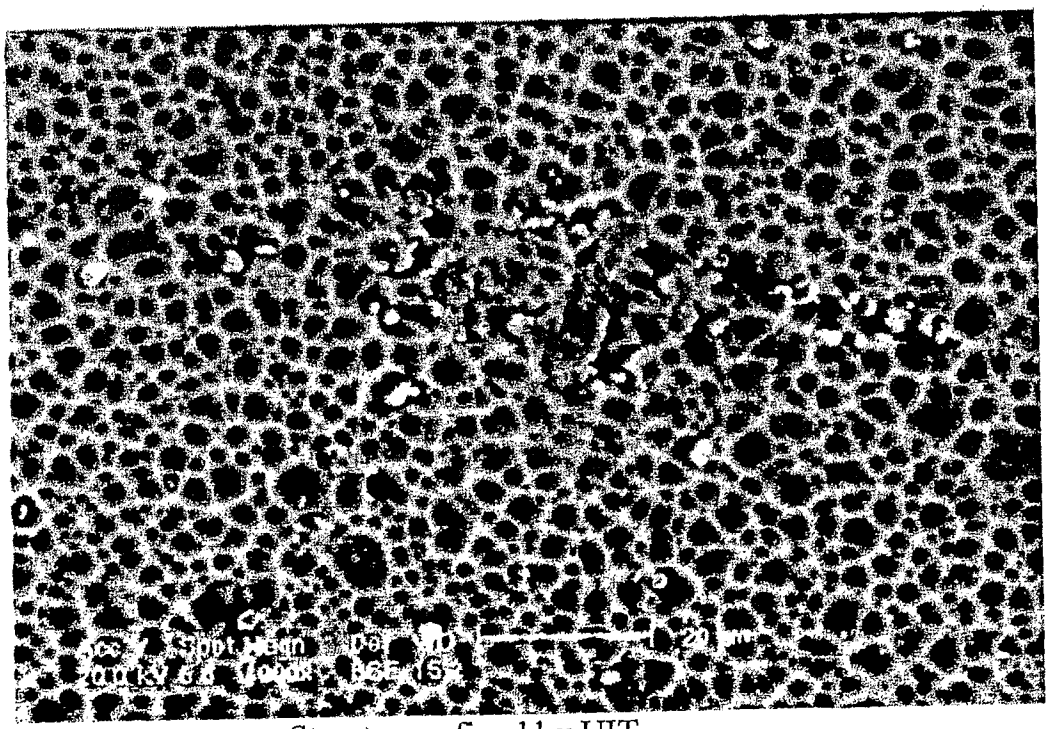

Structure refined by UIT

FIGURE 82

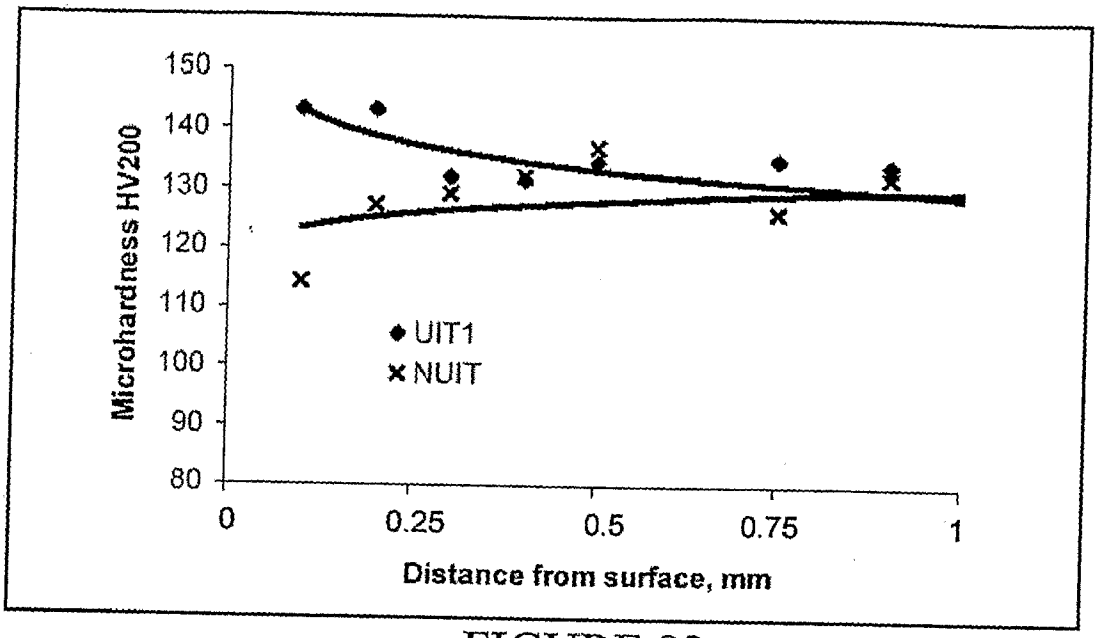

FIGURE 83

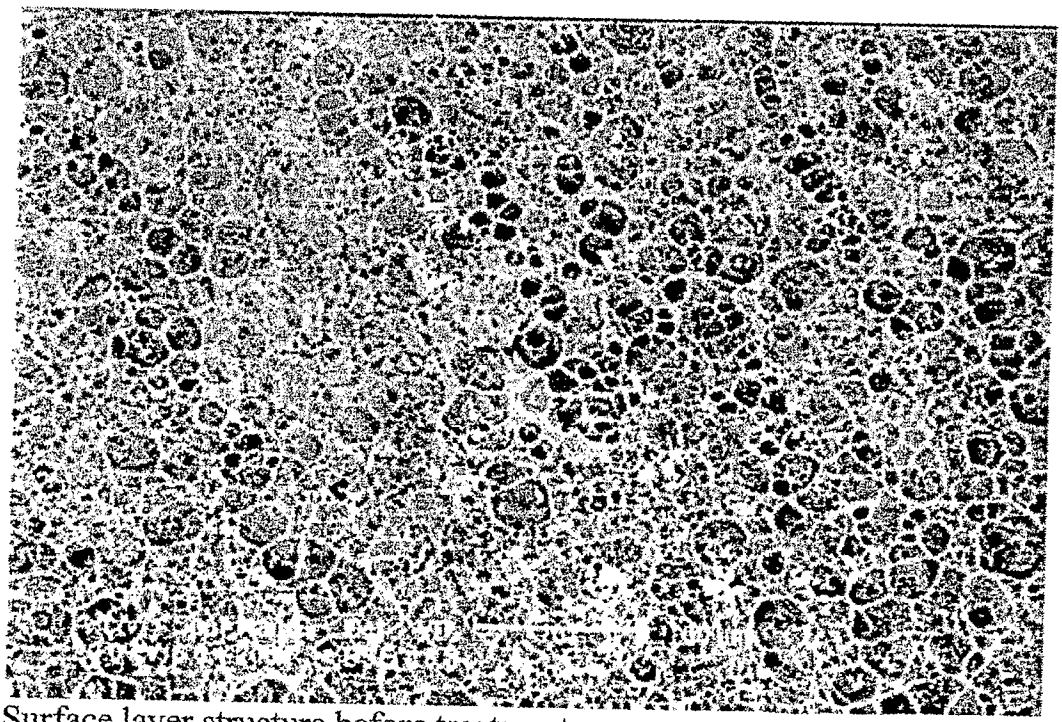

Surface layer structure before treatment

FIGURE 84

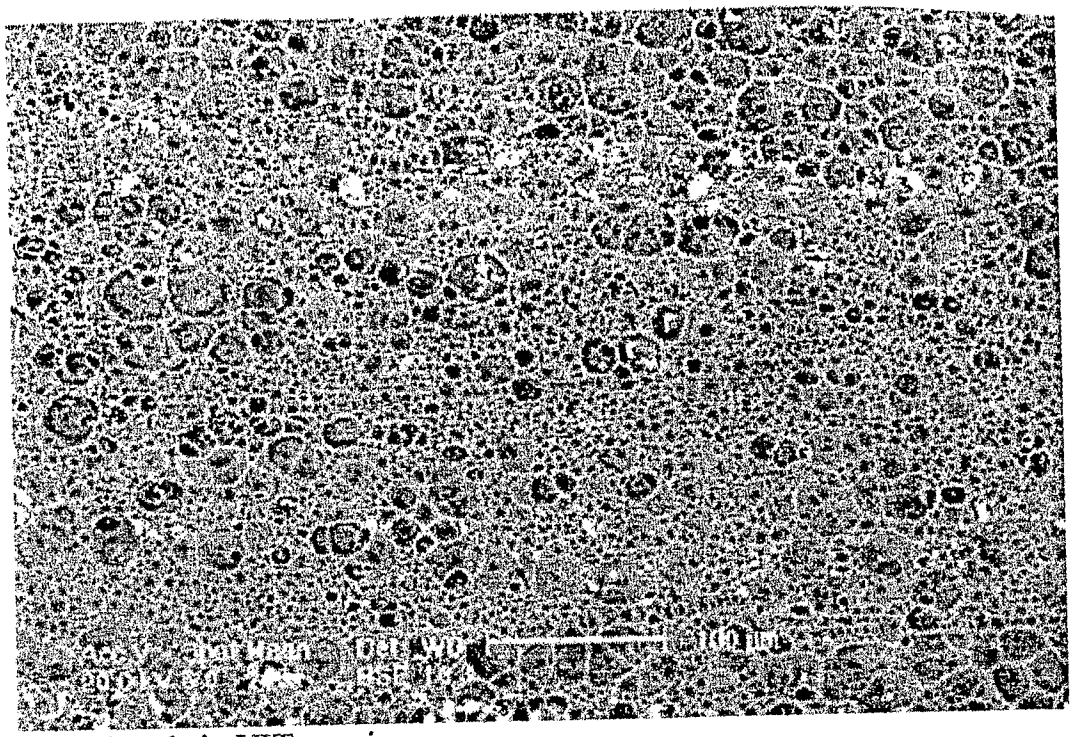

Microbands in UIT specimen

FIGURE 85

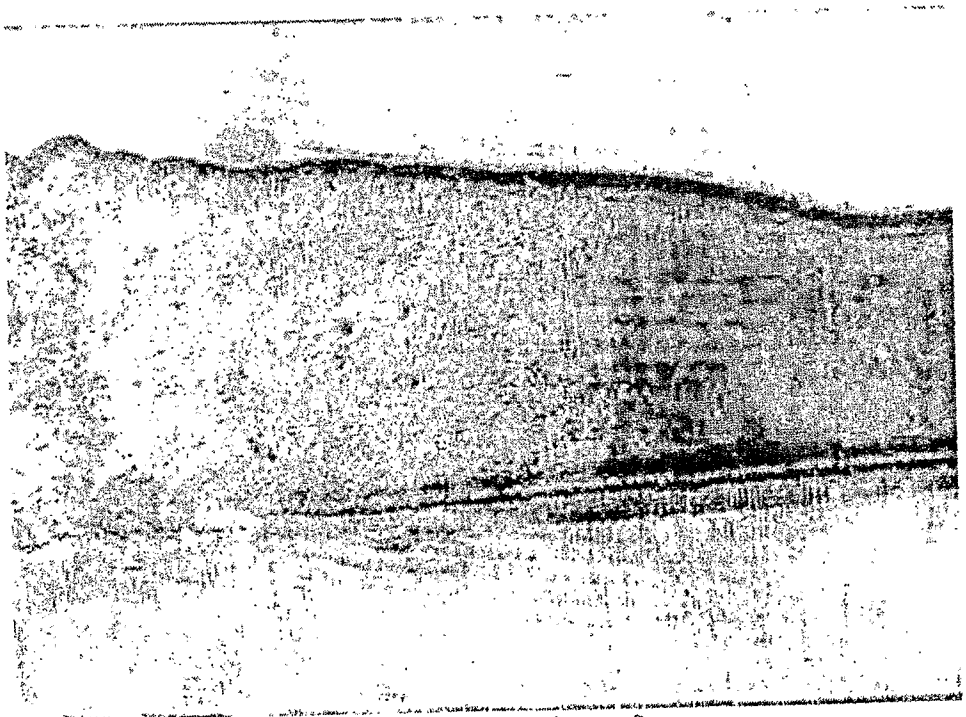

Corrosion damage on untreated sample surface

FIGURE 86

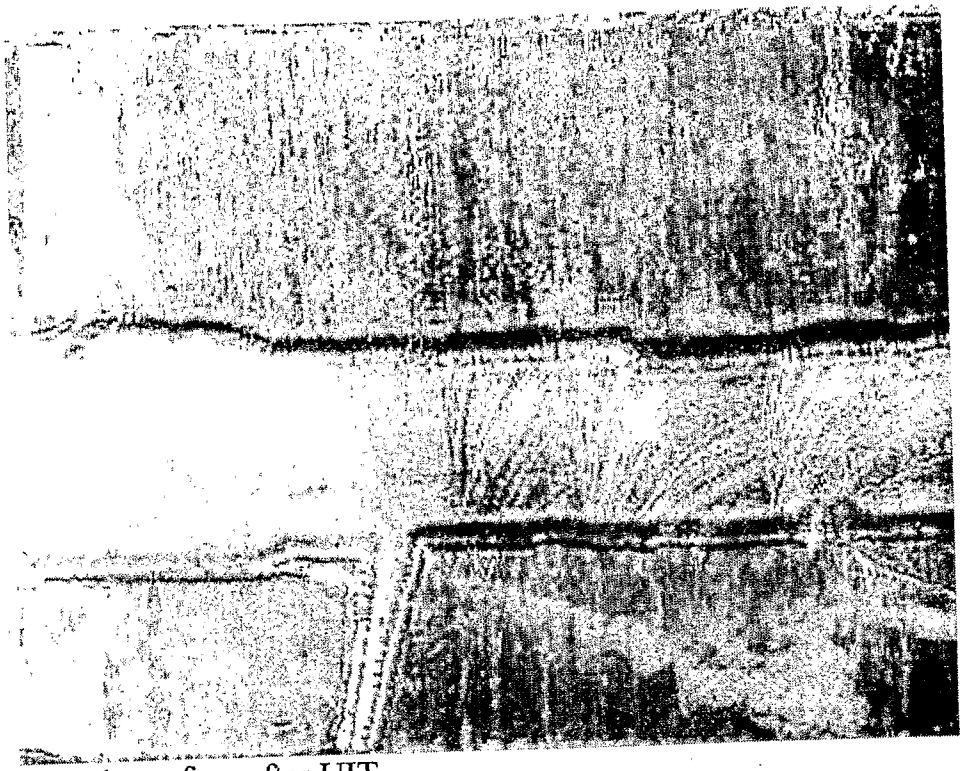

Sample surface after UIT

FIGURE 87

FIGURE 88

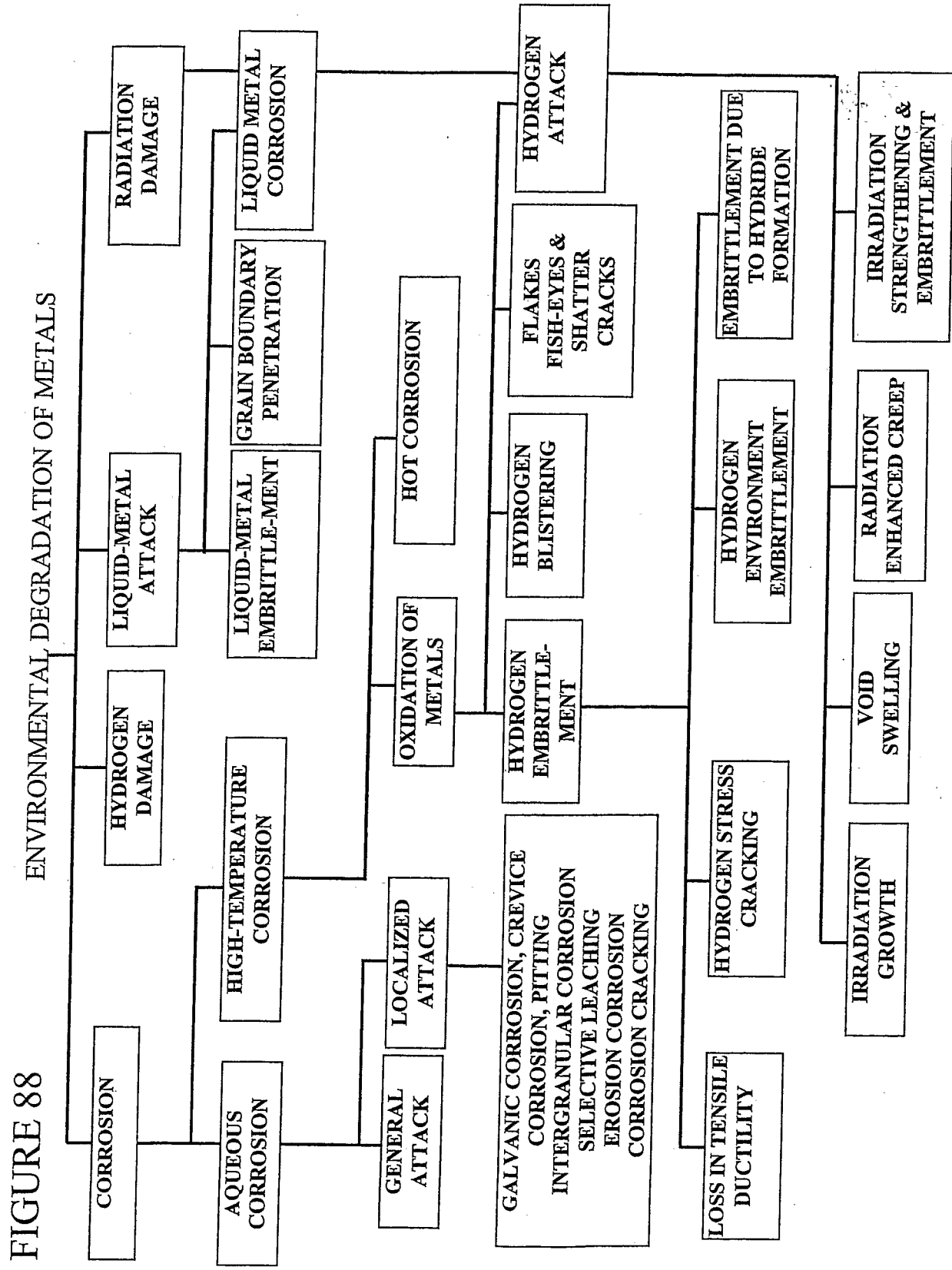
ENVIRONMENTAL DEGRADATION OF METALS
CORROSION
RADIATION DAMAGE
HYDROGEN DAMAGE
LIQUID-METAL ATTACK
LIQUID METAL CORROSION
GRAIN BOUNDARY PENETRATION
LIQUID-METAL EMBRITTLE-MENT
HIGH-TEMPERATURE CORROSION
OXIDATION OF METALS
HOT CORROSION
HYDROGEN ATTACK
HYDROGEN BLISTERING
FLAKES FISH-EYES & SHATTER CRACKS
AQUEOUS CORROSION
GENERAL ATTACK
LOCALIZED ATTACK
HYDROGEN EMBRITTLE-MENT
EMBRITTLEMENT DUE TO HYDRIDE FORMATION
HYDROGEN ENVIRONMENT EMBRITTLEMENT
IRRADIATION STRENGTHENING & EMBRITTLEMENT
RADIATION ENHANCED CREEP
VOID SWELLING
IRRADIATION GROWTH
HYDROGEN STRESS CRACKING
GALVANIC CORROSION, CREVICE CORROSION, PITTING
INTERGRANULAR CORROSION
SELECTIVE LEACHING
EROSION CORROSION
CORROSION CRACKING
LOSS IN TENSILE DUCTILITY